HYDROMETEOROLOGICAL REPORT NO. 34

METEOROLOGY OF FLOOD-PRODUCING STORMS IN THE MISSISSIPPI RIVER BASIN

Washington
July 1956

HYDROMETEOROLOGICAL REPORTS

(Nos. 6–22 Numbered Retroactively)

No. 1. Maximum possible precipitation over the Ompompanoosuc Basin above Union Village, Vt. 1943.*
No. 2. Maximum possible precipitation over the Ohio River Basin above Pittsburgh, Pa. 1942.*
No. 3. Maximum possible precipitation over the Sacramento Basin of California. 1943.*
No. 4. Maximum possible precipitation over the Panama Canal Basin. 1943.*
No. 5. Thunderstorm rainfall. 1947.*
No. 6. A preliminary report on the probable occurrence of excessive precipitation over Fort Supply Basin, Okla. 1938.*
No. 7. Worst probable meteorological condition on Mill Creek, Butler, and Hamilton Counties, Ohio. 1937. (Unpublished.) Supplement, 1938.*
No. 8. A hydrometeorological analysis of possible maximum precipitation over St. Francis River Basin above Wappapello, Mo. 1938.*
No. 9. A report on the possible occurrence of maximum precipitation over White River Basin above Mud Mountain Dam site, Wash. 1939.*
No. 10. Maximum possible rainfall over the Arkansas River Basin above Caddoa, Colo. 1939.* Supplement, 1939.*
No. 11. A preliminary report on the maximum possible precipitation over the Dorena, Cottage Grove, and Fern Ridge Basins in the Willamette Basin, Oreg. 1939.*
No. 12. Maximum possible precipitation over the Red River Basin above Denison, Tex. 1939.*
No. 13. A report on the maximum possible precipitation over Cherry Creek Basin in Colorado. 1940.*
No. 14. The frequency of flood-producing rainfall over the Pajaro River Basin in California. 1940.*
No. 15. A report on depth-frequency relations of thunderstorm rainfall on the Sevier Basin, Utah. 1941.*
No. 16. A preliminary report on the maximum possible precipitation over the Potomac and Rappahannock River Basins. 1943.*
No. 17. Maximum possible precipitation over the Pecos Basin of New Mexico. 1944. (Unpublished.)
No. 18. Tentative estimates of maximum possible flood-producing meteorological conditions in the Columbia River Basin. 1945.*
No. 19. Preliminary report on depth-duration-frequency characteristics of precipitation over the Muskingum Basin for 1- to 9-week periods. 1945.*
No. 20. An estimate of maximum possible flood-producing meteorological conditions in the Missouri River Basin above Garrison Dam site. 1945.*
No. 21. A hydrometeorological study of the Los Angeles area. 1939.*
No. 21A. Preliminary report on maximum possible precipitation, Los Angeles area, California. 1944.*
No. 21B. Revised report on maximum possible precipitation, Los Angeles area, California. 1945.*
No. 22. An estimate of maximum possible flood-producing meteorological conditions in the Missouri River Basin between Garrison and Fort Randall. 1946.*
No. 23. Generalized estimates of maximum possible precipitation over the United States east of the 105th meridian, for areas of 10, 200, and 500 square miles. 1947.
No. 24. Maximum possible precipitation over the San Joaquin Basin, Calif. 1947.
No. 25. Representative 12-hour dewpoints in major United States storms east of the Continental Divide. 1947.*
No. 25A. Representative 12-hour dewpoints in major United States storms east of the Continental Divide. 2d edition. 1949.
No. 26. Analysis of winds over Lake Okeechobee during tropical storm of August 26–27, 1949. 1951.
No. 27. Estimate of maximum possible precipitation, Rio Grande Basin, Fort Quitman to Zapata. 1951.*
No. 28. Generalized estimate of maximum possible precipitation over New England and New York. 1952.*
No. 29. Seasonal variation of the standard project storm for areas of 200 and 1,000 square miles east of 105th meridian. 1953.*
No. 30. Meteorology of floods at St. Louis. 1953. (Unpublished.)
No. 31. Analysis and synthesis of hurricane wind patterns over Lake Okeechobee, Florida. 1954.
No. 32. Characteristics of United States hurricanes pertinent to levee design for Lake Okeechobee, Florida. 1954.
No. 33. Seasonal variation of the probable maximum precipitation east of the 105th meridian for areas from 10 to 1,000 square miles and durations of 6, 12, 24, and 48 hours. 1956.

* Out of print.

U. S. Department of Commerce
Weather Bureau

U. S. Department of Army
Corps of Engineers

HYDROMETEOROLOGICAL REPORT NO. 34

METEOROLOGY OF FLOOD-PRODUCING STORMS IN THE MISSISSIPPI RIVER BASIN

Prepared by
George A. Lott and Vance A. Myers
Hydrologic Services Division
Hydrometeorological Section

Washington, D. C.
July 1956

For sale by the Superintendent of Documents, U. S. Government Printing Office, Washington 25, D. C. - Price $1.25

CONTENTS

CONTENTS (cont'd)

FIGURES

FIGURES (cont'd)

FIGURES (cont'd)

FIGURES (cont'd)

FIGURES (cont'd)

FIGURES (cont'd)

FIGURES (cont'd)

INTRODUCTION

On assignment from the Office of the Chief of Engineers, Department of the Army, the Hydrometeorological Section of the U. S. Weather Bureau undertook a comprehensive examination of the meteorology pertinent to the flood potential of the Mississippi River below the mouth of the Missouri River. The purpose of the meteorological study was to enable the Corps of Engineers to "determine flood magnitudes that will be used as a basis for establishing leevee grades on the main stem of the Mississippi River and for planning, designing, and determining benefit valuations of a large number of other comprehensive flood control works within the Mississippi River Basin."[1/] The meteorological study was divided into three parts, survey of the causes of heavy precipitation in the central Mississippi Valley, detailed synoptic analysis of large Mississippi Valley rainstorms, including the largest of record, and, in collaboration with the Corps of Engineers, combining those storms into hypothetical flood sequences. The first two phases are presented here; the last phase will be presented separately.

This report is primarily concerned with intensive precipitation falling as rain over the central part of the Mississippi River Basin during the months of January through July. Other precipitation in the Basin is relatively ineffective in producing floods on the main stem. Snow melt is not negligible in Mississippi floods but has never been the primary cause of a historical Lower Mississippi flood. Portions of the Mississippi River Basin west of approximately 100° W longitude and north of approximately 43° N latitude contribute little to floods on the main stem below St. Louis because of flood control reservoirs and hydrologic factors. Major floods are not experienced from August to December because the ground, dried during the summer, has an accumulated capacity to soak up water; any hypothetical flood between August and December would be overshadowed for design purposes by a hypothetical flood of the same likelihood of occurrence between January and July. The latter would be drastically more severe.

During the January-July flood season there is a gradual shift from east to west in the area of the Basin most likely to make the largest contribution to a main stem flood. Over the western tributaries, where the spring precipitation potential is several times that of winter, the greatest flood threat is in spring and early summer. Over the Ohio the precipitation potential varies little from month to month; the flood threat thereby decreases during the spring as infiltration and evapo-

ration rates rise. Average winter and spring precipitation are shown in figures 1 and 2.

The 19 storms analyzed in detail in chapter II are those chosen by the Corps of Engineers and the Hydrometeorological Section as the most appropriate of the storms for which precipitation data has been collected and organized in the Corps of Engineers' Storm Study Program[2/] to serve as prototypes of the precipitation of the design flood. Shown with the analyzed weather maps are concurrent short-period isohyetal patterns (for 6- or 12-hour intervals), probably the most comprehensive compilation of its kind appearing in the literature to date. This combination of maps should enable the reader to make a more precise comparison of rainfall patterns with associated weather events than is possible with the meteorological material usually available.

Chapter I

METEOROLOGY OF EXCESSIVE RAINS IN CENTRAL MISSISSIPPI RIVER BASIN IN WINTER AND SPRING

A. The Precipitation Process

The account of our present knowledge of the precipitation process is voluminous, complex, and incomplete and is dispersed through many textbooks and periodicals. It appears, however, that four conditions are necessary for the production of precipitation of more than drizzle intensity: 1) a mechanism to produce cooling of the air below the saturation temperature; 2) a mechanism to promote condensation of the super-saturated water vapor into cloud droplets; 3) a mechanism to produce growth of cloud droplets to raindrops; 4) a mechanism to produce a sufficient rate of accumulation of moisture in the atmosphere above one location to account for observed rainfall intensities. So far as is known, a simultaneous occurrence of all these mechanisms is a sufficient condition for heavy rainfall. Present knowledge of these four is summarized briefly.

Mechanism for cooling--lifting

Physical studies have shown that the following methods of cooling are too small to account for other than light drizzle or fog: adiabatic cooling by horizontal motion toward lower pressure, radiational cooling, cooling by contact with colder land or sea surface, and mixing of two air masses. To account for moderate or heavy rainfall amounts, adiabatic cooling by ascending motion is believed to be the only mechanism capable of producing a sufficiently rapid lowering of the temperature. The rate at which the amount of vapor content necessary for saturation decreases with cooling may be called the rate of production of moisture excess over-saturation. Fulks[3/] has constructed a chart showing the rate of production of moisture excess in a layer in terms of the temperature and moisture in the layer and the upward speed of the layer. This is reproduced in figure 3. The figure demonstrates that if the rate of precipitation is equal to the rate of production of moisture excess great upward speeds must accompany such heavy rainfall rates as occur in thunderstorms. This seems to be true even with some allowance for horizontal convergence of the falling raindrops, which causes the precipitation rate to be greater than the rate of production of moisture excess. More moderate vertical veloc-

ities will account for the rainfall intensities commonly experienced in long-duration large-area winter rainstorms.

Mechanism for condensation--the nuclei and molecular diffusion

Lowering of the temperature of the air below the dewpoint and consequent production of moisture excess over saturation does not necessarily require that condensation will occur, at least in the laboratory. Air from which all foreign particles have been washed can be cooled in the laboratory until the relative humidity is several hundred percent before droplets of liquid water form, presumably on aggregates of molecules. By contrast, in ordinary open air only a very slight degree of supersaturation can be obtained. This is because droplets form around particles of some foreign substance, commonly referred to as condensation nuclei. These particles are much smaller than the dust particles seen in a beam of light in a dark room and are studied by observing the condensed droplets in cooled air. Ordinary dust particles are not effective condensation nuclei, however. For example, one investigator found that beating a carpet in a room did not change the condensation nuclei count. That the nuclei are of terrestrial origin is evidenced by the fact that the number in the atmosphere decreases rapidly with height. Salt particles from evaporated sea spray and certain products of combustion are known to be effective condensation nuclei. There are probably other kinds also. There are probably always more than enough effective condensation nuclei present in the lower layers of the atmosphere to take care of any possible degree of the supersaturation. The present state of knowledge about condensation nuclei is summarized by Houghton[4/] and by Junge[5/]. In this study it will be assumed that if air in the lower atmosphere is cooled to saturation, condensation will occur.

Mechanism for droplet growth--collision and coexistence of ice crystals and water droplets

Clouds are colloidal-like suspensions of water droplets, or aerosols. Clouds vary in their colloidal stability - the tendency of the droplets not to coalesce and to remain too small to overcome the frictional resistence to falling. The two processes regarded as most effective for drop growth are the difference in falling speed between large droplets and small droplets, whereby the big droplets sweep up the little droplets, and the coexistence of ice crystals and water droplets. In the second process the difference in equilibrium saturation vapor pressure over water and over ice requires that vapor evaporate from the water drops and condense on the ice crystals. The latter grow large enough to fall out of the clouds. This last is the classical theory of Bergeron and Findeisen. Houghton has suggested that the ice crystal effect may be most important in the early stages of droplet growth and the collision effect

in the later stages. It has also been shown that the collision effect alone can start precipitation in a warm cloud containing no ice crystals if the liquid water content is initially high, the cloud is moderately deep, and the cloud's drop size distribution is broad.

Mechanism for accumulation of moisture--convergence

The amount of liquid water in a cloud or even the total water vapor in a column does not equal the amount of rain often observed to fall in an hour or less. One of the ways the liquid water content of clouds has been measured is by capturing the water while flying through the cloud in an airplane. The water content of most clouds is of the order of magnitude of one-tenth to five-tenth grams per cubic meter.* Even a cloud twenty thousand feet thick would contain only a few hundredths of an inch of liquid water. If all the liquid water in most clouds could be induced to fall to the earth as precipitation the amount of precipitation would still be very small.

In a vertical column an inch of water vapor is a high value and two inches is an extreme value. Furthermore, there is usually more water vapor in the vertical column after a rain than before. It is evident that convergence of air toward a heavy rain area is necessary to replenish the water vapor constantly and condense new cloud droplets which in turn coalesce to form new rain drops or snow flakes. Such convergence is also necessarily present in association with the rising motions in a rainstorm in order to satisfy the simple principle of continuity of mass.

In summary, the meteorological factors to be examined in accounting for major cool-season rainstorms in the central Mississippi Valley are those that transport moisture toward the rain area and continually replenish the moisture during the period of the rainstorm, and those related to convergence and lifting. It will be assumed that when these requirements for rain are fulfilled, the physical processes of condensation, droplet growth, and falling of the drops will operate efficiently.

* May be as much as 2 gm m^{-3} in heavy cu. In clouds 20,000 ft thick this works out to about 0.5 inch of liquid water. JGC.

B. Vertical Motions

The rising motion needed to release rain may be induced in any of three ways or a combination of them. The wind may ascend a mountain slope. This orographic process is a major cause, for example, of the heavy winter rains of the Coast and Cascade Ranges of the Pacific Northwest. Orographic release of rain, however, while important for local floods within the Mississippi Basin, is of little consequence for floods on the

Mississippi River itself. The second lifting process is associated with vertical instability in the atmosphere and is a result of the excess of solar heating at the surface of the earth as compared with aloft. The third process, the lifting of warm air masses over colder air masses, is the process of most importance to Mississippi floods and is the result of excess of solar heating in the south as compared with the north.

C. Instability

When a quantity of air near the surface of the earth reaches such a temperature and water vapor content that if it is lifted to some great height--taking into account the release of latent heat of condensation--its temperature will exceed that of the surrounding air at that height, a state exists that is termed latent instability.* If the warm moist surface air can be lifted above the level at which condensation begins, then the convection will proceed spontaneously with an updraft in the warm moist air from which precipitation falls and surrounding descent of cooler air, as shown schmatically in figure 4. The thunderstorm, the tornado, and the hurricane are all products of the release of latent instability. Their kinetic energy is in large measure derived from the release of the heat of condensation. A second method of creating latent instability is for low-level winds to carry warm moist surface air northward under air that is progressively cooler at a high level. The Lower Mississippi Valley and adjacent Gulf drainage is the most favored region of the United States for the development of latent instability in the cool season by this process. This is evidenced by the January-through-April frequency of thunderstorms (figure 5).

A portion of the atmosphere in which the moist adiabatic temperature distribution prevails (curve B of figure 4) is in a neutral state of vertical equilibrium and neither induces nor inhibits rain but serves as a chimney through which moist air will readily rise and release rain if induced to do so by another process. It appears that for major Mississippi Valley rains in which thunderstorms are not prominent the vertical lapse rate is generally near this neutral state or slightly more unstable. Temperature differences between 1.5-km and 5-km elevations (4,921 and 16,404 feet) and concurrent 6-hour precipitation for the major rainstorm in January 1937 are shown in figure 6. The

*The name latent instability is taken from Petterssen, "Weather Analysis and Forecasting," 1940, p. 62.

area of temperature difference exceeding the moist adiabatic lapse rate is delineated in the figure by T-shaped symbols; the heavy rain, it can be noted, is in or near this area. Too much stability may terminate the rain. The map for January 23, 1937, (figure 6C) suggests that the rain was cut off when the stability became too great in the region where the other rain-producing factors were still present. A similar stability analysis for two other storms showed a comparable distribution of the precipitation with respect to the area of moist adiabatic temperature difference. In none of the three storms was there much precipitation more than one degree on the stable side from the moist adiabatic temperature-difference line.

The development of latent instability is the inevitable result of the manner in which the earth and its atmosphere absorb solar radiation. According to Houghton[6/], the average annual absorption of solar energy over the Northern Hemisphere amounts to about 461 langleys (calories per square centimeter of horizontal surface) per day, of which 64 langleys are absorbed by clear air, 72 langleys by clouds, and the remaining 325 langleys at the surface of the earth. Only about a third of this intensive heating at the surface of the earth is dissipated by net upward radiation from ground and sea. The remainder is transferred to the bottom of the atmosphere by conduction of heat from ground and sea to the air and by evaporation of water vapor into the air. (These account for about one-fifth and about one-half of the 325 langleys, respectively.) This warming and moistening of the air from below continues until latent instability is developed either locally or in some region to which the warmed and moistened surface air is transported.

The energy added to the atmosphere by evaporation from below is in the form of latent heat. This latent heat is converted to sensible heat in the atmosphere at the level at which precipitation forms and falls out. As this is always at a greater height, frequently a very much greater height, than the level of evaporation, the water-vapor cycle has great importance in transporting the excess surface heat upward into the atmosphere.

D. Horizontal Temperature Contrast

The importance of horizontal temperature gradients in the production of heavy rainfall is verified by the fact that all winter and spring rain in the Mississippi Valley of proportions to swell rivers is observed near fronts, that is, not more than 100 miles from the position of the front at the ground into the warm air and not more than twice that distance into the cold air. Unusually strong temperature gradients existed at the fronts associated with several of the storms described in the second chapter of this report. All of these strong fronts were

formed and maintained between air currents that in a few days had brought into juxtaposition air from sources of temperature modification thousands of miles apart--warm air from south and east of the Gulf of Mexico and cold air from central or western Canada. Some typical horizontal trajectories of air parcels computed for major storms are depicted in figures 7 to 11. These trajectories are for the gradient level (about 1500 feet) and, in the more recent storms, for two higher levels also. The trajectories terminate in the warm air and in the cold air on opposite sides of a rainfall center. The methods for computing the trajectories are described in the appendix, page 16. It can be noted in figures 9, 10, and 11 that the warm-air trajectories turn clockwise with height and the cold-air trajectories turn in the opposite direction, as required by the thermal wind relationship.* Thus, the oppositely directed wind currents near the surface are associated with more parallel currents aloft.

A front or horizontal temperature gradient in the atmosphere is not effective in releasing rain unless there is a wind component in the warm air directed across the temperature gradient.** The intensities of the normal wind component and of the front or horizontal temperature gradient may be combined by measuring the apparent horizontal advection of temperature on a chart on which simultaneous winds and isotherms are

*The cold-air trajectory in figure 10 turns in the opposite direction. This paradox is explained by the fact that the terminal point of the cold-air trajectories at North Platte, Nebr. is on the west side of a fairly intense Low. At the time of the terminal point, the cold air at North Platte, which had flowed from Canada as depicted by the trajectories, was being followed by warmer air which had swept around the north side of the cyclonic center. Thus, there was actually warm advection in this region and the wind therefore turned clockwise instead of counterclockwise with height.

**With a fast-moving cold front there may be only a net component toward the front, that is, the front may be overtaking the warm air.

depicted.* Recognizing the role of advection in releasing rain helps account for the fact that the heaviest precipitation in the frontal zone, as often as not, is on the warm side of the front. Motion up the frontal surface cannot account for such rain, as fronts always slope toward the cold air. Advection within the warm air, however, may be stronger than across the front, in spite of the much weaker temperature gradient, by virtue of a high wind directed almost at right angles to the isotherms. There is some theoretical and empirical evidence that the gradient of the advection is more important than its absolute magnitude in producing vertical motions. A point in the wind-temperature field where the advection is greater than at any surrounding point may be likened to a gas burner under a tank of water, or to the formation of a cumulus cloud over a hot field surrounded by cooler woods. In all three instances the concentrated warming induces concentrated ascent surrounded by more diffuse return descent. The centers of greatest comparative advection may be located by constructing first a chart of values of the advection and secondly a chart of values of $A_1 + A_2 + A_3 + A_4 - 4A$, where A is the value of the advection at a point and the other terms are the advection at a fixed distance north, east, south, and west of the point. Charts of the comparative or differential advection are shown in figures 145, 157, and 173 and the associated rainfall in figures 141, 156, and 172.

The ultimate cause of the interplay of cold and warm air masses in the Mississippi Valley, with the warm air continually seeking to flow north and rise above the cold air which in turn seeks to sink and underrun the warm air, is the latitudinal variation of insolation. The mean annual excess of local heating (by sunshine) over local cooling (by radiation to space) at low latitudes on the earth is known to be exactly equaled by the excess of cooling over heating at high latitudes, since the mean

*The instantaneous advection at a standard time for weather observations is obtained by dividing the wind speed, observed or geostrophic, by the distance between isotherms in the direction of the wind. The mean apparent advection over a period of time may be obtained by moving the isotherms on an initial map with the speed and direction of the wind for a designated number of hours and taking the difference between the initial and final temperatures at points. Details of the latter procedure are described by Appleby[22].

The horizontal advection of temperature is only a necessary condition here; it is not sufficient. The necessary and sufficient condition for the production of rainfall in this process is that there be horizontal advection of moisture convergent. Why not make this clear?

J.G.

temperature of the earth does not change appreciably from year to year. The excess of heat must be transported by the atmosphere, and to a small extent by the ocean, to the region of excess of cooling. The latitudinal variation of the annual and January mean of solar radiation absorbed by the earth and atmosphere, and the outgoing long-wave radiation through the top of the atmosphere (the only net cooling process) as computed by Houghton[6/] are depicted in figure 12. The poleward flux of heat necessary to maintain a balance is also shown. This mean poleward flux is both in the form of sensible heat (warm air moving northward and being replaced by chilled air) and latent heat (moisture evaporated from the ocean in the south being precipitated in the north). The Mississippi Valley, by virtue of its geographical position - between warm ocean immediately to the south and cold continental region of excess cooling to the north, with no protective intervening mountains - is especially favored to receive copious rain as warmed air seeks to flow northward and rise above cold air and cold air seeks to underrun the warm air and push southward. The rising motions inherent in this process release precipitation through adiabatic cooling of the warm air.

E. The Moist Inflow

Large-volume cool-season rainstorms in the central Mississippi Valley are supported by an inflow of tropical air from the Caribbean Sea or from the Atlantic Ocean south of 25° N. This is illustrated by the warm-air trajectories in figures 7 through 11. Trajectories computed for half a dozen other storms (not shown) were similar. As a further investigation of the source of the moisture for winter storms, the isobars through New Orleans on 36 selected days of heavy rain in the Mississippi Valley during January and February were traced onto a map (figure 13). These isobars are rough approximations of low-level trajectories. Figure 13 and the other trajectory figures are rather convincing evidence that passage of air over the Gulf of Mexico alone is probably not adequate for the air to acquire enough moisture to support a major rainstorm and that a longer travel over warmer water is required. Comparison of the trajectories with mean sea-surface temperatures suggests that to impart a given dewpoint to an air current entering the southern United States a water surface with a temperature 8 to 10 F° warmer is required. Typical sea-level dewpoints at the Gulf Coast in January and February are in the upper 60's (°F) in tropical air which flows from an area where the water temperature is in excess of 77° F (figure 14). By May, inflow dewpoints at the Gulf Coast are in the lower 70's while the water temperature in the source region has risen to above 80° F (figure 15).

The volume of precipitation occurring over the eastern and central United States in winter or spring appears to be about equal to the moisture transported across the Gulf Coast a few hours before, as demonstrated by computations for two and a half months. Daily northward transport of moisture between the ground and 400 mb (approximately 24,000 feet) across the 30th parallel (approximately along the Gulf Coast) between the longitudes of San Antonio, Tex., and Tallahassee, Fla., during March 1951 is plotted against the daily fall of precipitation upwind from the San Antonio-Tallahassee base line in figure 16. The daily values for vapor transport were obtained by assuming that the rate at 0900 CST was maintained for 24 hours*. The daily precipitation was obtained by planimetering daily isohyetal maps for the 24-hour period ending at 0630 CST. One explanation of the precipitation inflow relationship is that the inflow is mostly at a low level, and before passing off the East Coast or into Canada this low-level moisture current in winter and spring will normally encounter a horizontal temperature gradient. Ascent and precipitation result. Only rarely in winter and early spring will very warm weather prevail over such a large area that tropical air will flow through the United States from the Gulf without encountering sufficient temperature gradients to release precipitation. Accumulated values of water-vapor transport and precipitation data in figure 16 are presented in figure 17. This diagram shows that for the month as a whole the precipitation was approximately 80% of the vapor inflow. By contrast, the precipitation for the heavy rain period from the 25th through the 29th was very nearly 100% of the vapor inflow.

The relationship between precipitation and the moist inflow immediately prior to it is not usually as close in summer as it is in winter for three reasons: (a) evapo-transpiration contributes appreciable moisture to the air from the land in summer, (b) several days transit time may elapse from coast to point of precipitation, (c) circumstances are more favorable for moisture to flow through the country without precipitation. At times of very heavy rain in summer, however, the relationship should hold, since a strong inflow against a temperature gradient is necessary. During the first half of July 1951, the month of the spectacular Kansas flood, this was found to be the case.

*Details of the procedure for computing moist inflow through the San Antonio-Tallahassee cross section are give in the appendix, page 17.

The largest transport of moisture across 30° N is at a much lower level than that at which the precipitation clouds form. It is typical for the moisture transport, both in individual storms and in seasonal means, to be concentrated in a jet of restricted horizontal and vertical extent at the 2000-ft or 3000-ft elevation, just above the layer in which the wind speed is reduced by surface friction. Mean winter (December, January, February) and summer (June, July, August) cross sections of moisture-vapor transport at 30° N for the year 1949 have been prepared by Benton and Estoque[7/]. These are reproduced in figures 18 and 19 of this report. The mean winter jet is centered over New Orleans at an elevation of about 2000 feet and the mean summer jet slightly to the west at the same elevation. The mean seasonal moist inflow is substantial; if the average inflow vertically above New Orleans (figure 18) were released as precipitation, it would be sufficient to deposit about .60 inch of rain per day for the entire season along a line 500 miles long.

Two moisture-transport cross sections at 30° N prepared by the Hydrometeorological Section for a single observation time during an intense and widespread rain (figures 20 and 21) show the same low-level jet pattern as the seasonal means. Figure 20 illustrates the transport at the time of the heaviest rain in a large winter rainstorm that extended from northern Texas to Illinois; figure 21 illustrates that during the record-breaking spring rainstorm centered at Warner, Okla. The latter storm is described in detail in chapter II of this report. The 6-hour isohyetal patterns before, during, and after the inflow of figure 21 are depicted in figures 141, 143, and 144. Study of numerous surface and upper-level maps by the Hydrometeorological Section suggests that these low-level jet patterns of moisture transport are typical for large volume rainstorms.

Prevailing wind direction over the Mississippi Valley from the Gulf Coast at the elevation of maximum moist inflow has a direct relationship to the distribution of both average precipitation and the frequency and magnitude of rainstorms of flood-producing proportions. The pattern of the number of miles in an average winter (December-February) that the air at a height of 1000 meters (3281 feet) flows from a bearing toward the Gulf (figure 22) may be compared with the normal winter precipitation (figure 1)*.

*The miles of wind in figure 22 are computed from figure 73 of "Airway Meteorological Atlas," U. S. Weather Bureau, Washington, D. C., 1942. The wind roses in that figure were compiled from all pilot-balloon observations of record up through 1939.

Winds from a direction within the marked sectors of figure 22 obviously do not necessarily represent transport from the Gulf, nor is all of the transport from the Gulf included within the marked sectors. The wind-flow totals are, however, qualitatively indicative of the influence of the wind in determining the normal and storm precipitation. A typical distribution of water-vapor transport throughout the United States for a heavy rain in the Mississippi Valley is illustrated by charts of mean water-vapor transport at four levels in January 1949, a heavy rain month, (figure 23). The arc of the axis of moisture-flow at all levels is from the Gulf Coast toward Pittsburgh, then off the East Coast. the average transports are the vector means of the 62 twice-daily instantaneous transport vectors, which are in turn the product of the wind vector and the specific humidity (950 mb based on once-daily vectors). The vector directions are depicted by arrows, the magnitudes by numbers and isopleths. The 850-, 700-, and 500-mb levels are after Benton[8/].

F. The Circulation Pattern

The moist inflow, temperature contrast, and instability necessary for heavy rain in the middle and lower Mississippi Basin during winter and early spring is produced by a specific over-all pattern of atmospheric wind flow. Scores of cold-season Mississippi storms reviewed each had the following characteristics: (a) There was a front near the rain area. (b) There was a High centered in the western Atlantic. (The warm moist inflow is around the western edge of this High.) (c) There was a High centered in the eastern Pacific. This is a necessary partner to: (d) a trough in the West with the trough line* between the rain area and the Pacific Coast, or just off the Pacific Coast. The trough, while extending from the ground into the stratosphere, is not as well-defined at the surface as at levels above about 5000 feet. Practically none of the heavy precipitation falls east of the 10,000-ft trough line. (e) There was a high-pressure area in the north-central United States or southern Canada. This may have appeared as a separate High center, or as the extension of a High centered in western Canada, the Great Basin High, or the East Pacific High. The role of this High or extension of a High is to pour cold

*A trough line in this report is defined as lying through the southernmost points on U-shaped isobars, or through the southernmost and northernmost points of closed isobars.

Canadian air around its eastern edge into the central United States. Often the High is more clearly defined a day or two before the rain than at the time of the rain. There was frequently, but not necessarily, an active Low between this High and the East Pacific High.

The circulation of the air associated with this pressure distribution, shown schematically in figure 24, is directly related to the physical processes involved in the heavy rainfall. The warm moist low-level flow around the western edge of the Atlantic High carries a relatively narrow tongue of warm air northward parallel to the front. The wind-across-isotherms pattern necessary for rain is obtained at the head of this warm tongue and across the front itself. As this warm tongue advances, the temperature at the surface will rise more rapidly than in the southwesterly current at a higher elevation above it in which there will be little change in temperature, thus developing and maintaining the degree of instability necessary for rain. This typical rain situation is not only favorable for rain but also for cyclogenesis, which in turn facilitates the release of rain. The flow pattern and temperature fields described are not independent but are strictly interrelated. The temperature field fixes the rate of decrease of pressure with height, and the pressure field, in turn, is closely related to the wind.

The pressure systems and circulation associated with major rainstorms from April through June are similar to those described above for winter rainstorms, but some of the pressure systems and circulations are weaker. Rain in summer is conditioned to a greater extent on smaller-scale vagaries of wind, moisture, horizontal temperature gradient, and stability than in winter. The upper-air troughs are of shorter wave length and the trough line is, of necessity, close to the rain area rather than far to the west as in some winter cases. This, of course, is because displacement of the trough line far to the west of the rain area is observed only in association with unusually cold air. In the late spring and early summer season Highs are not necessarily in simultaneous position to feed cold air and warm air toward the rain area. The interaction may be between an active warm-air current and a more or less stagnant cold mass or between an active cold current and a stagnant warm and moist mass. In either case the stagnant mass originally moved into position as part of the circulation around a High two or three days before.

Tropical storms and hurricanes sometimes move into the Lower Mississippi Valley in the summer months and must be considered as an important threat of excessive rain in that area after the early part of June. The Atlantic subtropical

anticyclone is displaced to the north of its mean annual position in summer, and the Gulf of Mexico is frequently in the zone of easterly winds. Tropical disturbances may move inland in this belt of easterlies swinging from the east or central Gulf up into the Mississippi Valley.

Appendix

Supplementary data and computational procedures

Note 1. Dates of isobars in figure 13. January 10, 11, 1913; January 26, 27, 28, 29, 30, and 31, 1916; February 11, 12, and 13, 1927; January 1, 1932; January 9, 10, 14, 17, 20, 21, 22, and 24, 1937; February 14, 15, 16, and 17, 1938; January 2, 3, 4, 5, 6, 10, 11, 12, 13, 14, 15, and 16, 1950.

Note 2. Procedure for computing trajectories in figures 7-11. Trajectories were traced backward from a selected terminal point by computing displacements on successive weather maps. For older storms, surface maps were available every 12 hours within the United States and every 24 hours beyond. For later storms, surface maps were available every 6 hours and upper-air maps every 12 hours. Every map was considered as depicting the mean winds and pressures for a period of time centered on the time of the map, for example, upper-air charts for 9 a.m. and 9 p.m. CST were considered as means of the period from 3 a.m. to 3 p.m. and 3 p.m. to 3 a.m., respectively. To construct an upper-air trajectory ending at 9 p.m., the flow was computed backward from the selected terminal point for 6 hours on the 9 p.m. chart, giving a 3 p.m. position; this position was transferred to the 9 a.m. chart and carried back 12 hours, giving the 3 a.m. position; this position was in turn transferred to the preceding map, and a 12-hour displacement computed, etc. Displacements were computed on the basis of observed winds at map time, if wind observations were available. If no winds were available, the geostrophic wind, computed from the pressure field, was used. The trajectories in figures 7-11 are in general based on observed winds within the United States and on the geostrophic wind beyond. At the gradient level (the level at which surface friction becomes negligible) observed 1000-ft or 2000-ft winds were employed. Surface winds were not used. Test comparisons of geostrophic and wind-based trajectories for the same times and terminal points demonstrated that it was important at all levels to employ observed winds instead of geostrophic winds near a Low or front. The angle of the real wind across isobars at 5000 feet was sufficient near the terminal points of many trajectories that use of the geostrophic wind would have given an entirely erroneous warm-inflow trajectory from over northern Mexico instead of the more nearly correct trajectory from over the Gulf. Beyond the United States the pressure patterns were such that the across-isobar accelerations would be small and the geostrophic wind a good approximation of the real wind, with one exception. The 5000-ft trajectories

tended to become indefinite below about 20° N in the vicinity of the Yucatan Peninsula in a region where the pressure gradient was often so light that it exercised poor control on the wind.

To substitute the gradient wind (not the gradient-level wind, but the theoretical wind which includes centrifugal force in addition to the terms included in the geostrophic wind) for the geostrophic wind offers no improvement, as only the speed and not the direction of the computed wind would have been different. The non-geostrophic direction of the real wind was the essential element in starting geostrophic trajectories off on the wrong foot.

Note 3. Source of data and explanation of figure 12, "Latitudinal Variation of Heat Balance." The annual insolation and cooling curves are from values by Houghton[6/]. The insolation curve shows the average daily absorption of solar radiation in a vertical column of atmosphere and earth of one square cent centimeter horizontal cross section. The cooling curve shows the mean daily long-wave radiation passing upward through the top of the atmosphere. The January curves of insolation and cooling are derived by adjusting Gabites'[28/] monthly values upward by the ratio of Houghton's to Gabites' annual totals (ratio 1.08 for insolation and 1.095 for cooling). The ocean at atmosphere flux curve is from values by Houghton of the mean annual northward transport of heat necessary to maintain the heat balance, in units of calories per day through a vertical strip facing south, one centimeter wide and extending from the bottom of the ocean to the top of the atmosphere. According to Sverdrup, Johnson, and Fleming[29/] ocean currents account for much less than 10% of the total transport. The rate of transport of heat during winter exceeds the mean annual values at all latitudes[28/].

Note 4. Definition of gm/cm-mb-sec. The unit gm/cm-mb-sec is defined as the mass of water vapor, in grams, flowing in one second through a vertical rectangle normal to the flow one centimeter wide and of such vertical extent that the pressure difference between the bottom and top of the rectangle is one millibar. The convenience of this unit is that water-vapor transports may be readily evaluated from the wind and the conventional unit of moisture content of the air, the mixing ratio, without regard to the particular density of air at any particular height. Equal areas in figures 17-20 represent equal transports.

Note 5. Computation of moist inflow in figures 20 and 21. The inflow of water vapor (I_{1000}) in inch-square-miles per 24-hours between San Antonio and Tallahassee in the layer extending from 1000 mb to 999 mb, was obtained from the expression:

$$I_{1000} = 0.549 \left(\Delta h_1 \bar{q}_1 + \Delta h_2 \bar{q}_2 \right)$$

where Δh_1 is the difference, in feet, of the height of the 1000-mb surface between Burwood, La., and San Antonio, Tex., Δh_2 is the height difference between Tallahassee, Fla., and Burwood. The $\bar{q}$'s are the respective mean mixing ratios over the two intervals, in grams of water vapor per kilogram of dry air, and are approximated by:

$$\bar{q}_1 = \frac{q_{SAT} + 2q_{LCH} + q_{BRJ}}{4}$$

$$\bar{q}_2 = \frac{q_{BRJ} + 2q_{VPS}}{3}$$

The subscripts SAT, LCH, BRJ, and VPS refer to San Antonio, Tex., Lake Charles, La., Burwood, Tex., and Valparaiso, Fla., respectively. All terms are observed directly at raob stations at approximately 9 a.m. CST, except the data at Tallahassee, not a raob station. Heights and mixing ratios there were interpolated between adjacent stations on a map.

Similar values of the inflow were computed for 1-mb layers at 925 mb, 850 mb, 700 mb, and 500 mb. The total inflow I_T from the surface to 400 mb was then obtained from:

$$I_T = 37.5(I_{1000}) + 75(I_{925}) + 112.5(I_{850}) + 175(I_{700}) + 200(I_{500})$$

The constant multipliers in the above expression are equal to the number of millibars from the midpoint between two layers to the next higher midpoint between layers.

The 1000-, 850-, 700-, and 500-mb data were readily available on standard constant-pressure charts. Heights and mixing ratios at 925 mb were obtained by averaging the corresponding 1000-mb and 850-mb heights and mixing ratios. Investigation determined that a 925-mb layer should be included and that the data could be approximated in that fashion.

Use of the multiplier of 37.5 for the I_{1000} overestimates the inflow by assigning full geostrophic value to the wind in the 1000-mb to 962.5-mb layer, neglecting the fact that the wind is reduced by surface friction, but underestimates the inflow by ignoring inflow between 1000 mb and the ground. Investigation showed that in the mean the two effects approximately compensate for each other.

Chapter II

MAJOR RAINSTORMS OVER THE MISSISSIPPI RIVER BASIN

Introduction

This section will be devoted to a detailed meteorological analysis of major rain-producing storms over the Ohio and Mississippi Valleys.

Selection of the storms for this part of the study was made from sequences considered pertinent by the Corps of Engineers. These storms do not represent exclusively the largest of record but were chosen in part on account of the floods they produced and their adaptability for synthetic flood sequences. This selection is therefore restricted to storms that have occurred during the months that historically have produced floods, or storms that could reasonably be transposed in time to the flood season.

Each storm is treated, first, with respect to the large-scale circulation pattern (a section of the Northern Hemisphere Maps for the storm period starting before the first burst is included) and, second, with respect to a more detailed picture (a series of maps covering the area of significant rain and vicinity). Adjacent to the small-scale maps will be found the incremental isohyetal maps, showing the distribution of the principal rainfall.

The similarities and differences among the storms will be treated, together with any anomalies of note. Other weather charts, including a presentation of differential advection, are shown for the later storms for which extensive upper-air data are available. (For a definition and short account of the significance of differential advection, see page 9).

The 12-hour representative dewpoint* and the maximum possible dewpoint for the date of occurrence of the storm will be given together with the potential moisture adjustment. Also, where pertinent to the hypothetical flood sequences referred to

*The highest dewpoint (reduced to 1000 mb) persisting for 12 hours in the rain-producing air mass where it lay at the surface upstream from the rainfall center, "Generalized Estimates of Maximum Possible Precipitation," Hydrometeorological Report No. 23, Washington, 1947. pp. 18-19.

on page 1, an estimation will be made of the minimum time interval necessary at which moisture would be available to permit another heavy rainstorm, regardless of type to follow the storm, taking into consideration meteorological characteristics that are essential to its mechanism. Intervals preceding the storms are similarly treated.

Storm of January 17-25, 1937 (OR 5-6)

January 1937 may represent conditions near the extreme for January under our present climatic regime for the persistence of the warm moist current that, on the average, sweeps westward through the Antilles. During an average winter month, cold dry air periodically sweeps through the Gulf of Mexico into the northern Caribbean Sea cutting off the flow of tropical air for several days at a time. In January 1937, however, no cold air was able to pass southern Florida until the 30th of the month and even then by only a few miles. The southeastern Gulf was, therefore, overlain by unmodified tropical air all month. At the same time, temperatures in the western half of the country were much below normal, approaching record lows in some of the Rocky Mountain States. Frontal activity, as might be expected was both frequent and intense. In fact, the mean surface position of the polar front for January 1937 was 400-500 miles north of its most frequent January position through central and southern Florida. Although storms were numerous throughout the entire month, a period of particularly intense frontal activity accompanied by almost continuous rain in the eastern United States occurred during the 17th through the 25th. The detailed surface weather maps (figures 28, 30, 32, and 34), 1500-meter charts (figures 36-39), and 6-hourly incremental isohyetal maps (figures 29, 31, 33 and 35) are restricted to this period*. Three-thousand-meter charts for the storm period are available as part of the Historical Weather Map Series[9/]. A series of isohyetal maps covering longer time intervals (2 to 30 days) are contained in the Monthly Weather Review[10/]. This comprehensive report also contains a meteorological analysis and a comparison of the 1937 flood with historic floods on the Mississippi and Ohio Rivers up to that time. There are some differences in analysis of fronts and isobars on the large-scale surface weather maps and the detailed maps for the same area and time.

* It should be pointed out that the upper-air observations are not strictly synchronous. Observation times vary from station to station, in some cases by many hours, but this has been taken into consideration in the drawing of the various isolines. The time of observation is plotted with each report.

This has come about because more data was available for the detailed maps and because more concentrated attention could be paid to the exact placement of fronts, etc., over the much smaller area. In case of difference, the analysis on the detailed charts will be the one referred to in the text. The large-scale surface weather maps in this report (figures 25-27), are taken from the Northern Hemisphere Sea Level Series[11/].

It may be noted that pressure was much above normal[12/] to the east of Florida during the storm period and indeed had been since before January 1. Above-normal pressure is almost always present in the western Atlantic at the time of heavy rainfall in the Mississippi Valley. The cause of such persistent above-normal pressures in the sub-tropical belt is not yet known. The Pacific High cell was also much stronger and its average position at a higher latitude than normal. This situation tends to bring arctic air into the western states accompanied by a semi-permanent trough aloft, while at a distance of one-half wave length downwind the ridge aloft is found near the East Coast of the United States. This sets up a persistent southwesterly flow aloft over the Mississippi and Ohio Valleys-- a necessary condition for heavy rains in this region.

The major precipitation of the storm period fell in three main bursts, one on the 17th, one on the 21st, and the last on the 24th. These bursts were associated with frontal cyclones in various stages of their life histories. Although a small quantity of snow was on the ground at the beginning of the period in some localities, the amount did not materially add to the magnitude of the flood.

As the first rain burst commenced over the Ohio Valley, the following rather characteristic synoptic weather picture prevailed (figure 25). A Low of Pacific origin was situated in the western Plains with intensely cold air northwest of it, a cold anticyclone was moving off the New England Coast, and the semi-permanent Atlantic sub-tropical anticyclone extended westward into the Gulf of Mexico. The large-scale maps show in detail the surface weather situation in the eastern part of the country during the first burst (figure 28). The front between the tropical air and the cold air over the northeastern United States exhibits various contortions due in part to the effect of the mountains. Although the Low system seems complex in this case, at upper levels a simple southwesterly flow of moist air is evident over the eastern United States. An airplane sounding taken at Murfreesboro, Tenn., in the warm air current just before the first burst is included (figure 40). An outstanding feature of this sounding is the saturation of the air above the inversion at 935 mb. The temperatures in this layer are exceeded by only about 10% of the observations in January[13/], and since high temperatures are not always

accompained by high moisture charges, it may be inferred that the water-vapor content of the air was even more unusual.

After the rains of the 17th and 18th, an extension of an arctic High moved eastward along the northern border of the United States, while at the same time a second Pacific Low with its attendant upper-air trough was located in the mountain states on the 19th (figure 25). By morning of the 20th, while the front accompanying the Pacific Low lay near the longitude of El Paso, a rapidly deepening secondary wave cyclone had formed over Kansas (figure 26). By evening of the 20th this secondary Low was occluded and centered in northern Wisconsin. Moderate warm-front rains occurred over the Ohio Valley on the 20th with a heavy burst (the most intense of the January 1937 storm) due to the passage of the occluded front early on the 21st (figure 31). The Murfreesboro sounding for the morning of the 21st is shown in figure 40. Moisture values at this time were even higher than on the 17th in the critical 900-to 700-mb layer. Moreover, latent instability was present in this layer, a condition prevailing in most heavy rainstorms.

The cold front that extended from the occluded front became stationary on the 21st through Tennessee and Kentucky (figure 30). Almost continuous wave action along this front prevailed until the 23rd. A brief break in the rainfall over the Ohio Valley occurred during the morning of the 23rd (figure 32). This was due to a weak thrust of arctic air that temporarily shunted off the moist upper current to the south and east of the Ohio Valley.

On the 24th the polar front again moved northward at the instigation of still another Pacific Low (figure 27) and caused the third and last major rain burst over the Ohio Valley. The Murfreesboro sounding for January 24 (figure 40) was taken in the warm inflow air during this last rain burst of the 1937 storm. Compared with the previous soundings, somewhat drier conditions in the layers above 850 mb are apparent and probably account in part for the lighter rain observed in this last burst. But latent instability was present in some of the layers and moisture below the 850-mb level was still an extraordinarily high value. The track of this last Pacific Low of the storm period was north of the tracks of its two predecessors, having entered the United States near Williston, N. Dak., (figure 27). The effect, rain-wise, was similar to that in the storms with a more southerly track, but the subsequent air-mass movements were different, for the dry, cold air mass stopped the rain over the Ohio Valley on the morning of the 25th (figure 34).

The final front that swept cold, dry air over the eastern

United States did not penetrate beyond the middle of the Gulf of Mexico. This event may allow a quick resurgence of moisture into the Mississippi Valley if a rather deep trough should happen to be approaching the Mississippi Valley from the west. Records indicate that this outcome did not occur in the 1937 storm, but rather a very weak trough passed through the northern Plains and Great Lakes region on the 27th and 28th. Depending on the depth (intensity) of the incoming trough, heavy rain under favorable circumstances can begin in the Ohio Valley about 48 hours from the ending of the preceding heavy rainfall. The evidence for this statement proceeds from observations of many winter storms that regularly traverse this stormy region.

The representative 12-hour surface dewpoint for the storm is 66° F, while the maximum observed dewpoint in January at the same location is 68° F. This allows an increase of 10% in the rainfall values on the basis of surface moisture adjustment only.

Storm of March 24-25, 1904 (UMV 2-4)

The heavy rains of March 24-25, 1904, in the area of interest, which extends from northwestern Arkansas to southwestern Ohio, fell when an intense cold front moved into the area from the northwest. Thunderstorms occurred ahead of this front in tropical maritime air flowing northward from the Gulf of Mexico. A wave then developed in Oklahoma and moved rapidly northeastward along the front across the area of interest, causing heavy rains. Although no upper-air data are available, the warm air moving northward was presumably very moist in the lower levels and unstable.

For at least 10 days prior to this storm only light rains had been recorded in the area. On March 22 a deepening Low moved inland from the Pacific over northern California. This Low moved rapidly east-northeastward across the Rockies to Nebraska by 0700 CST of March 24 (figure 41). At that time the pressure distribution was such that tropical maritime air started moving northward from the Gulf of Mexico toward the Low center while cold Canadian air began to move rapidly southeastward in the rear of the Low east of the Continental Divide, causing it to become occluded by 0700 CST March 25 (figure 42). By then the center had advanced to just northwest of Lake Superior, and the cold front at that time extended from north of Lake Huron southwestward to about South Bend, Ind., and West Plains, Mo. thence westward between Tulsa and Oklahoma City, Okla., to about Amarillo, Tex. The strong temperature contrast between the two air masses is shown by the reports at 0700 CST March 25 (figure 44) from Cairo, Ill., and St. Louis, Mo. Cairo reported 68° F with a south wind and St. Louis 42° F with a north wind. The heavy rains in the area of interest began in northwestern Arkansas

in the six hours ending at 1800 CST, March 24, and advanced northeastward to southwestern Ohio by 0600 CST, March 25, (figure 46). These rains appear to have been principally thunderstorms in the warm air southeast of the cold front, although some rain fell behind the cold front as it advanced into the area.

A weak Low center formed on the cold front in western Oklahoma on the evening of March 24 and moved eastward along the front. The southeastward movement of the front was retarded as the Low moved along it. General heavy rains attended by thundershowers fell north of the front for several hundred miles ahead of the Low center, while heavy cold-front thundershowers occurred behind the Low center as the cold air resumed its southeastward movement.

By early morning of March 26 (figure 45) the Low center had passed to the northeast, and cold air had swept southeastward far enough to end the rain in the area of interest. The cold air advanced across the Gulf of Mexico and western Caribbean during the next few days, displacing the tropical maritime air at the surface. It was not until the morning of March 30 that warm moist air again appeared at the surface in the Gulf States.

The representative maximum 12-hour dewpoint for the storm has been computed as 62° F, located 300 miles south-southeast of the Willow Springs, Mo., rainfall center. The maximum 12-hour dewpoint in this area at this time of year is 72° F, allowing an upward adjustment of 63%.

The March 23-25, 1904 storm was preceded by a frontal rainstorm of ordinary intensity about 48 hours before. The quantity of moisture, however, was sufficient at that time to have allowed a major rainstorm to take place if the lifting mechanism had been more efficient. Moreover, the front that accompanied the rainstorm of March 21-22, 1904, did not pass into the Gulf of Mexico thus allowing the tropical air to remain over the Lower Mississippi Valley. Therefore under most favorable circumstances a storm of major proportions could occur at a minimum of one day prior to the beginning of UMV 2-4.

Storm of January 10-11, 1913 (LMV 1-9)

Heavy rainfall of the storm of January 10-11, 1913, extended through Arkansas and northwestern Kentucky. This storm occurred only 2 to 3 days after the end of another moderately heavy rainstorm of the Ohio Valley and was located just southeast of it. The highest rainfall amount was 7.5 inches and the isohyetal pattern is oriented approximately in an east-northeast west-southwest direction.

Temperatures throughout the month of January in the United States east of the Rocky Mountains were much above normal and the ground was unfrozen at the time of this rainstorm. There was no snow cover.

One of the synoptic features commonly noted with heavy rainstorms in the central and eastern United States is the presence of a more or less stationary high-pressure cell centered near Bermuda area with a ridge extending westward over the Gulf States. This situation existed prior to and during the January 10-11 storm as the Atlantic sub-tropical anticyclone was reinforced by a large high-pressure cell moving across the United States on January 8-9 (figure 47).

Following the High, which reached the East Coast on January 9, was a weak Low moving across the Rocky Mountains. This Low then intensified east of the mountains on the 10th and was followed by an outbreak of polar air. The rain began in the Ohio Valley well in advance of the frontal trough.

The predominant feature of this storm which probably accounts for more of the rainfall than any one factor is the depression first noticeable on the map of 0700 CST, January 10, over the northwestern Gulf of Mexico. This depression formed on the remnant of the front that moved into the Gulf and western Atlantic on January 8 and started moving northwestward around the anticyclone over the Southeastern States. By 1900 CST of the 10th, this depression had reached southern Arkansas, accounting for the first significant rainfall of the storm (figure 51). The detailed surface map for this time (figure 50) indicates precipitation due to convergence in the frontal trough and overrunning of warm moist tropical air to the north of the front.

The detailed surface map for 0700 CST, January 11, (figure 50) shows that the maritime tropical air at the surface had pushed northward and eastward to western Tennessee. Rainfall was still occurring in the frontal zone and had spread a considerable distance to the northeast, a favorable location for overrunning. During the 12 hours prior to this map time the polar air to the northwest had moved only a short distance southeastward, allowing time for the advection of warm moist air into the interior and prolonging the period of rainfall.

By 1900 CST, January 11, (figure 52) the polar front had advanced more rapidly southeastward and was located in the storm area. The isohyetal pattern for the 12 hours previous to this time (figure 51) shows one of the largest bursts of rainfall associated with frontal passage.

The surface map for 0700 CST, January 12, (figure 52) shows that the rainfall had ended in the area of this storm with the advancement southeastward of the polar high-pressure cell.

In summary it might be stressed that the principal causes of this storm were the advection of unstable, maritime tropical air well into the interior of the United States along with the slight depression moving inland from the Gulf of Mexico, and the lifting of this warm moist air by the much colder polar air on the 11th. Professor F. J. Walz, writing in the Monthly Weather Review for January 1913, mentions the occurrence of thunderstorms in Kentucky and Tennessee on the 11th, an indication of the instability in the maritime tropical air mass which undoubtedly contributed much toward the occurrence of the large volume of rainfall.

The storm of LMV 1-9 was preceded by a major rainstorm (OR 6-17) on January 6-8 with an interval of about two and one-half days separation between the significant rains. The front from OR 6-17 penetrated a little beyond mid-Gulf on January 9, thus making a minimum interval of about 2 days a possibility under most favorable conditions that a heavy rainstorm could precede LMV 1-9.

The 12-hour representative reduced dewpoint of LMV 1-9 was 63° F which allows a 28% upward adjustment in place of occurrence.

Storm of March 23-27, 1913 (OR 1-15)

In this storm, the major rain bursts were associated with a series of waves on a quasi-stationary front, the type generally considered to be the most important heavy-rain producer in the central United States. Isohyetal maps were prepared for the main bursts, which occurred between morning of the 24th and evening of the 25th.

Light rains two days before the storm (March 21) had left the ground wet enough so that the early period of intense rain saturated it. The resulting surface conditions were conducive to a large runoff.

Here, as in almost all flood-producing storms in the central United States, the pressure was much above normal over the Bermuda area. During the 4-day period, March 23-26, 1913, the pressure averaged about 1035 mb at Bermuda in contrast to a normal 1019 mb for this period. The warm air current brought into the southern United States by the Bermuda High was

characterized by dewpoints ranging as high as the upper 60's (°F) within about 3 F° of the maximum observed dewpoints for the area and season.

During the same time, a polar High centered in southern Canada on the morning of the 24th (figure 53) poured unseasonably cold air into the central Plains States. The average temperature at Havre, Mont., during the period of the storm was 34 F° below normal.

From detailed weather charts two lines of discontinuity were found to lie between the Bermuda High and the arctic High, one, the major polar front, extended southwestward from a cyclone center near Sault Ste. Marie, Mich., at 0700 CST, March 24, (figure 55) the other lay within the warm sector of the same cyclone. The second discontinuity line, the important one so far as the heavy rain was concerned, was probably formed originally as an instability line. The formation of instability lines in the warm sector of winter cyclones is a rather common occurrence in the central United States[14/].

Very rarely, however, does the instability line become oriented in such a way as to lie nearly at right angles to the incoming low-level southerly jet. The temperature contrast component of the differential advection in the instability-line case is supplied by the agency of rain cooling. A combination of factors, including cooling due to the melting snow at upper levels and the cold rain resulting at lower levels and local cooling by moist-adiabatic descent of air in the rain area are responsible for the temperature falls behind the instability line. After the cool air mass between the two discontinuities was formed, the southern edge then acted like a front, having had waves on it over a period of 36 hours. The temperature gradient thus interposed in the strong northward-moving air current formed a band of differential advection which was alternately augmented and diminished as waves moved along the discontinuity. This trigger mechanism, in conjunction with the probable latent instability of the warm air mass, resulted in heavy rains centered between the two lines of discontinuity. Although warm differential advection was noted as having existed behind the northern front, much less rain fell in that area. This is to be explained by the depletion of moisture by the huge convective system immediately upwind (south of this other-wise-favorable area for heavy rain).

Because of an almost perfect balance between the forces urging the cold air southward and the warm air northward (at the earth's surface), the zone of interaction remained nearly

stationary for 48 hours. Indeed, this balance of forces must be a necessary condition for the quasi-stationary frontal-type storm, for once mastery by one or the other of the two air masses is obtained a new set of rain-producing conditions must be set up to start the process again.

The conditions that followed the March 1913 storm were such that a high moisture charge could not quickly return to the central United States. The cold front swept the tropical air out of the entire Gulf of Mexico region. Under favorable circumstances the moisture necessary for flood-producing storms would take a minimum of 3 days to reestablish itself after the ending of a storm of the March 1913 type.

The 12-hour representative dewpoint for this storm is 67° F. The maximum possible dewpoint is 71° F, which allows an upward moisture adjustment of 21% in place.

Storm of January 26-31, 1916 (MR 2-13)

The heavy rainstorm of January 26-31, 1916, occurred after a period of above-average precipitation in the central United States. In Missouri and Illinois moderate rains prior to the storm (on the 20th,21st, and 22nd) saturated the soil and made conditions favorable for greater runoff. For the most part, snow melt did not add appreciably to the flood.

Figures 61, 62, and 64 are detailed weather maps of the storm area at 24-hr intervals, and figure 63 shows 12-hourly isohyetal maps in the area of greatest interest. In large measure the rains shown were responsible for this mid-winter flood.

Evolution of the pressure configuration that foreshadows and accompanies so many flood-producing rainstorms was very clear in this storm. A large High of partly Pacific and partly Arctic origin moved off the New England coast on the 24th, (figures 58 and 60 showing the large-scale weather maps). During the next few days the High remained at almost the same longitude, gradually settling southward, thus directing air northward into Texas, Louisiana, and areas to the north for many days. As in many cases preceding extensive rains in the central United States, the Atlantic High was transformed into a warm High (i.e., the anticyclonic circulation gradually extended higher and higher above the surface anticyclonic rotation). This, then, as in other major Mississippi Valley storms, allowed a warm southerly current to enter the Lower Mississippi Valley in depth--an important factor affecting the volume of precipitation.

The other major factor affecting this precipitation, the cold northern High, was of fresh arctic origin. The average temperature at Bismark, N. Dak., for the period January 26-31 was about 25 degrees below normal. Separating the two large Highs was a quasi-stationary front in a trough of low pressure extending on the 26th (figure 61) from central Wisconsin to the Texas Panhandle and thence westward to the Pacific.

In addition to the interaction of the two large Highs, the remnants of the two Pacific storms and their attendant upper-level troughs periodically intensified the southerly wind current. While opposing flows of air are a necessary condition for heavy rainfall, strong southerly winds with their constant replenishment of moisture are of utmost importance, since heavy rainfall cannot continue unless the supply of moisture is maintained. The troughs from the west caused cyclones to form between the Highs, giving rise to an intensification of the winds, and thus, the rainfall. One cyclone formation took place late on the 26th and during the 27th (figure 61), and another on the 30th (figure 64).

The detailed weather charts show that the front between the contrasting Highs was double in structure on the morning of the 26th, (figure 61). This kind of structure is fairly common in the case of cold air retreating northward (a warm front) and reflects a marked change in frontal slope above the northernmost surface frontal position. During the afternoon and evening of the 26th, a southward surge of cold air took place over central Oklahoma. A Low, formed on its forward edge, was situated on the Texas-Oklahoma border near Ardmore, Okla., at 1900 CST (not shown in figures). Very heavy rainfall was experienced ahead of this Low as it moved northeastward during the night (figure 63). On the 27th (figure 61) the wave that had formed in northern Texas was centered along the northern border of Illinois. An acceleration of the polar front produced by this wave gave rise to an instability line during the night of the 26th-27th. Moderate rains over central Missouri and Arkansas (figure 63) were the result of this instability line as it swept eastward and southeastward.

A lull in the rainfall took place during the daylight hours of the 27th as the arctic air pushed southward to extreme northwestern Louisiana. A wave soon formed on the front near Shreveport, La., followed by two more in rapid succession during the next 18 hours (figures 61 and 62). The heavy rain centered in southern Arkansas (figure 63) was associated with these waves,

A polar front retreated northward across the area of interest during the night of the 28th-29th, the rainfall became

light and consequently is not shown. On the morning of the 29th, however, a frontal system of Pacific origin was entering the area of interest from the west (figure 62). This front soon merged with the retreating polar front, thus reinforcing the tmeperature contrast. Under the influence of the Pacific system's upper-air trough, a series of waves formed along the combined front (figure 64), which settled slowly southward during the next 48 hours causing the last burst of the storm, illustrated in figure 63.

After the slowly moving cold front moved south of the area of interest, the very cold, dry air mass engulfed the Mississippi Valley and the rains stopped.

The 12-hour representative dewpoint for this storm was 63° F. The maximum dewpoint for the area is 68° F, allowing a 28% upward adjustment of moisture in the place of occurrence.

Storm of February 11-14, 1927 (LMV 4-6)

The weather had been dry for several months before the occurrence of this storm, otherwise the rain associated with it would have produced a much greater flood[15/]. There was no snow cover because temperatures had been distinctly warmer than normal for the whole winter, particularly in the South, and snowfall had been limited to northern districts of the country and mountain areas[16/].

Despite the southerly latitude of this storm, the large-scale synoptic features were very similar to those in more northerly storms. (The large-scale weather maps for this storm will be found in figures 65-66.) The Bermuda High, while not developed at the outset of this storm period, increased in intensity on the 12th and became a dominant influence over the Gulf of Mexico and the Southeastern States thereafter. The cold air mass extended somewhat further to the south than usual in this Gulf Coast storm. The temperature in the cold air mass, however, did not depart significantly from normal--in contrast to most winter storms reviewed in this report.

The main burst, that of the 13th, was associated with a warm-sector convective system (the eastern boundary is usually designated as an instability line). Frontal activity, however, contributed to the storm rainfall totals on all days of the storm. This type of rainfall situation is rather common in the Gulf States and accounts for many of the greatest flood-producing storms in that region.

The wave that caused this rainstorm formed on a front that moved into the northwestern Gulf of Mexico on February 7. The large polar anticyclone behind the front continued to move

slowly southeastward so that on February 9 it covered most of the United States and, now almost stationary, was oriented almost east-west across the northern Gulf.

By 0700 CST, February 12, (figure 67 shows details of the synoptic situation) the front had started to move northward and the wave which had begun to form on it was centered just south of Meridian, Miss. At the time of the map, rain had already started around the wave with thunderstorms in the warm sector. The Polar High, which by this time was modified considerably, had moved into the western Atlantic allowing northward movement of the wave. Meanwhile, another polar High was moving into the north-central part of the country. The isohyetal pattern for the 12 hours ending at 1000 CST, February 12, (figure 68) shows rainfall amounts up to 3.4 inches.

The movement of the cold High in this case was very rapid, its center moving from near 100° W longitude in southern Canada on the morning of the 12th (figure 65), to about 75° W longitude on the following morning. The speed of the cold center of action is of great importance, since the cold High provides the bulk of the temperature contrast in all storms; the faster the rate of eastward motion of the High, the less chance for southward penetration of the cold air mass. In consequence, the temperature contrast in this storm was less intense than in other winter storms, as was the rainfall. What was wanting in extreme temperature contrast was partially made up by a rather strong southerly wind jet. On the day of the maximum rain burst, the fortuitous interaction of a trough entering the area from the west and the sudden build-up of the Atlantic sub-tropical High caused a material strengthening of the warm-sector winds. This, in conjunction with the temperature gradient existing over Louisiana and southern Mississippi, gave rise to an area of warm differential advection, which in turn was able to release the latent instability of the incoming warm air mass.

By 0700 CST, February 13, (figure 69) the frontal wave had continued northward and thunderstorms were numerous in the maritime tropical air of the warm sector. Another indication of the squall-line type weather in this area was the occurrence of a small tornado in southern Louisiana. The heaviest rainfall occurred near this time, as indicated by the isohyetal pattern for the 12 hours ending at 1000 CST, February 13, (figure 68) in which up to 7.5 inches fell in south-central Louisiana.

Later on February 13 (figure 69), the wave occluded rapidly and moved northeastward, the rain coming to an end with the passage of the wave's cold front through the area early on February 14. The heavy rainfall of this storm totaled as much

as 10.55 inches at Clinton, La.

The 12-hour representative dewpoint for this storm was 66° F. The maximum dewpoint for this area is 72° F, allowing a 34% upward adjustment of moisture in the place of occurrence.

Storm of April 12-16, 1927 (LMV 4-8)

The heavy rainstorm of April 12-16, 1927,occurred over the area from eastern Texas to southern Illinois and from eastern Oklahoma to northeastern Mississippi. Amounts of rainfall up to approximately 12 inches occurred in north-central Arkansas and up to 9.6 inches in central Louisiana. Over much of this area the precipitation during March and the first part of April had also been far in excess of normal, so that ground moisture was high and rivers of the section were in flood during the greater part of the month; some had the highest stages ever known[17/]. Due to the moderate temperatures and heavy rains prior to this storm there was no snow cover at the time.

For several days prior to this rainstorm a large cyclone moved slowly southeastward across the Rocky Mountains combining with a Low near the Mexican border on April 9-10 (figures 70-71). During this time pressure was high over the eastern part of the country with a frontal trough separating the warm high ridge over the southeast from the polar anticyclone to the north. This same synoptic situation persisted for several days prior to the beginning of the rainfall with only a slight southeastward drift of the polar anticyclone.

The major synoptic feature associated with this storm was the Low centered over western Texas on April 12 ,(figure 74). While no upper-air data was available, slow-moving Lows of this kind are usually associated with a deep upper-air trough. Most of the rainfall was a result of thunderstorms, which were accompained by a number of hailstorms and tornadoes in advance of the Low[17/].

The first isohyetal pattern for the 12 hours ending 1500 CST, April 12, (figure 76) shows some small areas of rainfall due to thunderstorms in eastern Oklahoma and northwestern Arkansas and a more intense area of more than 4 inches in southeastern Tennessee. The details associated with the latter area cannot be determined from the available data, but it was in a pressure-fall area and in favorable location for convergence and overrunning of warm, moist, tropical air from the southwest.

The isohyetal pattern for the 12 hours ending 0300 CST, April 13, (figure 76) shows considerable rainfall from eastern

Oklahoma to central Tennessee and northward to southeastern Missouri. The surface data near this time (figure 75) indicates that numerous thunderstorms account for most of this precipitation. The late afternoon and evening increase of precipitation at the time of maximum heating indicates that the increase of instability due to low-level warming was an important factor. However, it is likely that the chief cause of the precipitation was convergence in the cyclonic flow of maritime tropical air northward in advance of the Low in Texas and with the warm frontal depression that had dissipated or merged with the cold front to the north by 0700 CST, April 13.

The isohyetal pattern ending 1500 CST, April 13, shows a continuation of heavy rain, mostly in northwestern Arkansas and eastern Oklahoma, a favorable location for squall lines in relation to the Low in northern Texas and the frontal system to the north.

The isohyetal pattern for the 12 hours ending 0300 CST, April 14, (figure 76) shows the pattern of rainfall still in the warm sector formed by the cold front approaching from the west and another front to the north. From an examination of the surface maps at approximately this time (figure 77) the rainfall seems to be largely a result of thunderstorms, indicating instability and strong convective activity. Windstorms, hail, and a few tornadoes occurred in eastern Texas as the front passed[17/]. The small area of heavy rain in eastern Texas also seems to be the result of local storms associated with the frontal passage.

The remaining isohyetal patterns of this storm (figure 78) appear to be very closely associated with the frontal passage from the west. The weather maps show most of the thunderstorm activity along this front which moved on across the area, bringing heavy bursts of precipitation, the isohyetal patterns progressing eastward with the front. The rainfall came to an end on April 16 as the front moved out of the area.

The end of the rainfall was brought about by the cessation of convergent flow in the frontal trough over the area of intrest and the advection of cooler and drier air over the area. The High following this front was very small, scarcely larger than the rain-cooled area usually following squall lines.

The fact that another rainstorm with amounts up to 9 inches occurred over Kansas and Missouri from April 7-9 (MR 3-11) and heavy rain occurred in Tennessee (OR 7-5) from April 9 to the beginning of the storm of April 12-16, (LMV 4-8), indicates that a previous storm could have occurred over the area of LMV 4-8 from April 7-12. The only requirement would be a slight shifting of the location of the frontal waves which caused

MR 3-11 and OR 7-5 over the area of LMV 4-8. It is evident, that, in effect, LMV 4-8 could have been extended in time for at least 5 days with no break in the rainfall over the same area in which it occurred.

The 12-hour representative reduced dewpoint observed in LMV 4-8 was 72° F. The maximum dewpoint to be expected in the area at that time of year is 76° F, permitting a 22% moisture adjustment in place.

Storm of April 17-21, 1927 (SW 2-4)

The major rain burst of this storm occurred in the warm sector of a quickly-developing wave cyclone (figure 81) rather than with a series of waves along a quasi-stationary front. The isohyetal map for the major burst is shown in figure 82.

As a result of previous heavy rains, ground moisture was high during this storm. However, there was no snow cover, due in part to these rains and in part to high temperatures prior to the storm.

The juxtaposition of large air masses of radically different properties is clearly evident in this storm. The average surface temperature for Bismark, N. Dak., for the 20th was 19 F° below normal. To the south, in Louisiana, Texas,and Mississippi, dewpoints were in the upper 60's and lower 70's, or within about 5 F° of the maximum observed values in the area for the time of year.

Despite the fact that most of the rain was not of frontal type, the large-scale circulation pattern exhibited the usual features found to accompany great frontal storms in the Mississippi Valley (figures 72-73). A large High was centered near Bermuda, directing a warm moist southerly current into the lower Mississippi Valley; a cold High straddled the Continental Divide over extreme southern Canada, with a fast-moving offshoot of the cold Canadian High centered in northern Iowa on the morning of the 20th. Between the two contrasting air masses lay a frontal zone extending from the Ohio Valley west-southwestward to the Texas Panhandle. South of this frontal zone in central and northern Arkansas (see figure 81 for detailed weather maps) an area of intense rainfall developed during the early morning of the 20th (figure 82). The southern boundary of this rain area had the characteristics of an instability line in that it was able to move southward against a strong southerly surface wind. Cooperative observer data made possible the exact placement of the instability line and the detailed delineation of the isothermal field in the storm. It may be noted that the temperature gradient was strongest in the

coldest air north of the front and weakest in the tropical air. It adopted an intermediate value over northern Arkansas. Over Arkansas, however, the air flow at the gradient level was strong from the south. Thus, in this critical region, the combination of a moderate temperature gradient with a strong wind at right angles to it gave relatively faster warming than any surrounding area (warm differential advection). This created a favored area for strong vertical velocities and, since the air was very moist, for heavy rain.

In this storm the main polar High invaded the Great Plains very quickly after the set-up for heavy rain was realized. As noted in chapter I, the factors producing heavy rain are also conducive to cyclone development. It is thought that if the relative heating extends in great depth, large pressure falls ensue, allowing a deep Low to form, thus bringing the heavy rain in a given area to an early end (deepening cyclones are generally not stationary). This concatenation of events apparently obtained in this storm, though no direct evidence is possible due to the absence of upper-air data. The ridge in the east finally gave way to the frontal passage on April 21 which brought an end to the precipitation in the area of interest.

The 12-hour representative dewpoint for this storm was 66° F. The maximum dewpoint for this area is 75° F, allowing a 55% upward moisture adjustment in the place of occurrence.

Storm of June 28-30, 1928 (OR 7-10)

The heavy rainstorm of June 28-30, 1928, occurred principally in Kentucky, Tennessee, and parts of Missouri. The largest amount of rainfall recorded was 10.16 inches at Clinton, Tenn. Most of the precipitation was the result of severe thunderstorms in moist tropical air that was moving northward and northeastward from the Gulf of Mexico.

June was a remarkably wet month over practically all parts of the country from the Rocky Mountains eastward, and the precipitation was rather uniformly distributed during the various portions of the month[18]. This indicates that soil moisture was relatively high.

As is frequent for the month of June, the movement of pressure patterns across the United States was rather sluggish. From June 23 to 26 (figure 83) an occluding wave cyclone moved from western Texas into Ontario. Following this cyclone a weak anticyclone of modified polar air traveled to the Atlantic Coast by June 27. In advance of this anticyclone was a weak cold front which on the 27th reached from the western Atlantic through the Gulf States and northwestward into a Low over the

Southwest. This weak front interferred very little with the ridge of high pressure which extended from the Atlantic subtropical anticyclone westward over the Gulf States while the High following it partially merged with the Atlantic subtropical anticyclone. This series of events started repeating itself early on June 28, as the Low in the Southwest started intensifying and moving northeastward, accounting for the first heavy burst of rainfall of this storm.

The isohyetal pattern for the 12 hours ending 1300 CST, June 28, (figure 87) shows a heavy burst of more than 4 inches in southwestern Missouri and more than 5 inches in western Kentucky. The detailed surface map for 0700 CST, June 28 (figure 85) shows a weak warm front moving northward across the area with thunderstorms occurring on both sides of the front. The weather pattern here indicates that most of the rainfall was due to thunderstorms caused by horizontal convergence of the moist, maritime tropical air moving northward over the area. An indication of the instability present in this northward-flowing air was the occurrence of two tornadoes on the afternoon of June 28 in southern Iowa just north of the heavy rainfall area.

The next isohyetal map, which is for the 12 hours ending 0100 CST, June 29 (figure 87), shows an increase of rainfall in northeastern Tennessee and eastern Kentucky as the warm-front trough advanced across the area as part of an open wave with a Low to the northwest from which a cold front extended southwestward. This system is illustrated by the surface map for 1900 EST, June 28, (figure 86). The cause of rainfall was still convergence in the warm-front trough as discussed above, with the addition of orographic lifting over the more mountainous terrain of northeastern Tennessee and eastern Kentucky. It should be pointed out that surface dewpoints in the maritime tropical air flowing northward were in the 70's, indicating a plentiful supply of moisture. At 0100 CST, June 29, two tornadic windstorms were reported near Nashville, Tenn., in this northward flowing current of moist tropical air along with the thunderstorms and heavy rainfall which occurred near this time.

The heaviest 12-hour burst of rainfall of the storm occurred during the period ending at 1300 CST, June 29, (figure 87), where 4 or 5 inches fell over parts of northeastern Tennessee and Kentucky. The detailed surface maps for 0700 and 1900 CST, June 29, (figures 86 and 88) show a cold front, with a large trough of maritime tropical air in advance of it, approaching the area during this time. Convergent flow in the trough in advance of the front and orographic lifting of the moist unstable air mass over the mountainous terrain seems to account for most of the rainfall.

The isohyetal pattern for the 12 hours ending 0100 CST,

June 30, (figure 87) shows a smaller amount of precipitation than the previous periods, and the surface maps show that it was more directly associated with the frontal passage over the area. The final isohyetal pattern for the 12 hours ending 1300 CST, June 30 (figure 89) shows only a small area of rainfall in southwestern Missouri as a result of thunderstorms in advance of a warm-front trough moving in from the southwest.

Very little upper-air data are available for this storm because of the early date of occurrence. However, the winds aloft over the eastern United States on June 28 were southerly up to about 1500 meters gradually shifting to southwesterly above this level. Upper-air humidities for June were well above normal upward through the 2000-meter level at Broken Arrow, Okla.,[19], the nearest recording station to the air current flowing over this area of interest.

In judging the minimum time interval likely between OR 7-10 and a preceding heavy rainstorm, the frontal movements as they occurred leading to OR 7-10 may be used as a guide. A cold front passed through the area of interest early on June 25, accompanied by moderate rainfall. The front subsequently moved to the Gulf Coast and returned northward, becoming an integral factor in the mechanism of OR 7-10. This rocking motion of a cold front followed by a warm front can occur somewhat more rapidly than in the case of OR 7-10. Under most favorable conditions it is probable that heavy rains could be expected from this combination of synoptic features with a minimum interval of two rainless days.

The 12-hour representative reduced dewpoint observed in OR 7-10 was 72° F. The maximum dewpoint to be expected in this area the same time of year is 78° F permitting a 41% moisture adjustment in place.

Storm of December 22-24, 1932 (SW 2-9)

The storm of December 22-24, 1932, produced rainfall amounts up to 8.4 inches. Isohyetal charts were constructed in 12-hourly increments covering the area from north-central Texas through Oklahoma and extreme northwestern Arkansas to southwestern Missouri. Detailed surface weather maps for intervals of 12 hours covering the storm area for December 21-24, inclusive, were also drawn. The storm is the first of those studied in this report for which fairly comprehensive upper-air charts are available[11].

A High that becomes stationary over the Atlantic Coast States with a ridge aloft extending westward along the Gulf States seems to be a prerequisite for large winter rainstorms over the southern Plains and the Ohio and Mississippi Valleys.

Another common feature of these storms is the formation or intensification of a surface cyclone in the Southwest or somewhere just east of the Rocky Mountains as an upper-level trough moves across the mountains and intensifies on the eastern slopes. All of these features were present in the storm of December 22-24, 1932.

The surface high-pressure cell, which covered most of the southern half of the nation on December 19 (figure 91) persisted over the Southeastern States, and circulation around this High resulted in the inflow of warm moist air into the southern Plains and Valley States. Along with the northward flow of air from the western Gulf was a depression, the remnant of an old polar front that had moved into the Gulf several days previously. The depression moved into eastern Texas on December 21 and decreased in intensity after moving inland. Nevertheless there was moderate precipitation associated with it in Louisiana and adjacent areas.

The remnants of an old Pacific occluded front had become about stationary from north-central Texas northeastward on December 21. The surface map for 0700 CST, December 22, (figure 94) shows that the depression from the Gulf had dissipated at the surface. About this time a most important development was the re-energizing of the old Pacific front by the influx of warm moist air during the 22nd. This not only increased the temperature gradient but also added the moisture and instability factors necessary for very heavy rainfall.

Most of the rainfall of this storm occurred on December 23, as shown by the isohyetal patterns ending at noon and midnight (figure 96). Rapid cyclogenesis over southern Texas and northern Mexico was associated with this rainfall. This surface cyclogenesis occurred as an upper-air trough, associated with another Pacific occluded front which entered the West Coast on December 20 (figure 91), approached the area from the west.

As the wave that developed on the front in the area of this storm on December 22 occluded and deepened, it moved northeastward, accounting in large measure for the northeast-southwest orientation of the isohyetal pattern. This is the usual direction of movement of these storms throughout this general area, with slight variations possible. One of the main reasons for this is the flow pattern associated with a persistent ridge over the Southeastern States, which plays a major role in the development of the storm by circulating warm moist air, usually maritime tropical, into the storm area.

The rainfall of this storm ended as the cyclone that produced it moved out of the area to the northeast.

The estimation of the minimum interval of time necessary between the beginning of SW 2-9 and the end of a preceding heavy rainstorm, preserving the meteorological factors that form an integral part of SW 2-9, would require, among other things, that the northern Gulf of Mexico be covered with air of polar origin. This is a necessary condition for the formation of the frontal wave that was the prelude to SW 2-9. A wave of this sort allows low-level moisture to penetrate to high levels, thus augmenting the total precipitable water of the inflow air. Frontal waves in this area usually require that the preceding front reach near the Yucatan Peninsula, thus necessitating a minimum of 3 days between heavy rains in the Oklahoma area.

The 12-hour representative reduced dewpoint observed in SW 2-9 was 64° F. The maximum dewpoint to be expected in this area is 71° F permitting a 41% moisture adjustment in place.

Storm of July 22-25, 1933 (LMV 2-26)

During the 4-day period ending on the evening of July 25, 1933, a tropical depression, the second one of the month traversing the western Gulf of Mexico, produced 21.30 inches of rain at Logansport, La., and 19.46 inches at Shreveport, La.

The tropical disturbance that caused this storm originated in the Caribbean Sea about a week prior to its entry into the United States. It crossed the Yucatan Peninsula on the 18th and started to recurve to the north in the western Gulf of Mexico on the 21st and 22nd (figure 98). The track of the depression as it affected the area of interest is shown on the last of the detailed weather maps (figure 105). At no time in its history did the storm reach hurricane intensity. Only winds up to 35 mph were noted as it crossed the Texas Coast about 70 miles southwest of Galveston. The forward speed of the storm was about 12 mph and its direction almost due north until the evening of the 23rd when it was centered near Tyler, Tex., (figure 101). After this time the storm rebounded sharply toward the southeast at about 4 mph. The change in direction was occasioned by the approach of a cold front behind which strong anticyclogenesis had taken place during the 24-hour period ending on the morning of July 23 (figure 101). A radical change in direction of a tropical storm or even a complete loop is not unknown, especially after the storm moves out of the tropical zone. Another characteristic of sharp recurvature is a slowing of the forward motion of the storm as a whole. This slowing tends to concentrate the rainfall instead of spreading it out over a large area and has been responsible for some of the heaviest rainfalls along the Gulf and Atlantic Coasts.

Light rains commenced over northern Louisiana during the daylight hours of July 22 as the cyclonic circulation about the tropical disturbance moved inland. Cloudy skies and east winds lowered temperatures about 10 degrees below normal in the area of interest shortly before and during the storm. Heavy rains were experienced along a short section of the coasts of Texas and Louisiana from early morning of the 22nd till about noon of the 23rd (figure 102). An examination of the detailed surface maps for this period (figures 100-101) reveals a strong onshore wind in the northeastern and eastern portions of the tropical Low. Warm surface differential advection is shown over southern Louisiana and adjacent Gulf waters by the concentration of solenoids (the areas formed by the intersections of the isobars with isotherms - the smaller the area, the more intense the vertical motion indicated). This strong solenoidal field arose because of (1) cool air over the continent as contrasted by higher temperatures over the Gulf of Mexico, and (2) superposition upon this temperature gradient of an increase in wind due to the pressure fall associated with the tropical depression. The detailed map for 1900 CST, July 23, (figure 101) shows the pressure gradient, and consequently the wind velocity, greatly diminished along the coast, and corresponding to the time of the slackening of rainfall in the area. An increase in low-level friction as a result of the air motion from the open water to land is thought to increase turbulence sufficiently in the lower layers to touch off the latent instability and thus deposit more rain than would normally fall were the coast not there.

Beginning on the evening of July 23, when the storm became almost stationary (figure 101), the rainfall increased in intensity, as judged by the rates recorded at Shreveport, La., and nearby areas to the east and south. The area of warm differential advection, as shown by the surface charts, exhibits, in general, a close correspondence with the associated heavy rain areas as the storm drifted southeastward.

During the 26th the storm began to drift northward again and the rain decreased in intensity. This was due to a slow seepage of slightly cooler and drier air into the cyclonic circulation. The storm disappeared entirely on the 27th in the interior of the United States.

The 12-hour representative dewpoint for the storm was 76° F. The maximum dewpoint for the area is 78° F, allowing a 10% upward adjustment of moisture in the place of occurrence.

Storm of January 19-20, 1935 (LMV 1-19)

The heavy rains of January 19-20, 1935, extended from north northeastern Texas to central Kentucky and fell principally from a tongue of tropical maritime air flowing northeastward from the Gulf of Mexico.

The air masses involved in the storm were polar Canadian air moving slowly eastward over the eastern United States, tropical maritime air flowing northeastward from the Gulf of Mexico, and arctic air pushing southeastward over the Plains States east of the Continental Divide.

Moderate amounts of precipitation fell in Kentucky and Tennessee on January 15-16. Otherwise, precipitation in the area was light and scattered between January 10 and 18.

On the morning of January 18 (figure 106), polar Canadian air was circulating clockwise around an eastward-moving ridge of high pressure. A surface front between this polar air and tropical Gulf air extended from about San Antonio, Tex., to Brunswick, Ga. Lifting of the warm moist air as it flowed northeastward over the cold air to the north was causing light rain for about 350 miles north of the front, west of the 85th meridian.

The front moved southward over northern Florida and northward over Texas, Louisiana, and Mississippi during the next 12 hours, and by the evening of January 18 light to moderate rain had fallen over most of the area of interest.

The warm tongue of air continued to advance northeastward and reached the vicinity of Memphis, Tenn., by morning of January 19. Rain continued north of the front as the tropical Gulf air continued to flow northeastward, and moderate amounts were recorded in the area of interest at this time (figure 110).

During the next 24 hours, from the morning of the 19th to morning of the 20th, the eastern portion of the warm front moved northward in Alabama and inland across the coast of Georgia and the Carolinas while the western portion of the front did not move much at the surface. The heaviest precipitation during this same period fell north of the front in the area of interest (figure 112). The rain was fairly steady except in thundershowers north of the front in Texas. South of the front scattered light showers fell except in the vicinity of Shreveport, La., where a moderate early morning shower was apparently due to local steepening of the lapse rate.

By 0700 CST, January 20, (figure 111) a Low center had formed on the front in north-central Texas. This center moved to northeastern Louisiana and southeastern Arkansas and the surface warm tongue advanced northward into western Kentucky by evening of the 20th. The western portion of the front at 1900 CST, January 20, extended from about Cairo, Ill., to Galveston, Tex. During the day of the 20th the heaviest precipitation fell northeast of the advancing warm front near Nashville, Tenn., within the warm air northeast of the Low center in western Tennessee and northern Mississippi, and in southern and eastern Arkansas, northwestern Louisiana, and southeastern Texas behind the cold front, moving southeastward, southwest of the Low center.

The advancing edge of a modified arctic air mass at 1900 CST, January 20, extended from about Milwaukee, Wis., to San Antonio, Tex., and was advancing rapidly southeastward about 125 miles behind the primary front. The modified polar air between these two fronts was very moist due to the precipitation falling through it from the overlying tropical Gulf air. Consequently, when the modified arctic air approaching from the northwest lifted this air, a band of precipitation about 175 miles wide developed behind the arctic front and moderate to heavy amounts of rain, sleet, and snow were deposited in the area of interest after the front passed. Thundershowers were reported from some stations in this precipitation band.

By morning of January 21 (figure 113), the Low center had moved northeastward to Ohio, and the forward edge of the modified arctic air had advanced to a line from Ft. Wayne, Ind., to Nashville, Tenn., to Lake Charles, La. Precipitation continued in the northeastern quarter of the area of interest where nearly an inch fell at some stations during the next 24 hours (figure 112). Elsewhere in the area only light amounts were reported.

Another Low center formed in the Gulf south of Louisiana on the front between the tropical maritime air and the modified polar Canadian air by 1700 CST, January 21, (figure 113) and moved northeastward along the front. This Low drew the modified arctic air far to the south into the Gulf of Mexico and northern Caribbean Sea, displacing the tropical maritime air at the surface in the course of the next few days. Tropical maritime air did not reappear at any Gulf station at the surface until about January 30.

Since tropical air covered the entire Gulf of Mexico and adjacent coastal areas of the United States from January 15-21, inclusive, a heavy rainstorm was possible a very short time before LMV 1-19, so far as moisture was concerned. The frontal patterns were such that a release of this moisture charge would

have been possible in a minimum of one and a half days prior to the beginning of LMV 1-19.

The 12-hour representative dewpoint for LMV 1-19 was 63° F. The maximum possible dewpoint for the area is 69° F making possible a 35% upward adjustment of moisture in place.

Storm of June 13-18, 1935 (SW 2-13)

The heavy precipitation of June 13-18, 1935, in the area of interest extending from northeastern Texas across southeastern Oklahoma to northeastern Arkansas, fell during a prolonged period of precipitation which began in Texas about the 9th of June and covered most of the United States to the northeast and east during the ensuing two weeks. Figures 114-116 are the large-scale weather maps and figures 117-118, 120-122, and 124, the detailed weather maps for this storm.

The last heavy rain in the area of interest before the storm period fell on the 7th. On the afternoon of June 11 a weak trough of low pressure, reaching from the surface (figure 114) to above 10,000 feet, extended northward and southeastward from the vicinity of El Paso, Tex., slanting upward to the east. This trough gradually deepened while moving slowly eastward during the next few days.

Ahead of the trough, a broad deep current of maritime tropical air began to flow northward across the western Gulf Coast. This air had apparently had a long trajectory over the Gulf of Mexico and Caribbean Sea and had an unstable lapse rate. Much moisture had been carried to mid-troposphere levels by a tropical disturbance which passed inland over the southwestern Mexican Coast on June 12. Winds-aloft observations from Mexico indicate that it is probable that the air involved in this decadent tropical storm traveled northward along the Gulf Coast of Mexico and into Texas.

Between June 12 and 17, 1935, the maximum 24-hour June rainfall of record occurred at 23 precipitation stations located in Texas, Oklahoma, and Arkansas, having 10 years or more of record (through 1949).

Precipitation in the area of interest (figures 119 and 123) began as scattered light to moderate rains and thunderstorms in the moist tropical air flow. A combination of instability and lifting due to the gentle upslope from the Gulf was responsible for the spotty rains through the 14th. Strong daytime heating over Texas at this time of year was probably a contributing factor.

About midnight of the 14th-15th a great increase in the intensity of precipitation took place (figure 119). This was associated with a pressure-fall area that arrived from the south, embedded in the moist tropical flow. A reflection of this is shown on the detailed surface map for 0700 CST of June 15 (figure 120) in the weak Low center near Abilene, Tex. An extrapolation of the pressure-fall area backward through Mexico (approximately along the 100th meridian) indicates the possibility that this pressure-fall area was a remnant of the tropical storm that hit the Pacific Coast of Mexico on the 12th. A pressure wave of this sort traversing a mountain barrier and reuniting with a moist current on the other side is not common but, on the other hand, not unknown.

After the pressure wave passed northward out of the area of interest, rainfall immediately slackened (figure 123).

Falling pressure north and northwest of the area, caused by the approach of a frontal trough, induced a gradual wind shift at the gradient level from southerly on the morning of June 15 to southwesterly on the morning of the 16th over northern Texas, Oklahoma, and Arkansas. This shift occasioned a rainfall increase again during the morning of the 16th (figure 123), centered in Arkansas. The rainfall was confined, in general, to those regions where southwesterly wind flow encountered a more emphatic upslope. The rainfall, and wind flow causing it, continued until midday on the 17th.

The frontal trough, which had gradually been approaching the area of interest from the northwest, was responsible for the last burst of the storm (figure 123). Specifically, an instability line was formed ahead of the cold front in the trough during the afternoon of the 17th (see figure 122). A good indication of the different synoptic cause of this last burst is the general northeast-southwest orientation of the isohyets in contrast to the west-northwest to east-southeast orientation of the previous burst when orography had been a major factor.

The 12-hour representative dewpoint for the storm was 74° F. The maximum dewpoint for the area is 78° F, allowing a 21% upward adjustment of moisture in the place of occurrence.

Storm of February 14-19, 1938 (SW 2-17)

The heavy rainstorm of February 14-19, 1938, was centered in Arkansas and eastern Oklahoma, but large amounts of rainfall also fell in parts of bordering states. Up to 11 inches of rain fell at the center and considerable flooding resulted. Isohyetal maps for periods of 6 hours each have been constructed for the entire storm (figures 128, 130, 132, 134 and 136)

along with 12-hour detailed surface maps (figures 127, 129, 131, 133, 135, and 137) covering the storm area. Since this storm occurred before the rapid expansion of the upper-air observing network about 1940, detailed upper-air charts cannot be constructed. However, the general state of the atmosphere associated with this storm can be ascertained from what data are available.

The meterological events which led to this storm started early in February. An extension of the Pacific subtropical high-pressure cell over the Southwestern States on February 4-5 separated from the Pacific High and started moving eastward. On February 6-7 this high-pressure cell was reinforced by a polar High from Canada moving down through the northern Plains States. The combined high-pressure cell covered all of the eastern United States on February 8 and in the southern part extended as a high-pressure ridge westward through Texas. While the northern part of this High gave way to passing cyclones and polar Highs during the next week, the southern part, which extended westward through the Gulf States, persisted as an extension of the Atlantic subtropical high-pressure cell throughout the period of this storm. The residuum of this stationary high-pressure cell lay east-west from the western Atlantic through the Gulf States from February 9 through the storm period. This caused continuous flow of maritime tropical air across the Gulf of Mexico and into the southern half of the nation east of the Rocky Mountains.

A huge outbreak of polar continental air from Canada pushed as far southward as northern Texas and Arkansas on the 14th (figure 125) and became almost stationary. This High was oriented in a west-northwest to east-southeast direction on the 15th and 16th (figures 125 and 126), which in large measure was responsible for the rain falling as far west as it did. While there were some showers as the cold front separating this air mass from the maritime tropical air pushed southward, the heaviest rainfall did not start until the front became quasi-stationary. It will be shown below how the heaviest bursts of rainfall resulted from waves occurring along this front.

The first extremely heavy burst of rainfall with amounts up to 3 inches, occurred in Oklahoma after the surface cold front had become quasi-stationary in northeastern Texas. The surface map for 1900 CST on February 14 (figure 127) shows a slight wave on the front in northeastern Texas with a trough extending northward through eastern Oklahoma. Winds-aloft observations near this time show southerly winds from about 4000 feet through 10,000 feet over this area. The surface trough, therefore, appears to be the reflection at the surface of the advection of warm air of less density aloft. Convergence in this trough near the ground and overrunning of warm moist air aloft seem to account for the heavy downpour at this time

(figure 128). This condition persisted throughout the next 12 hours. After this the trough filled and a new surge of polar air began to push southward just east of the Rocky Mountains, approaching the storm area, and the rainfall amounts diminished (figures 129 and 130).

The high-pressure ridge accompanying this new surge of cold air had pushed southward into north Texas by 0700 CST of the 16th (figure 131), intensifying the trough over Oklahoma between this High and the one remaining to the northeast. The situation produced frontogenesis in the trough and more heavy bursts of precipitation (figure 132). The rainfall patterns of the 16th were oriented more or less along the frontal trough and progressed slowly southward and eastward along with the front. The movement of the colder air southeastward again seemed to cause the frontal trough to decrease in extent and the precipitation to diminish, but still rather heavy amounts continued to occur along the frontal zone.

The front again became about stationary over Arkansas late on the 17th (figure 133) and a wave began to form along the front at this locality. An increase in precipitation resulted, with isohyetal patterns oriented from southwest to northeast across Arkansas (figure 134). After this, the wave cyclone occluded rapidly and moved northeastward followed by the large high-pressure cell (figures 135 and 137) which brought an end to the precipitation in the storm area (figure 136).

There are enough upper-air data available for this storm to indicate the presence of a pronounced trough aloft which approached the area of rainfall slowly from the west. The presence of a deep trough at upper levels has been observed in association with many of the heavy rainfall situations. As is usually observed, the rainfall occurred under the eastward half of the mid-tropospheric trough.

The most obvious cause of precipitation in this storm was the lifting of the warm moist air with a recent trajectory over the Gulf of Mexico by the colder air mass to the north. This lifting or overrunning also resulted in the release of latent instability which appears to have been present in the maritime tropical air mass. Surface dewpoints in this air mass were generally in the 60's (°F) and moisture values aloft also indicate that there was a sufficient moisture charge for heavy rainfall, given the necessary physical processes to release it.

It can be noticed from several of the surface charts and isohyetal patterns that there was considerable rainfall in the warm air ahead of the cold front. This precipitation might be caused partially by the release of latent instability due to flow over the gradually rising terrain north and west of the Gulf Coast.

In estimating the minimum time interval that would be required between a severe Ohio Valley rainstorm followed by a storm similar to SW 2-17 in place, the frontal positions as they existed just prior to SW 2-17 must be considered an important factor. On February 13 a small Low moved through the Great Lakes region causing 3 to 4 inches of rain. The cold front accompanying this Low crossed the Ohio Valley during the afternoon and evening of the 13th attended by light precipitation. While heavier precipitation could have accompanied this frontal passage, it would require a deeper trough aloft. These deep troughs move slowly and it would take about 3 days and usually longer for one to follow another.

The 12-hour representative dewpoint for SW 2-17 was 64° F. The maximum possible dewpoint for the area is 70° F allowing a 35% upward adjustment of moisture.

Storm of May 8-10, 1943 (SW 2-20)

The Warner, Oklahoma storm of May 8-10, 1943 in which the title station measured 25 inches of rain in 48 hours, was the first of two exceptionally large storms that occurred within a remarkably short interval of time. The Mounds, Oklahoma storm, the second of the two, formed in conjunction with the very next front that entered the Mississippi Valley after the front associated with the Warner storm had passed into the Atlantic and Gulf of Mexico.

On May 6 the precursory signs of a favorable pressure and temperature condition for heavy rainfall could be observed. The weather map of that date (figure 138) shows a High off the East Coast, with a very strong southerly jet of tropical air developing in the Texas-Louisiana region. At the same time a large supply of polar air was entering the country from Canada. During the next two days there was a gradual migration of the polar air southward to the Texas-Arkansas area and into the strong southerly jet. The pressure was 5 mb to 7 mb above normal in Florida during the period of heavy rain. Above-normal pressure over the Florida Peninsula and to the east seems to be a necessary condition for an extended period of heavy rain in the Mississippi Valley. Detailed weather maps of the storm area from 1830 CST, May 8, to 0630 CST, May 10, (figures 140 and 142) were constructed. Broadly speaking, a series of stable waves followed by a deepening unstable wave characterized the weather maps for the Warner rainstorm. The rain at Warner was of the frontal thunderstorm type with the heaviest downpour occurring during the early hours of May 9.

At 1830 CST, May 8, (figure 140) the polar front extended from Cape Cod southwestward through the Ohio River Valley into a minor stable frontal wave in northeastern Arkansas, thence to a large nearly-stationary frontal wave near Dallas, Tex., and on to a low-pressure area in New Mexico. This new Mexican Low,

with its associated trough aloft, increased the low-level southerly wind jet over the Texas-Oklahoma area. To the north of the frontal zone an elongated, double-centered, high-pressure area stretched from the Great Lakes to the Rocky Mountains, with the main center located over northern Minnesota. The edge of this cold air dome supplied the temperature gradient, while the southerly jet associated with the eastward moving trough aloft supplied the air motion to set up a field of intense differential advection in the Oklahoma area on the 8th, 9th, and 10th (figure 145).

The pressure gradient to the west side of the Bermuda High was concentrated along the western Gulf Coast and provided the moisture supply to the trough in which the front lay. During the 12 to 24 hours previous to the heavy rain at Warner, rising surface pressures were experienced in the Mississippi Valley. The resulting filling of the trough to the east increased the pressure gradient and aided in setting up the warm-air advection in eastern Oklahoma.

During the afternoon of May 8, as the rain was starting (figure 141), the temperature difference at the ground between the center of heaviest rain and the warm side of the front 100 miles to the southeast was 30 F°. This gradient was abetted by oppositely directed surface winds converging at the front. An area of falling surface pressure was located over the storm center and coincided vertically with the center of strongest warm-air advection at 10,000 feet.

Differential advection computed for 3 observations at the 5000-ft level indicated warm advection over eastern Oklahoma throughout the storm period and a maximum during the period of heaviest rainfall. However, the value over the area of heaviest rain was exceeded in intensity by an area to the northeast and one to the southwest a few hundred miles along the front.

Coupled with the warm differential advection in the lower levels, 12-hour temperature-change charts for 10,000 feet indicate a maximum cooling aloft over the storm area during the early morning hours of May 9 when the heaviest rainfall was occurring. During the 12 hours ending 1100 CST, May 9, a 4 C° cooling was experienced at 10,000 feet, while in the same period a 4-6 C° low-level warming took place in eastern Oklahoma. The resulting instability, plus the effects of the frontal surface itself, were further factors contributing to the intense downpour during the early morning hours of May 9.

The front that brought cold dry air over the heavy rain area proceeded into the Gulf of Mexico and stalled (and frontolyzed) in the region of the Yucatan Peninsula. This would allow a resurgence of moist air into the central United States in about 3 days at a minimum. The observed time interval between the last significant rainfall in the Warner storm (SW 2-20) and the first significant rain of the Mounds storm (SW 2-21) was 3 1/2 days.

The 12-hour representative reduced dewpoint observed in SW 2-20 was 70° F and the maximum possible for the area and time of year is 76° F. This permits an upward moisture adjustment in place of 34%.

Storm of May 16-19, 1943 (SW 2-21)

The storm of May 16-19, 1943, in which up to more than 17 inches of rainfall occurred, extended from north-central Oklahoma northeastward to northwestern Ohio. The isohyetal patterns for periods of 6 hours have been plotted for this storm (figures 151 and 153). Detailed surface maps covering the period of the storm were also constructed (figures 149, 150, and 152).

The broad-scale pressure patterns of this storm are somewhat similar to those of January 1937 and other winter-time storms. The patterns consist of a stationary high pressure ridge over the Southeastern States and a quasi-stationary front extending northeastward from a low pressure area in western Texas.

The ridge over the Southeastern States had existed for several days prior to this storm and persisted throughout the period of rainfall (figures 146-148). The presence of this ridge appears to be common to most heavy rainfall storms in the central United States and plays a major role in their occurrence. It not only circulates warm moist air, usually maritime tropical, into the central part of the country, but by remaining stationary, it continues this flow and blocks the eastward movement of other systems. In the May 16-19, 1943 storm, the heavy rainfall occurred in the stationary frontal trough just to the northwest of the sub-tropical ridge over the southeast.

Another very important feature of the storm was the deep upper-air trough over the western United States. This trough moved very slowly eastward during the storm. These deep slow-moving upper-air troughs are associated with almost all winter-time heavy rainfall situations in the central part of the country.

A cyclone formed on May 15 in the southwest just east of the Rocky Mountains (figure 146). This cyclone had moved northeastward to Wisconsin at 0630 CST on May 16 (figure 149). The cold air moving southward on the western side of this cyclone formed the stationary front with the maritime tropical air moving northward from the Gulf. This front persisted throughout the period of heavy rainfall. The cyclone over Wisconsin on May 16 moved on into Canada and a large high-pressure cell of maritime polar air moved across the Rocky Mountains and southward into the southern Plains States.

The isohyetal patterns and detailed surface maps show that the rainfall started as showers and thunderstorms along the front late on May 16 after it became stationary and moved slightly northward. The first of this rainfall of importance was for the 6 hours ending at 2300 CST, May 16, (figure 151) when more than 4 inches fell over a small area between Oklahoma City and Tulsa. This burst of precipitation was the result of thunderstorms which occurred as the front moved northward over the area.

One of the heaviest bursts of precipitation is shown by the isohyetal pattern for the 6 hours ending at 0500 CST, May 17, with the largest amount in northeast Oklahoma. While the front remained in this vicinity, the unusually heavy rainfall of more than 6 inches in as many hours seems to require more of an explanation than just frontal lifting. The front lay in an inverted V-shaped trough extending from a small cyclone which developed in southeastern Colorado on the 16th and moved to the Texas Panhandle area. The 5000-ft chart shows a large cyclonic curvature of the streamlines in the area which is just far enough east to allow a continuous inflow of moist tropical air from the Gulf. The occurrence of thunderstorms on both sides of the front indicate convergence in the moist unstable air within this area of cyclonic curvature of streamlines. The flow here is also toward higher elevations making a further contribution to the vertical motion which releases the instability. The more nearly south-to-north flow of air at lower elevations accompanied by advection of higher temperatures insured a supply of moist unstable air into the area. The northern part of this isohyetal pattern, an inspection of the associated surface map reveals, seems to be more nearly the result of frontal lifting.

The next two isohyetal maps for the 6-hour periods ending at 1100 CST and 1700 CST on the 17th show an increase in rainfall northeastward along the front simultaneously with the advection of warmer temperatures into the area as shown by the 5000-ft chart.

The isohyetal pattern for the 6 hours ending 2300 CST, May 17, (figure 151) shows up to 6.6 inches of precipitation near Joplin, Mo. This extremely heavy burst of rainfall was the result of severe thunderstorms as a surge of cooler air pushed into the area, as examination of the detailed surface maps show (figure 150). The southeastward push of the cooler air resulted in a wave on the front which remained about stationary in the area with only a slight northeastward movement throughout the remainder of the period of the storm.

The isohyetal patterns for 0500 CST and 1100 CST, May 18, (figure 153) show a continuation of the rainfall but with lesser intensities. This decrease in intensity might be due partially to the decrease of convective activity during the night hours. Also, the wave that formed in northeastern Oklahoma the day before moved northeastward and weakened. The fact that only light amounts of rainfall occurred during the 6 hours ending at 1700 CST, May 18, was a result of the end of wave activity and only a slight trough along the front.

Later on the 18th another wave formed on the front in north-central Texas and moved northeastward causing the bursts of rainfall shown by the isohyetal patterns for 2300 CST, May 18, and 0500 CST on May 19. As the wave moved northeastward, the anticyclone, which had been about stationary over the Plains States for several days, intensified and moved southeastward (figure 152), bringing an end to the rainfall in the storm area at about noon on May 19.

The temperature difference between the two air masses involved in this storm were significantly strong. However, it differed from the major midwinter storms in that the cold air mass was maritime polar air coming in from the Pacific with more moderate temperatures. The maritime tropical air mass to the south was somewhat warmer than that of the midwinter storms with surface dewpoints in the 60's and low 70's, furnishing a large supply of moisture.

The 12-hour representative dewpoint of SW 2-21 is 71° F. The maximum possible 12-hour reduced dewpoint is 76° F, which permits a moisture adjustment of 28% in place.

For the next few days, following the cessation of rainfall, the front gradually moved southeastward to the Gulf Coast and the anticyclone following it intensified and, by May 22, covered most of the country east of the Rocky Mountains (figure 148). It seems reasonable to conclude that another major rainstorm could have developed as this High reached the eastern seaboard or 3 days after the end of the heavy rainfall of SW 2-21. The tropical air was in a position to make a rapid

reentry into the Mississippi Valley if a deep trough aloft had entered the Rocky Mountain area. This, however, did not happen following SW 2-21, so no major rainfall ensued at that time.

Storm of June 22, 1947 (MR 8-20)

The precipitation for June 1947 was above normal throughout a wide area of the country. Parts of Iowa, Missouri, Kansas, and Nebraska received about 4 to 8 inches more than normal. The high June 1947 rainfall, however, differed from other high rainfall months in that the precipitation originated from a series of small storms spread throughout the month rather than from a single intense 3- or 4-day storm period.

A previous study by the Hydrometeorological Section[20/] pointed out that a stronger-than-usual northward flow of Gulf air persisted throughout the month, although the moistness of the air remained approximately normal in the lower levels. The study also mentioned the unusual number of cold-air outbreaks over the north-central United States while a positive temperature departure existed in Texas. This gave rise to a stronger-than-normal north-south temperature gradient. The strong steady flow of air across the isotherms over the Kansas-Missouri region constituted a remarkably persistent area of warm differential temperature advection. Since this flow consists of moist tropical maritime air at this time of year, the differential advection resulted in heavy average rainfall over Iowa, Missouri, Kansas, and Nebraska.

This study will concern itself with the rainfall of one afternoon and evening, that of June 22. While this period contained an unusual small-area storm, the general rainfall in the central Plains States was typical of several storms of that June. Detailed synoptic weather maps, upper-air charts, and an analysis of stability conditions for the storm of June 22 will be found in the Monthly Weather Review[21/]. Large-scale weather charts for the period June 17-24 are shown in figures 154 and 155 of this report, while figure 156 illustrates the rainfall.

The large-scale weather patterns at the time of this storm were similar to those of the winter and early spring storms. Pressure was very high for the season along the East Coast, while the trough in the Midwest was much below normal. The pressure difference between the Atlantic Coast and western Kansas was about 25 mb, in contrast to a normal difference of about 5 mb. The surface moisture in the tropical air flow was also unusually high[21/].

Figure 157 shows the results of a study of differential temperature advection associated with the burst of rain on the

afternoon and evening of June 22. The details of computing differential temperature advection are essentially as set forth in the Monthly Weather Review[22/]. A short account of the significance of differential temperature advection will be found in chapter I of this report, its theoretical basis having been developed by Gilman[23/].

First, it may be noted that almost all of the heavy rainfall occurred within the area encompassed by the 12° C dewpoint line at the 850-mb level. Secondly, within this area, two other factors, warm differential advection and latent instability, outline the heavy rainfall region with comparative precision. The stippled area represents the region where the three factors coincided. This area may be compared directly to the observed rainfall in figure 156.

The duration of this particular rainfall burst was short-lived, as were most others throughout the month. An influx of dry, cool air from the northwest and west, together with a filling of the pressure trough, brought this rainfall to an end.

The 12-hour representative dewpoint for the storm was 75° F. The maximum dewpoint for the area is 78° F, allowing a 16% upward adjustment of moisture in the place of occurrence.

Storm of January 3-7, 1950

The area of heavy rainfall of this storm was at first oriented northeast-southwest from Lake Erie to northeastern Texas, with later displacement southeastward.

During the last few days of 1949, a large polar anticyclone slowly moved southeastward over the United States east of the Rocky Mountains and with considerable warming from below became a somewhat modified continental polar air mass as its center reached the Atlantic Coast on January 1 (figure 158). Upon reaching the Atlantic Coast and Gulf of Mexico, the surface temperatures and dewpoints in the western part of this anticyclone increased rapidly until by January 2, 1950, the air over the Gulf States had maritime tropical characteristics.

While the high pressure persisted over the Eastern States at the surface the first two days of January, a Low moved very slowly across the northern Rocky Mountains and extremely cold air from Canada poured southeastward into the northern Rockies and northern Plains States. By 0630 CST on January 3 (figure 160) the Low had moved eastward to the Great Lakes and a cold front extended from it into Oklahoma and northwestward to the Rocky Mountains. Until this time only light amounts of rainfall had occurred in the northward flow of maritime tropical air in

advance of the front.

The upper-level flow pattern of this storm resembled, to a very great extent, that of other heavy rainfall situations in the same general area, consisting of a deep trough over the western United States and a ridge over the Eastern States. This represents a reversal of the normal January circulation pattern in the United States[24/]. Klein[25/] points out that in good agreement with numerous studies the southerly flow in advance of a deep trough aloft is intimately associated with heavy precipitation and that"these findings can be attributed to the horizontal convergence, upward vertical motion, abundant moisture, and convective instability which characterize southerly flow from the Gulf of Mexico."

The isohyetal pattern for the 6 hours ending 1500 CST, January 3, (figure 162) shows the first major burst of rainfall of this storm. The rainfall as far northward as Farmington, Mo., (about 50 miles south of St. Louis) was all in the cold air at this time, indicating no rainfall until the frontal passage. However, in parts of Ohio, Indiana, and Illinois the rainfall extended ahead of the front due to an instability line in a trough ahead of the front. While there is no one generally-accepted theory explaining the mechanism of instability lines, their location is usually in a warm-air trough ahead of a cold front or in the warm sector of a cyclone[26/].

The isohyetal pattern for the 6 hours ending 2100 CST, January 3, (figure 162) is very similar to the preceding one and is located slightly southeast of it. The rainfall here seems to be due to the same causes as above. The surface map near the end of this period (figure 160) showed a small wave which had formed in northern Arkansas. A thunderstorm was in progress at Westplains, Miss., just north of this Low.

The isohyetal pattern for the 6 hours ending 0300 CST, January 4, (figure 163) covers a somewhat broader area than the previous 6-hourly periods, with a slight shifting southward of the largest amounts. The broader area of the rainfall seems to be due to the lag of the trough aloft behind the surface cold front, while the displacement southward of the rainfall pattern is probably associated with development of the small Low near northeastern Arkansas.

The isohyetal pattern for the 6 hours ending 0900 CST, January 4, (figure 163) shows a smaller amount of rainfall due to the fact that the cold front was past the area at the surface and colder drier air was becoming deeper. For the 12 hours following this time the rainfall was very light because of the continued progress of the cold air over the area.

From an examination of the surface maps alone, it is difficult to determine why there was so little rain in the area of this storm for the 12 hours ending 2100 CST, January 4, (figure 164) and its beginning again for the 6-hour period ending 0300 CST, January 5, (figure 165). The 850-mb and the 700-mb charts, however, reveal the approach from the west of a trough near to the area of the isohyetal pattern ending 0300 CST, January 5, and a more southerly flow of air with higher dewpoints over the area of rainfall.

The continuous progress of the trough aloft approaching the rain area and the front at the surface (figure 166) account for the occurrence of the remaining fall of this storm. Also, a Low which developed on the front near the Gulf Coast on January 5, and moved northeastward along the front while intensifying, was a contributing factor.

Finally, the movement of the Low to New England and progress of the cold front across the Appalachian Mountains, followed by the polar High (figure 159), brought an end to the rainfall over the Mississippi and Ohio Valleys.

For the next 3 days following the cessation of rainfall over the area of interest, the large polar High moved very slowly eastward, its center reaching the Atlantic Coast on January 9, blocking the entrance of another depression into the central United States and the return of rainfall until January 10.

Light to moderate rains occurred in the northward flowing air over the Ohio and Mississippi Valleys on January 1-2. This rainfall was associated with a weak trough aloft that preceded the major trough that caused the storm of January 3-7. The weak trough aloft was accompanied by a front that stalled over the central United States near Kansas City, Mo., on January 1. Since this system did not progress southward out of the area of Interest, and in fact did give moderate rains over the Mississippi Valley up to the time of the beginning of the January 3-7 storm, it is reasonable to suppose that under most favorable circumstances a heavy rainstorm could precede with no appreciable time interval.

The 12-hour representative dewpoint for this storm was 68° F. The maximum dewpoint for this area is 71° F, allowing an upward adjustment of 16%.

Storm of July 9-13, 1951 (MR 10-2)

A detailed meteorological analysis of the great Kansas storm and flood of July 1951 has appeard elsewhere[27/]. It is

the purpose of this section merely to stress some of the main large-scale features and to discuss one new concept--that of the role played by warm differential advection in releasing the large moisture charge in the overriding tropical air flow. Large-scale weather maps are shown in figures 170-171, isohyetal maps, restricted to the three major nocturnal bursts, in figure 172, and three 700-mb differential temperature advection charts corresponding to the aforementioned rain bursts in figure 173.

This storm was of a synoptic type very similar to those that occur in winter, yet it happened in the hottest time of the year. The opposing air flows, one around a sub-tropical High, the other, a part of the circulation pattern of a High of arctic origin (figure 170), are identical to the winter and spring storms discussed previously. The temperature contrast was less in this storm than in the others, but this was compensated for by the higher moisture charge of the tropical air. It is of interest to note that even in this midsummer storm the rain was ended by the influx of the cold, dry air from the north (figure 171).

The storm rainfall occurred almost entirely in the nighttime hours. This marked diurnal effect is a well-known characteristic of the Kansas region in summer and operates in storm periods as well as in periods of light, shower-type rainfall situations.

Page 9 of chapter I gives a short description of the significance of the gradient of horizontal temperature advection as a cause of vertical motions in the atmosphere. A detailed description of the method employed in the calculation of the differential advection is available in the Monthly Weather Review[22/].

A comparison of 700-mb warm differential temperature advection areas shown in figure 173 with the concurrent rainfall reveals the following association. Nearly all the heavy rain occurred in areas of warm differential advection, i.e., the atmosphere at the 700-mb level was warming faster relative to its surroundings over the heavy rain area than over areas of light or no rain. The location of the highest value of the differential advection, however, was not coincident with the point of heaviest rain. This is due in part to various approximations used in the calculations, e.g., the use of a single level to represent a layer.

Entered on the same diagrams are the dewpoint lines at the 850-mb level. The southerly jet of warm, moist air that is observed in many great storms is usually centered at about the 3000- to 4000-ft level above the ground, corresponding to the

850-mb level in this storm. It has been found in studies of rainfall situations on a day-to-day basis in the Hydrometeorological Section that 850-mb dewpoint values of 10° C to 12° C are sufficient to produce heavy rain if a mechanism to release the moisture is present. It will be noted that dewpoint values of up to about 18° C were observed in this storm period---nearly maximum conditions for this region.

Another important requirement for the production of heavy rain is a certain amount of instability (latent or real) present in the incoming current. In this storm the Showalter Index is used as a measure of the latent instability and is represented by figure 174. The values of the lines refer to the difference in the temperature between the 850-mb parcel lifted to the 500-mb level and the temperature observed at the 500-mb level. In general, significant rains have been found to be associated with differences of +1° C or less. It may be noted that in this storm the immediate source of the warm moist air, subsequently processed, was central and western Oklahoma. In this area, values range from +1/2° C to -7° C, or well within the range considered to be effective in heavy rainfall production.

In summary, investigation of this storm has shown that the air in the perpheral current was conditionally unstable to a high degree. This latent instability was touched off by the temperature field in conjunction with the wind field over the Kansas region as shown by the differentaial advection. The warm differential advection acted as both a trigger mechanism to release the instability and as a direct lifting agent upon the moist air itself.

The 12-hour representative dewpoint for the storm was 72° F. The maximum dewpoint for the area is 77° F allowing a 28% upward adjustment of moisture in the place of occurrence.

ACKNOWLEDGMENTS

The project leaders of this study were Vance A. Myers and George A. Lott, for the material in Chapters I and II, respectively, under the guidance of Charles S. Gilman, Chief of Section, and Robert W. Schloemer, former Assistant Chief of Section. The individual storm analyses were prepared by Morton H. Bailey, Calvin W. Cochrane, Nelson M. Kauffman, Lillian K. Rubin, William W. Swayne, Roger R. Watkins, and George Wu. Assistance was also lent by Ai E. Brown, Obie Y. Causey, Robert Frazier, James L. Keister, Cora Ludwig, and Harlan H. Vinnedge. Final editing was by Lillian K. Rubin. Drafting was by Nemesio O. Calub, Carroll W. Gardner, and Ishmael A. Santiago, and the final manuscript was typed by Edna L. Grooms and Billie Ann Neely.

REFERENCES

1. Mississippi River Commission, "Interim Report, Mississippi Project Flood Study" Vicksburg, Mississippi, November 1954.

2. Corps of Engineers, Department of the Army, "Storm Rainfall in the United States, Depth-Area-Duration Data." Washington, 1945.

3. J. R. Fulks, "Rate of Precipitation from Adiabatically Ascending Air," Monthly Weather Review, Vol. 63, No. 10, October 1935, p. 291.

4. Henry G. Houghton, "On the Physics of Clouds and Precipitation," Compendium of Meteorology, American Meteorological Society, Boston, 1951.

5. Christian Junge, "Nuclei of Atmospheric Condensation," Compendium of Meteorology, American Meteorological Society, Boston, 1951.

6. H. G. Houghton, "On the Annual Heat Balance of the Northern Hemisphere," Journal of Meteorology, Vol. II, No. 1, February, 1954, p. 1.

7. George S. Benton, and Mariano Estoque, "Water-Vapor Transfer Over the North American Continent," Journal of Meteorology, Vol. 11, No. 6, December, 1954, p. 467.

8. G. S. Benton, M. A. Estoque, and J. Dominitz, "An Evaluation of the Water Vapor Balance of the North American Continent," John Hopkins University, Dept. of Civil Engineering, July 1953.

9. U. S. Weather Bureau, "Daily Synoptic Series, Historical Weather Maps, Northern Hemisphere 3,000 Dynamic Meters".

10. Monthly Weather Review, Supplement No. 37, Washington, 1938.

11. U. S. Weather Bureau, "Daily Synoptic Series Historical Weather Maps, Northern Hemisphere Sea Level,". January 1899 to June 1939, incl.

12. U. S. Weather Bureau, "Normal Weather Maps, Northern Hemisphere Sea Level Pressure," Washington, D. C. April 1946.

References (cont'd)

13. Benjamin Ratner, "Temperature Frequencies in the Upper Air," U. S. Weather Bureau, Washington, D. C., January 1946.

14. D. T. Williams, "A Surface Micro-Study of Squall-Line Thunderstorms," Monthly Weather Review, Vol. 76, No. 11, November 1948, pp. 239-246.

15. H. C. Frankenfield, "Rivers and Floods," Monthly Weather Review, Vol. 55, No. 2, February 1927, pp. 95-97.

16. P. C. Day, "The Weather Elements," Monthly Weather Review, Vol. 55, No. 2, February 1927, pp. 90-92.

17. P. C. Day, "Weather in the United States," Monthly Weather Review, Vol. 55, No. 4, April 1927, pp. 194-198.

18. P. C. Day, "Weather in the United States," Monthly Weather Review, Vol. 56, No. 6, June 1928, pp. 234-238.

19. W. R. Stevens, "Aerological Observations," Monthly Weather Review, Vol. 56, No. 6, June 1928, pp. 233-234.

20. J. F. Appleby, "Meteorological Summary, Storms of May 30-June 2, 1947 (MR 8-8); June 2-7, 1947 (MR 8-10); June 16-18, 1947 (MR 8-18); June 18-23, 1947 (MR 8-20); and June 26-30, 1947 (MR 8-24)," Hydrometeorological Section, January 23, 1953.

21. G. A. Lott, "The World-Record 42-Minute Holt, Missouri, Rainstorm," Monthly Weather Review, Vol. 82, No. 2, February 1954, pp. 50-59.

22. J. F. Appleby, "Trajectory Method of Making Short-Range Forecast of Differential Temperature Advection Instability and Moisture," Monthly Weather Review, Vol. 82, No. 11, November 1954, pp. 320-334.

23. C. S. Gilman, "An Expansion of the Thermal Theory of Pressure Changes," ScD Thesis, Massachusetts Institute of Technology, 1949 (unpublished).

24. William H. Klein, "The Weather and Circulation of January 1950," Monthly Weather Review, Vol. 78, No. 1, January 1950, pp. 13-14.

References (cont'd)

25. William H. Klein, "Winter Precipitation as Related to the 700-mb Circulation." Bulletin of the American Meteorological Society, Vol. 29, No. 9, part 2, November 1948, pp. 439-453.

26. J. R. Fulks, "The Instability Line," Compendium of Meteorology, American Meteorological Society, Boston, 1951.

27. U. S. Weather Bureau, Hydrologic Services Division, "Kansas-Missouri Floods of June-July 1951," W. B. Technical Paper No. 17, July 1952.

28. J. F. Gabites, "Seasonal Variations in the Atmospheric Heat Balance," Cambridge, Massachusetts Institute of Technology, ScD Thesis, 147 pp.

29. H. U. Sverdrup, M. W. Johnson, and R. H. Fleming, "The Oceans, Their Physics, Chemistry and General Biology," New York, Prentice-Hall, Inc., 1942.

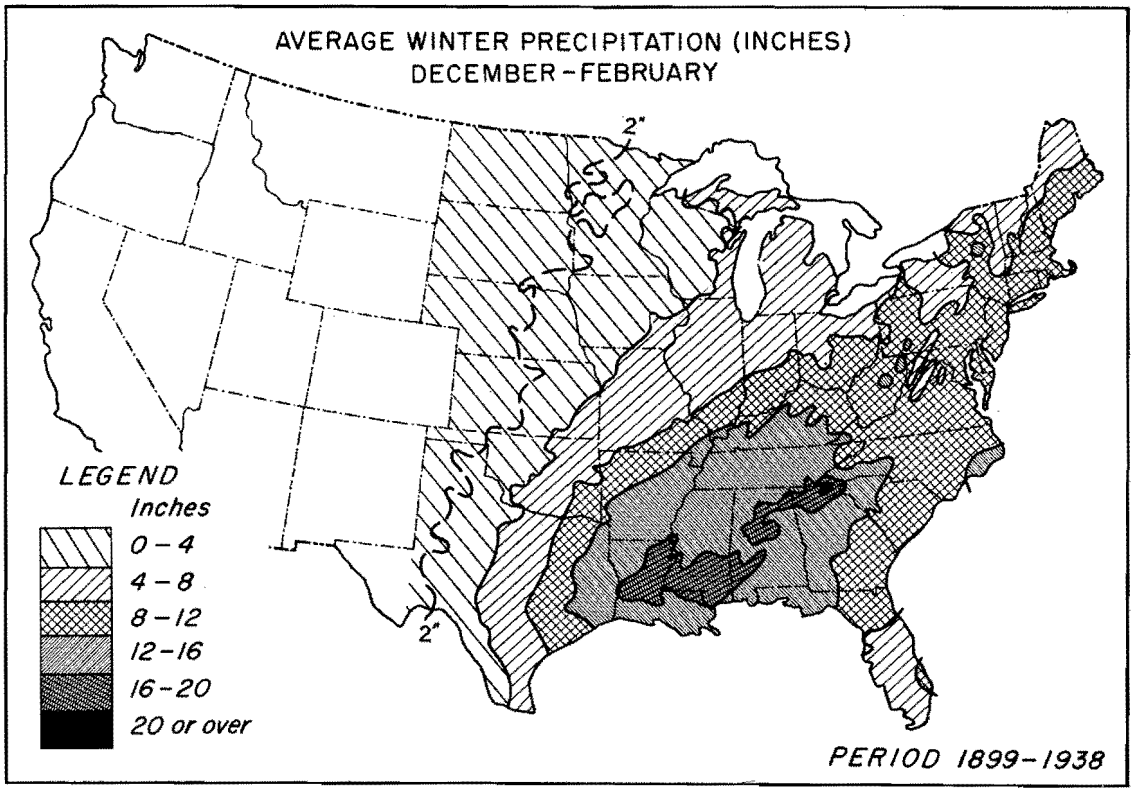

Figure 1

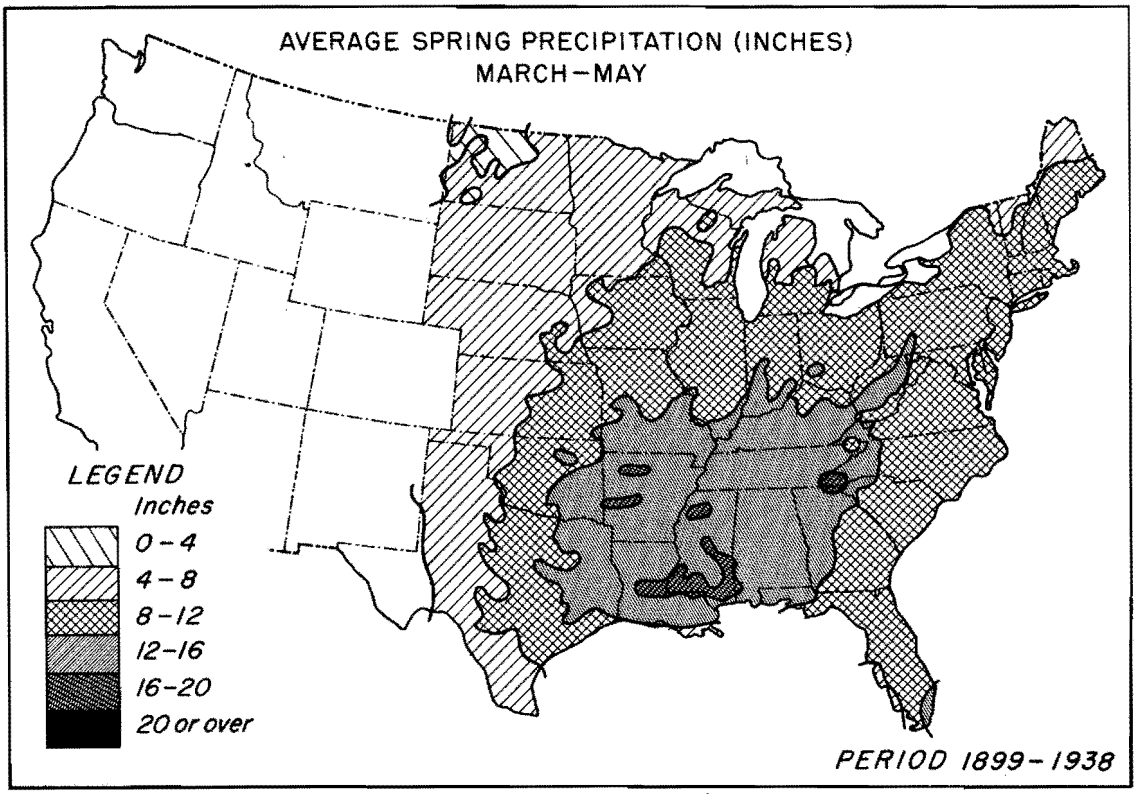

Figure 2

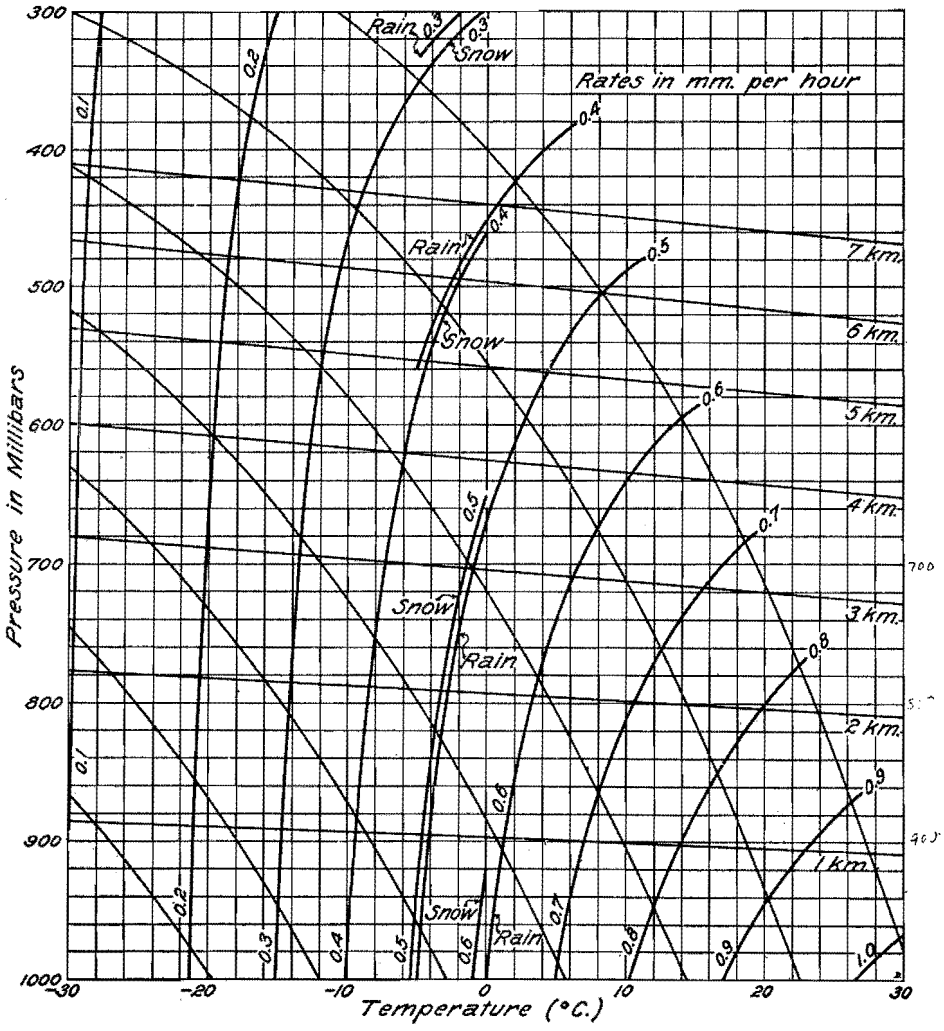

Rates of precipitation from adiabatically ascending air for a 100-meter layer with a vertical velocity of 1 meter per second.

Fig. 3.

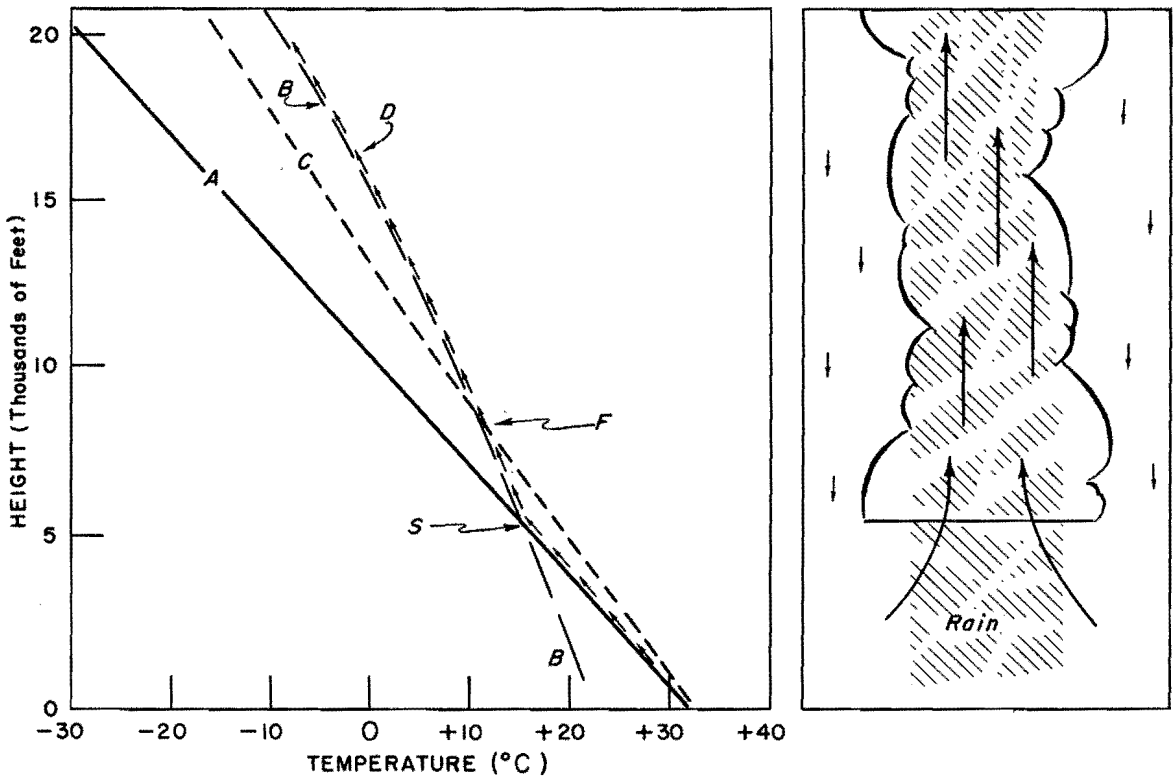

A - Adiabatic change of temperature with height for a dry air parcel.

B - Adiabatic change of temperature with height for a saturated air parcel. Release of latent heat of condensation on ascent accounts for the difference between A and B.

C - Typical pre-existing distribution of temperature with height in latently unstable atmosphere.

D - Temperature change with height of air parcel lifted from surface. Parcel containes water vapor and becomes saturated at S. Above F temperature of lifted parcel exceeds temperature of pre-existing air at same level, and convection proceeds spontaneously

SCHEMATIC REPRESENTATION OF RELEASE OF LATENT INSTABILITY

Figure 4

AVERAGE NUMBER OF DAYS WITH THUNDERSTORMS

Based on 217 First-Order Stations

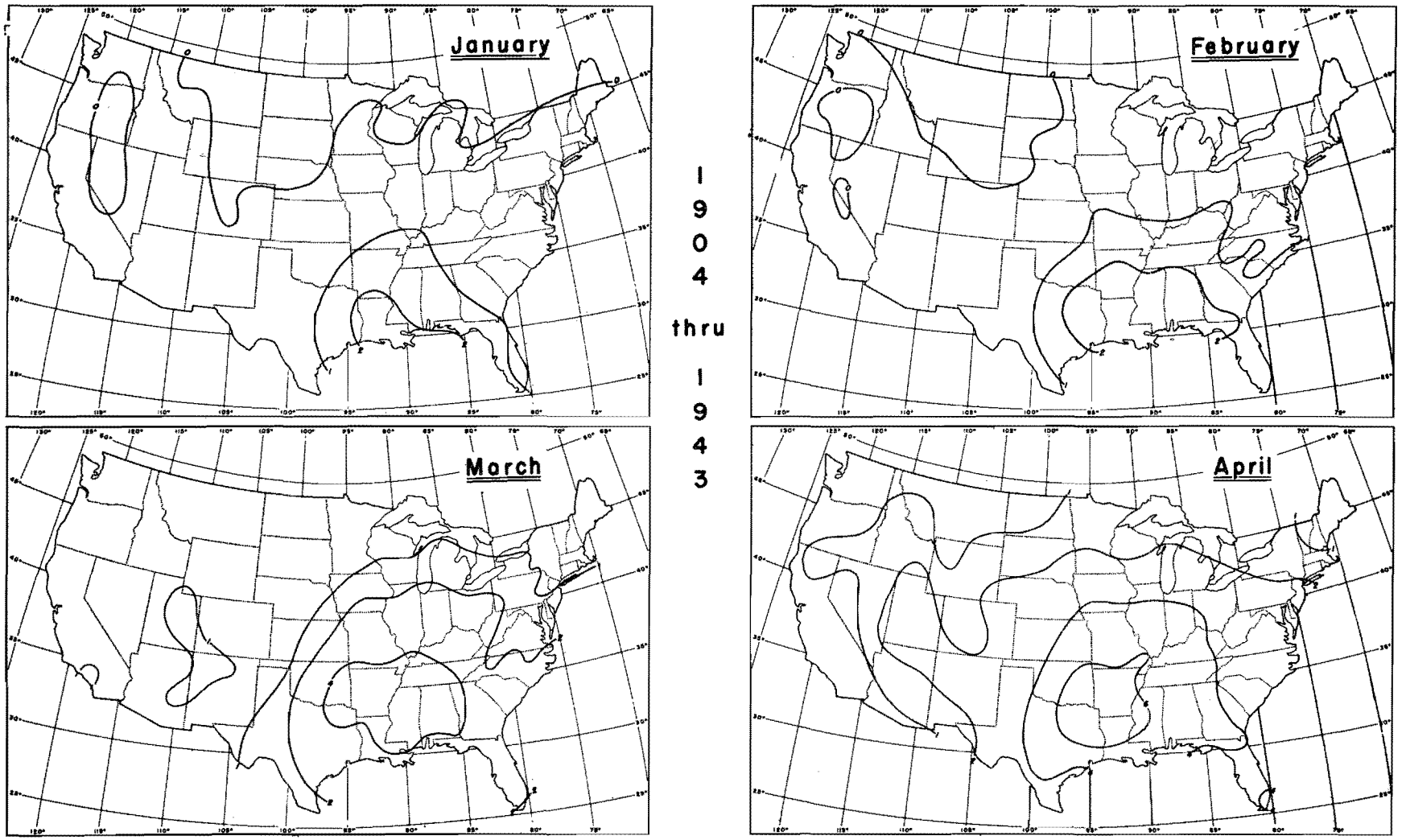

Figure 5.

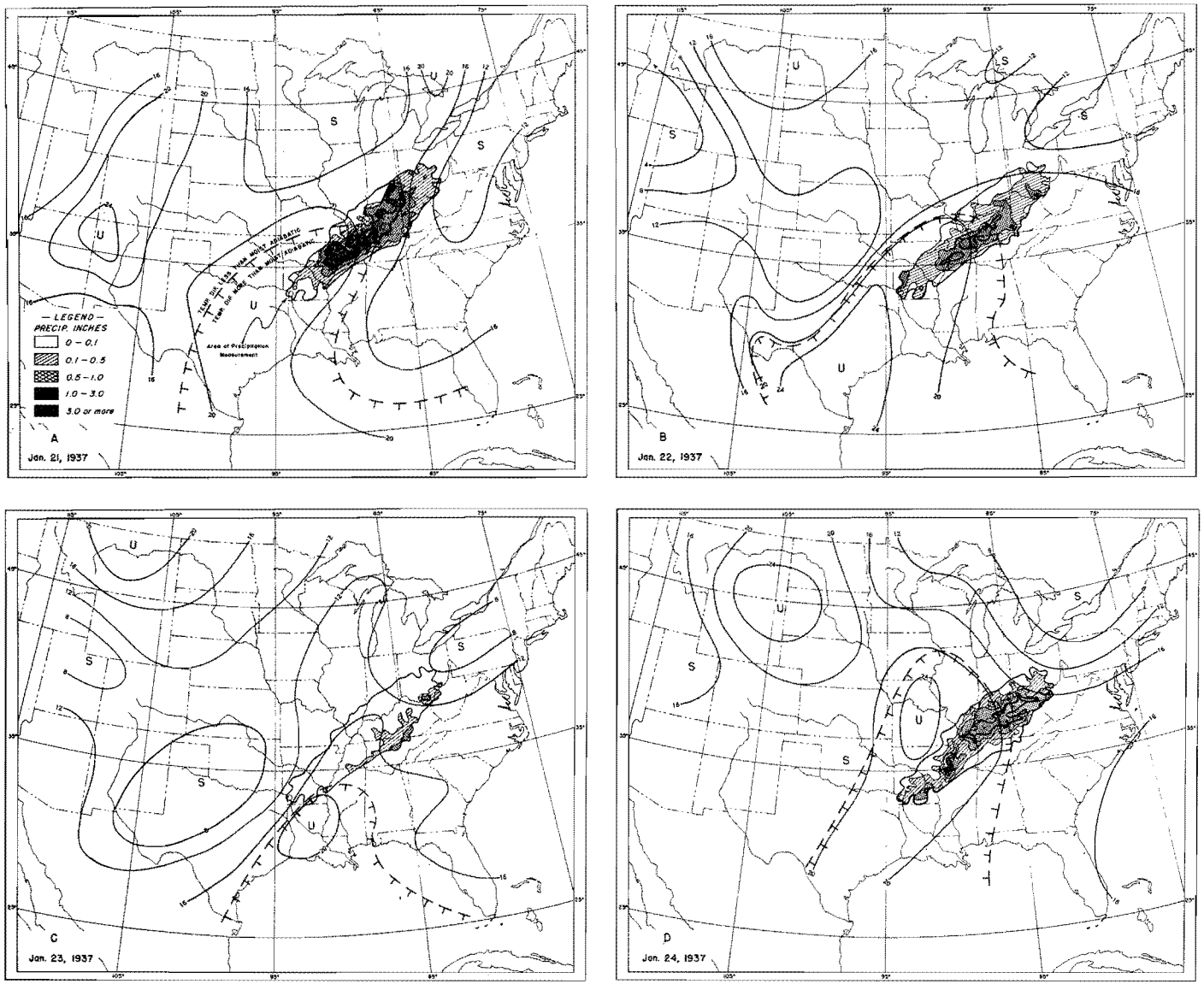

Figure 6. EXCESS OF TEMPERATURE (°C) AT 1.5 KM (4920 FT.) OVER 5 KM (16,400 FT.) AND CONCURRENT PRECIPITATION
Temperature difference – based on airplane soundings mostly between 2 a.m. and 6 a.m. CST Precipitation – 2 a.m. to 8 a.m. CST.

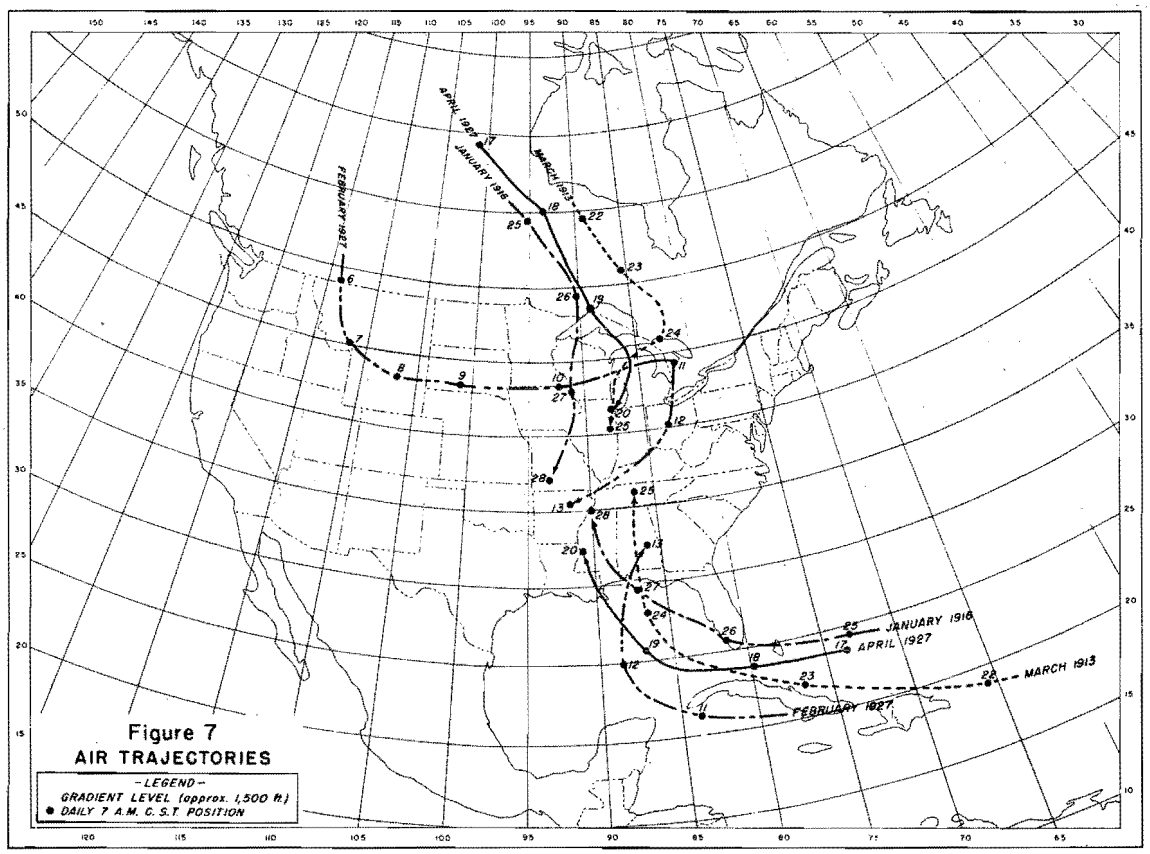

Figure 7
AIR TRAJECTORIES

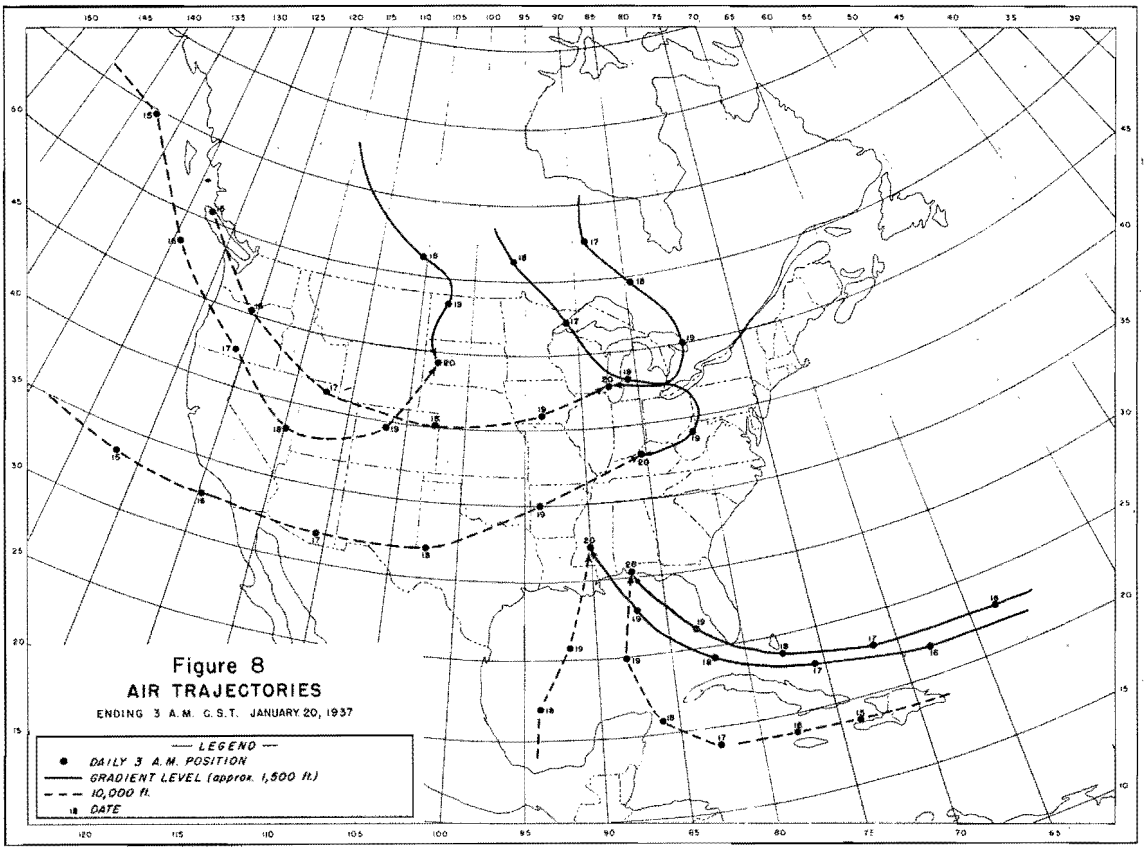

Figure 8
AIR TRAJECTORIES
ENDING 3 A.M. C.S.T. JANUARY 20, 1937

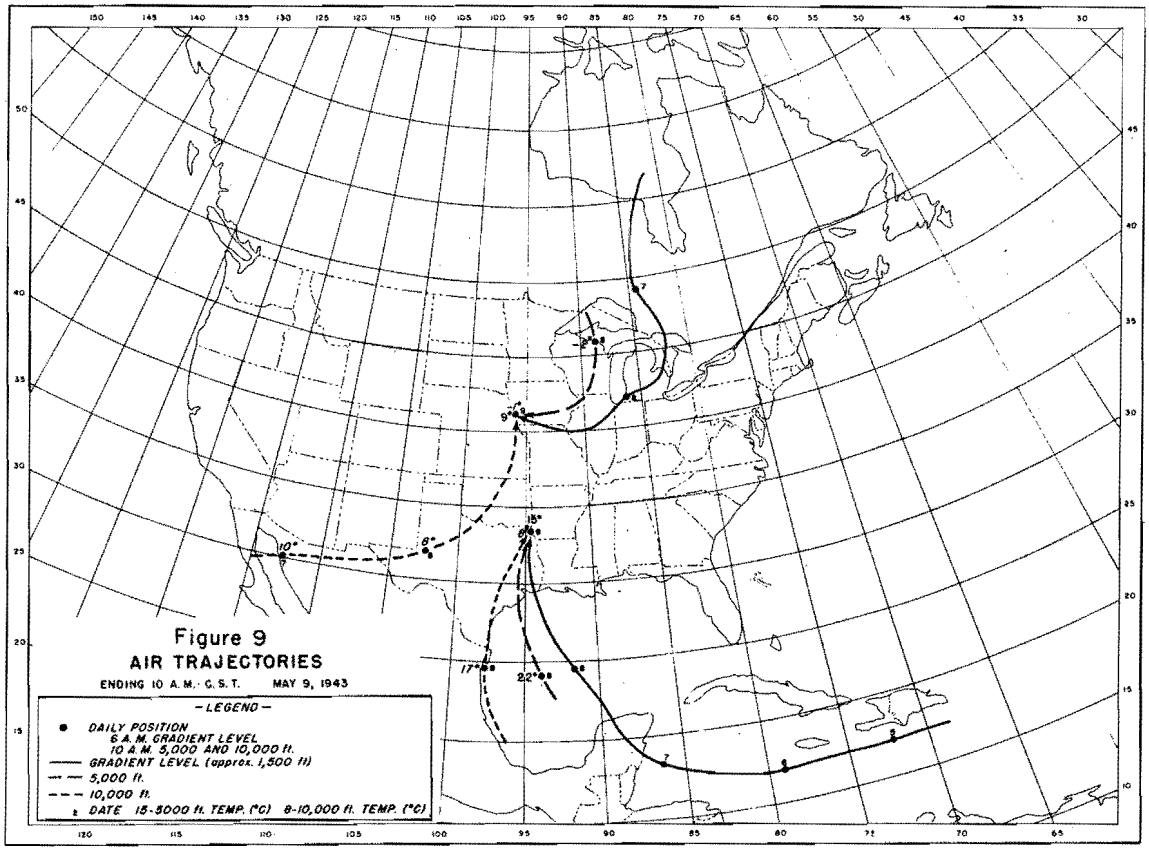
Figure 9
AIR TRAJECTORIES
ENDING 10 A.M. G.S.T. MAY 9, 1943
-LEGEND-
DAILY POSITION
6 A.M. GRADIENT LEVEL
10 A.M. 5,000 AND 10,000 ft.
GRADIENT LEVEL (approx. 1,500 ft)
5,000 ft.
10,000 ft.
DATE 15-5000 ft. TEMP. (°C) 8-10,000 ft. TEMP. (°C)

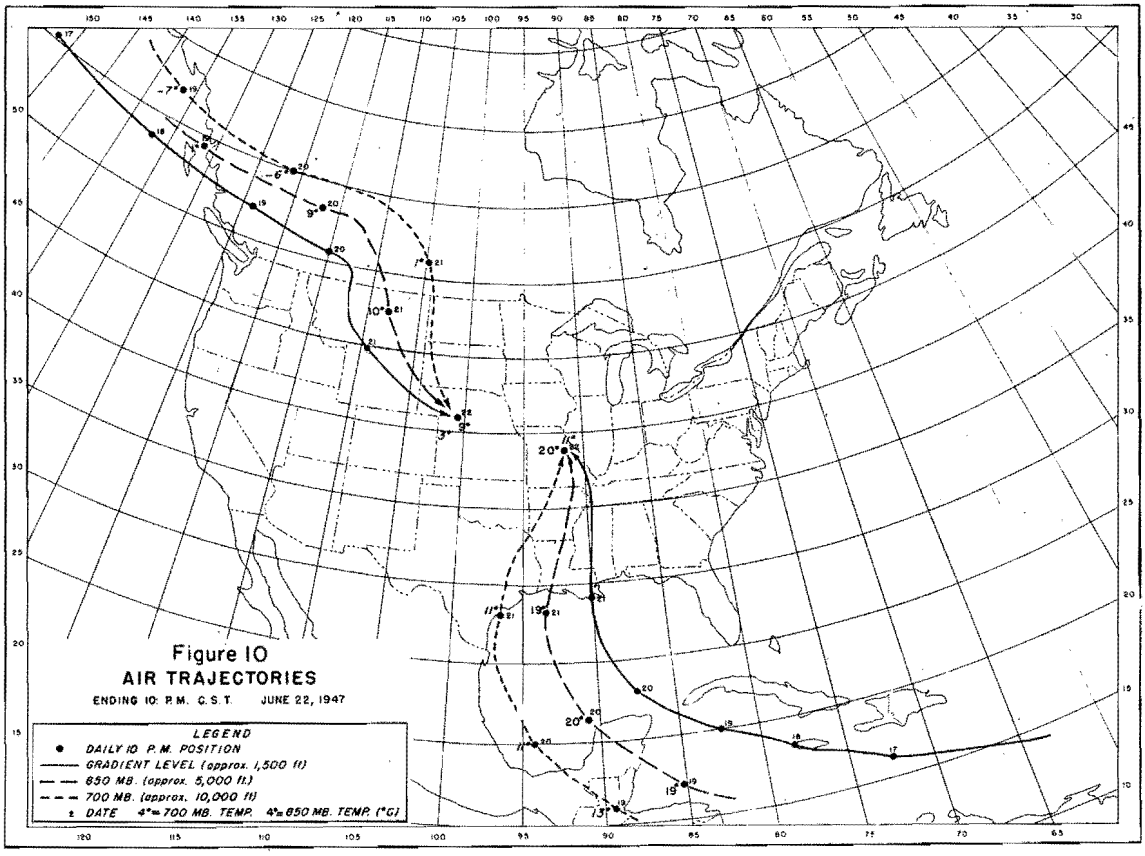
Figure 10
AIR TRAJECTORIES
ENDING 10 P.M. G.S.T. JUNE 22, 1947
LEGEND
DAILY 10 P.M. POSITION
GRADIENT LEVEL (approx. 1,500 ft)
850 MB. (approx. 5,000 ft.)
700 MB. (approx. 10,000 ft)
DATE 4°=700 MB. TEMP. 4°=850 MB. TEMP. (°C)

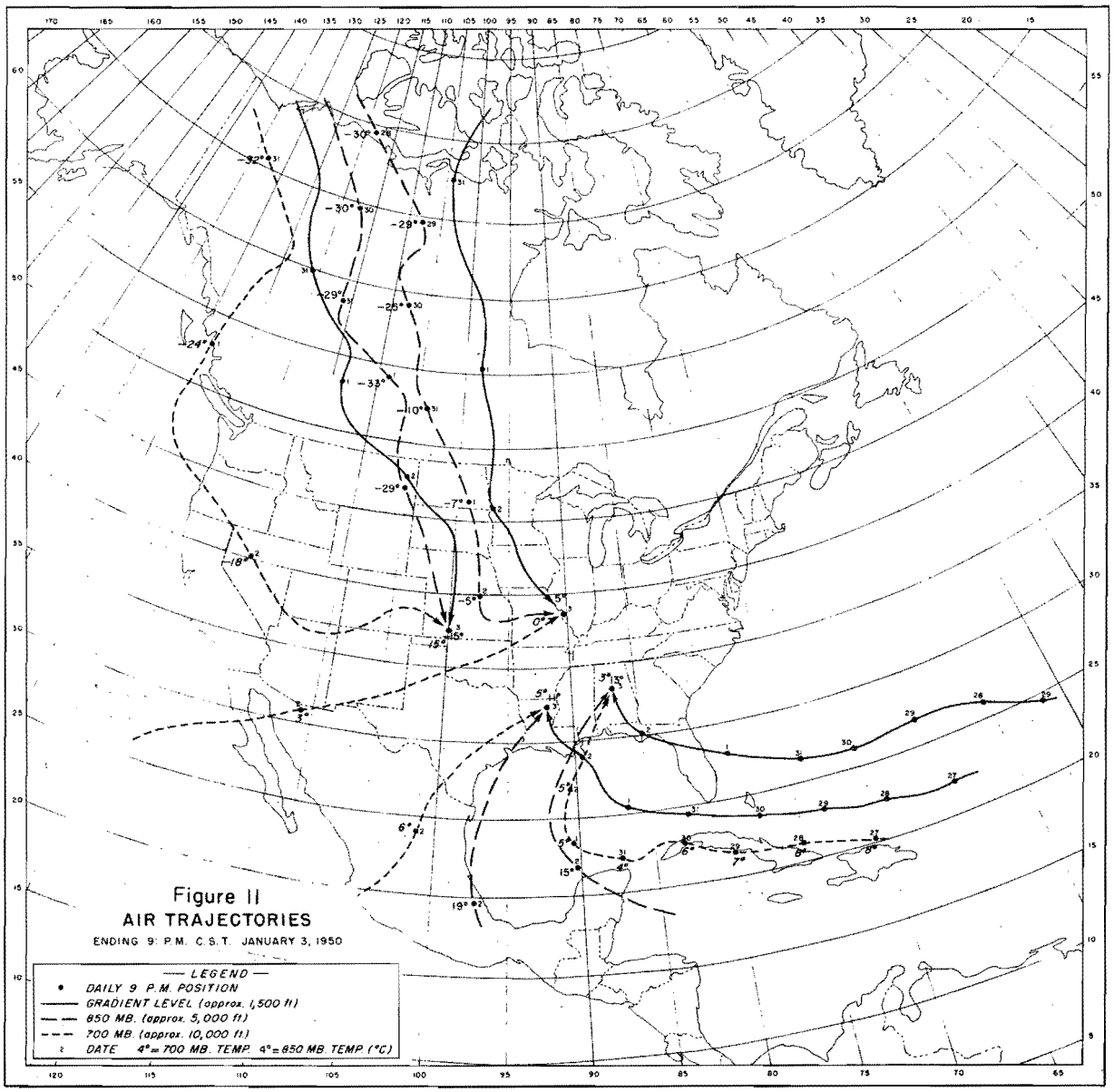
Figure II
AIR TRAJECTORIES
ENDING 9: P.M. C.S.T. JANUARY 3, 1950
— LEGEND —
DAILY 9 P.M. POSITION
GRADIENT LEVEL (approx. 1,500 ft)
850 MB. (approx. 5,000 ft)
700 MB. (approx. 10,000 ft)
DATE 4°= 700 MB. TEMP. 4°= 850 MB. TEMP. (°C.)

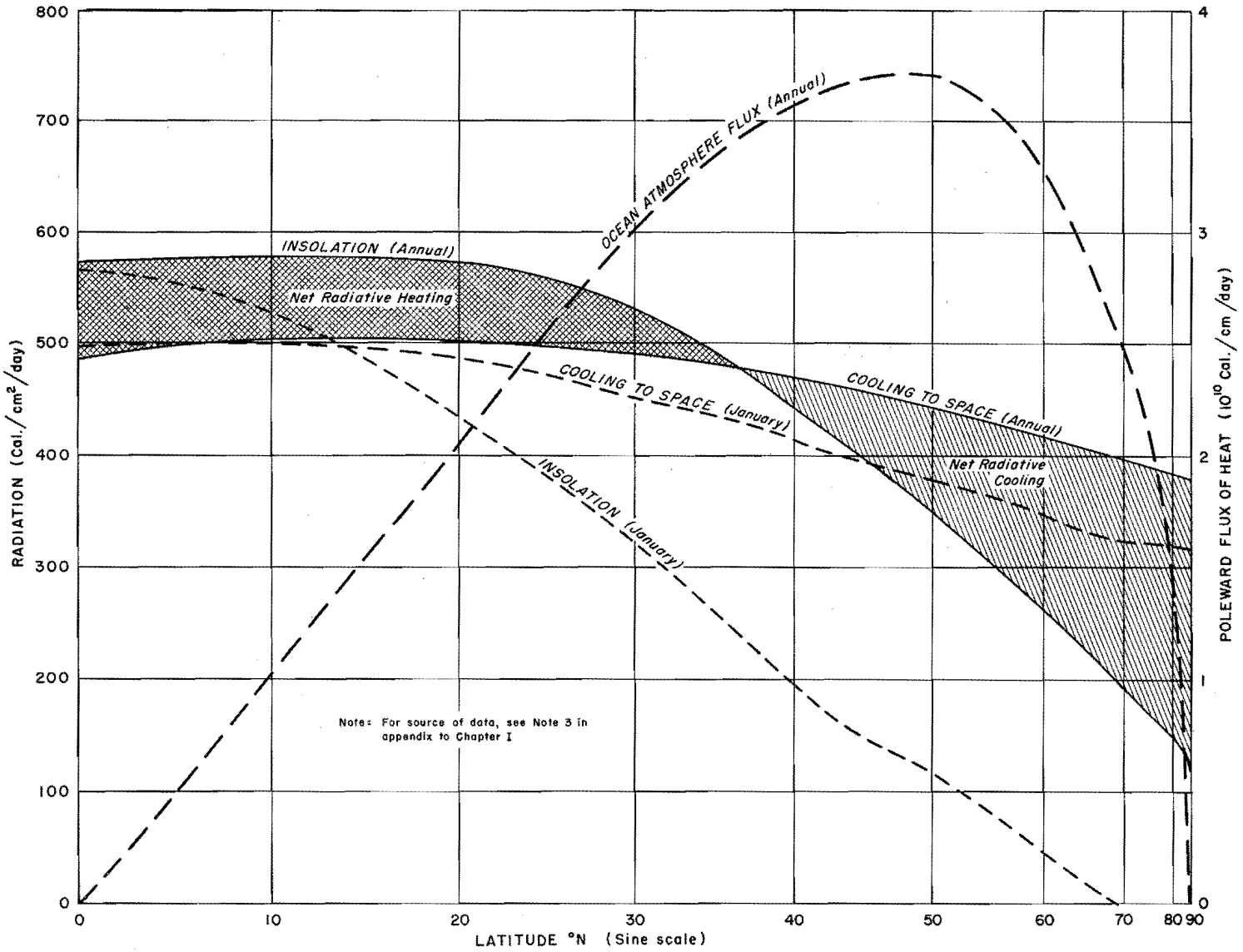

Figure 12. LATITUDINAL VARIATION OF HEAT BALANCE -- NORTHERN HEMISPHERE

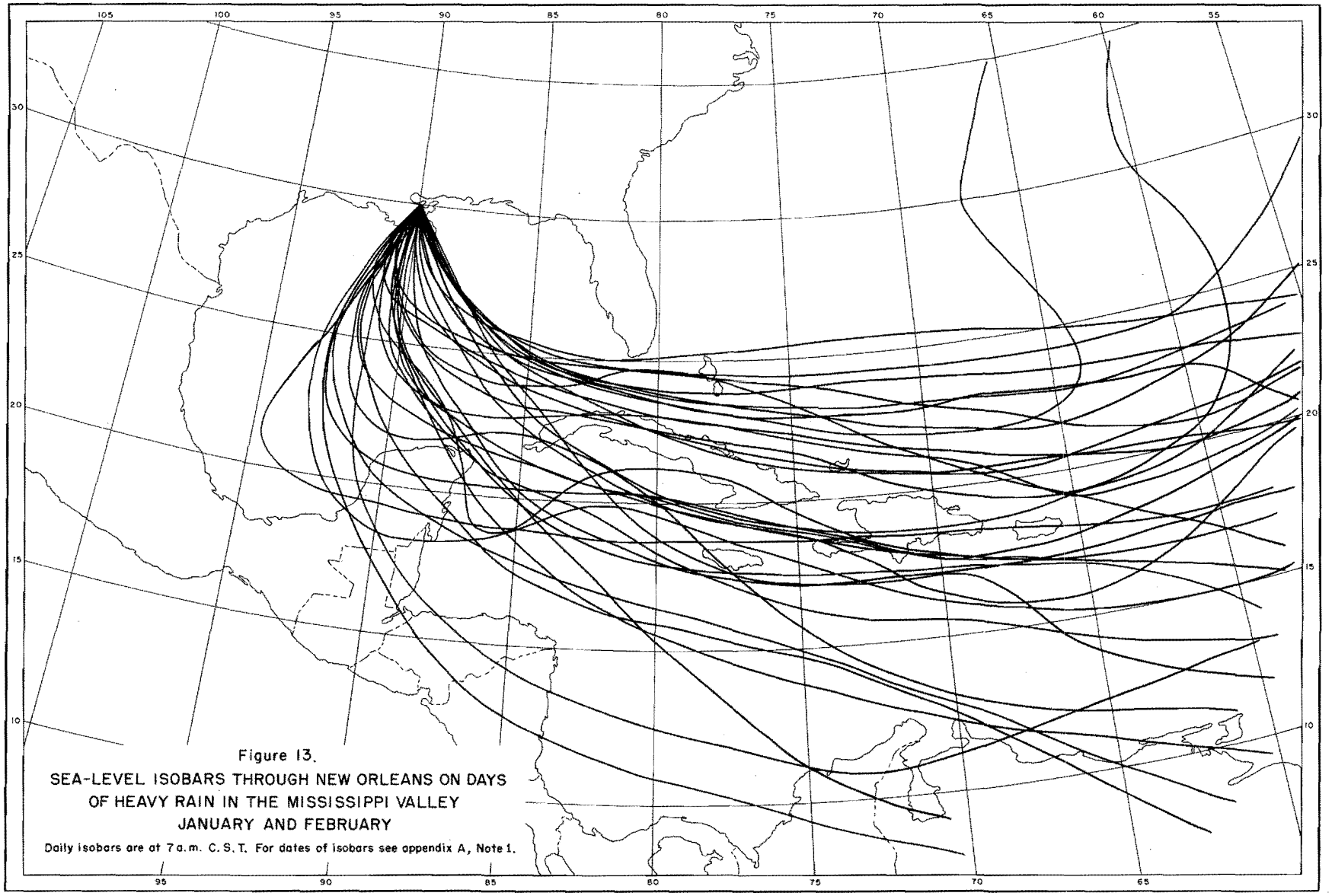

Figure 13.

SEA-LEVEL ISOBARS THROUGH NEW ORLEANS ON DAYS OF HEAVY RAIN IN THE MISSISSIPPI VALLEY JANUARY AND FEBRUARY

Daily isobars are at 7 a.m. C.S.T. For dates of isobars see appendix A, Note 1.

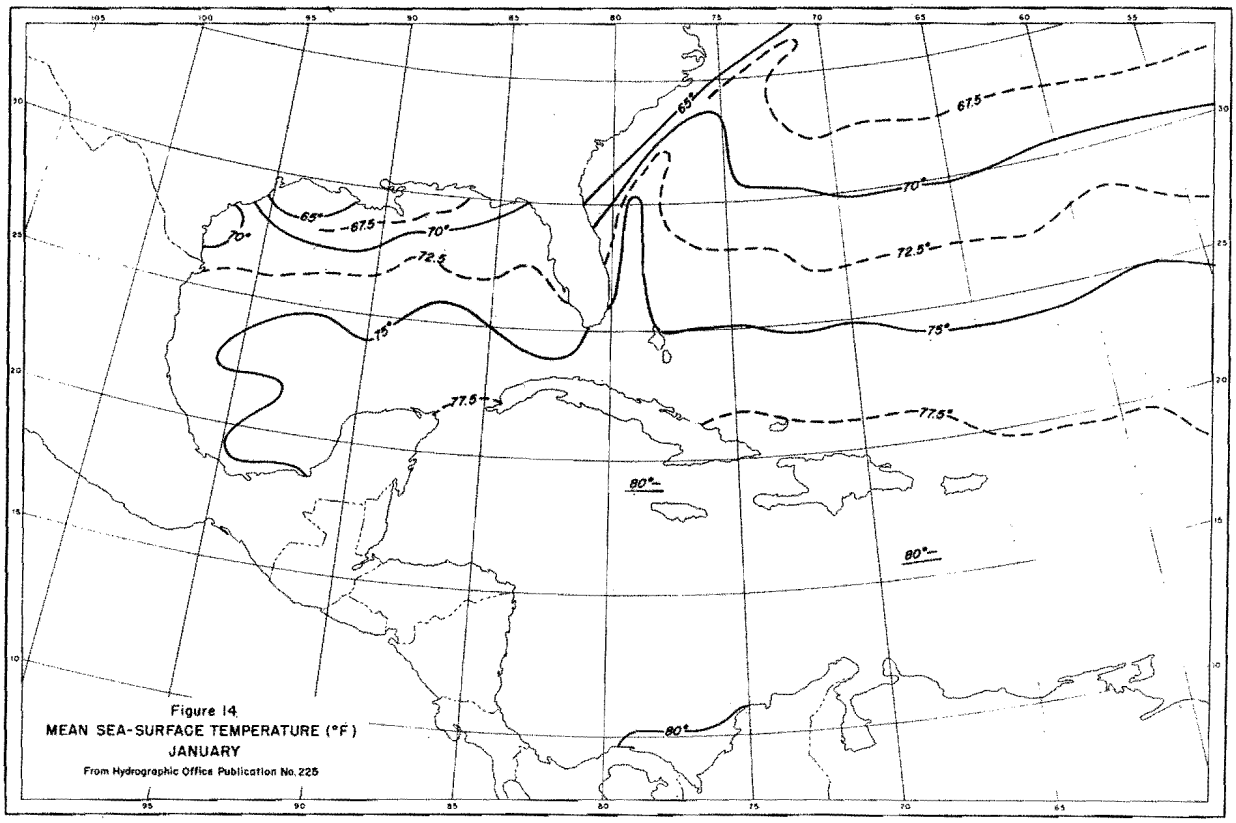

Figure 14.
MEAN SEA-SURFACE TEMPERATURE (°F)
JANUARY
From Hydrographic Office Publication No. 225

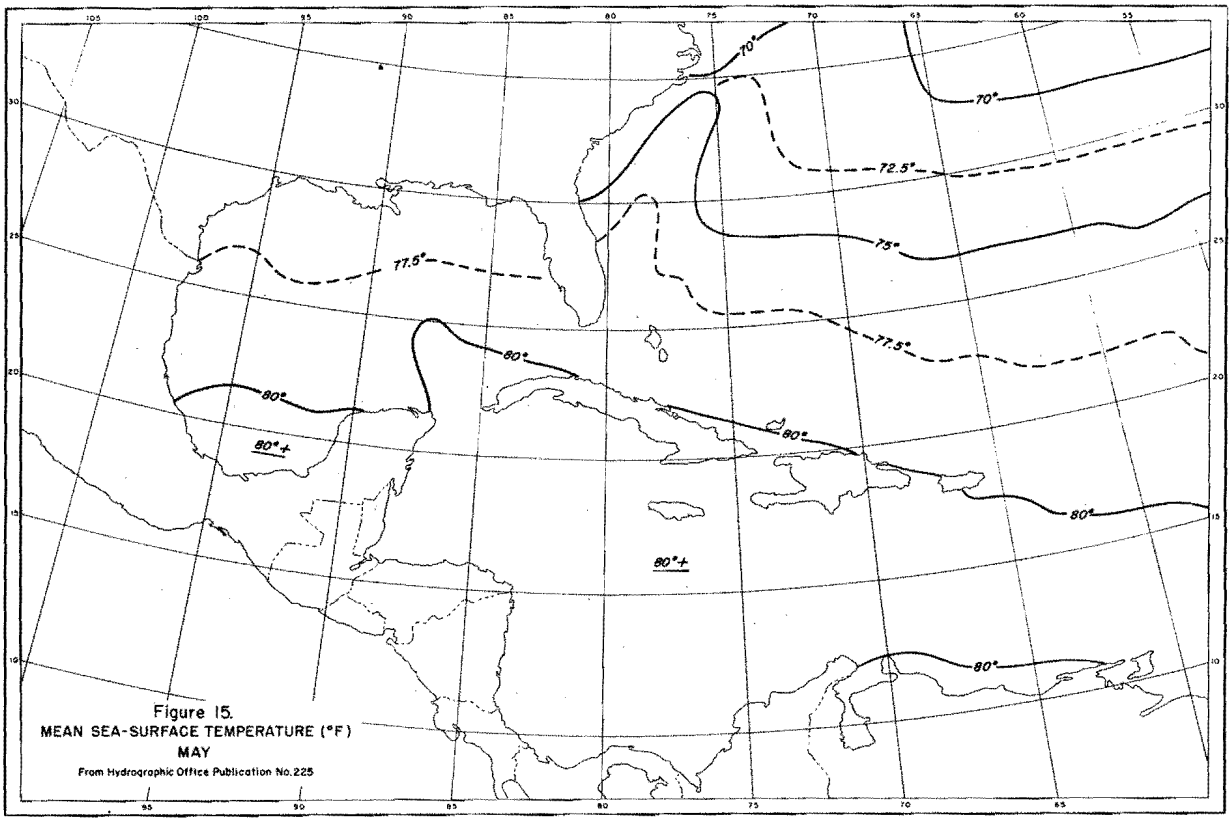

Figure 15.
MEAN SEA-SURFACE TEMPERATURE (°F)
MAY
From Hydrographic Office Publication No. 225

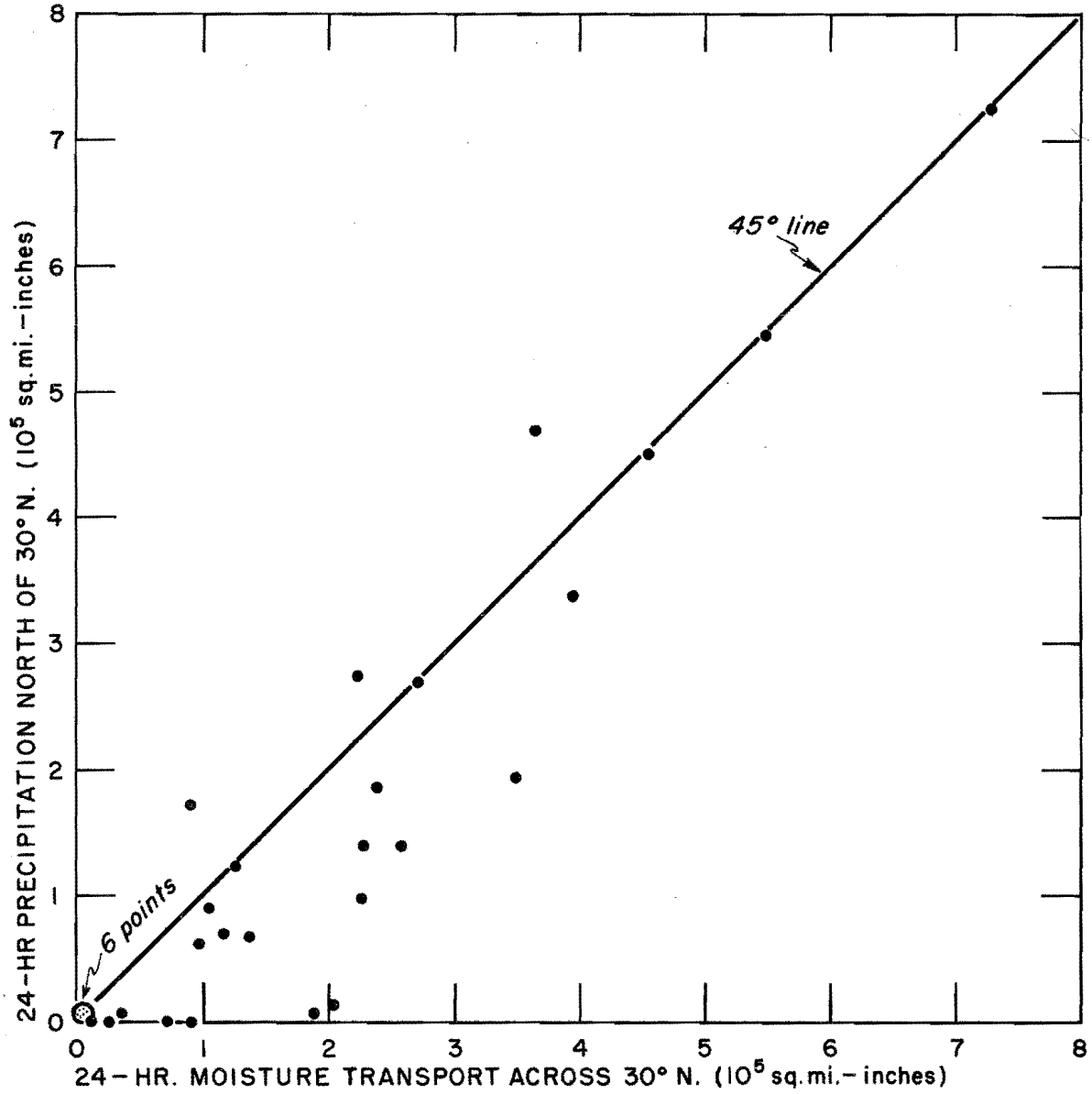

MOISTURE TRANSPORT: Vapor carried by windflow across 30° N between longitudes of Tallahassee, Florida and San Antonio, Texas, from ground to 400 mbs. (approx. 24,000 ft.) assuming rate at 9 a.m. CST is maintained for 24 hours. Based on radio balloon data. Unit of transport is vapor-equivalent of an inch of rain over one square mile.

PRECIPITATION: Observed precipitation from 6:30 a.m. CST day of moisture-transport measurement to 6:30 a.m. next day, over area within the United States estimated to be downwind at 3,000 - 5,000 feet from San Antonio - Tallahassee baseline.

Figure 16. TRANSPORT OF MOISTURE ACROSS 30° N.
VS.
24-HOUR PRECIPITATION NORTH OF 30° N.--MARCH 1951

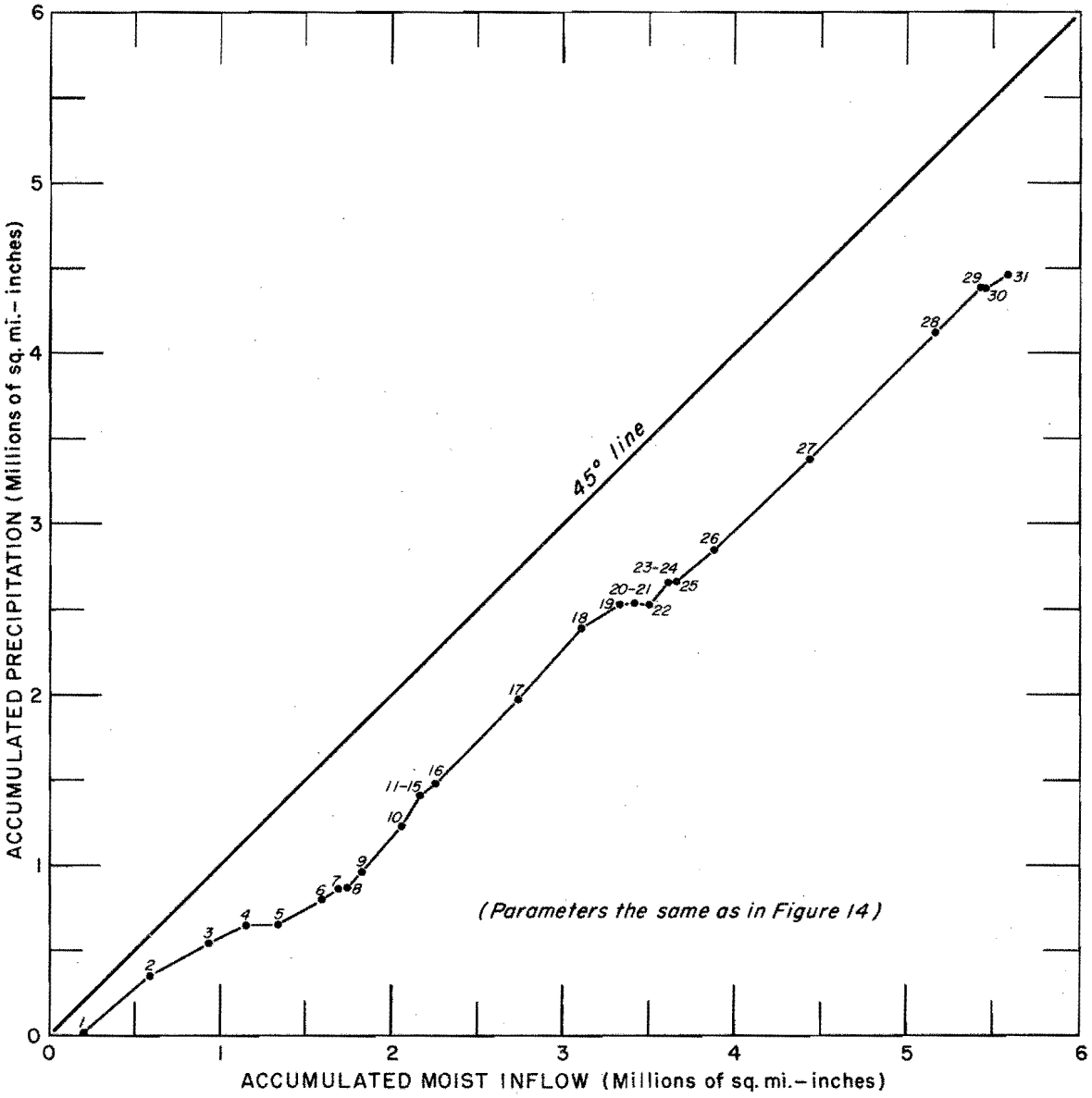

Figure 17. ACCUMULATED TRANSPORT OF MOISTURE ACROSS 30°N.
VS.
ACCUMULATED PRECIPITATION NORTH OF 30°N. -- MARCH 1951

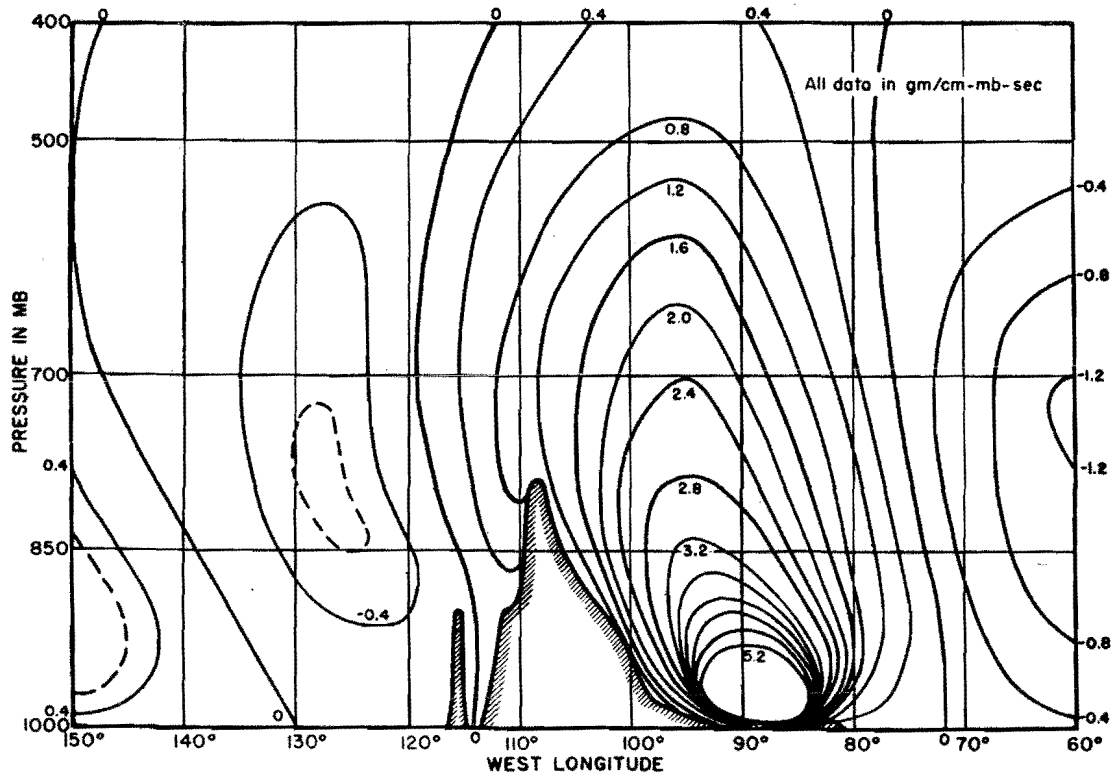

Figure 18. Meridional transport of water vapor across 30° N. latitude averaged for the Winter, 1949. (after Benton)

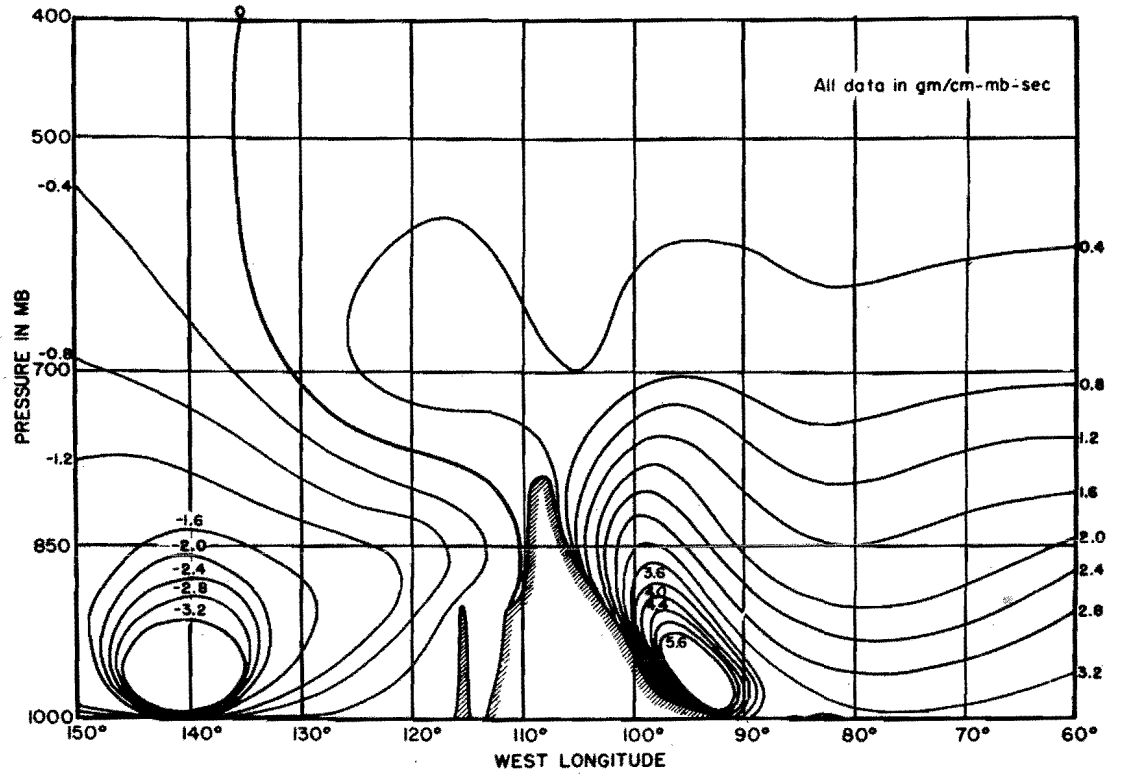

Figure 19. Meridional transport of water vapor across 30° N. latitude averaged for the Summer, 1949. (after Benton)

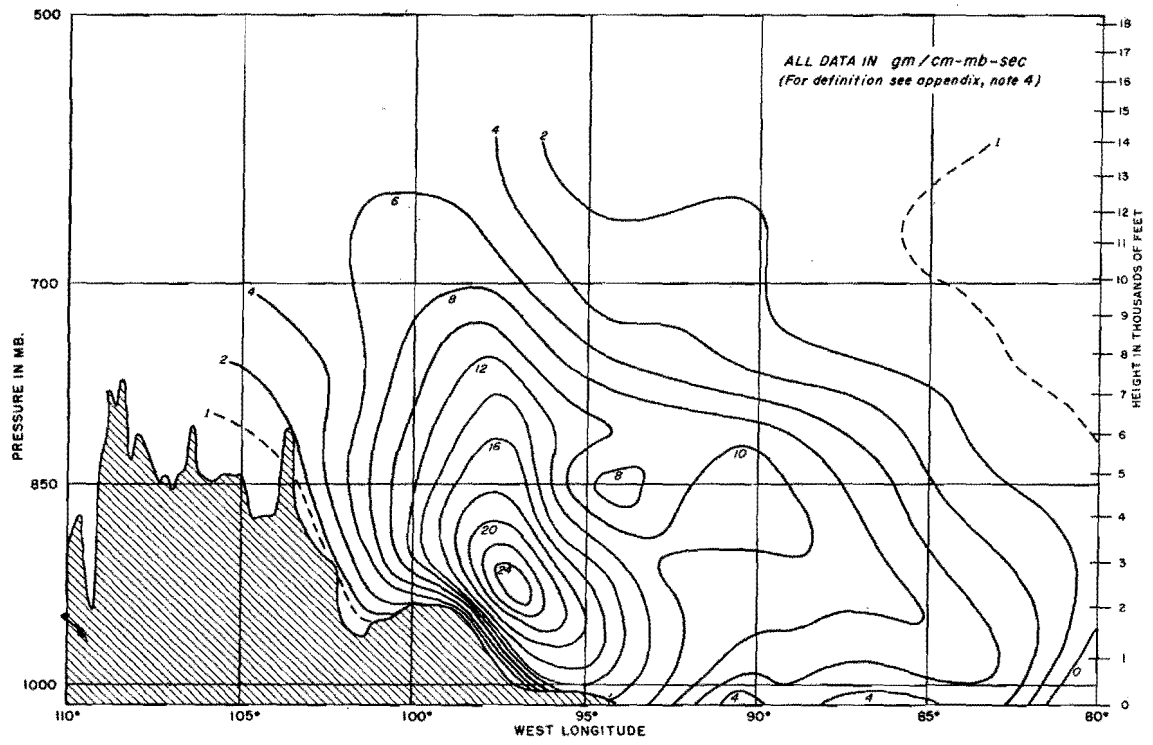

Figure 20. NORTHWARD TRANSPORT OF WATER VAPOR ACROSS 30° N. LAT. AT 9. A. M. CST, JANUARY 24, 1949

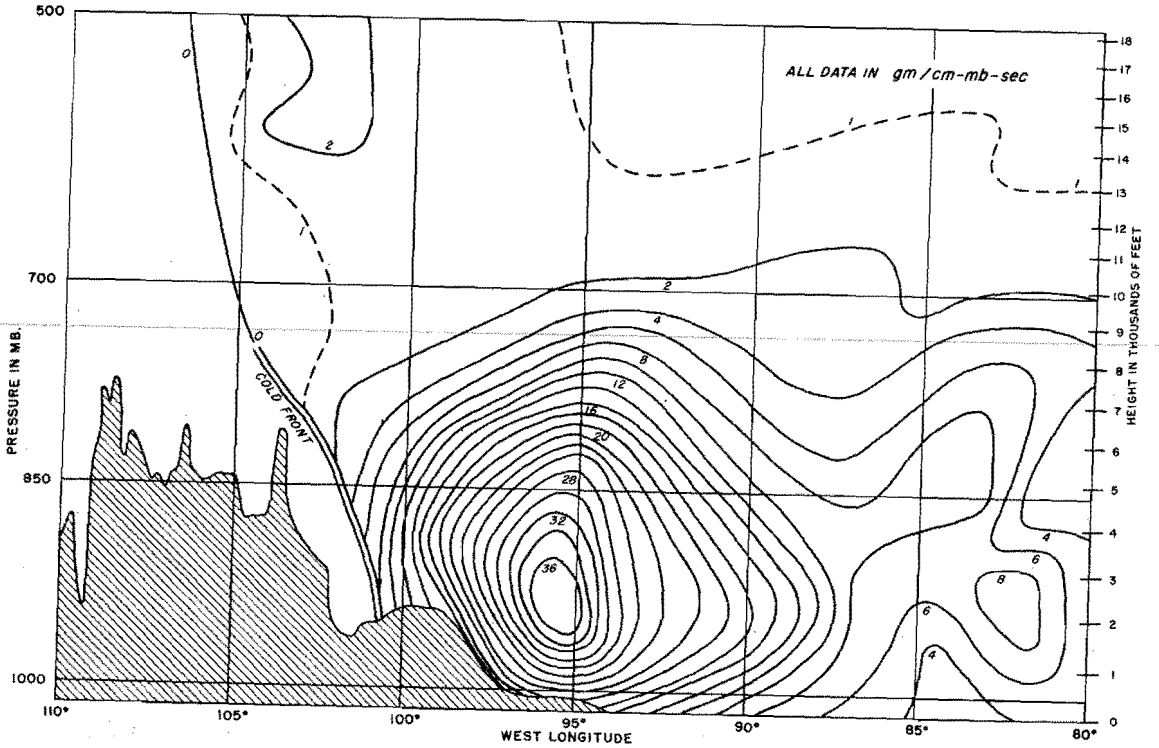

Figure 21. NORTHWARD TRANSPORT OF WATER VAPOR ACROSS 30° N. LAT. AT 9. P. M. CST, MAY 8, 1943

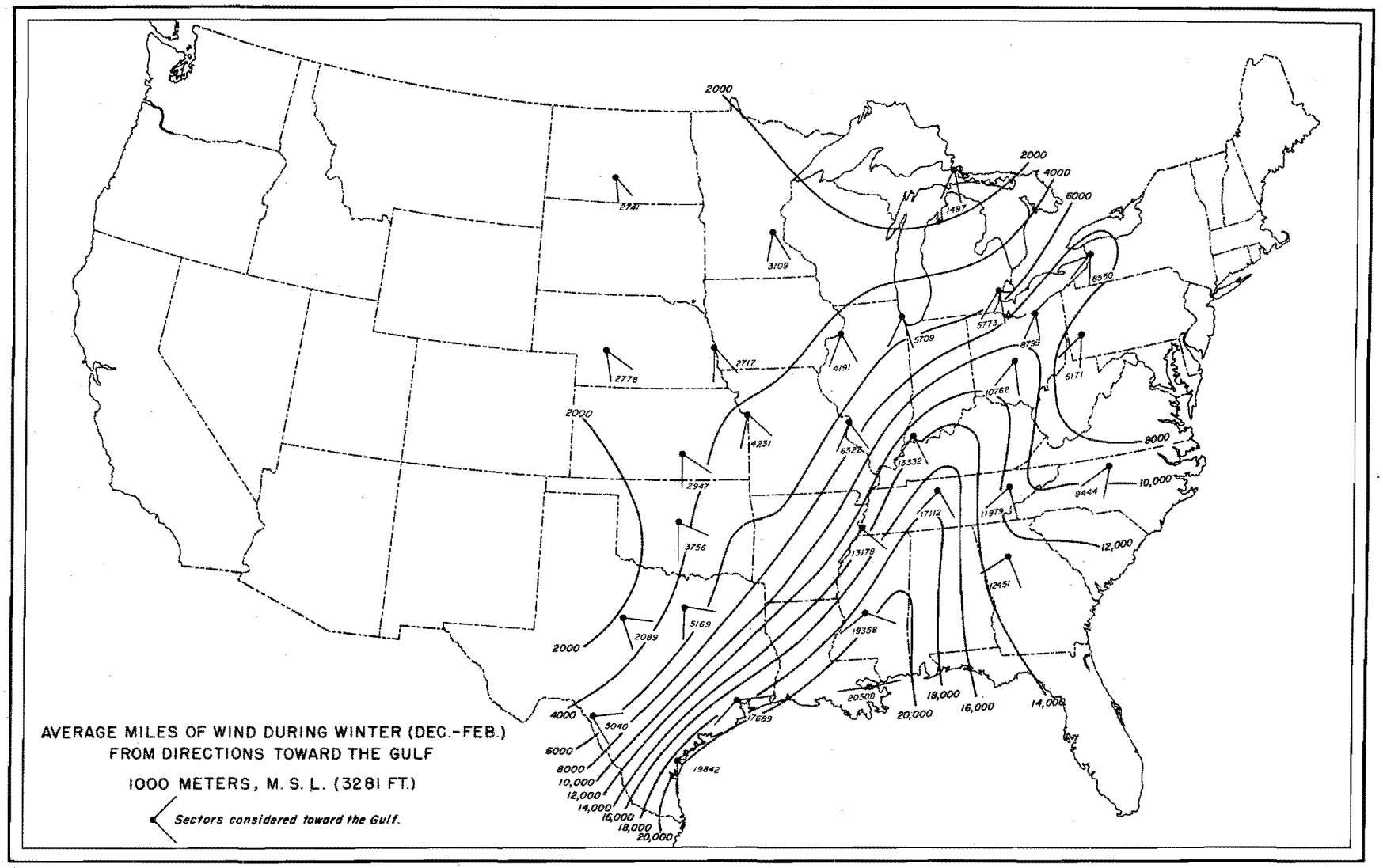
AVERAGE MILES OF WIND DURING WINTER (DEC.-FEB.)
FROM DIRECTIONS TOWARD THE GULF
1000 METERS, M. S. L. (3281 FT.)
Sectors considered toward the Gulf.
2000
4000
6000
8000
10,000
12,000
14,000
16,000
18,000
20,000
2741
3109
1497
8550
5773
5709
8793
6171
10762
6191
2778
2717
4231
6322
13332
9444
2947
3756
11979
17112
13178
12451
5169
2089
19358
20508
17689
19842
5040

Figure 22

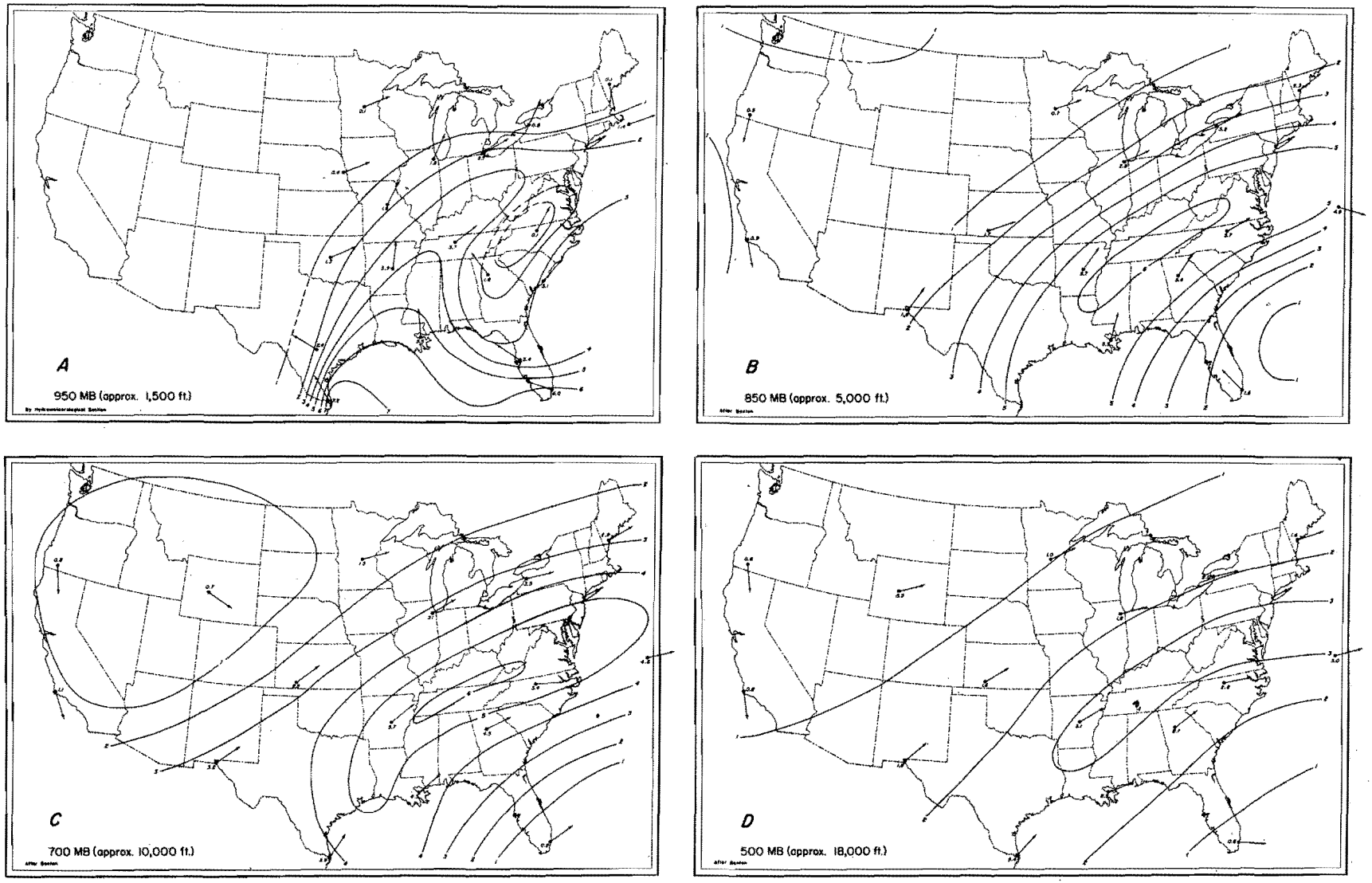

Figure 23. MEAN WATER VAPOR TRANSPORT (gm/cm-mb-sec) JANUARY 1949

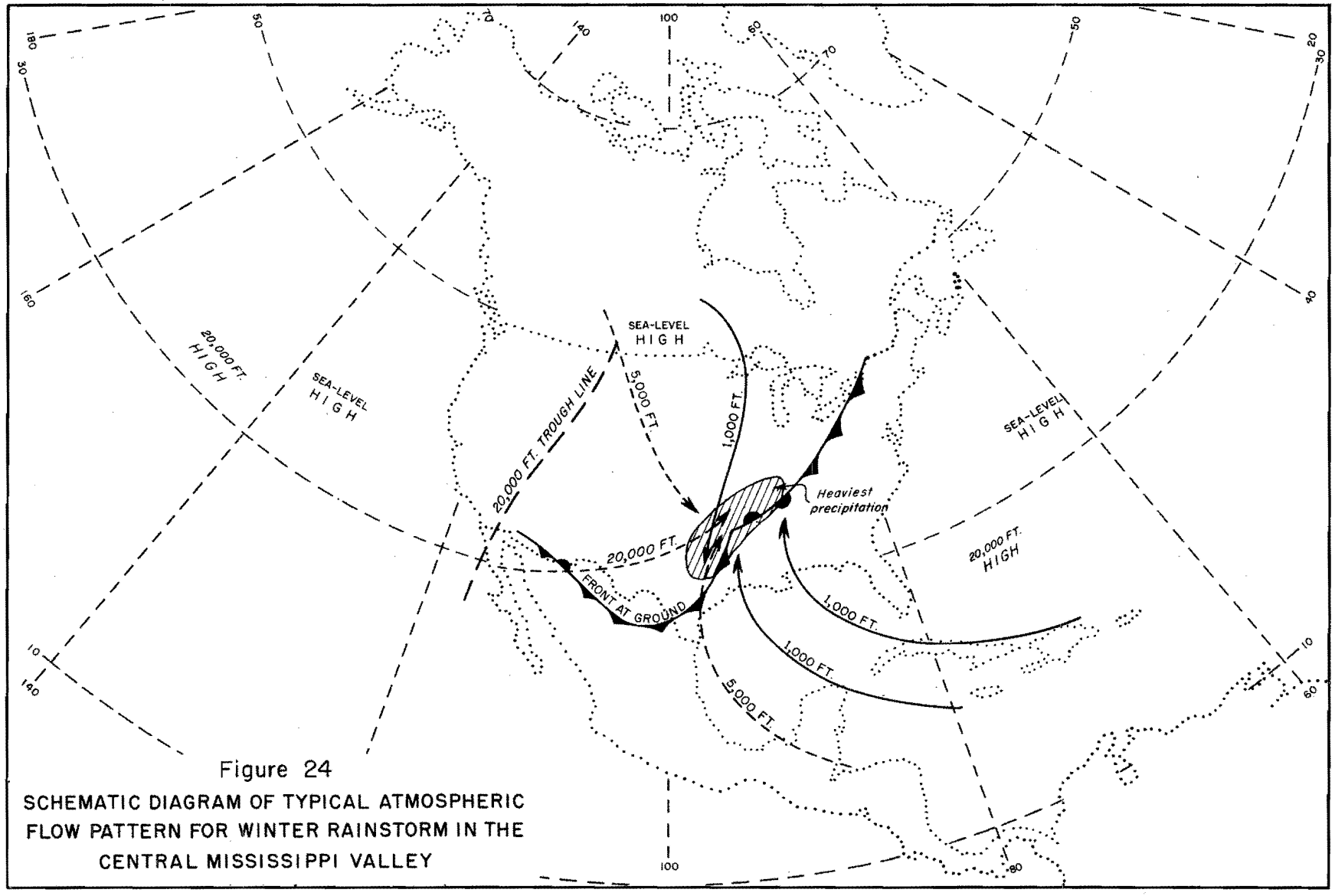

Figure 24

SCHEMATIC DIAGRAM OF TYPICAL ATMOSPHERIC FLOW PATTERN FOR WINTER RAINSTORM IN THE CENTRAL MISSISSIPPI VALLEY

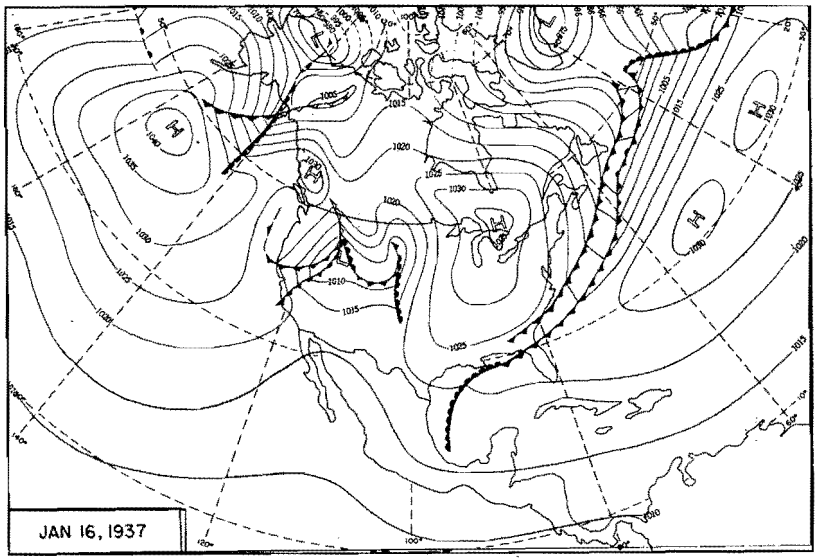

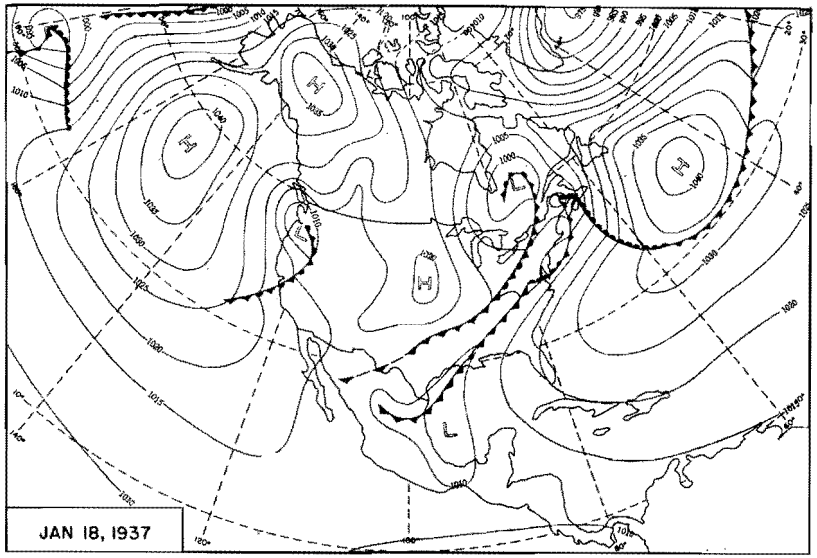

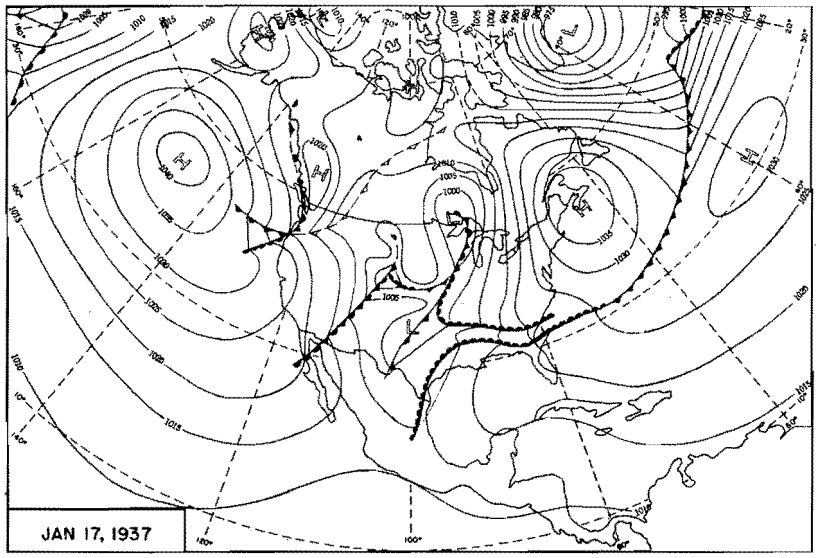

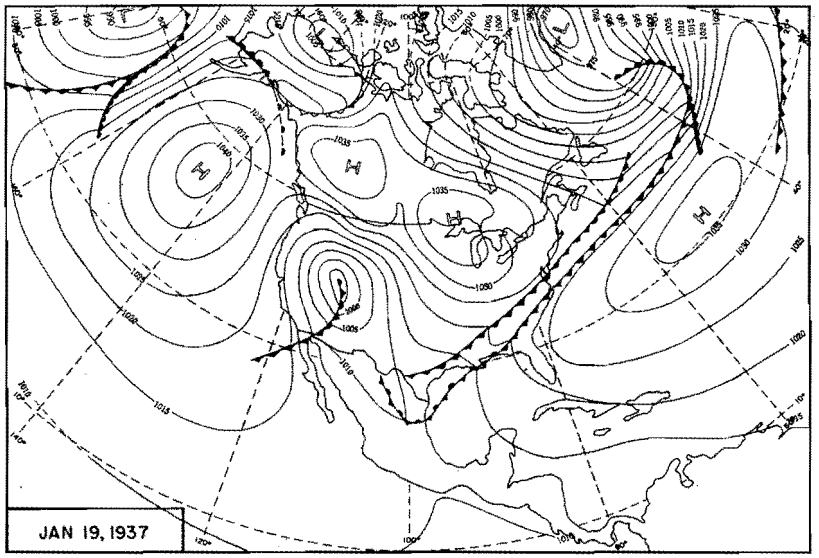

Figure 25. 0700 CST Northern Hemisphere Sea-Level Maps

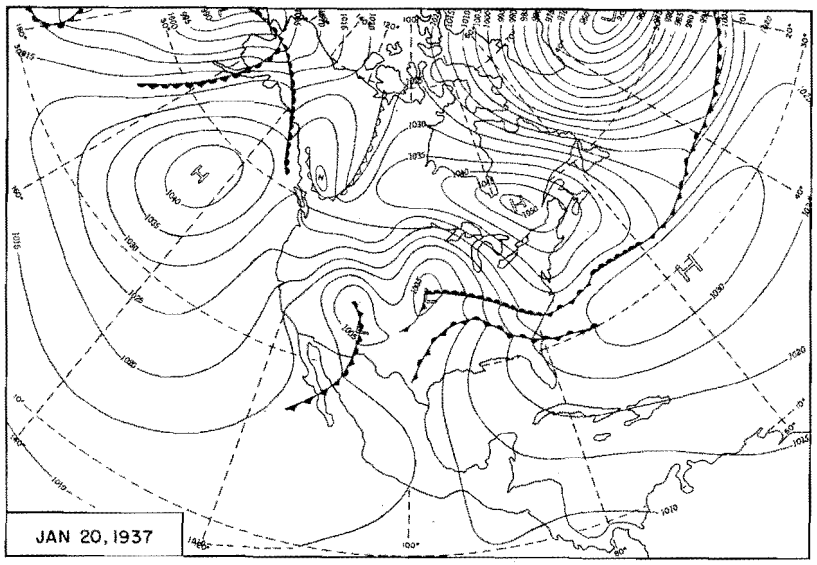

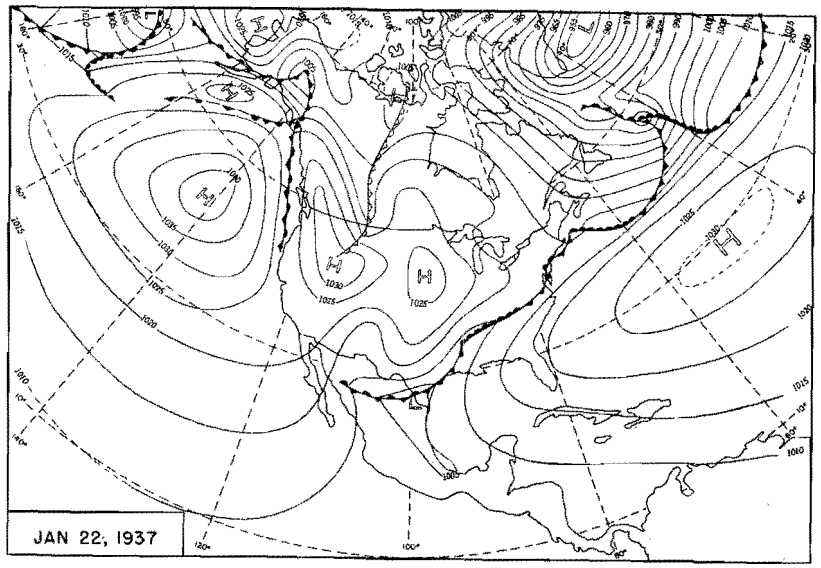

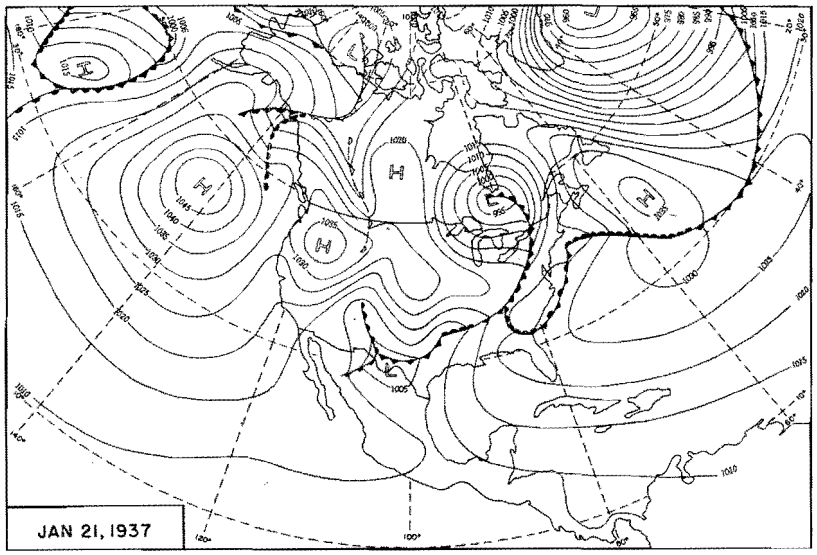

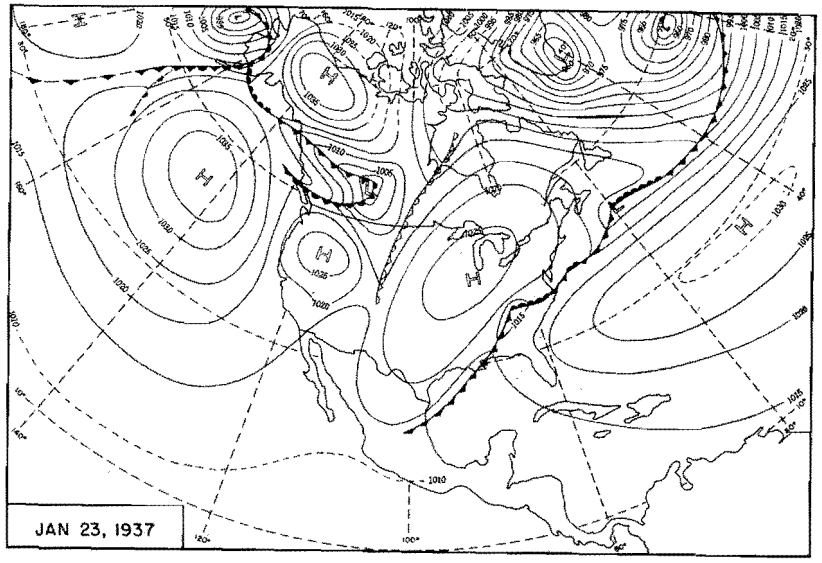

Figure 26. 0700 CST Northern Hemisphere Sea-Level Maps

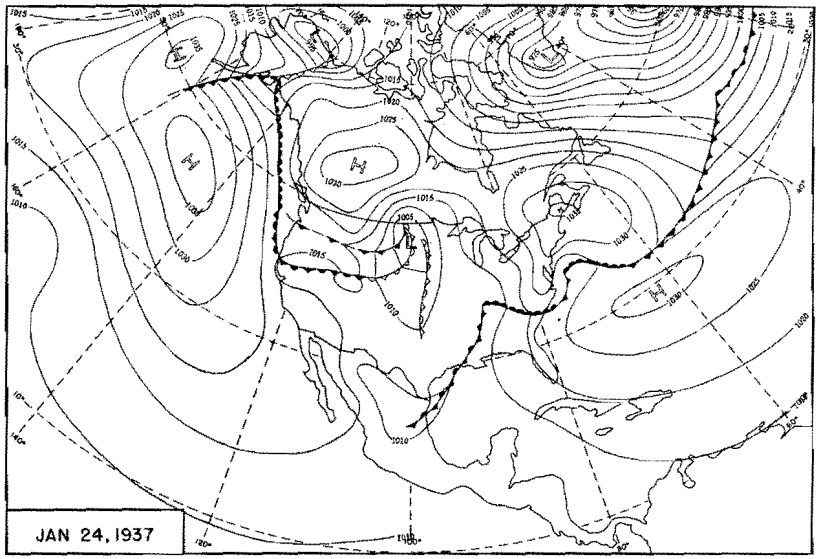

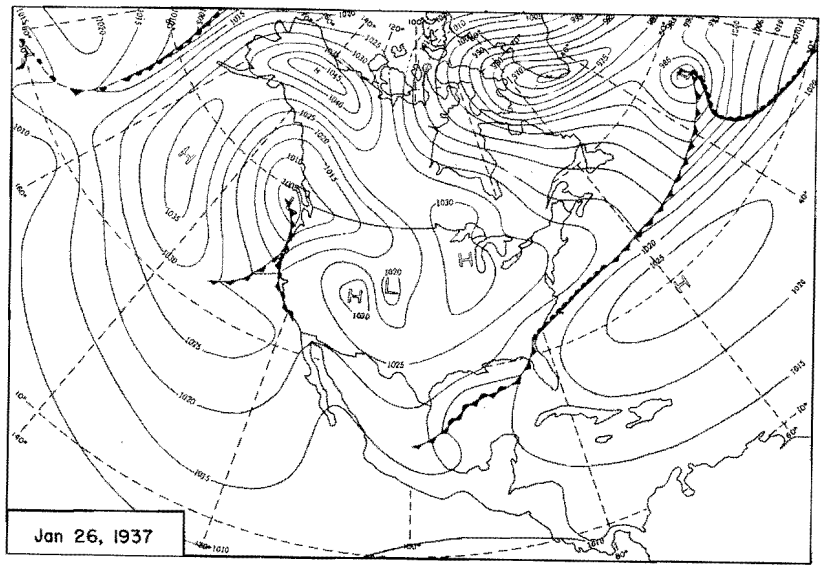

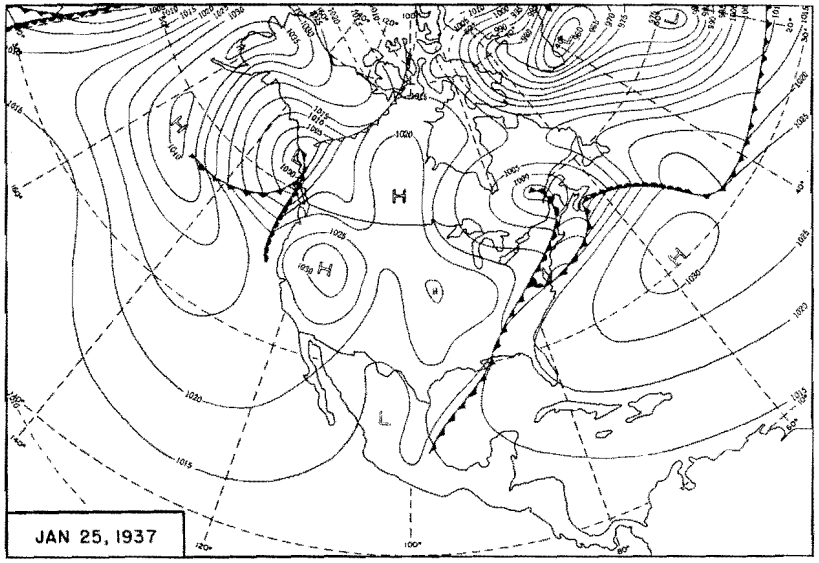

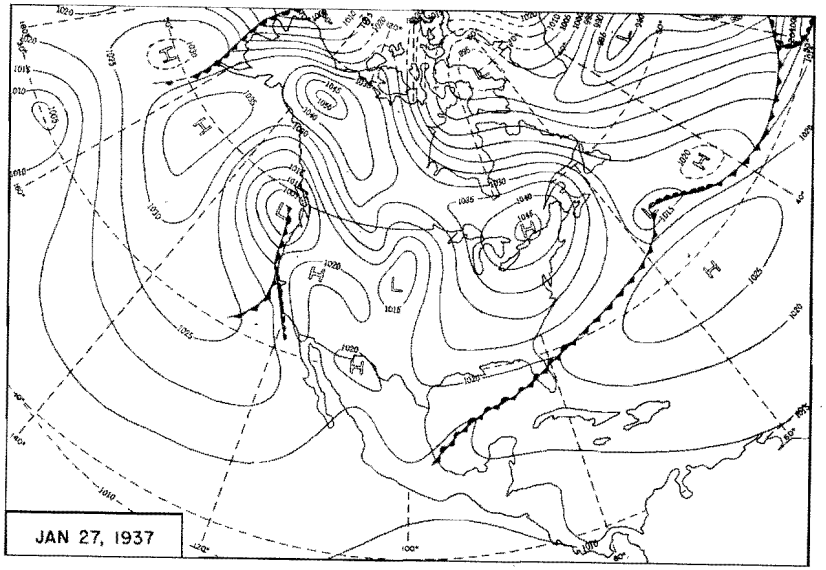

Figure 27. 0700 CST Northern Hemisphere Sea-Level Maps

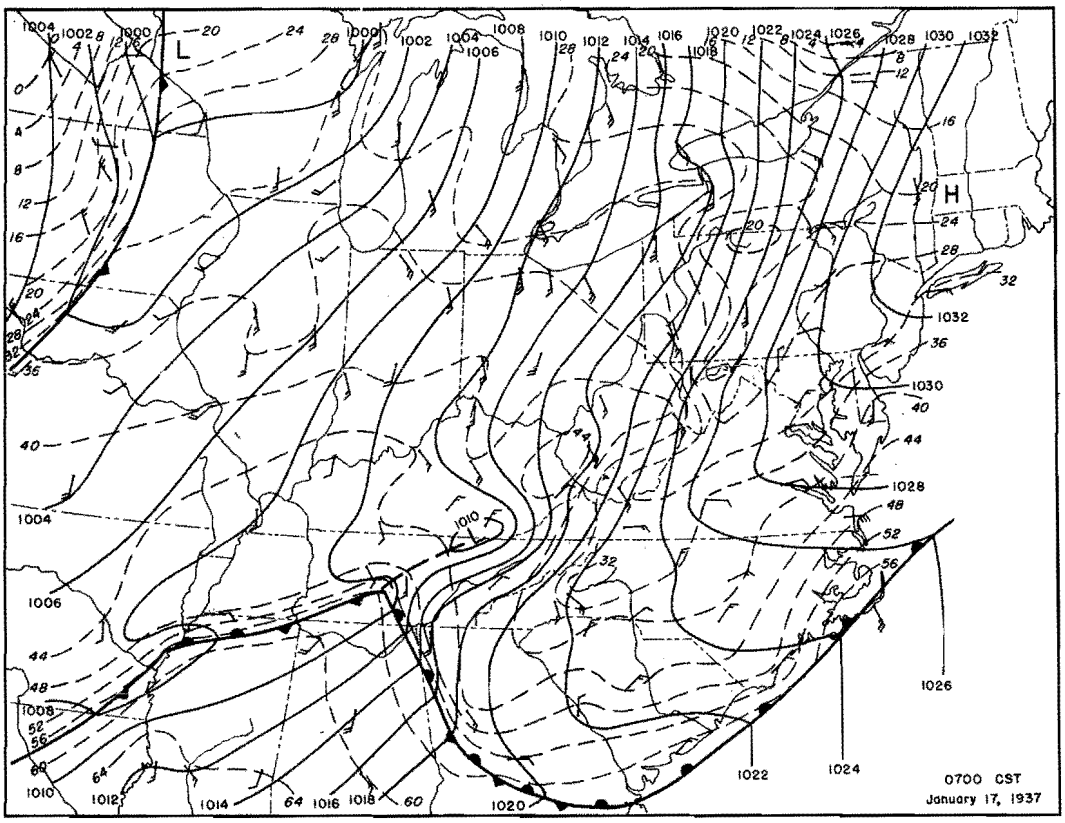

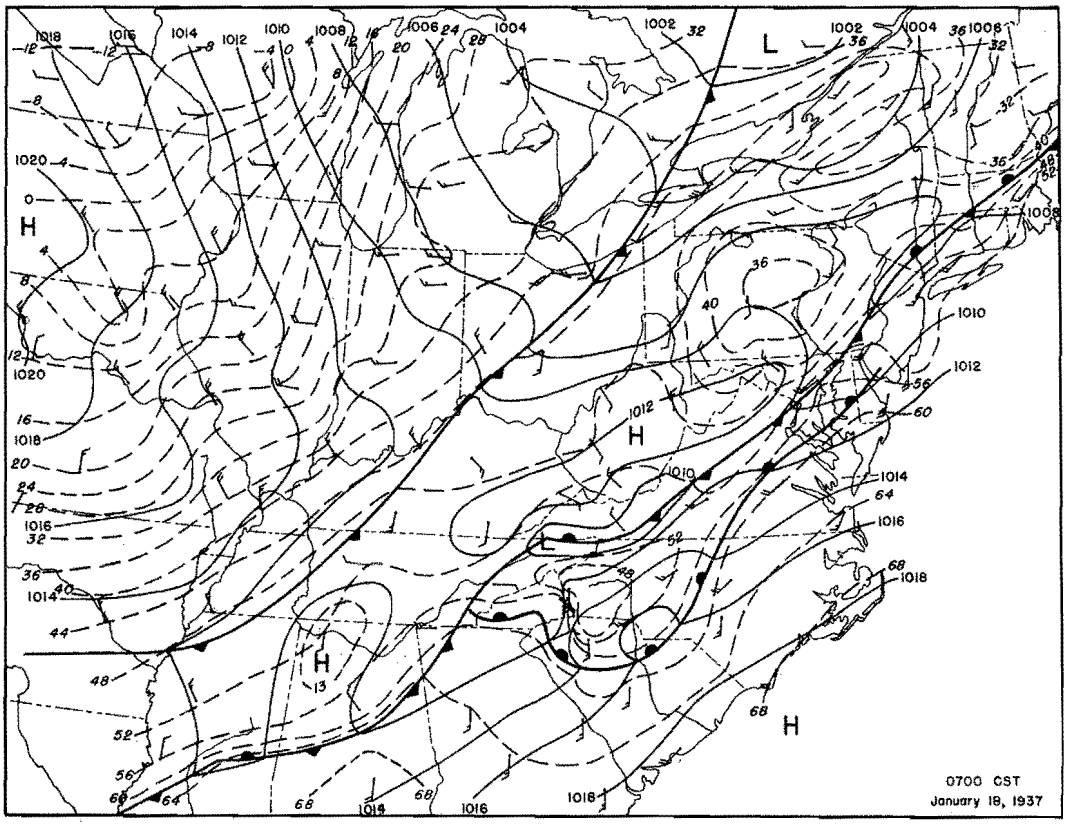

Figure 28. Detailed Surface Weather Maps

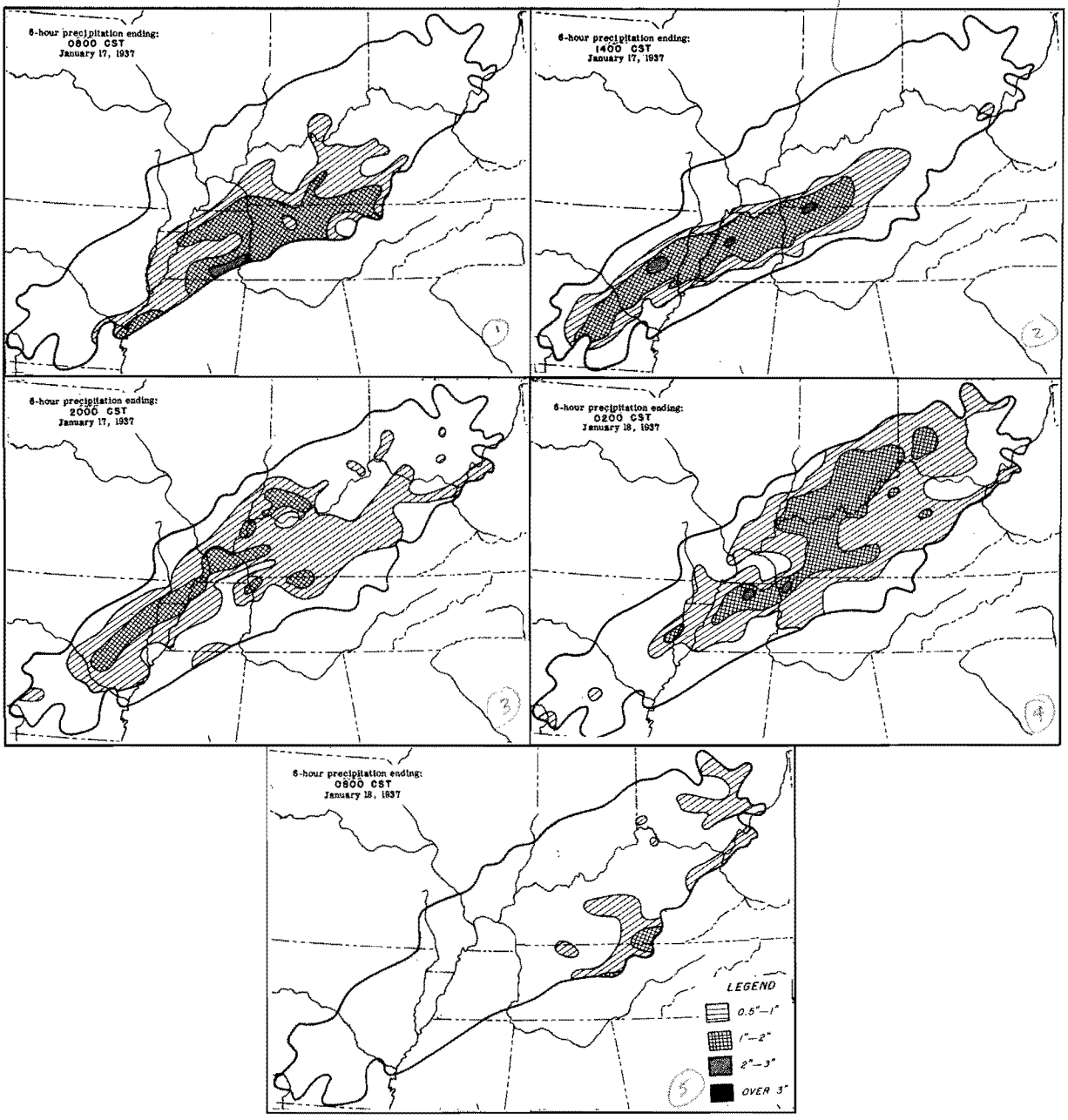

Figure 29. Incremental Isohyetal Patterns

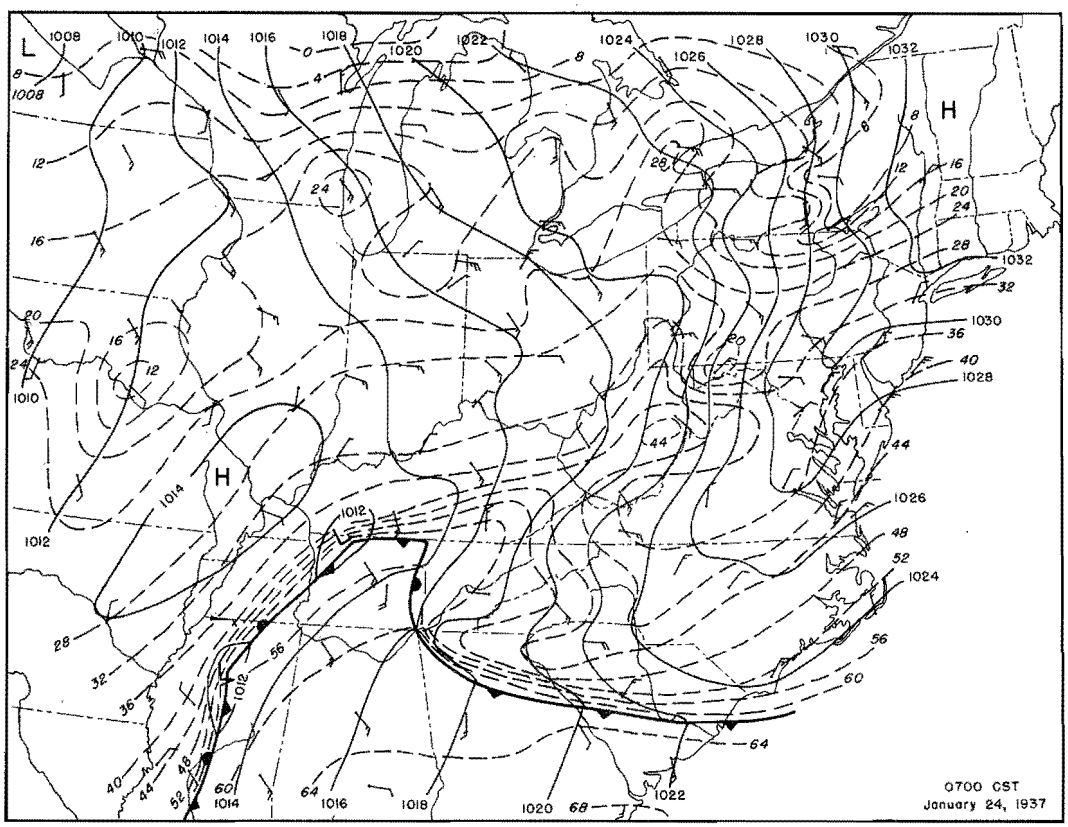

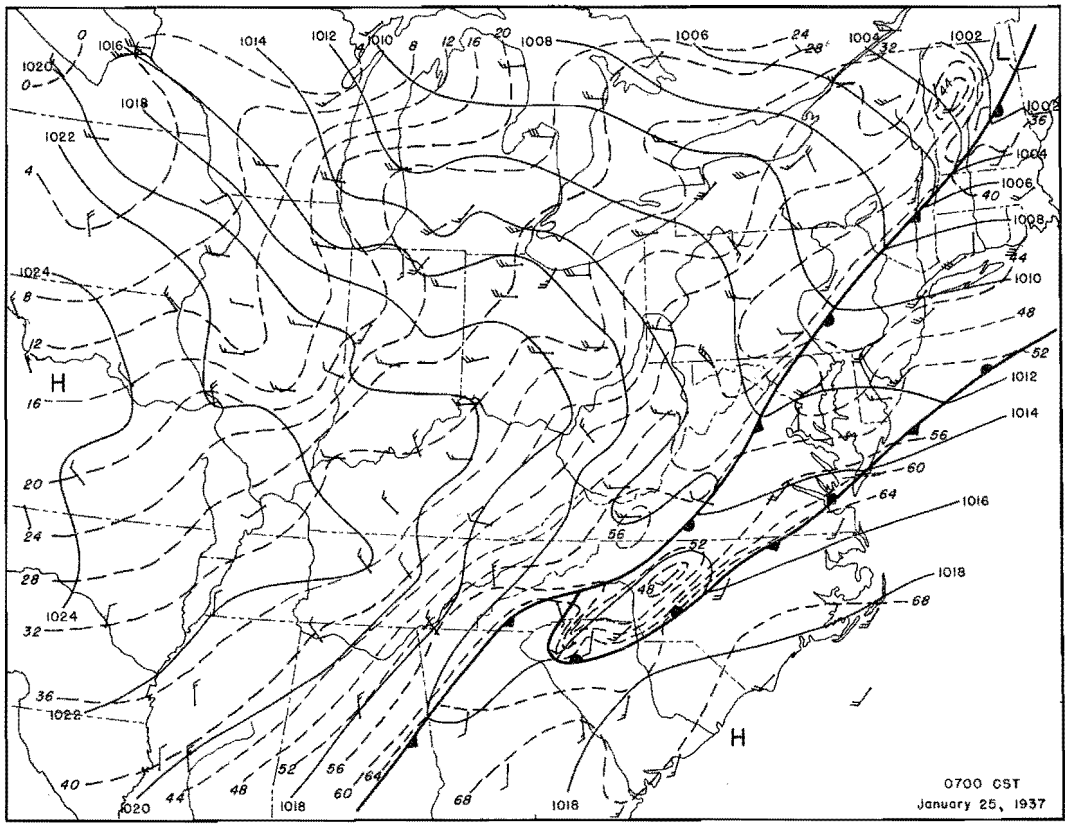

Figure 30 Detailed Surface Weather Maps

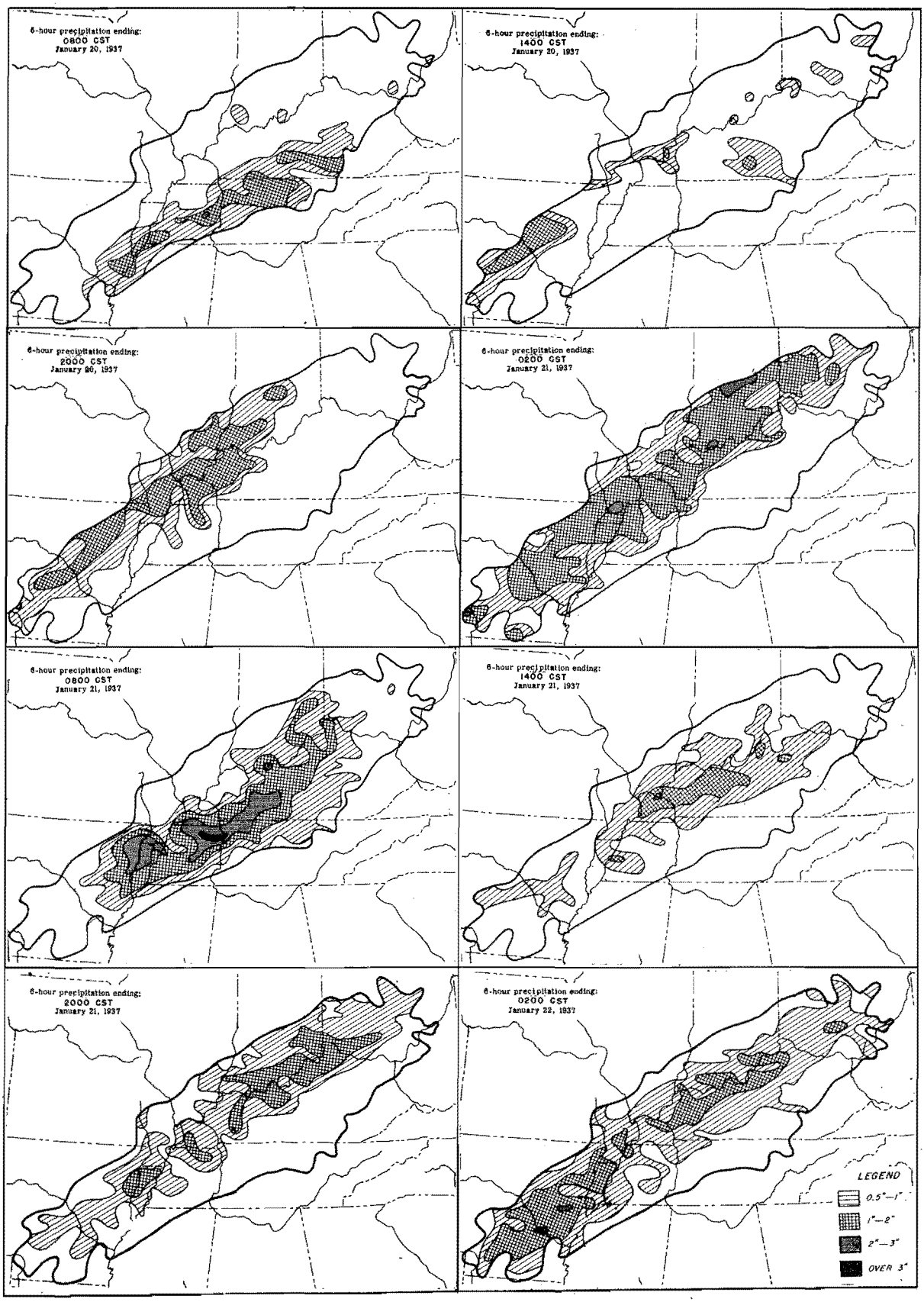

Figure 31. Incremental Isohyetal Patterns

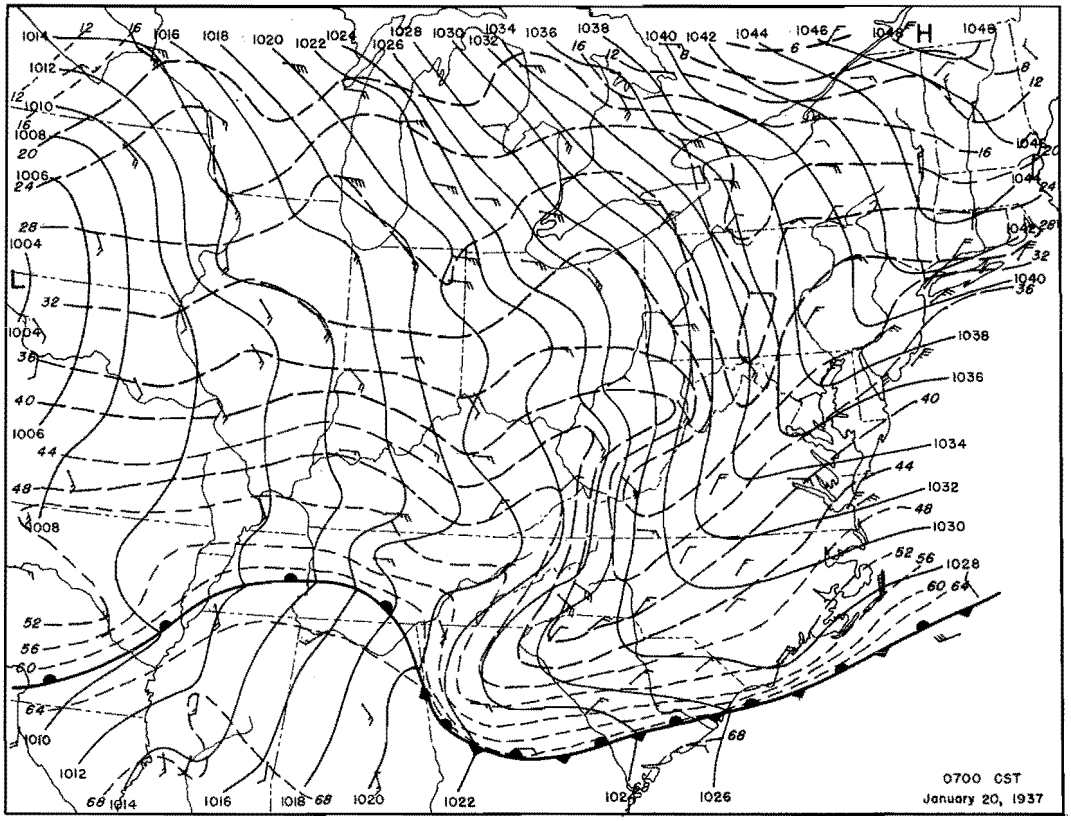

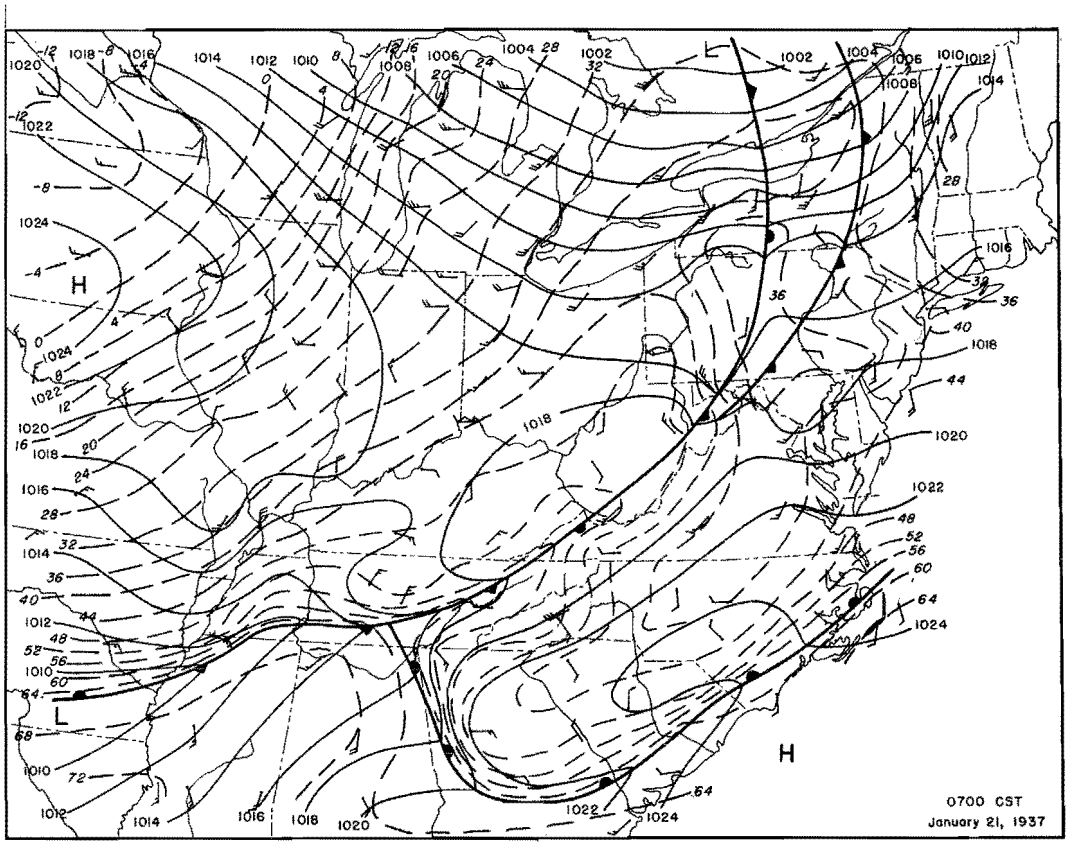

Figure 32. Detailed Surface Weather Maps

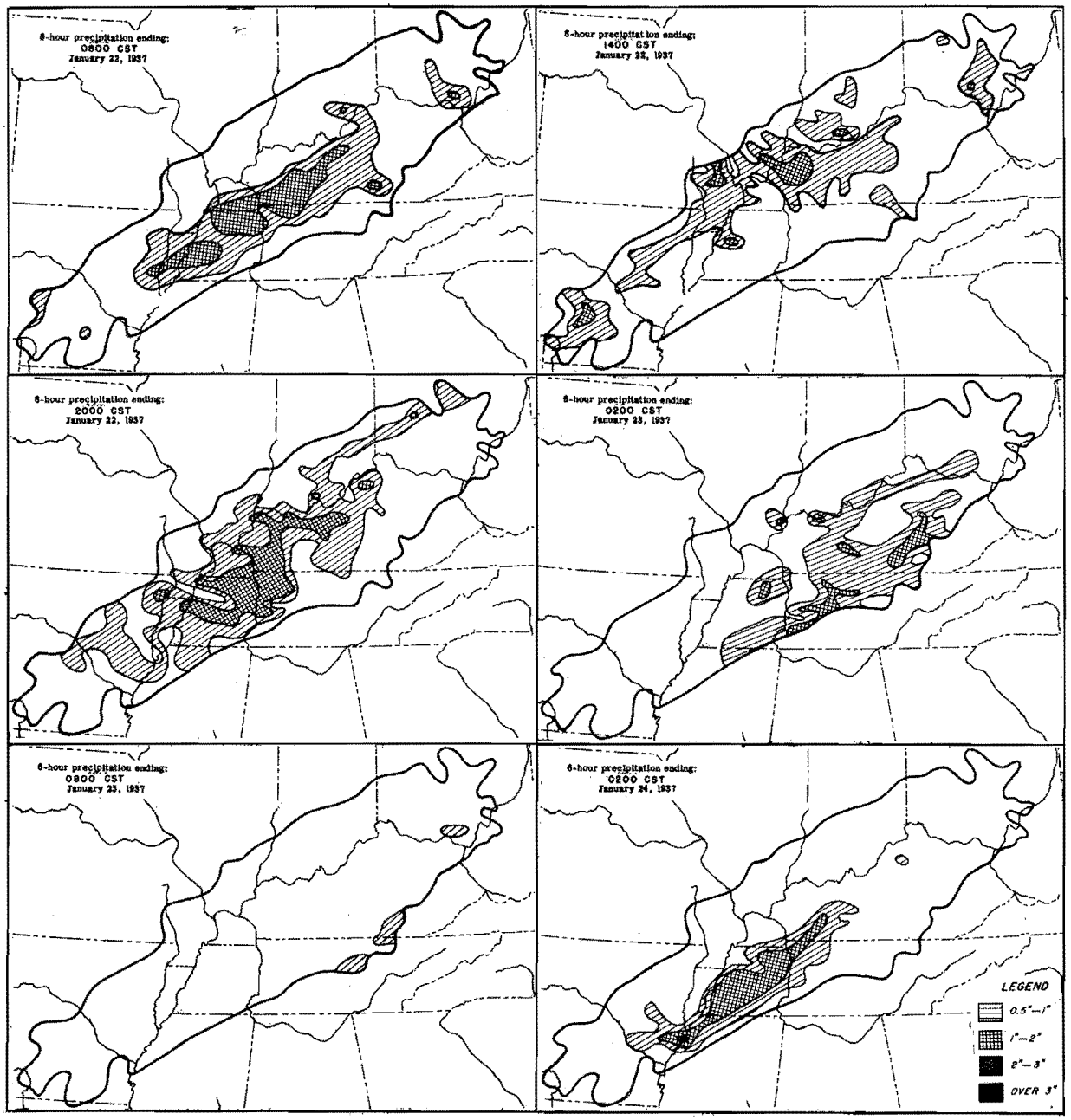

Figure 33. Incremental Isohyetal Patterns

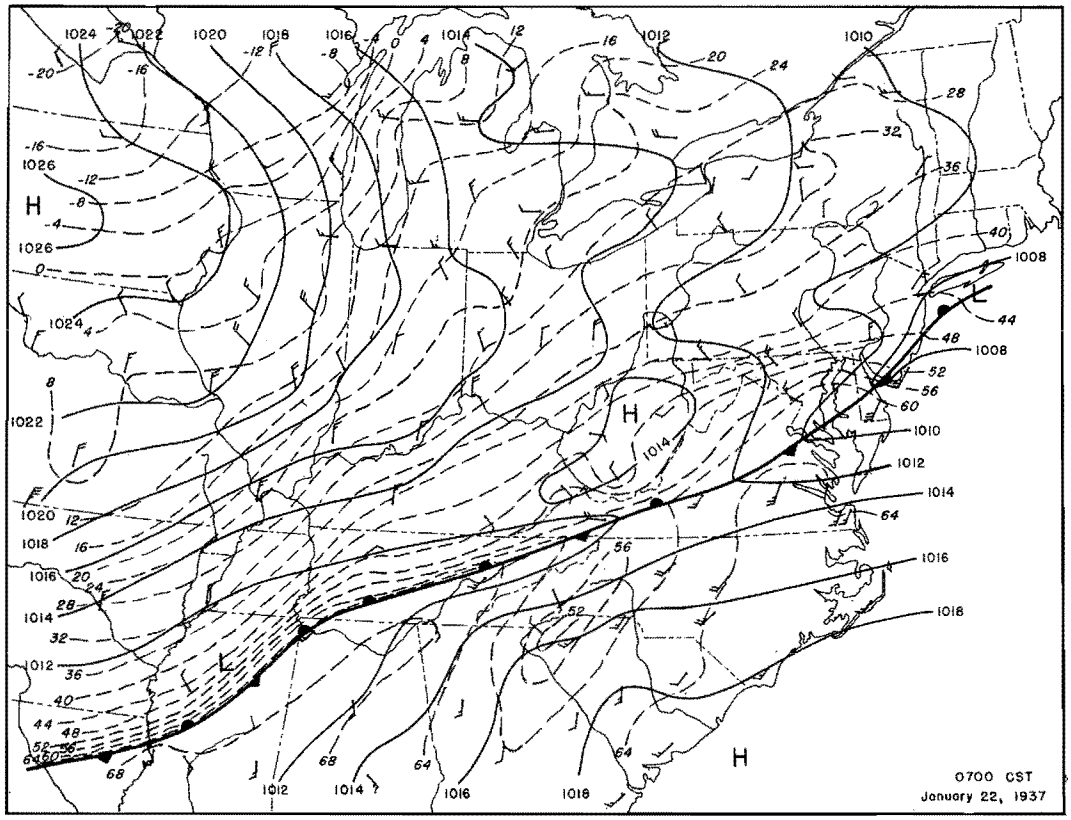

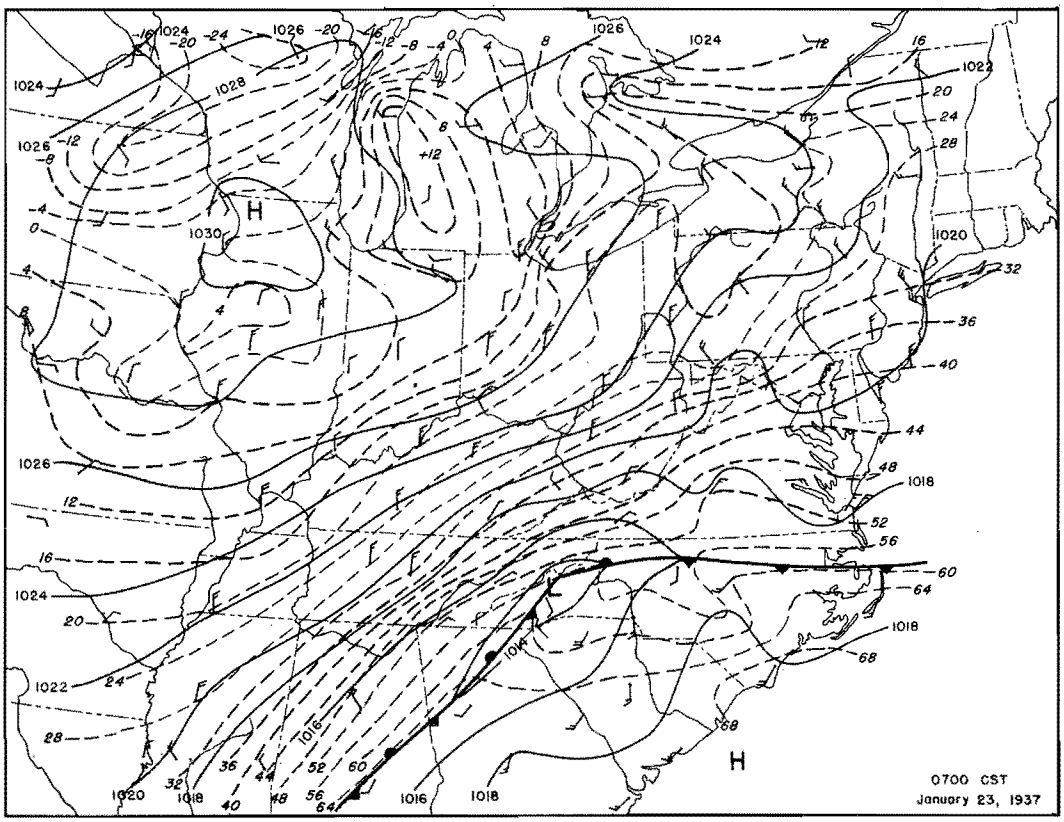

Figure 34. Detailed Surface Weather Maps

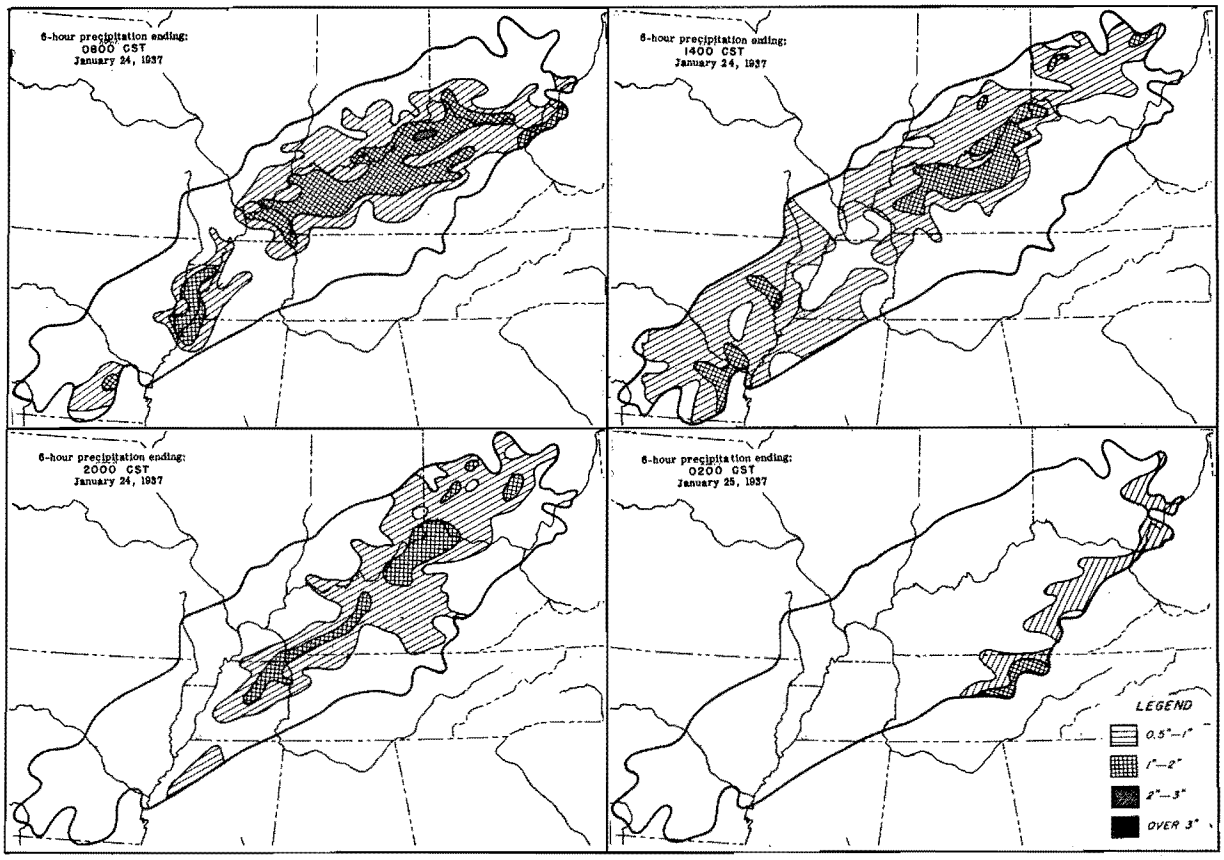

Figure 35. Incremental Isohyetal Patterns

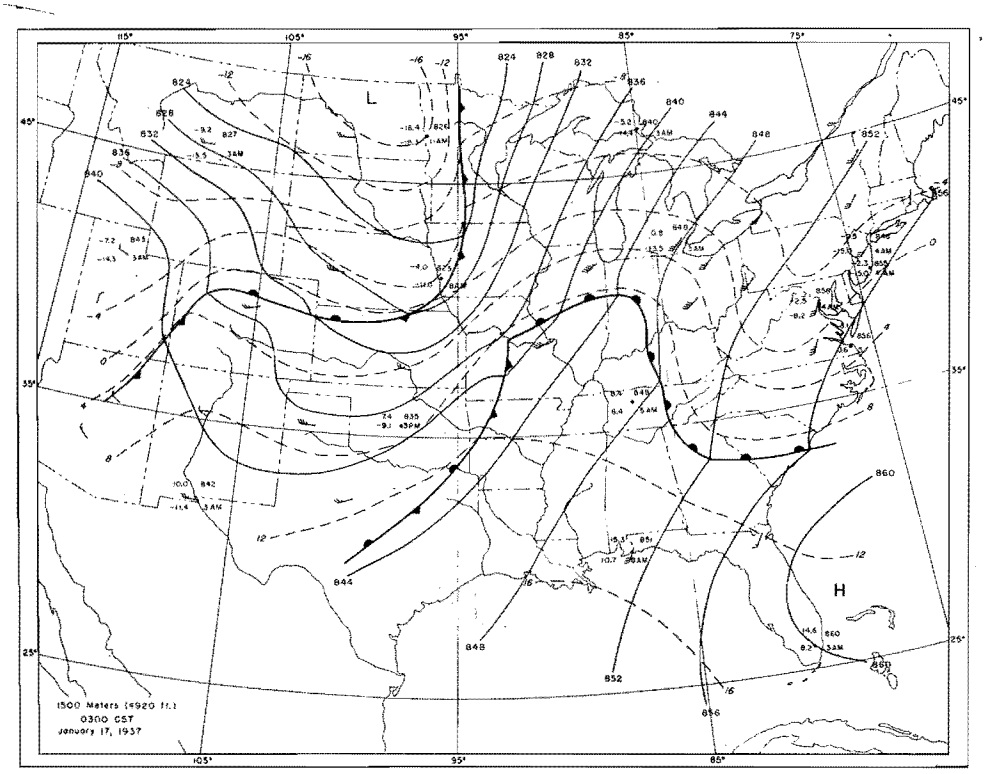

Figure 36. Constant Level Charts

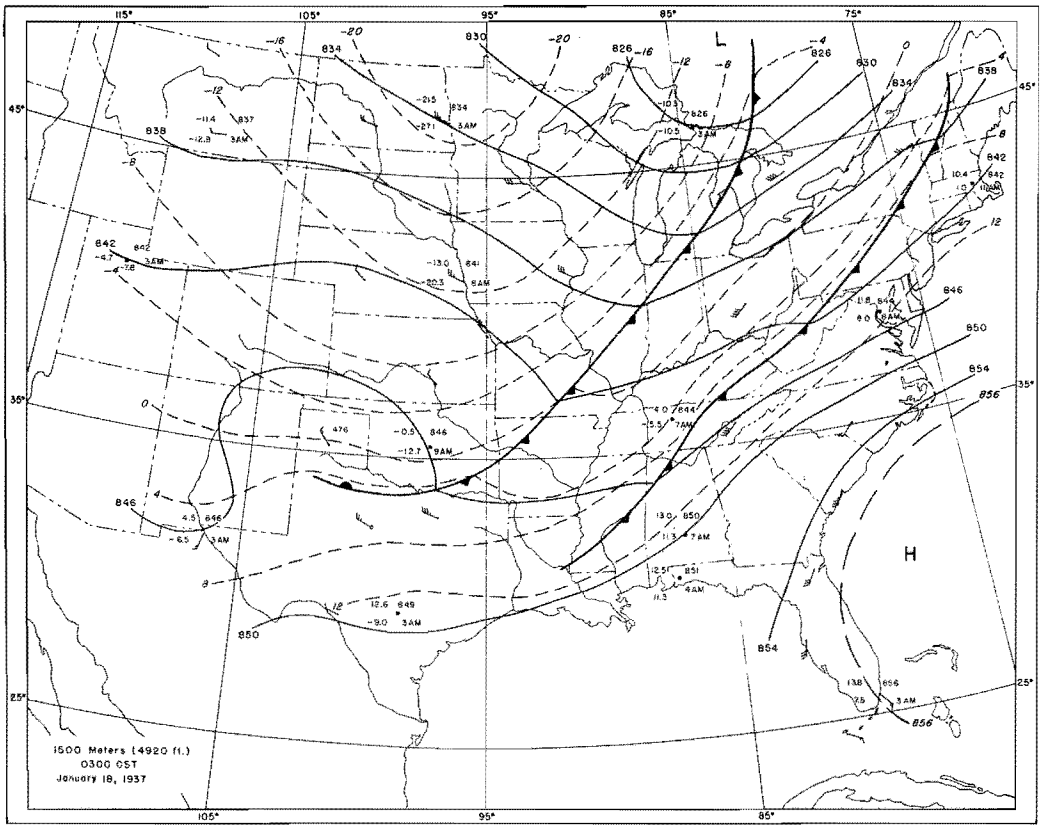

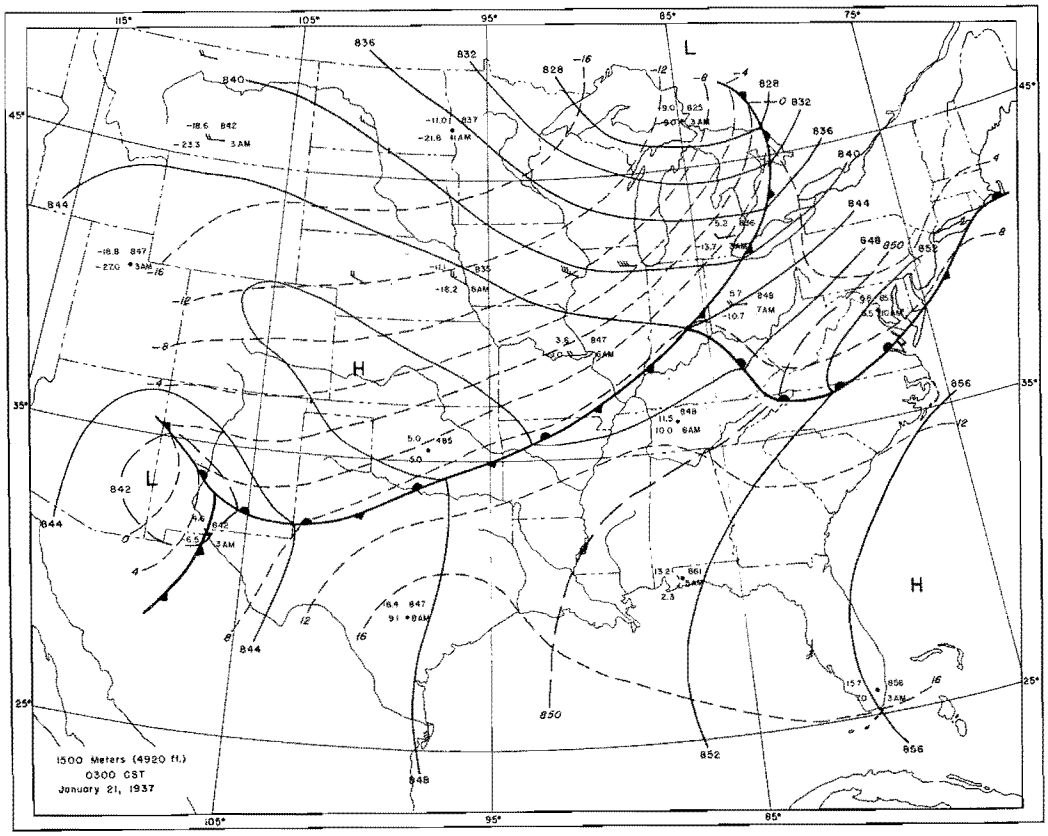

Figure 37. Constant Level Charts

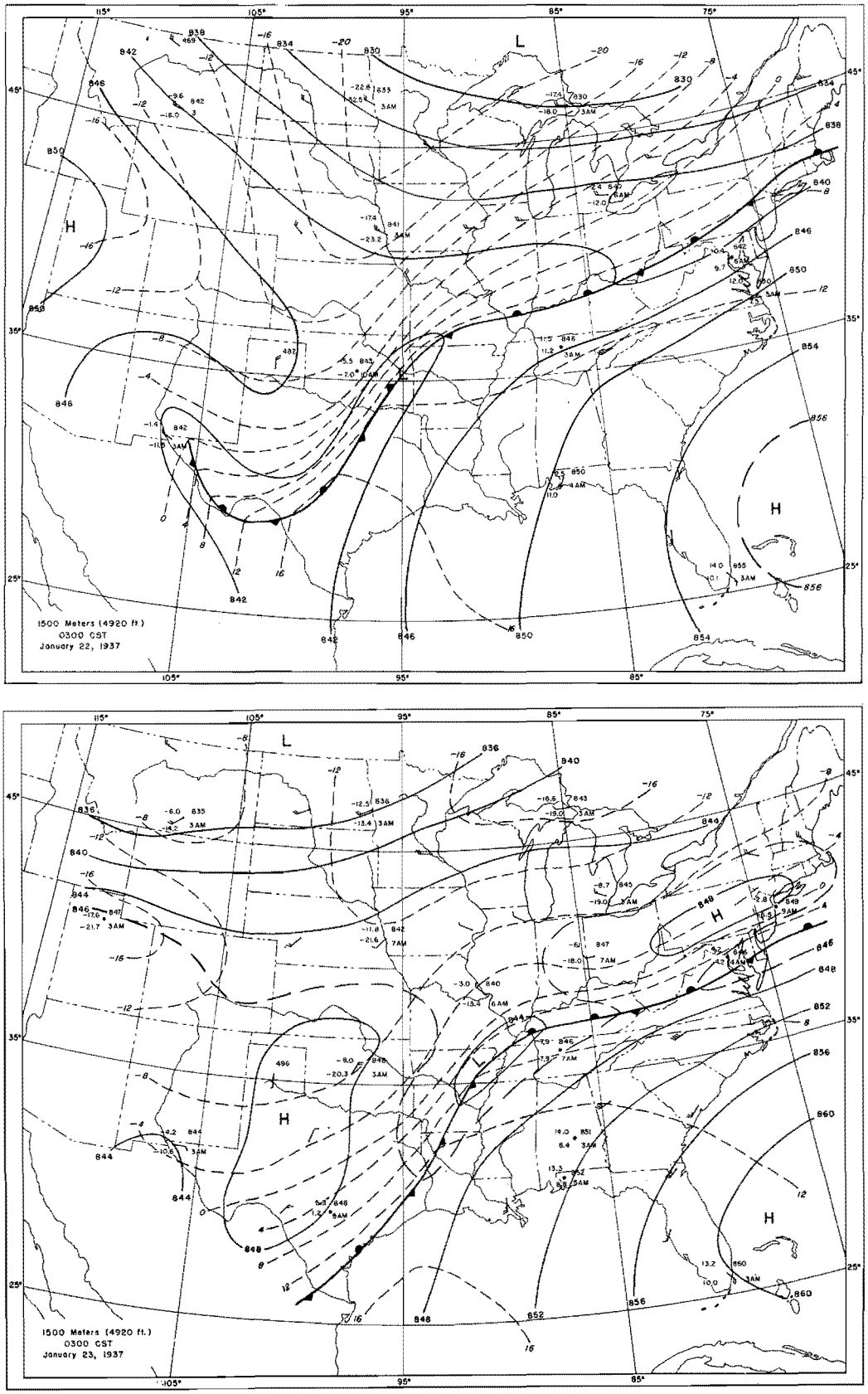

Figure 38. Constant Level Charts

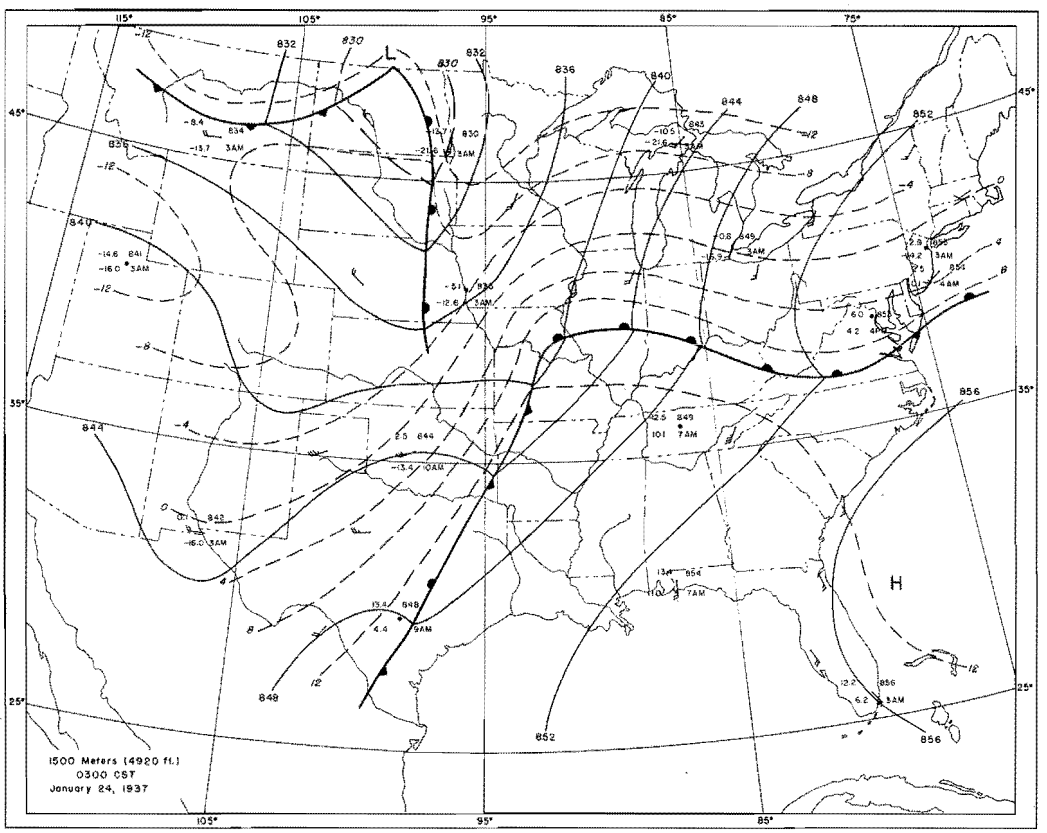

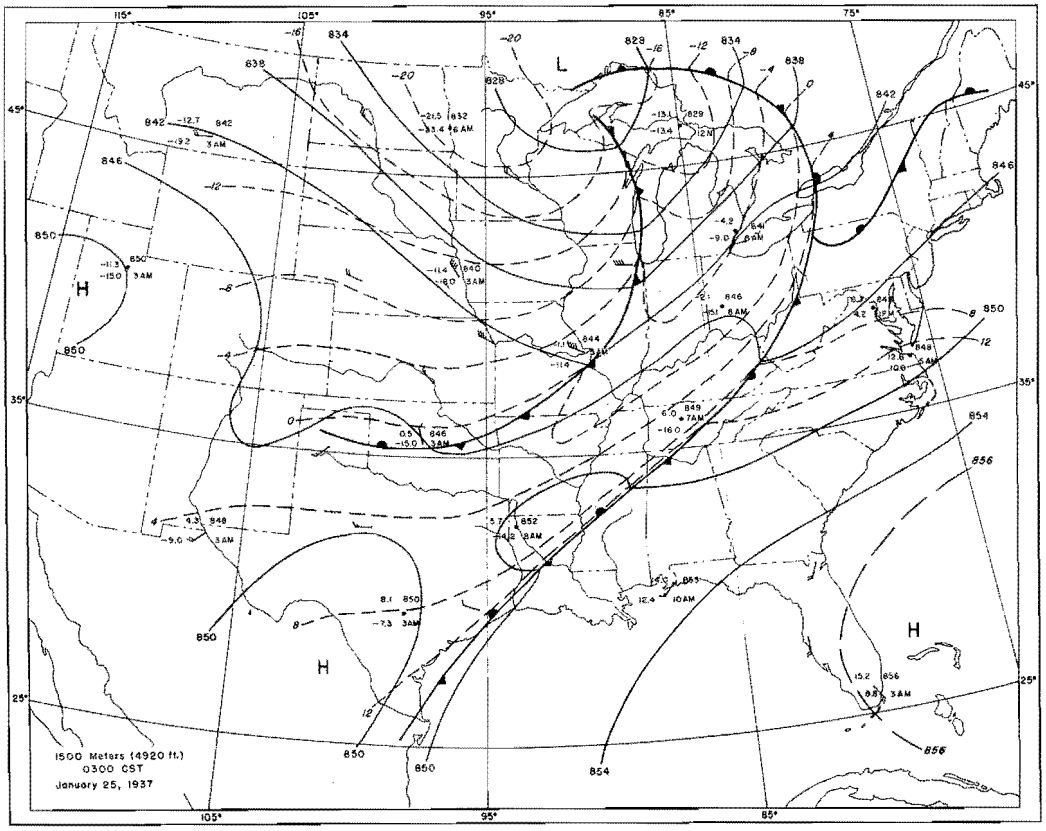

Figure 39. Constant Level Charts

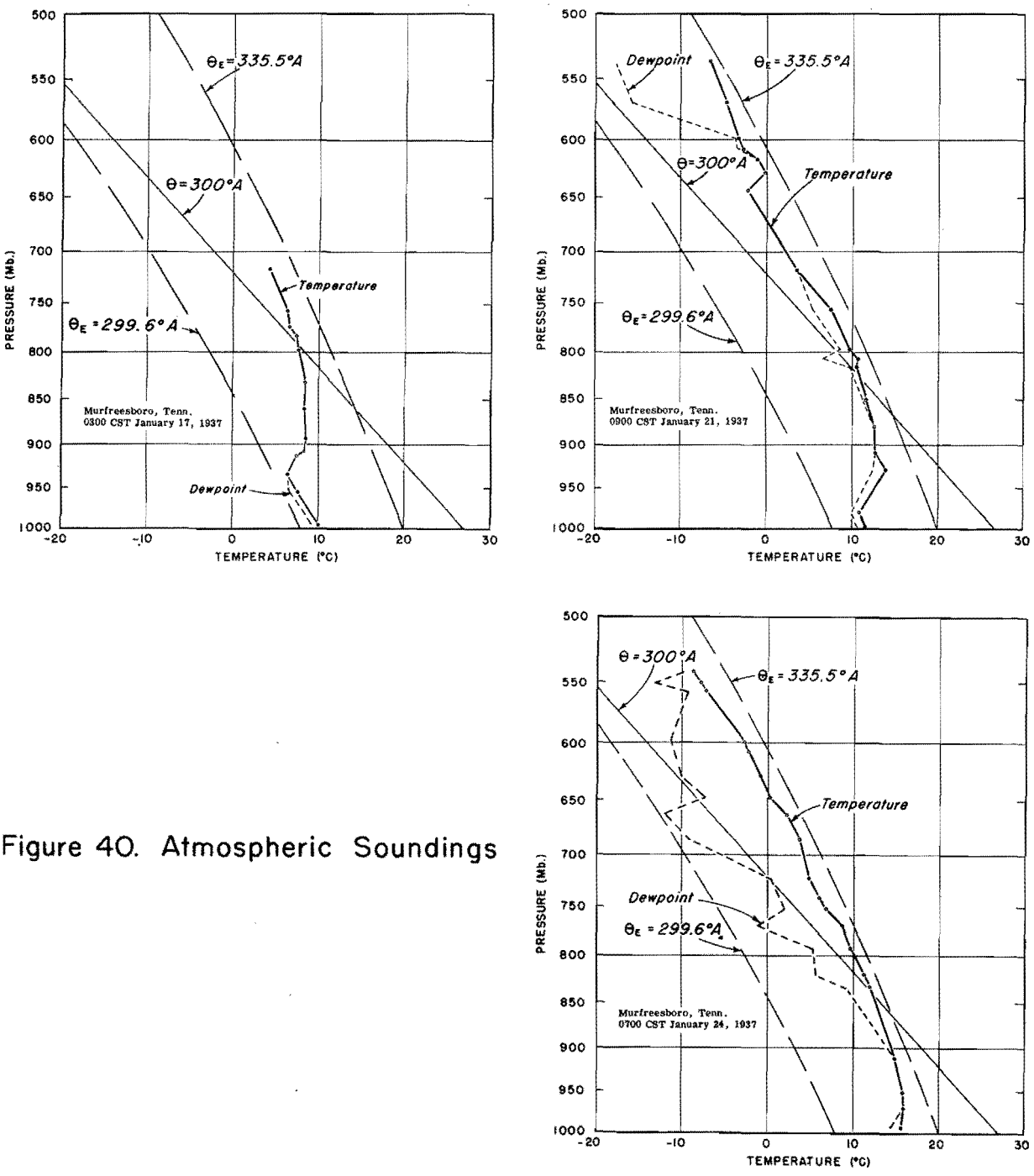

Figure 40. Atmospheric Soundings

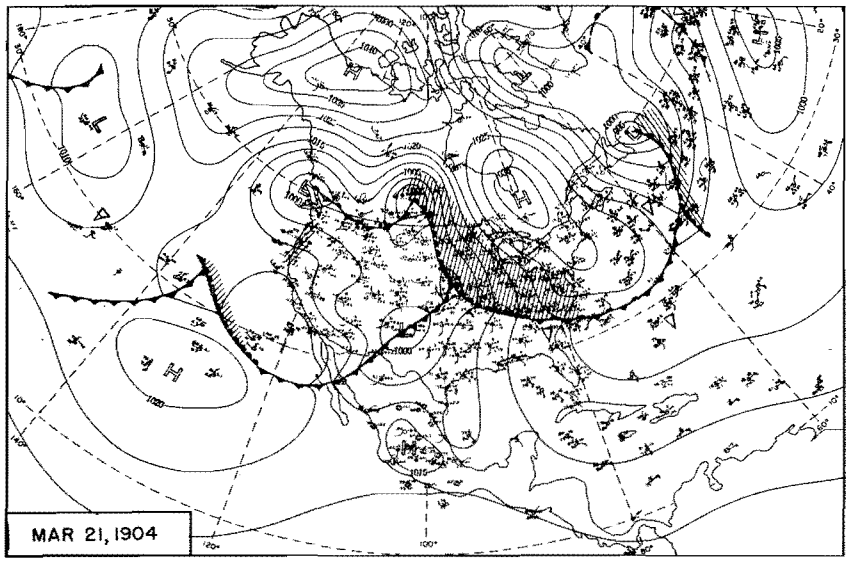

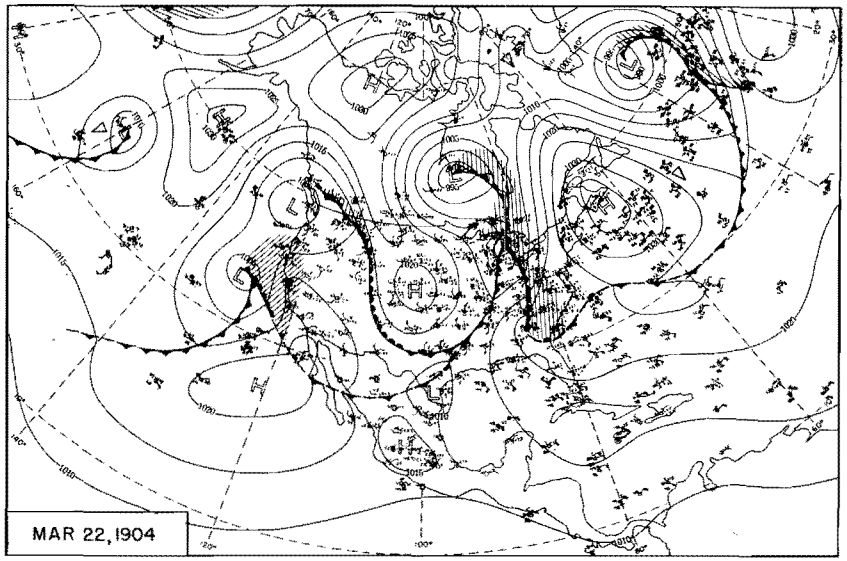

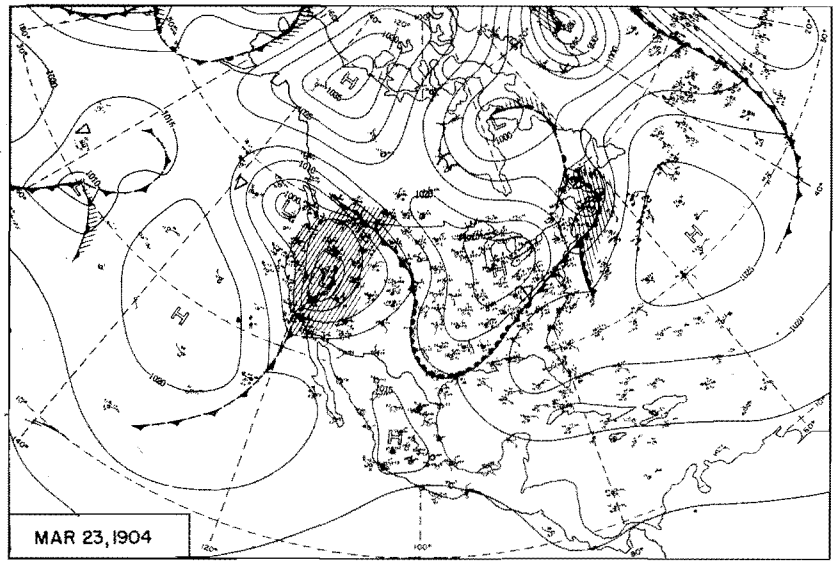

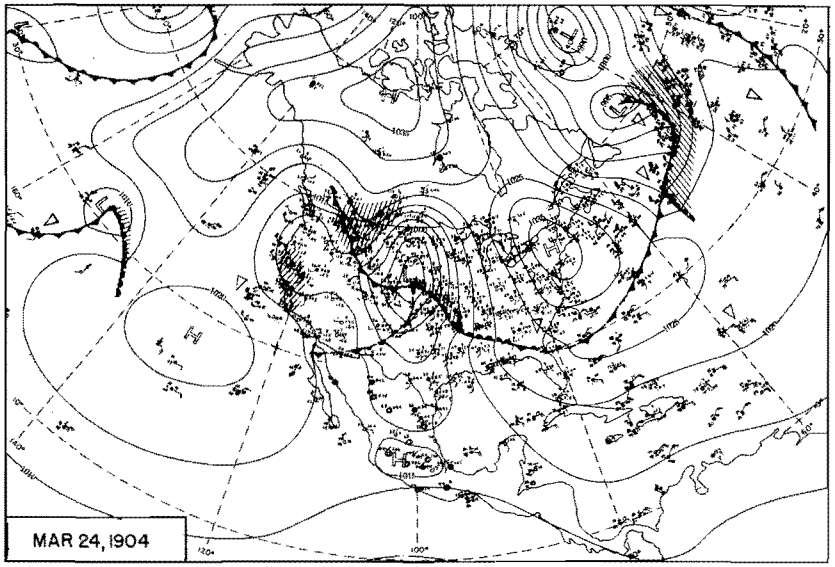

Figure 41. 0700 CST Northern Hemisphere Sea-Level Maps

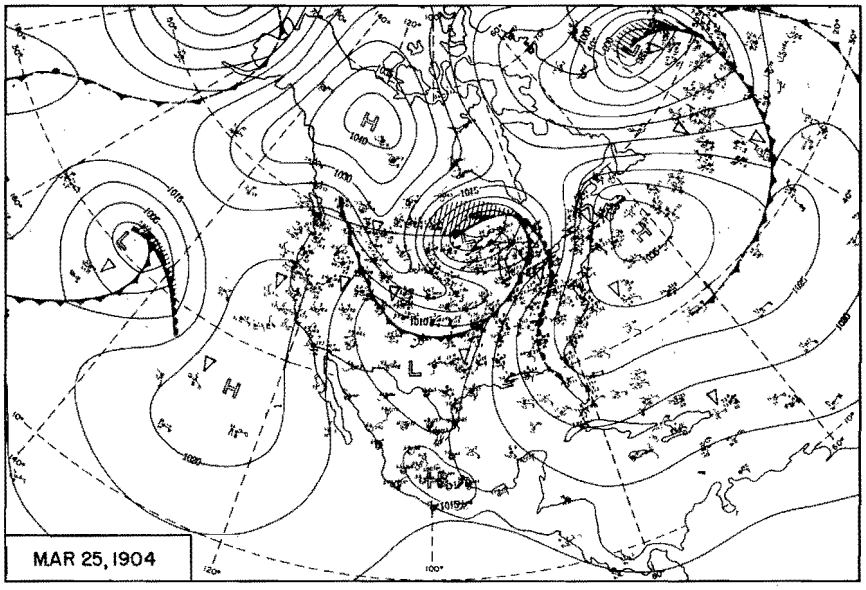

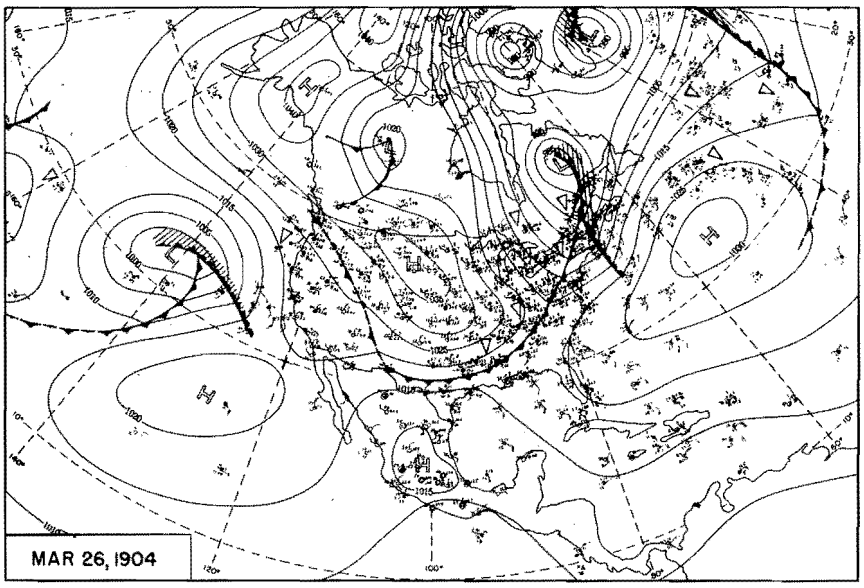

Figure 42. 0700 CST Northern Hemisphere Sea—Level Maps

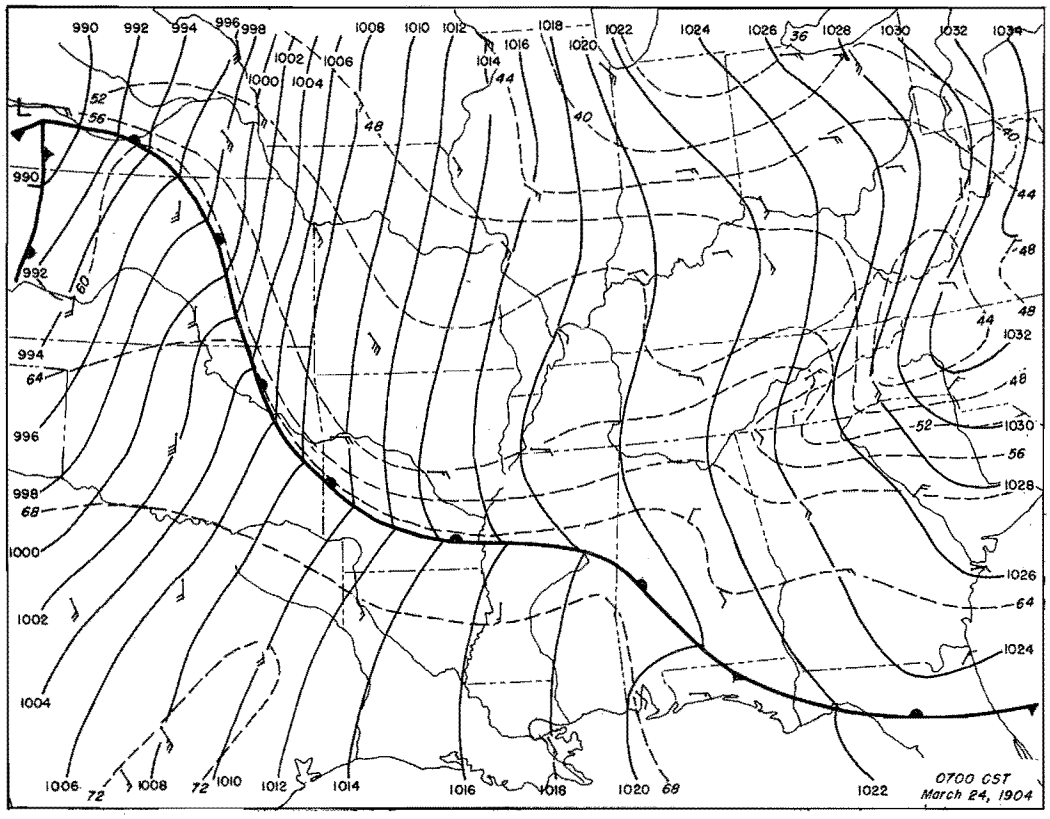

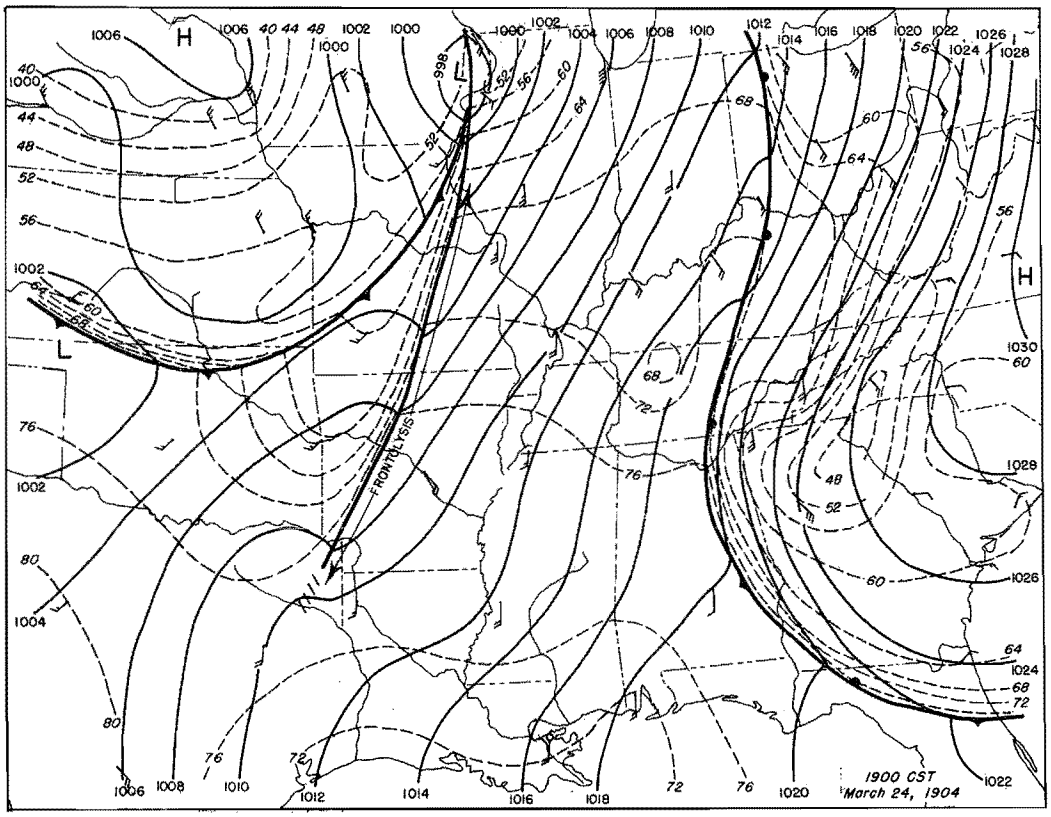

Figure 43. Detailed Surface Weather Maps

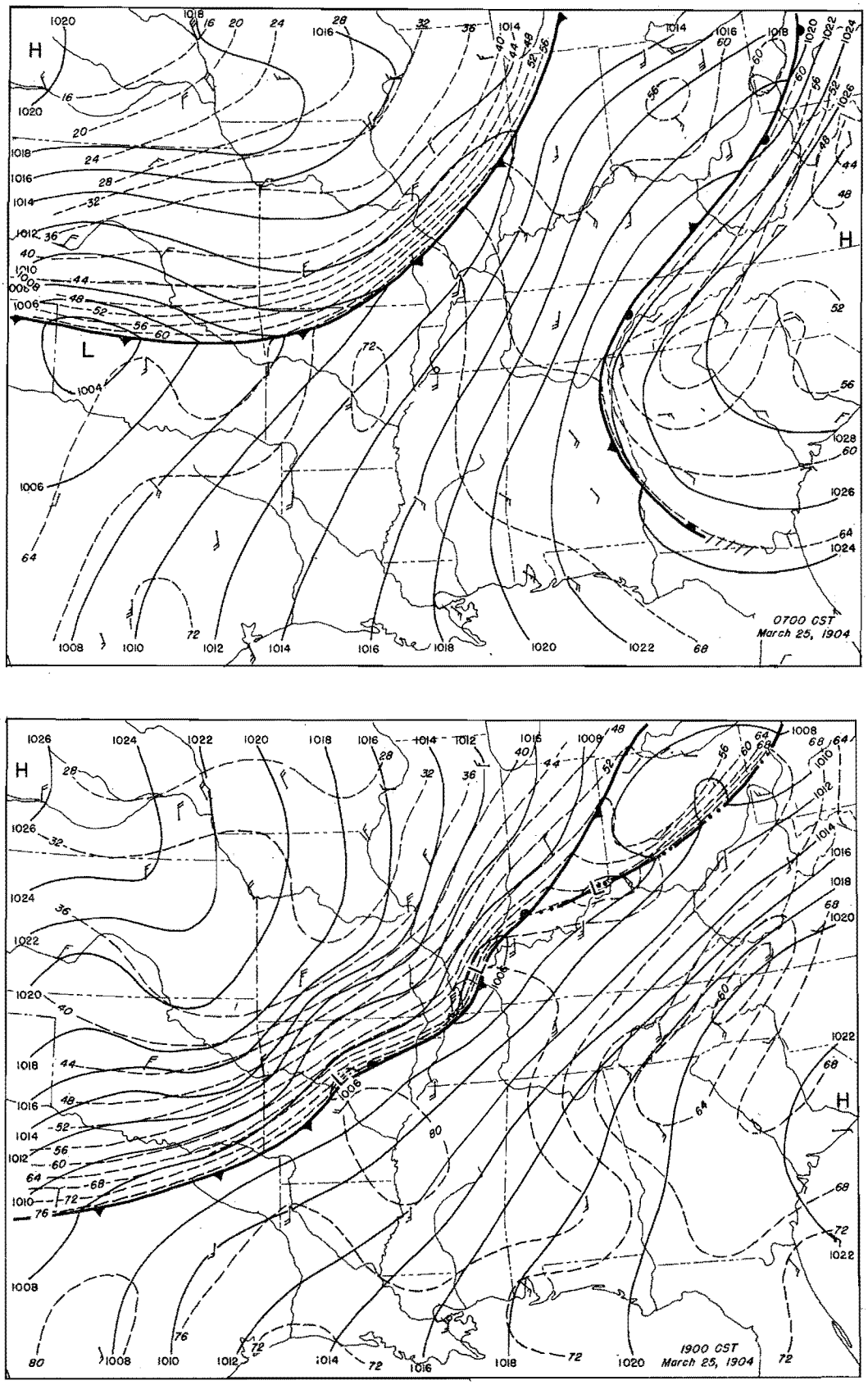

Figure 44. Detailed Surface Weather Maps.

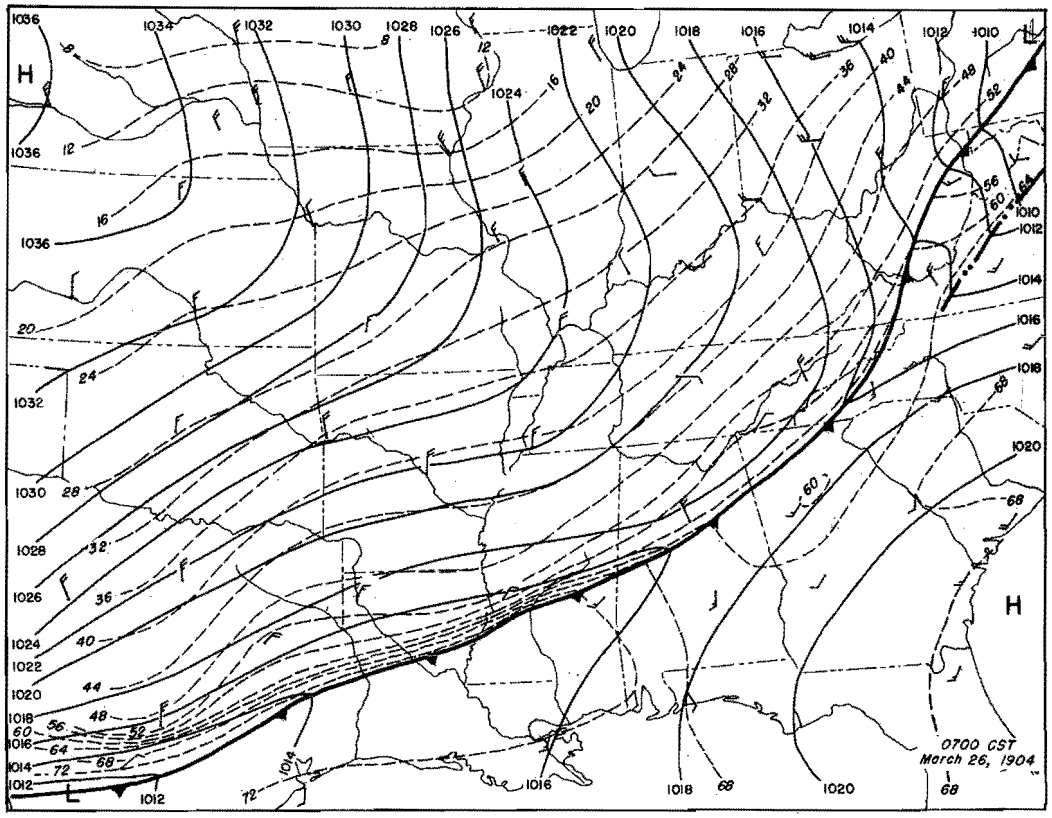

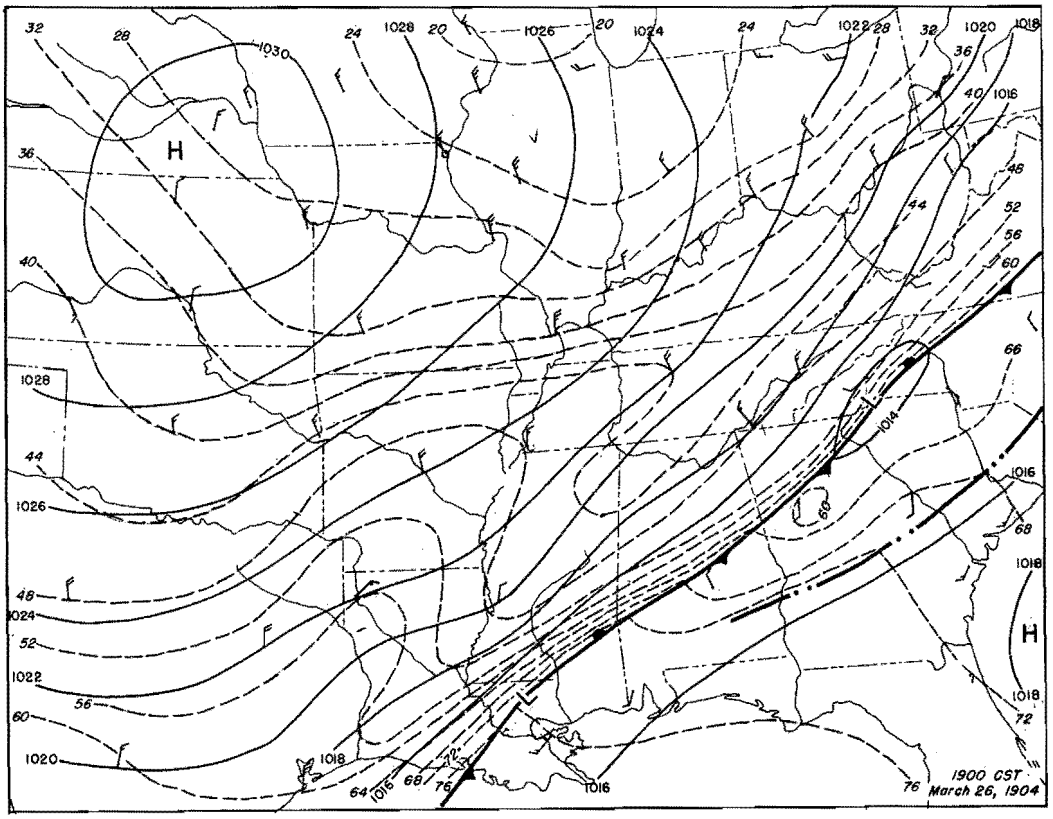

Figure 45. Detailed Surface Weather Maps

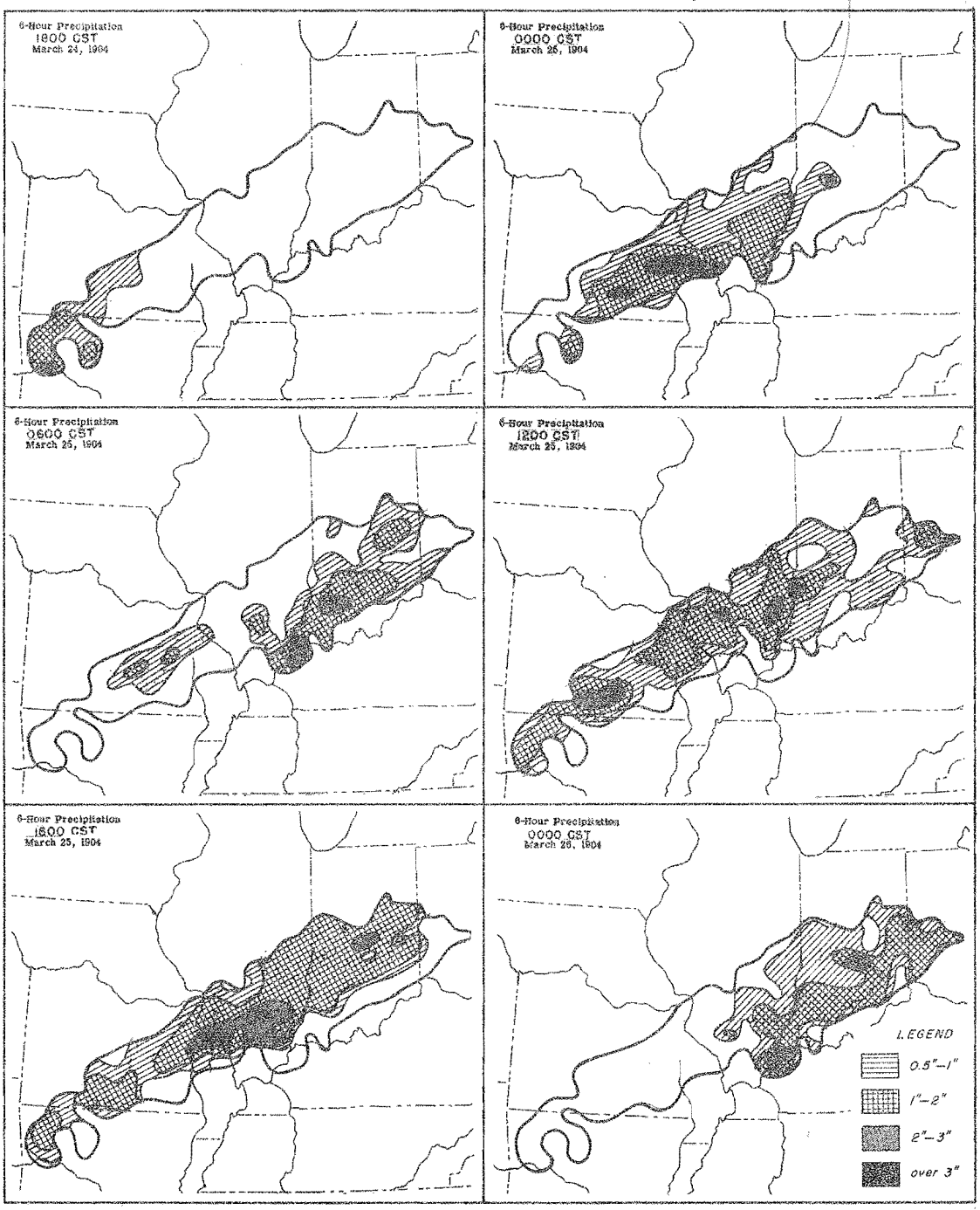

Figure 46. Incremental Isohyetal Patterns

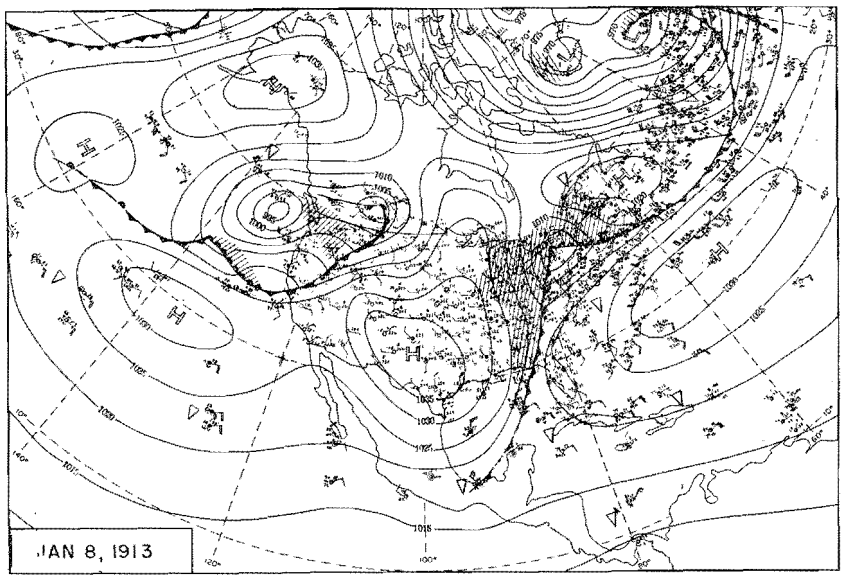

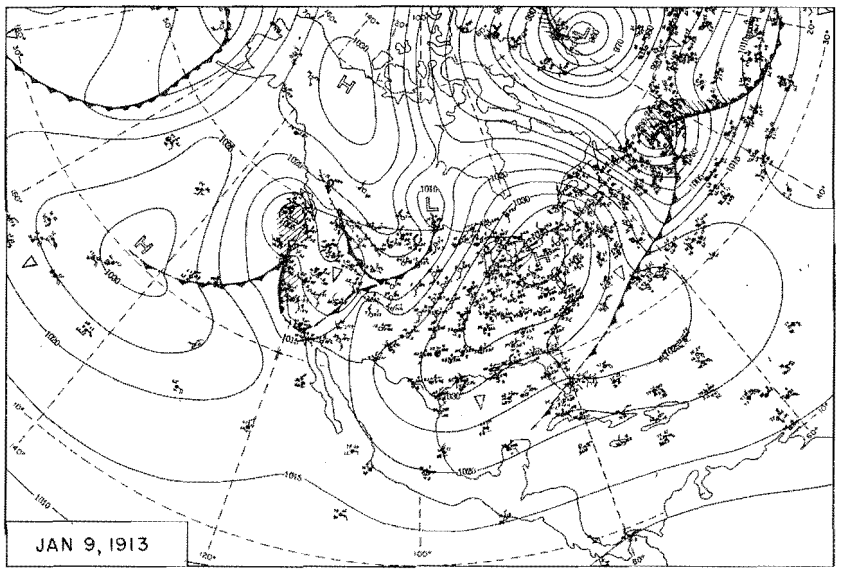

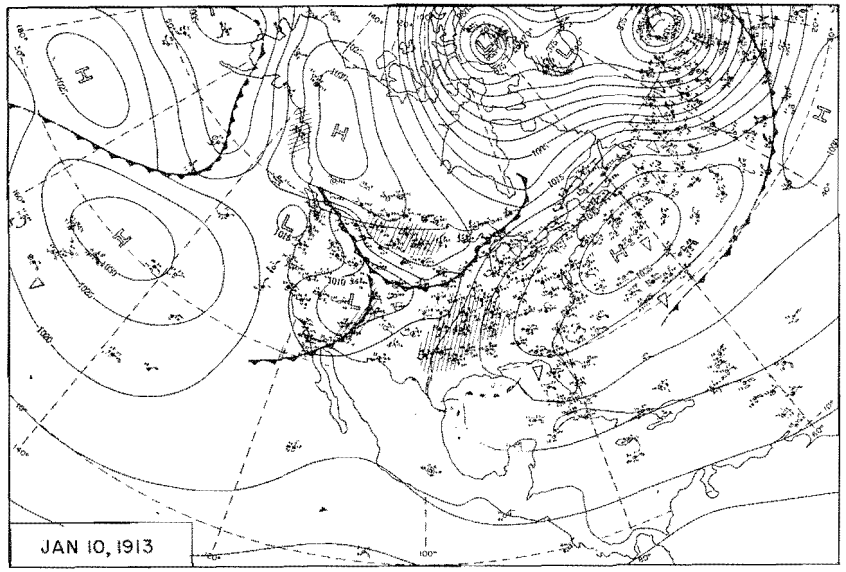

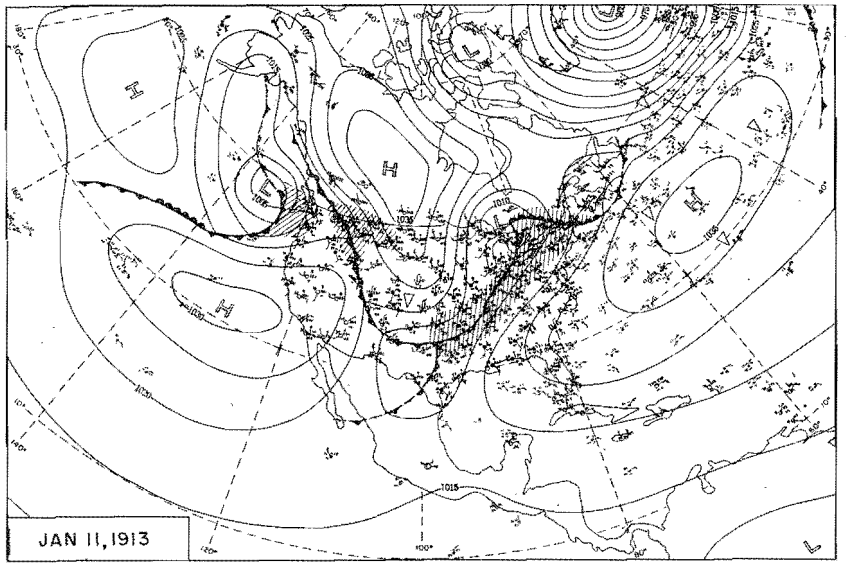

Figure 47. 0700 CST Northern Hemisphere Sea-Level Maps

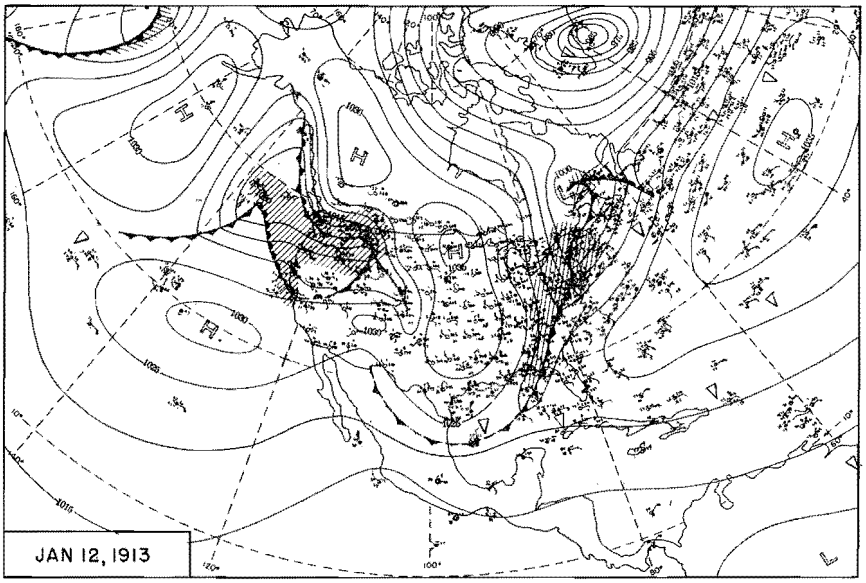

Figure 48. 0700 CST Northern Hemisphere Sea—Level Map

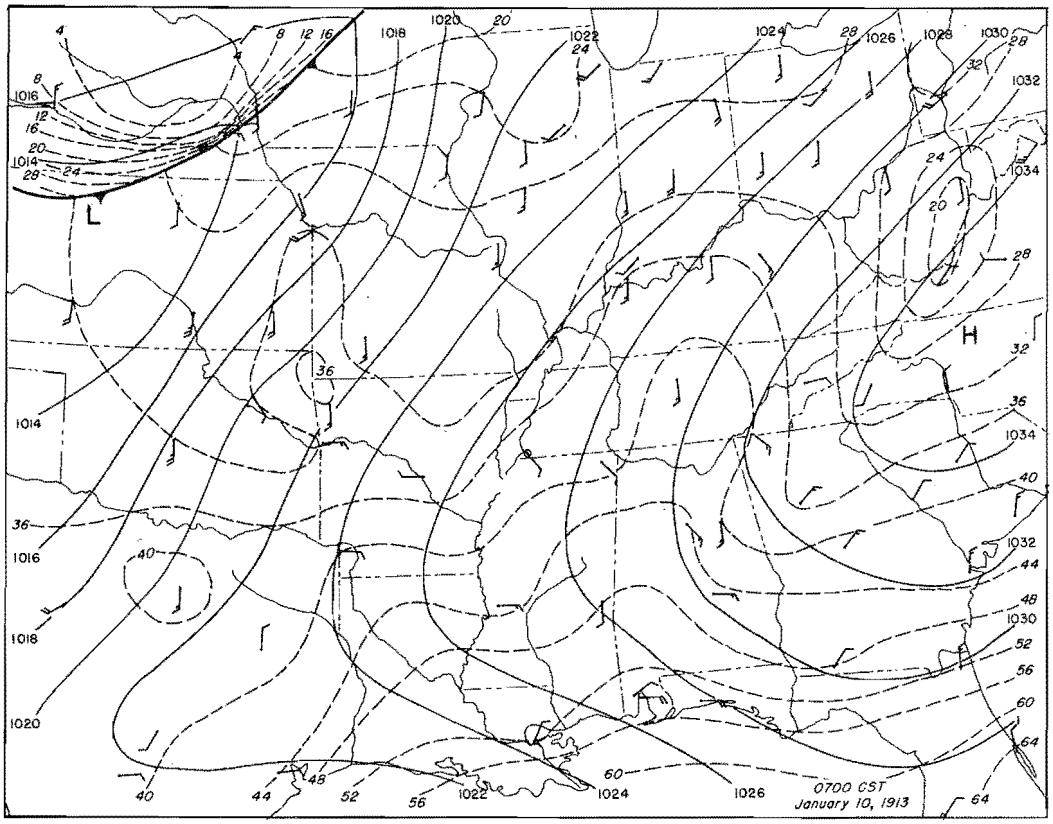

Figure 49. Detailed Surface Weather Map

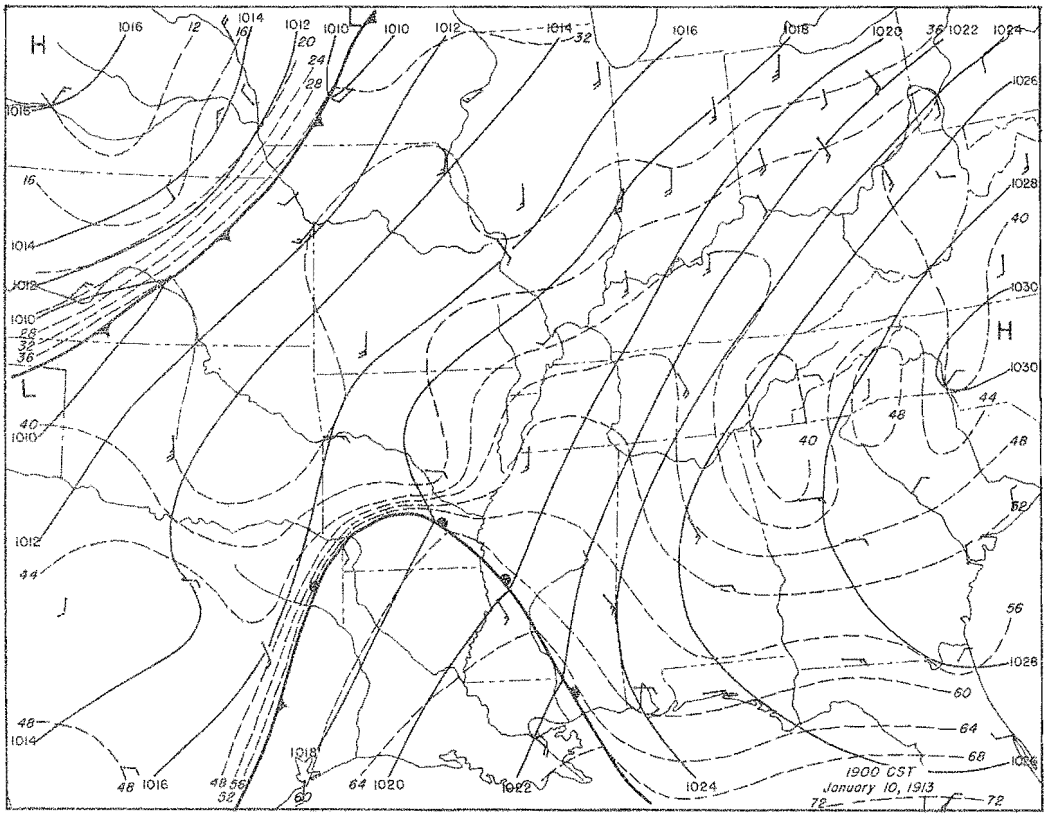

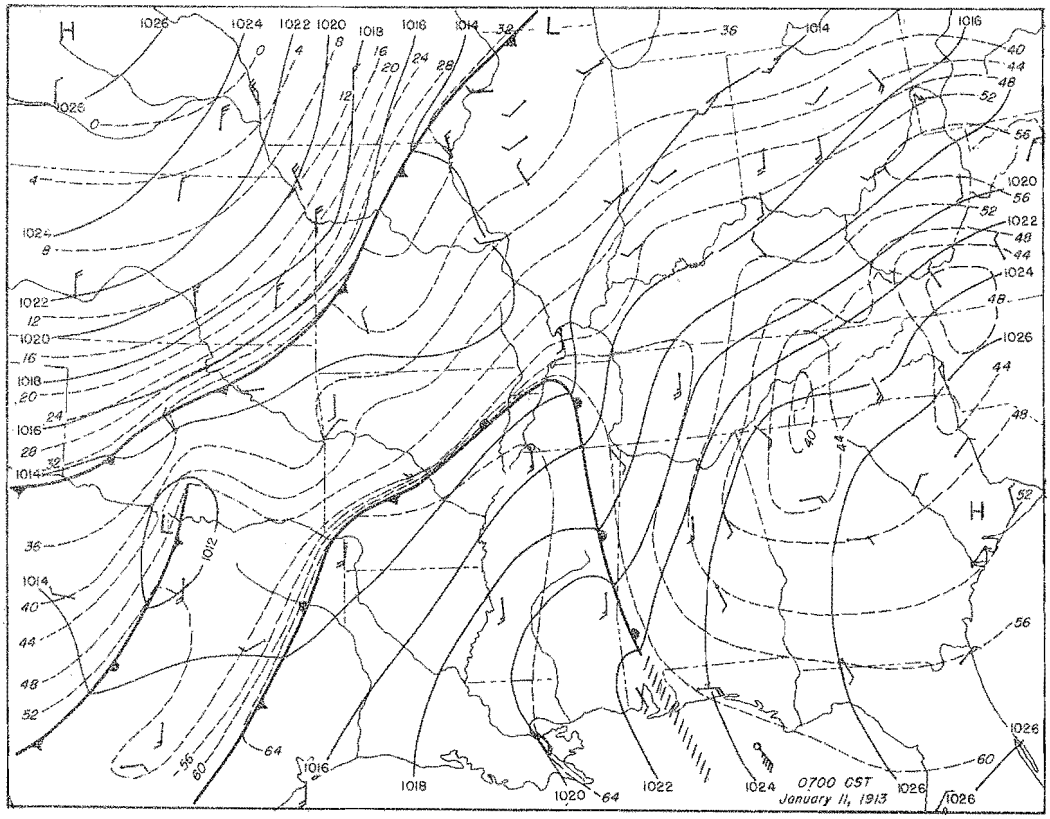

Figure 50. Detailed Surface Weather Maps

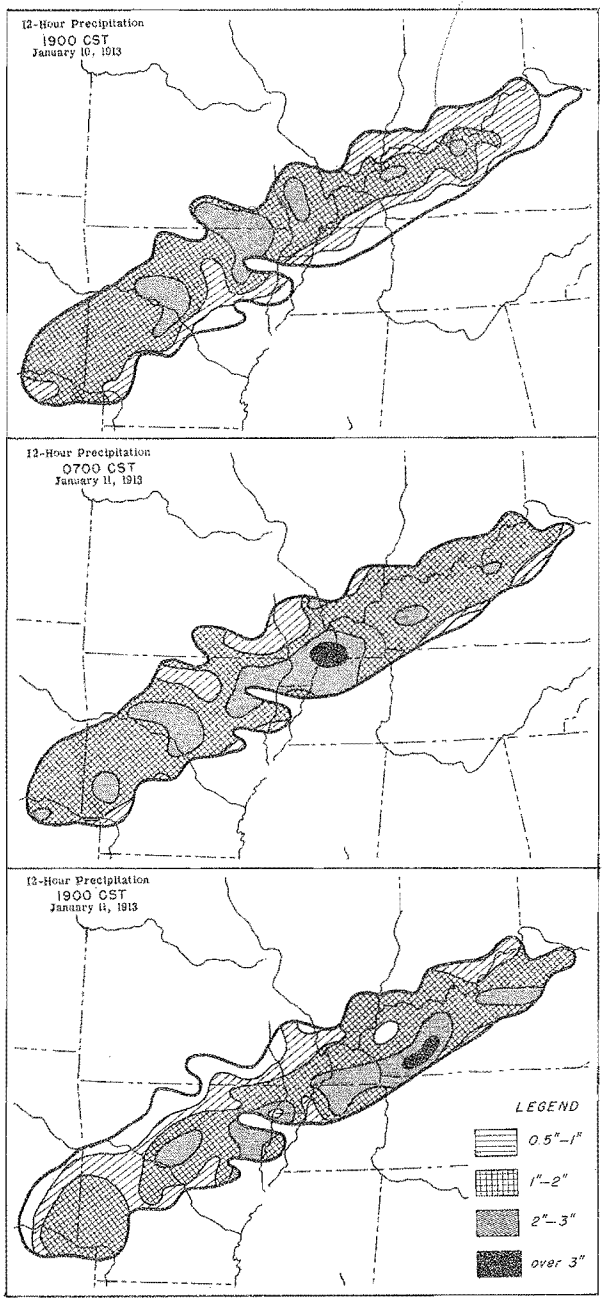

Figure 51. Incremental Isohyetal Patterns

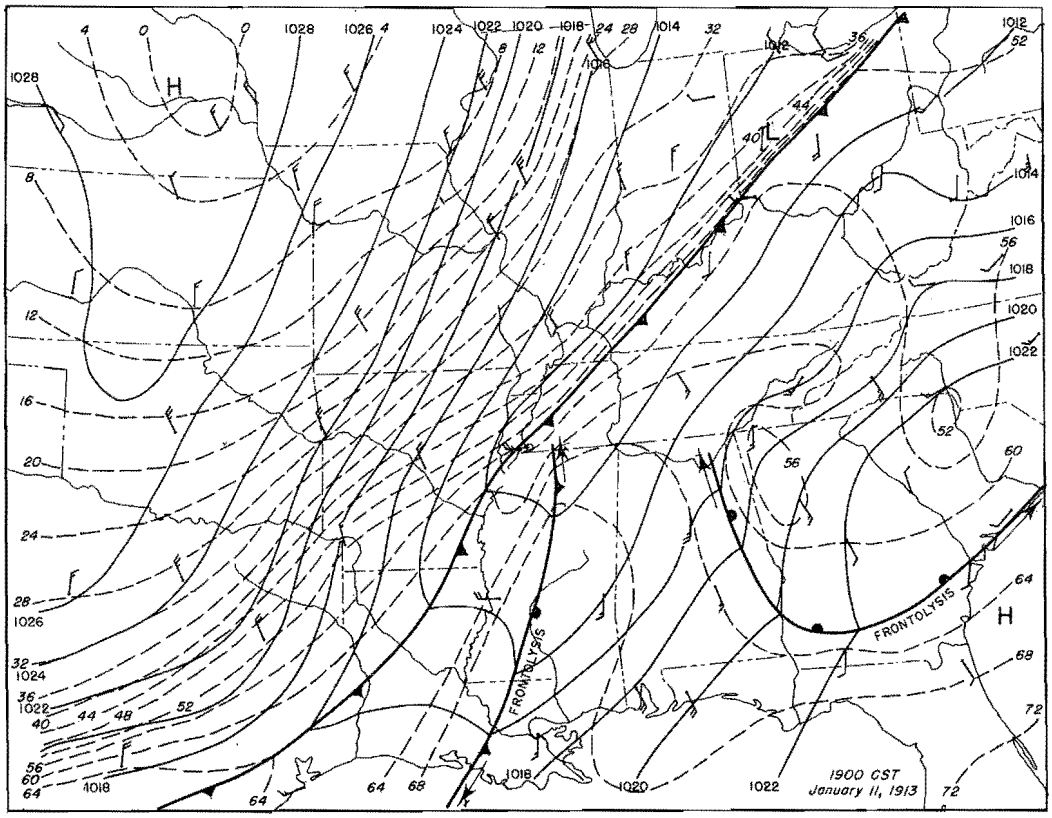

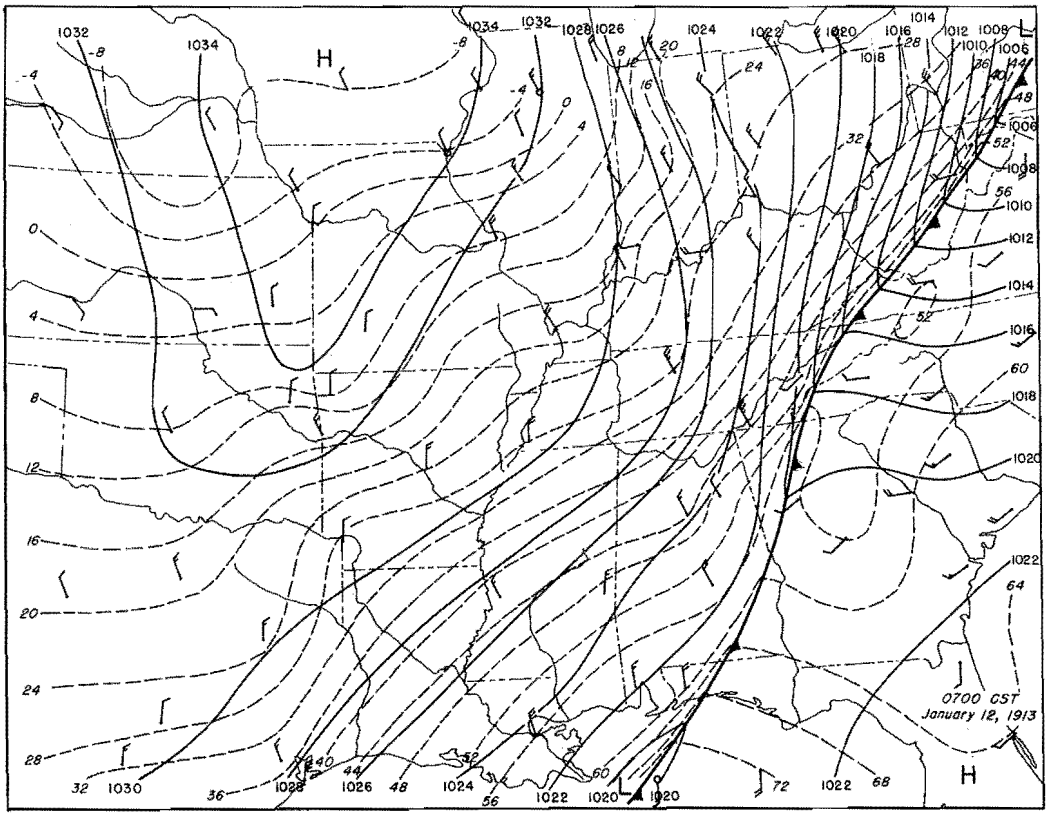

Figure 52. Detailed Surface Weather Maps

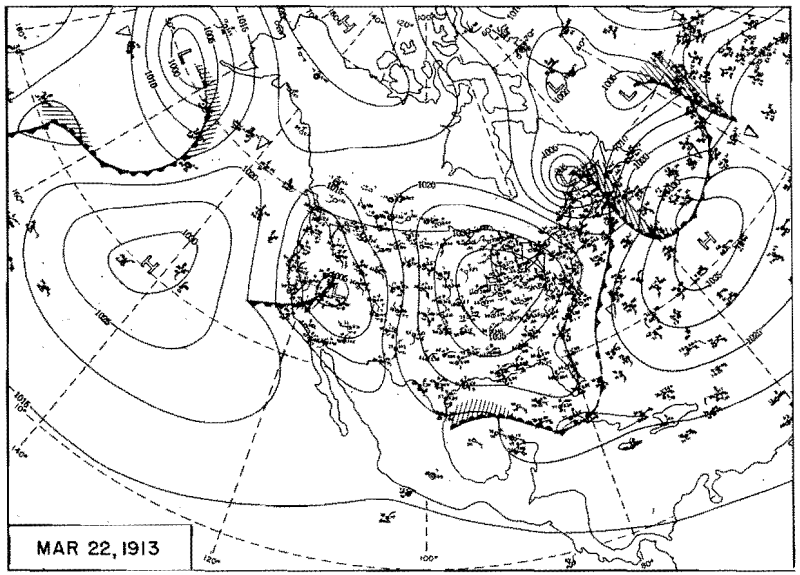

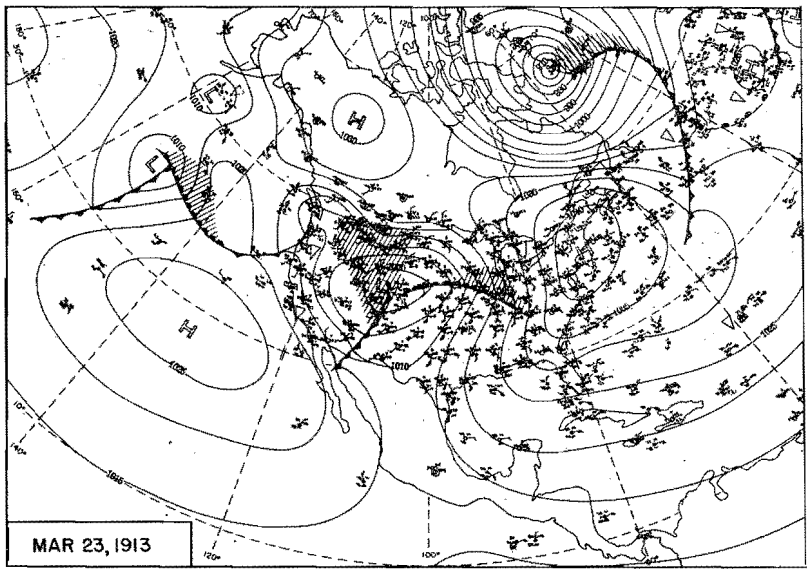

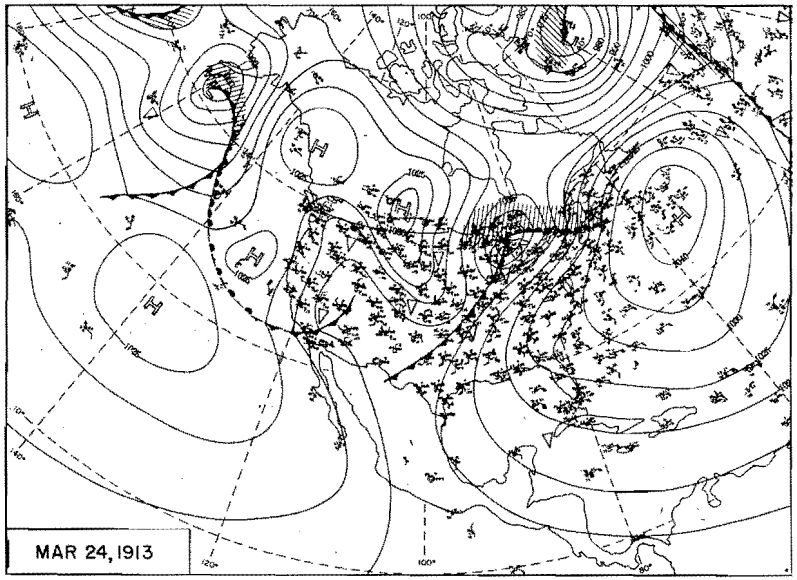

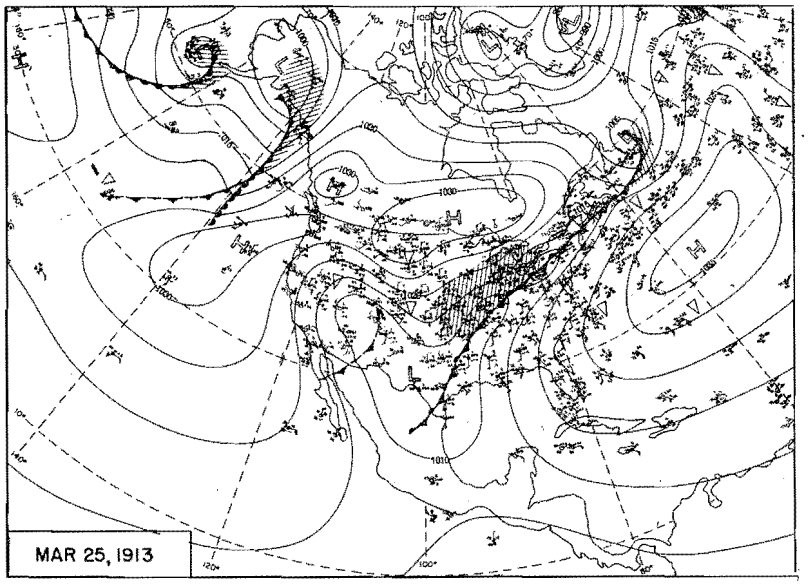

Figure 53. 0700 CST Northern Hemisphere Sea-Level Maps

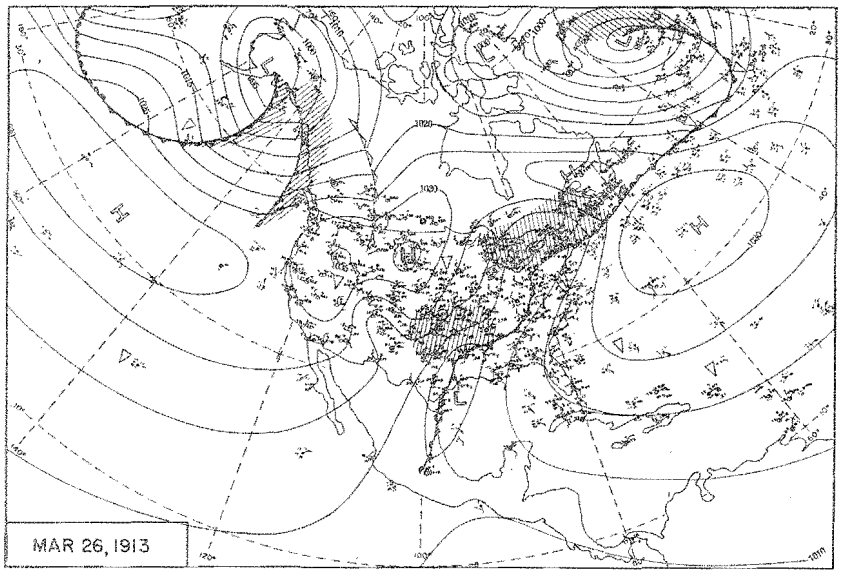

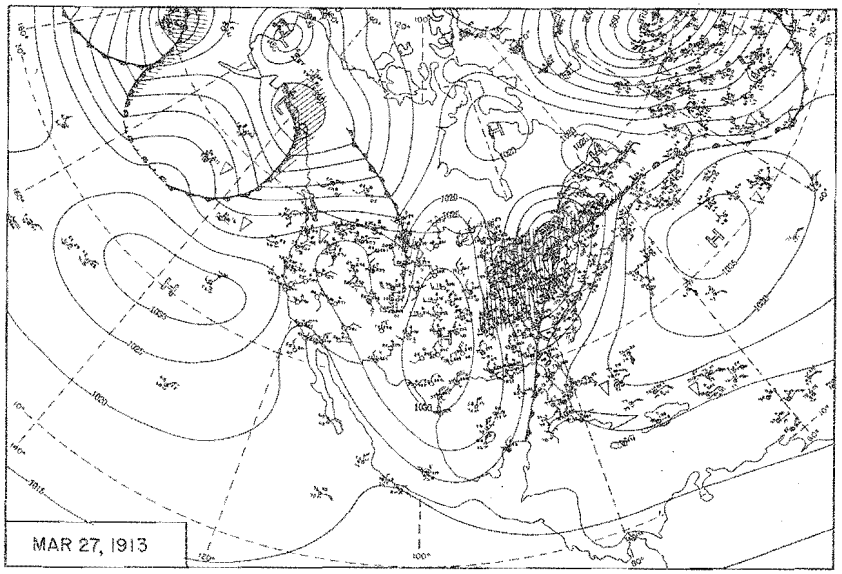

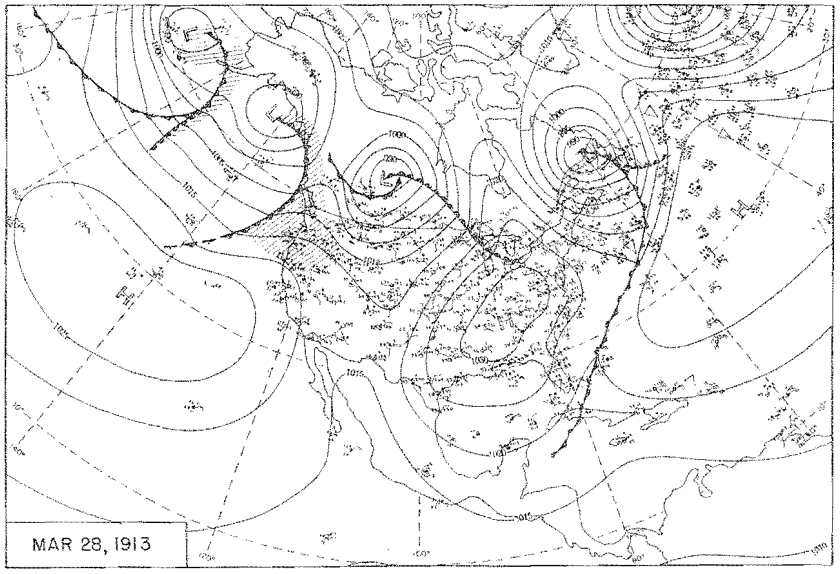

Figure 54. 0700 CST Northern Hemisphere Sea—Level Maps

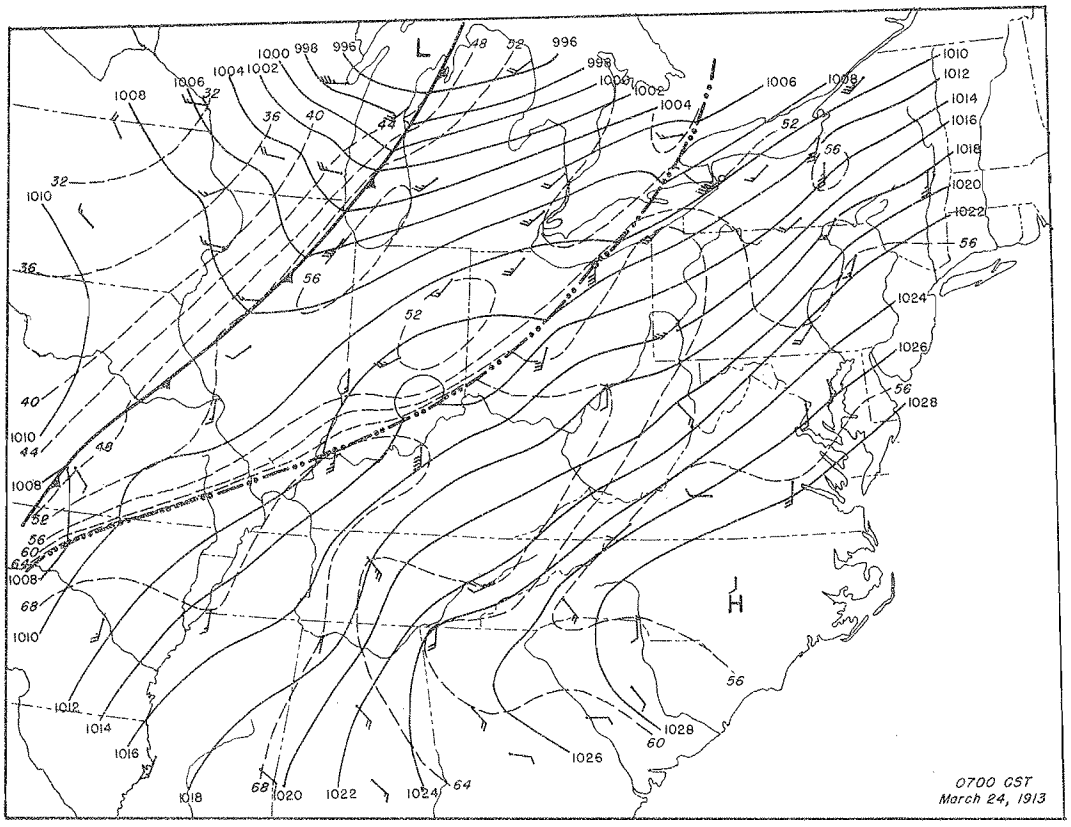

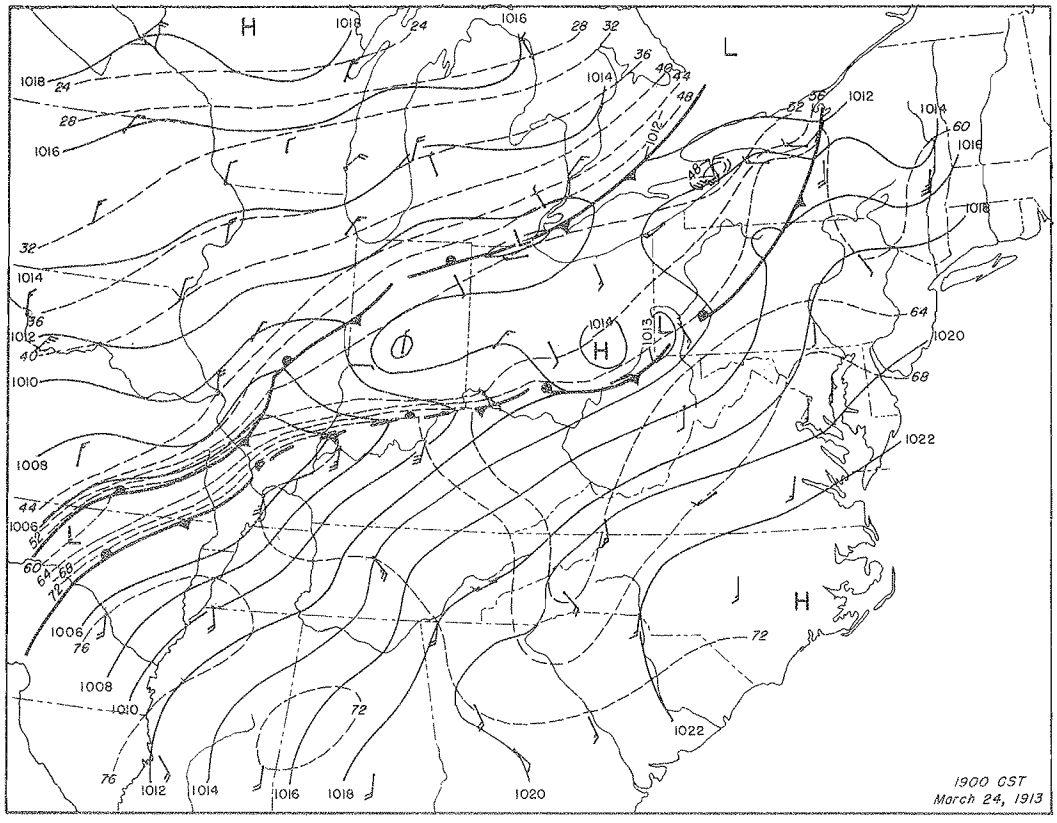

Figure 55. Detailed Surface Weather Maps

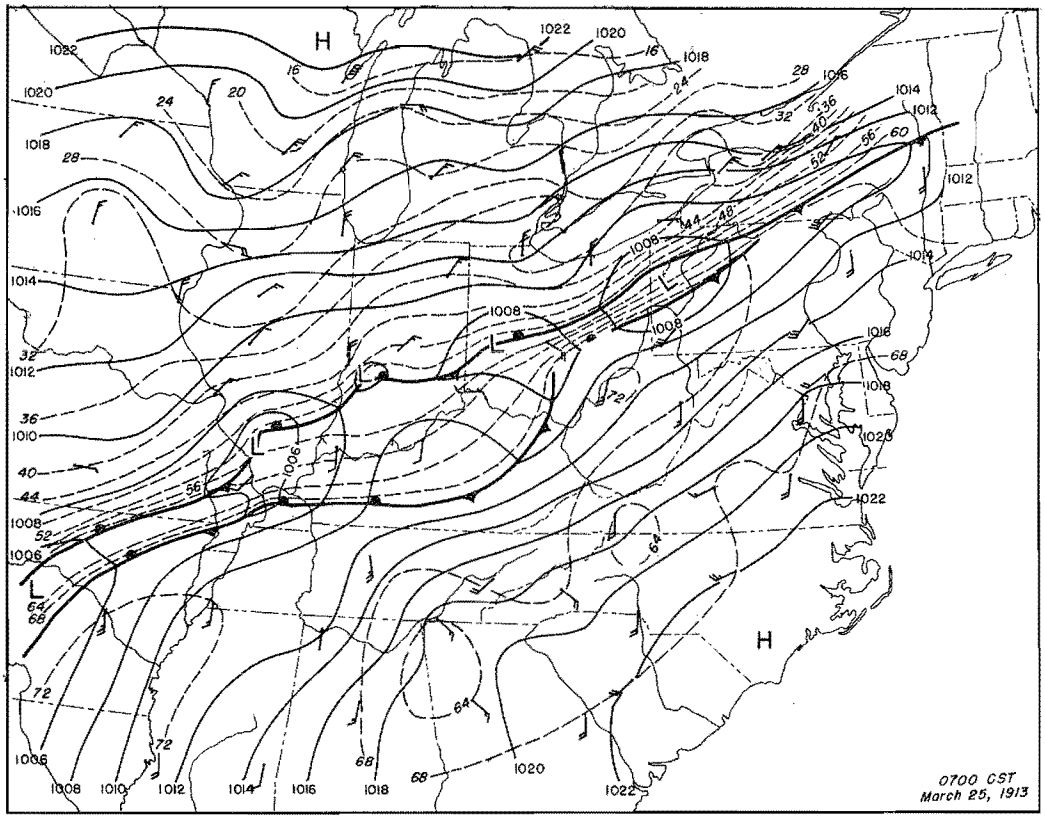

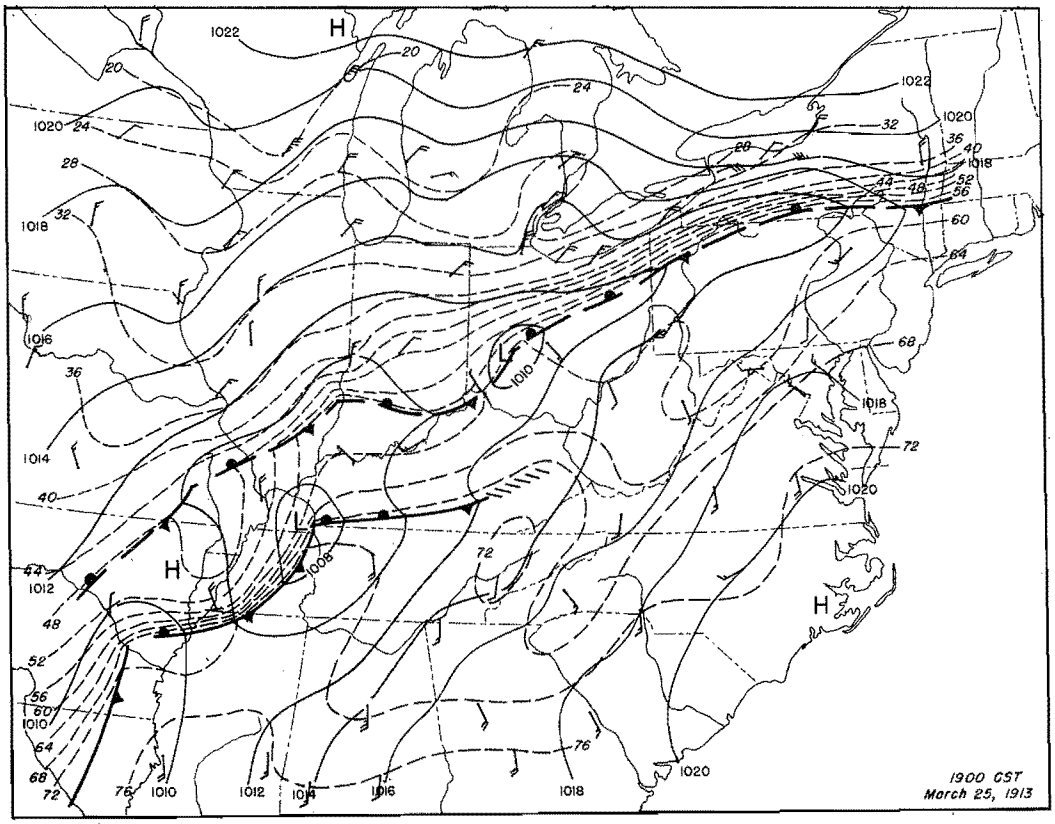

Figure 56. Detailed Surface Weather Maps

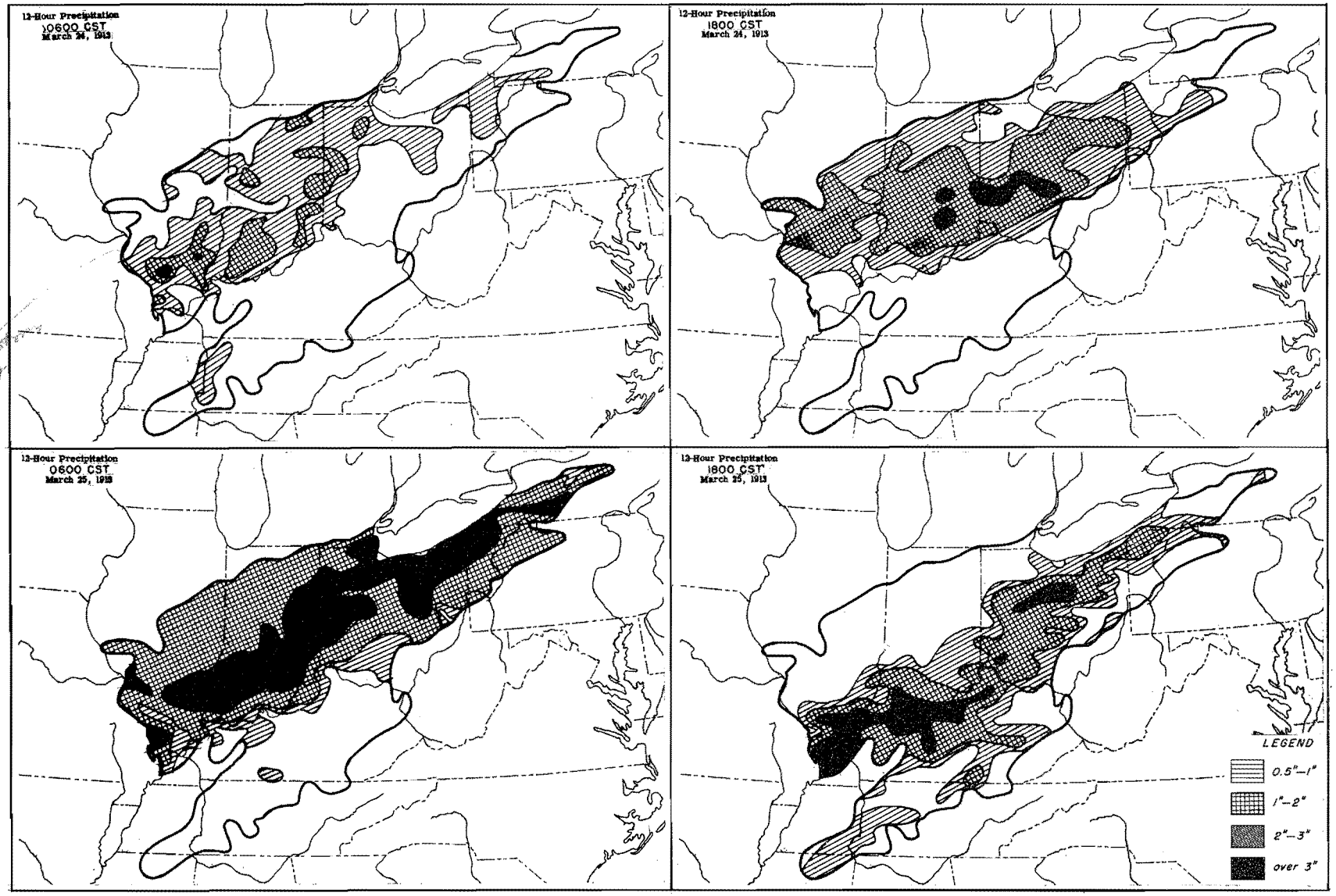

Figure 57. Incremental Isohyetal Patterns

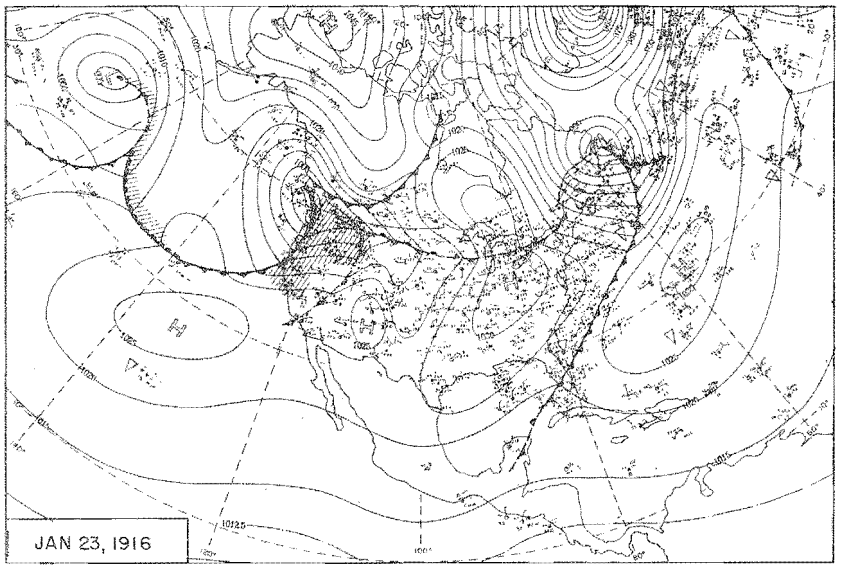

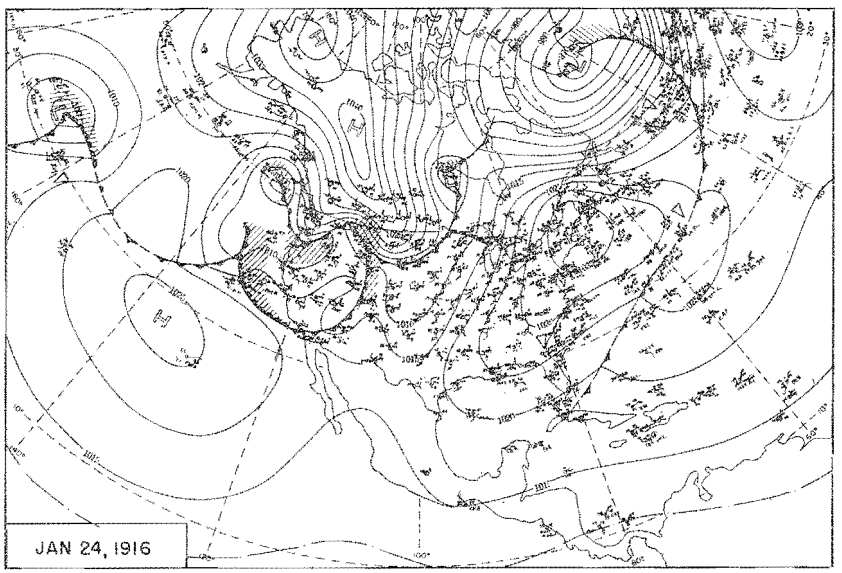

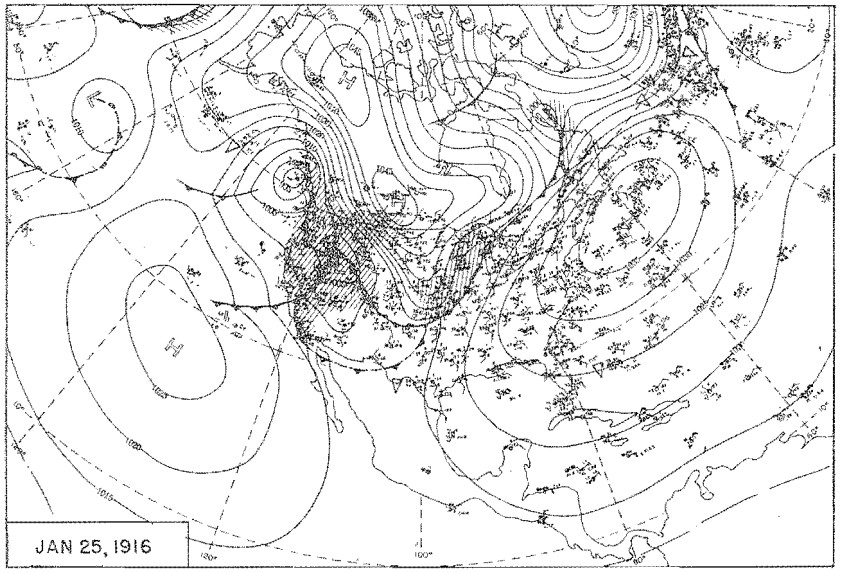

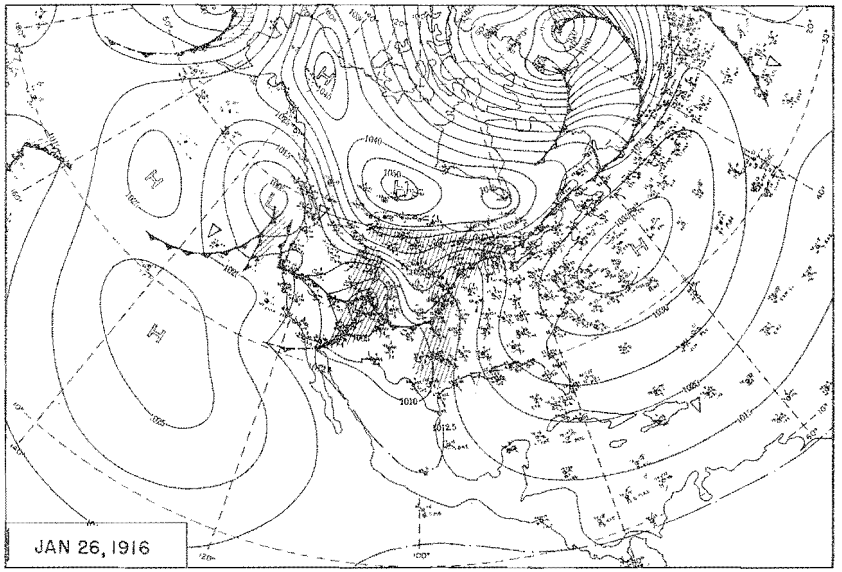

Figure 58. 0700 CST Northern Hemisphere Sea-Level Maps

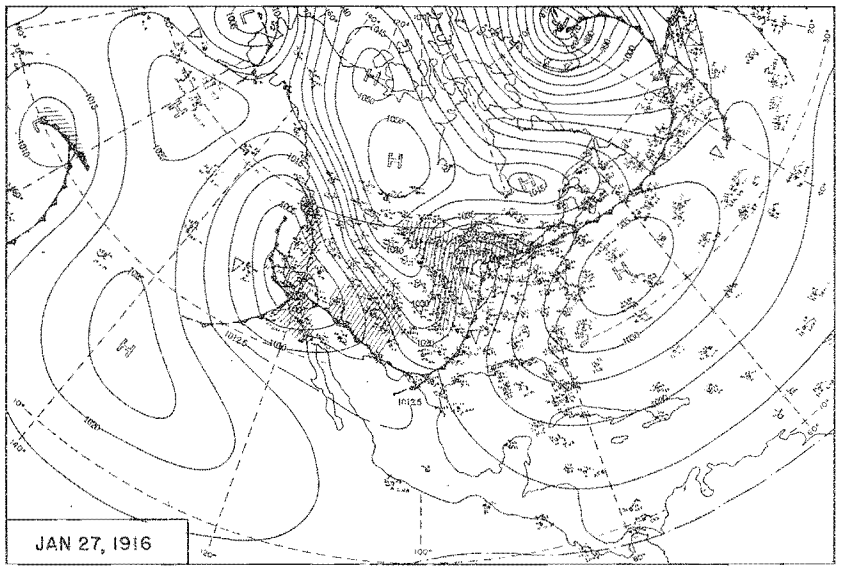

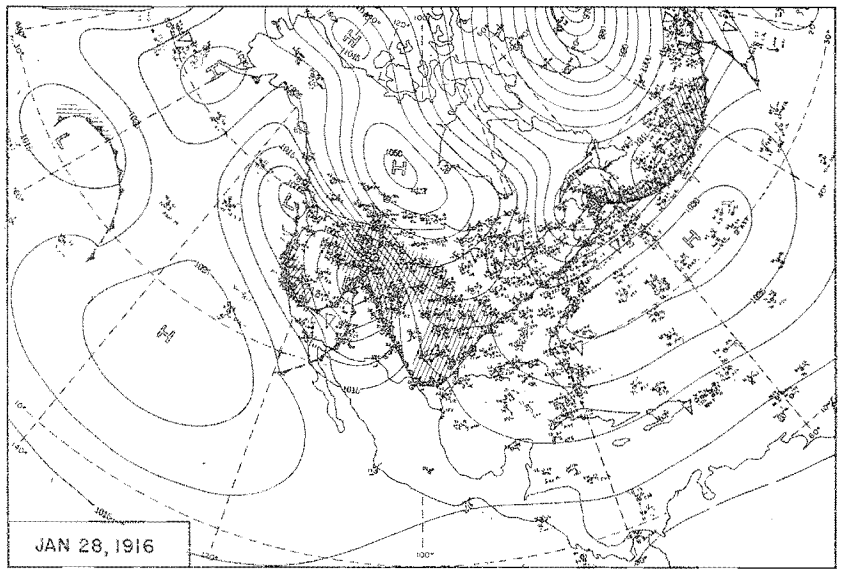

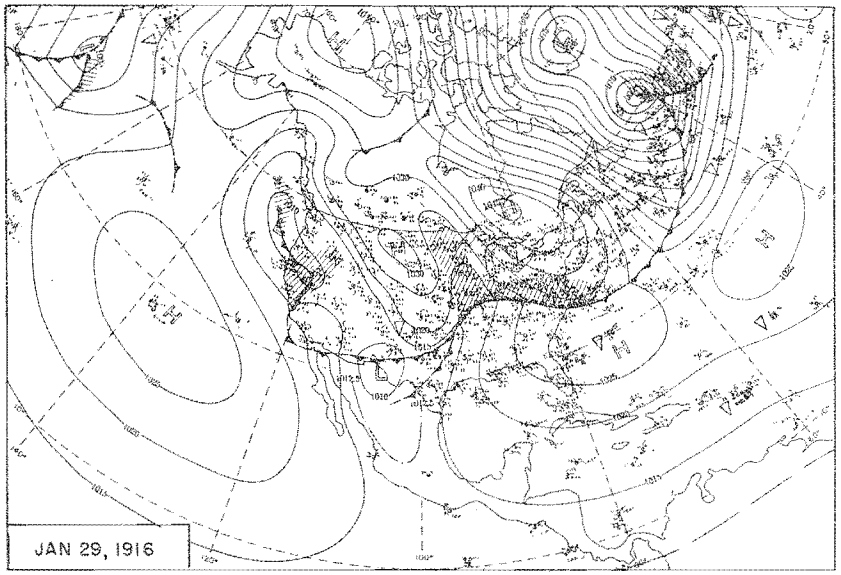

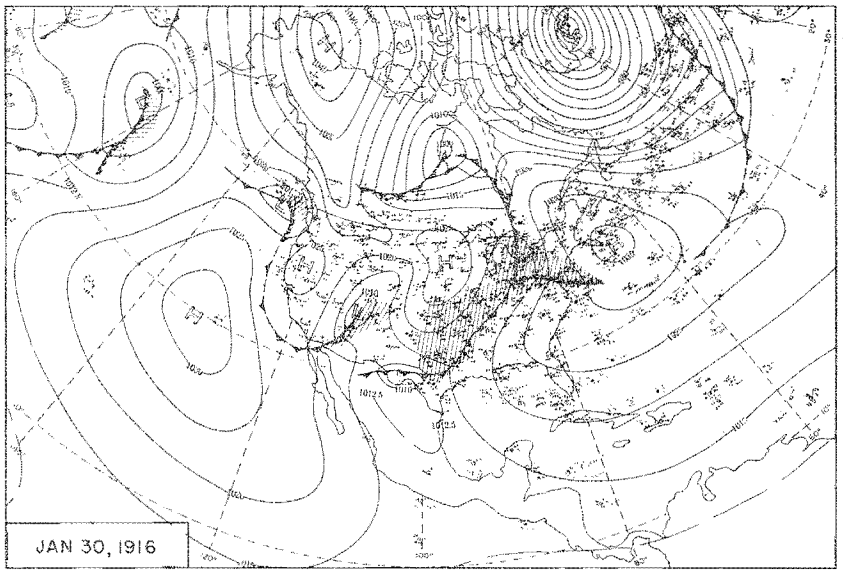

Figure 59. 0700 CST Northern Hemisphere Sea-Level Maps

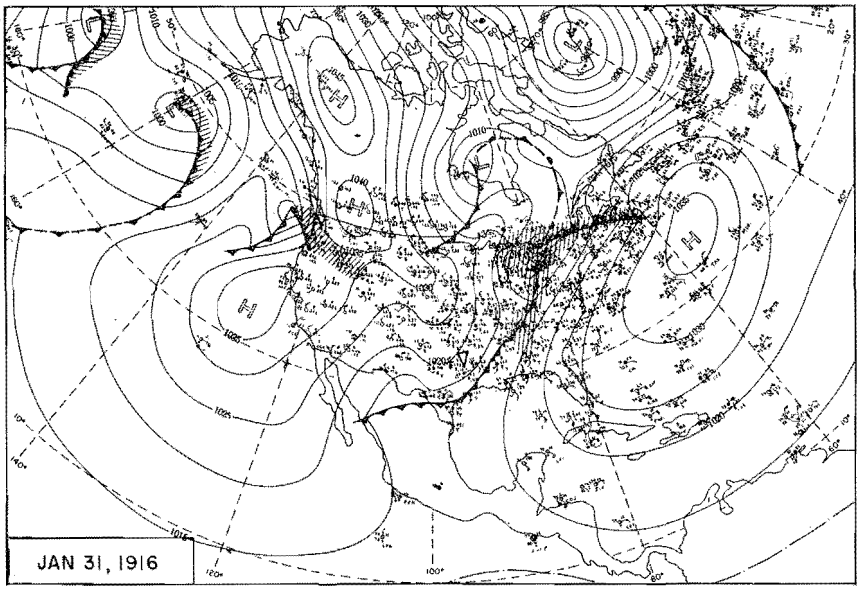

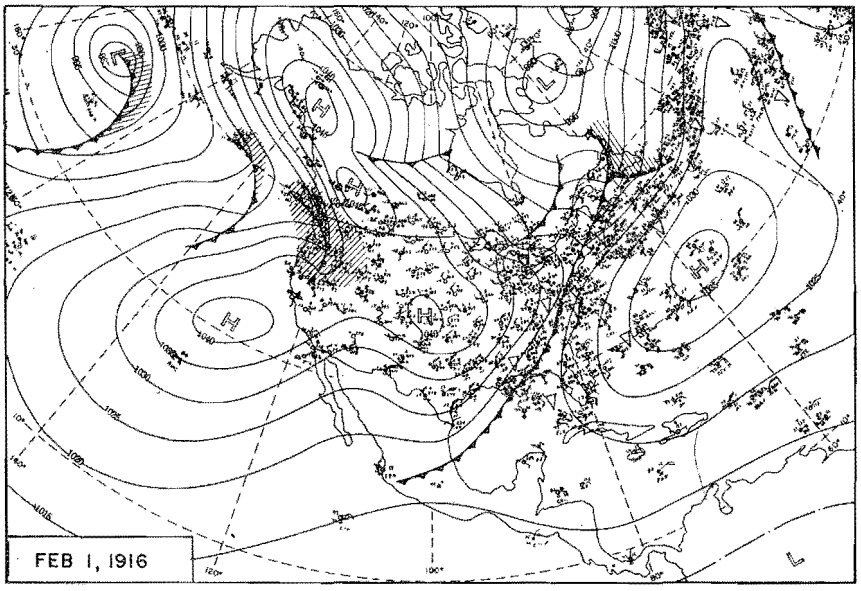

Figure 60. 0700 CST Northern Hemisphere Sea—Level Maps

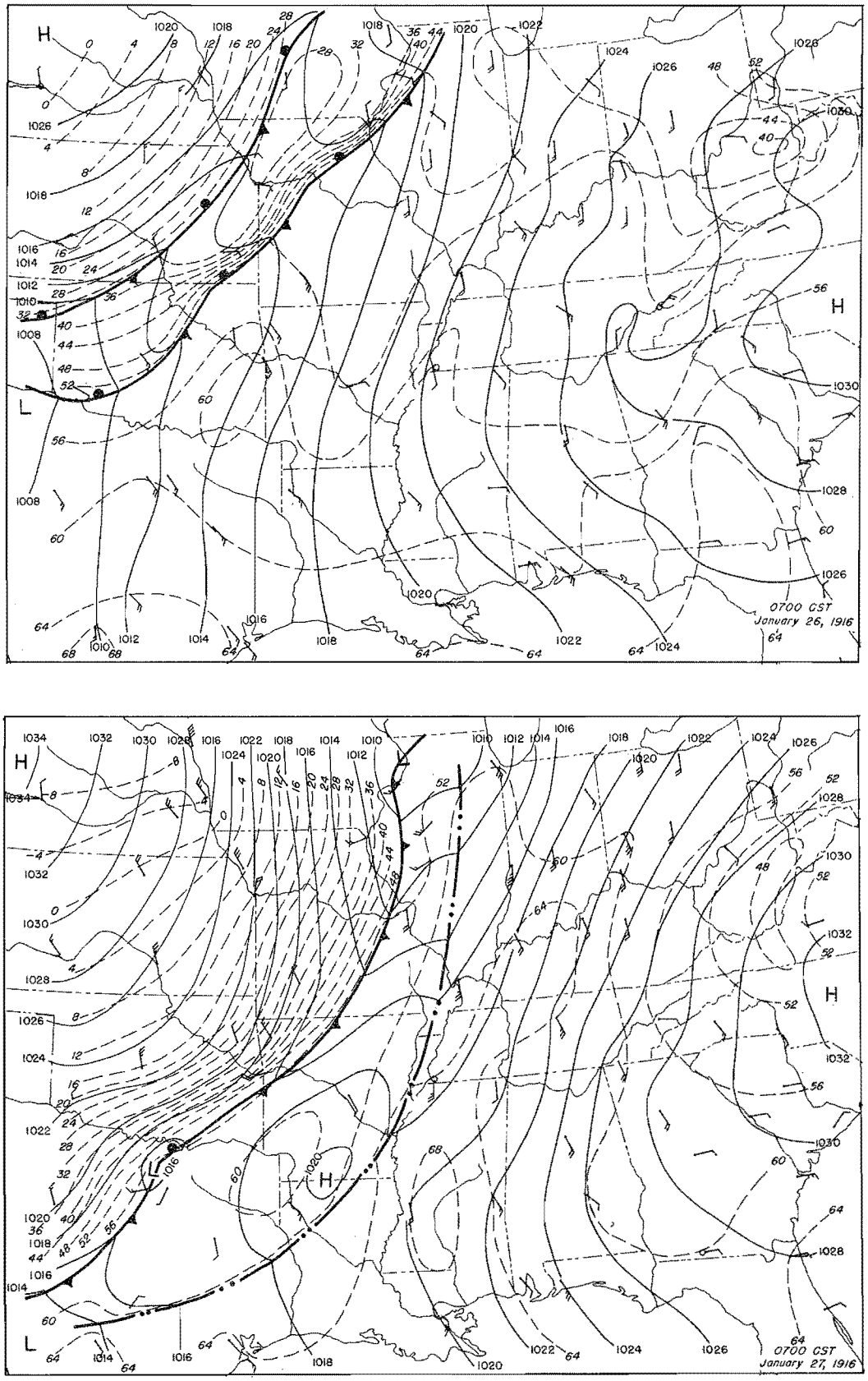

Figure 61. Detailed Surface Weather Maps

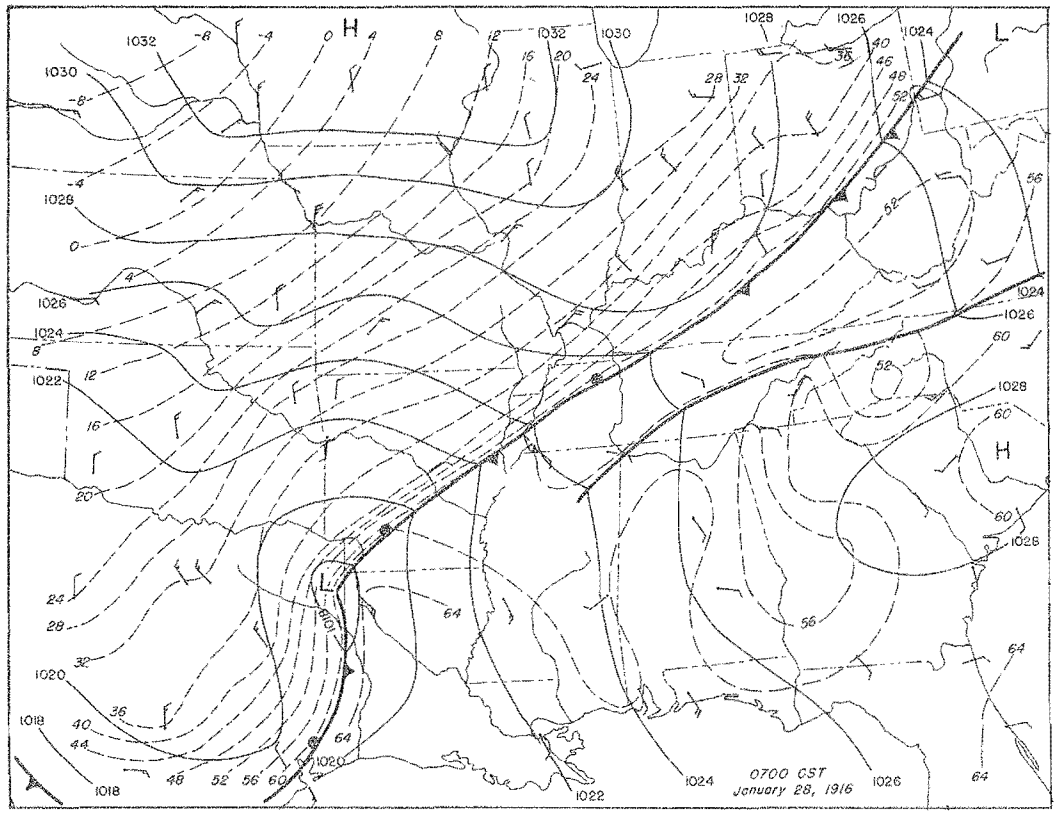

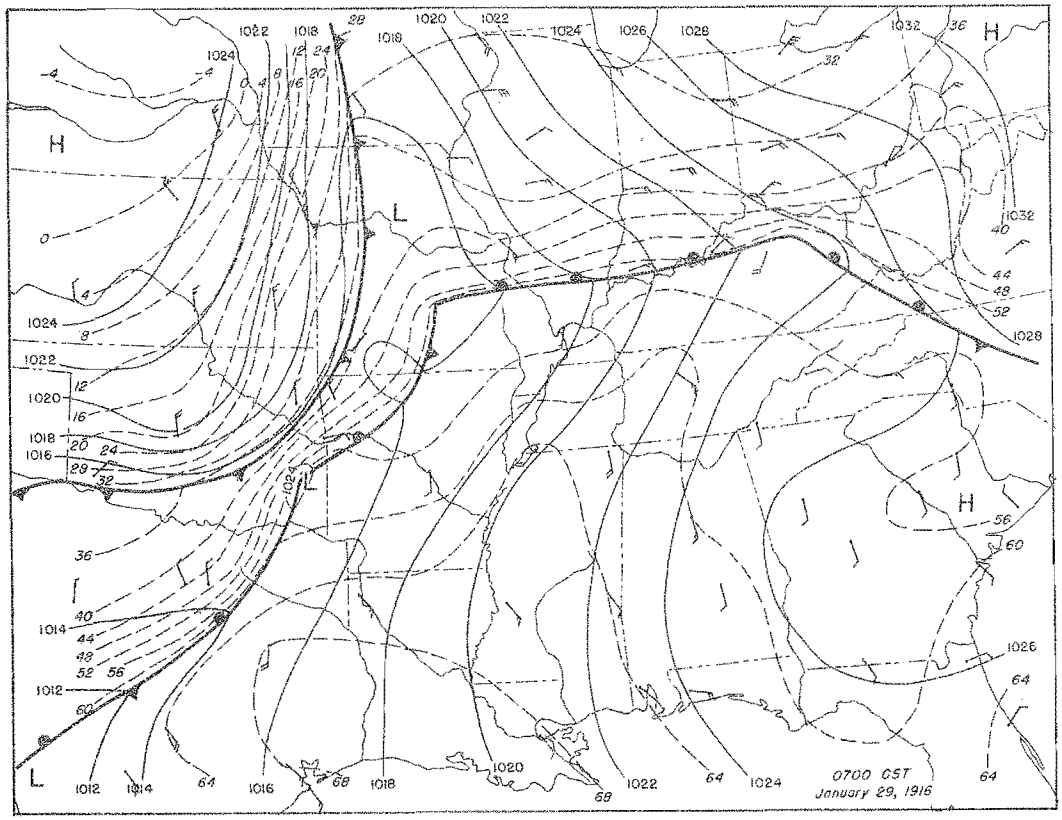

Figure 62. Detailed Surface Weather Maps

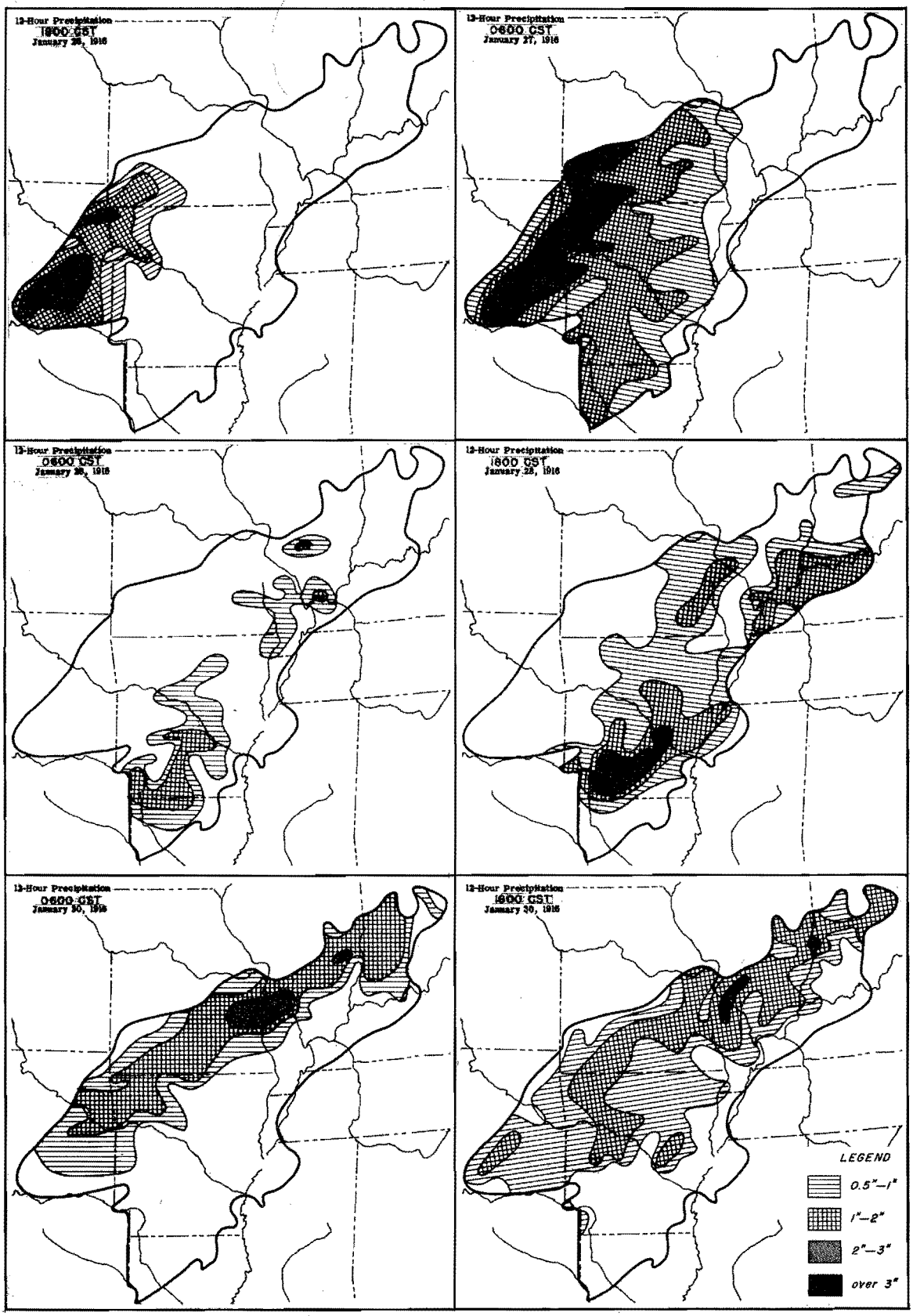

Figure 63. Incremental Isohyetal Patterns

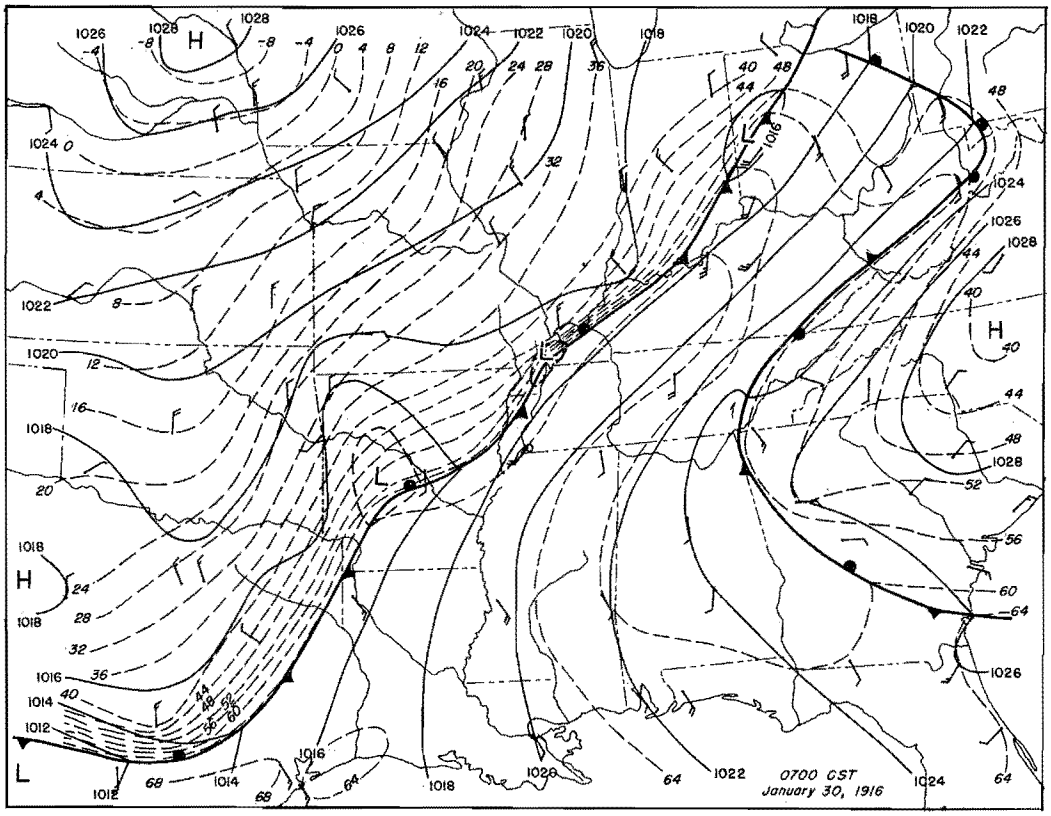

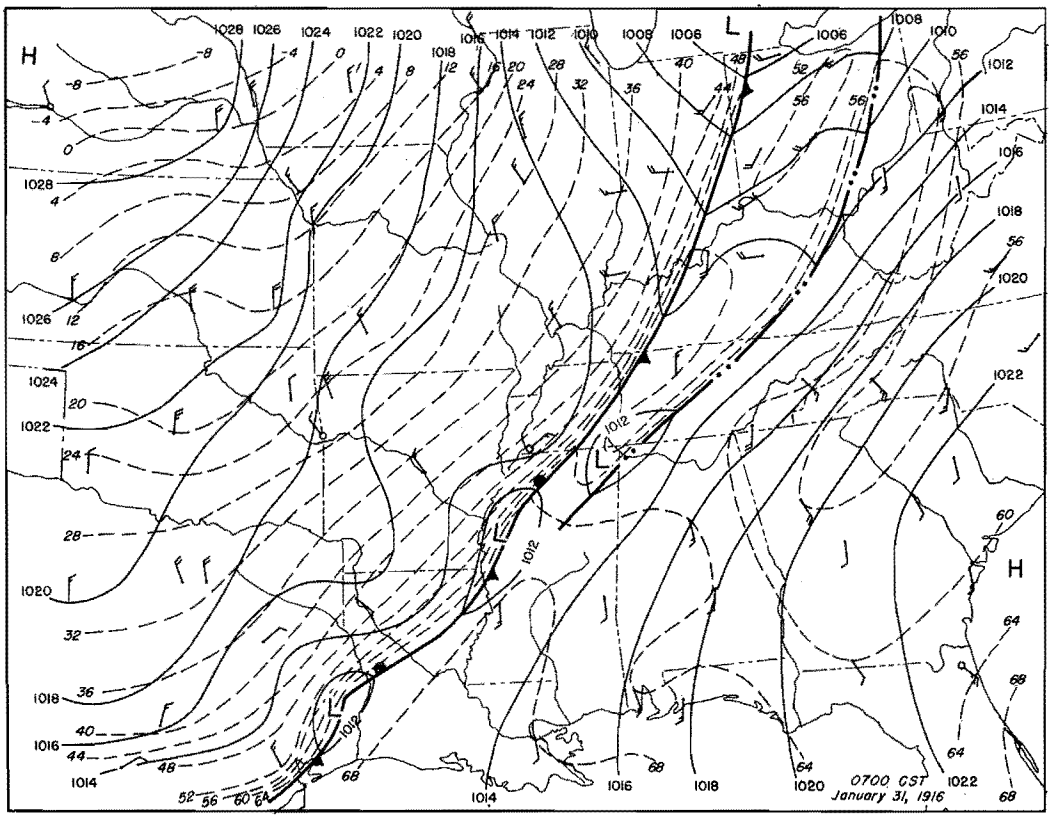

Figure 64. Detailed Surface Weather Maps

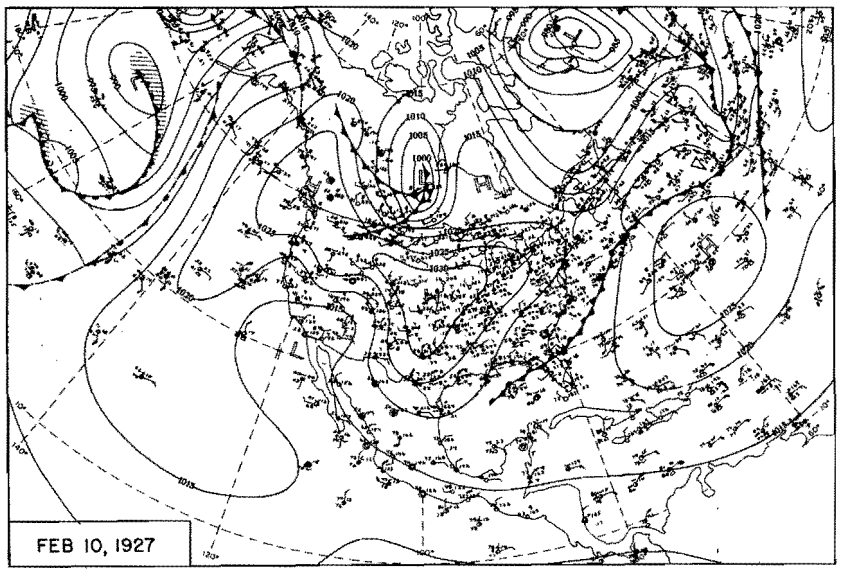

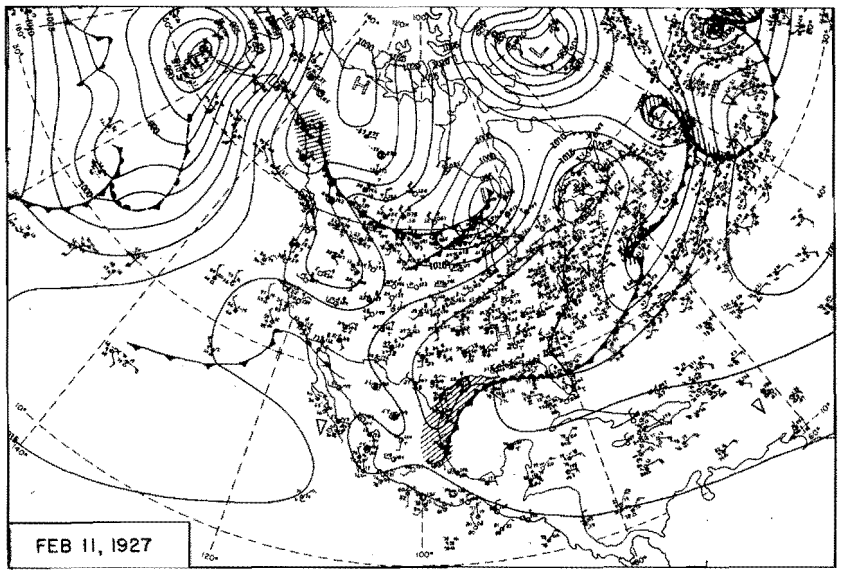

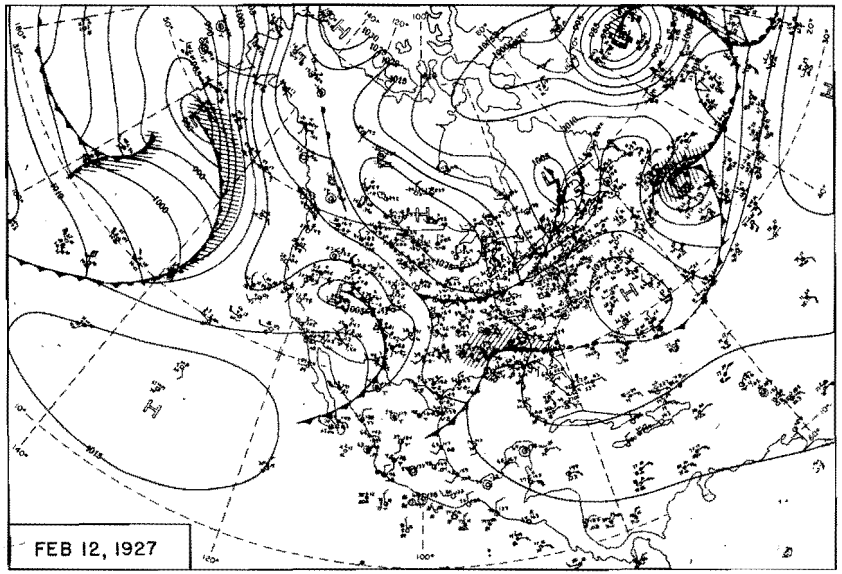

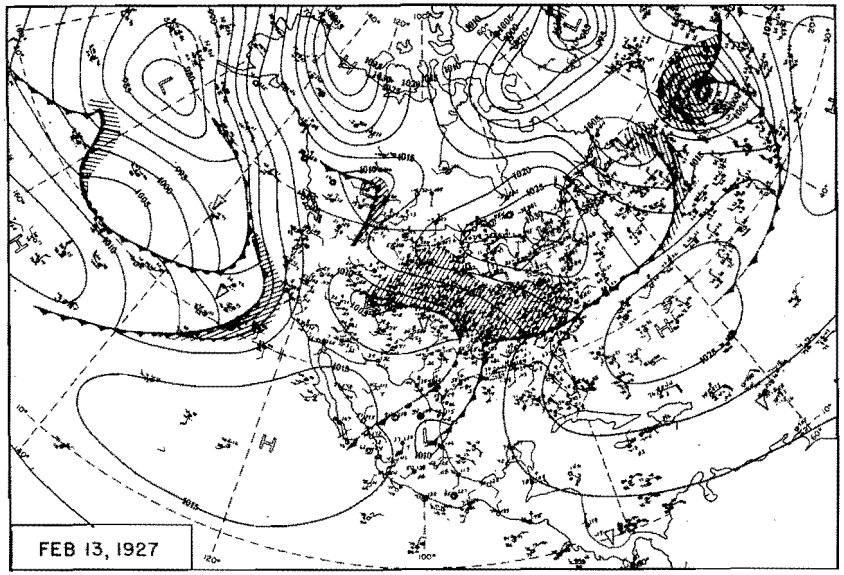

Figure 65. 0700 CST Northern Hemisphere Sea—Level Maps

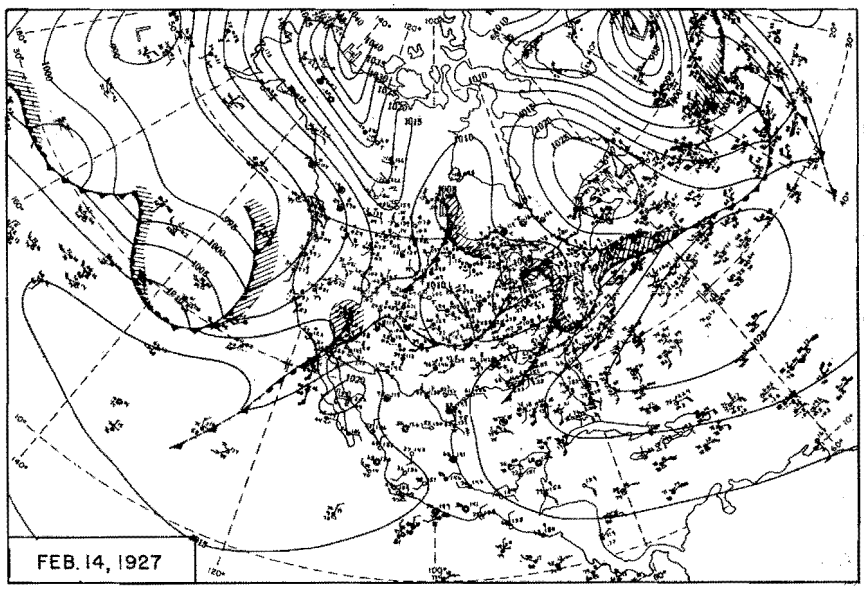

Figure 66. 0700 CST Northern Hemisphere Sea—Level Maps

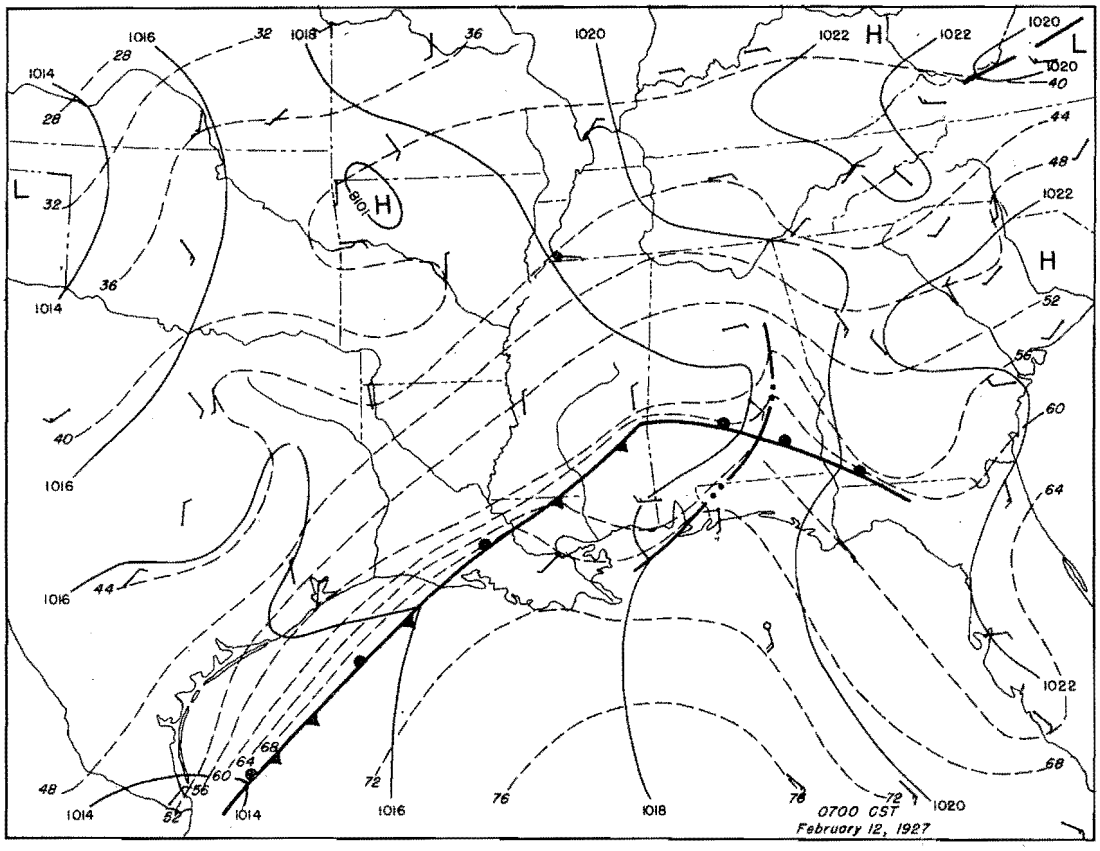

Figure 67. Detailed Surface Weather Map

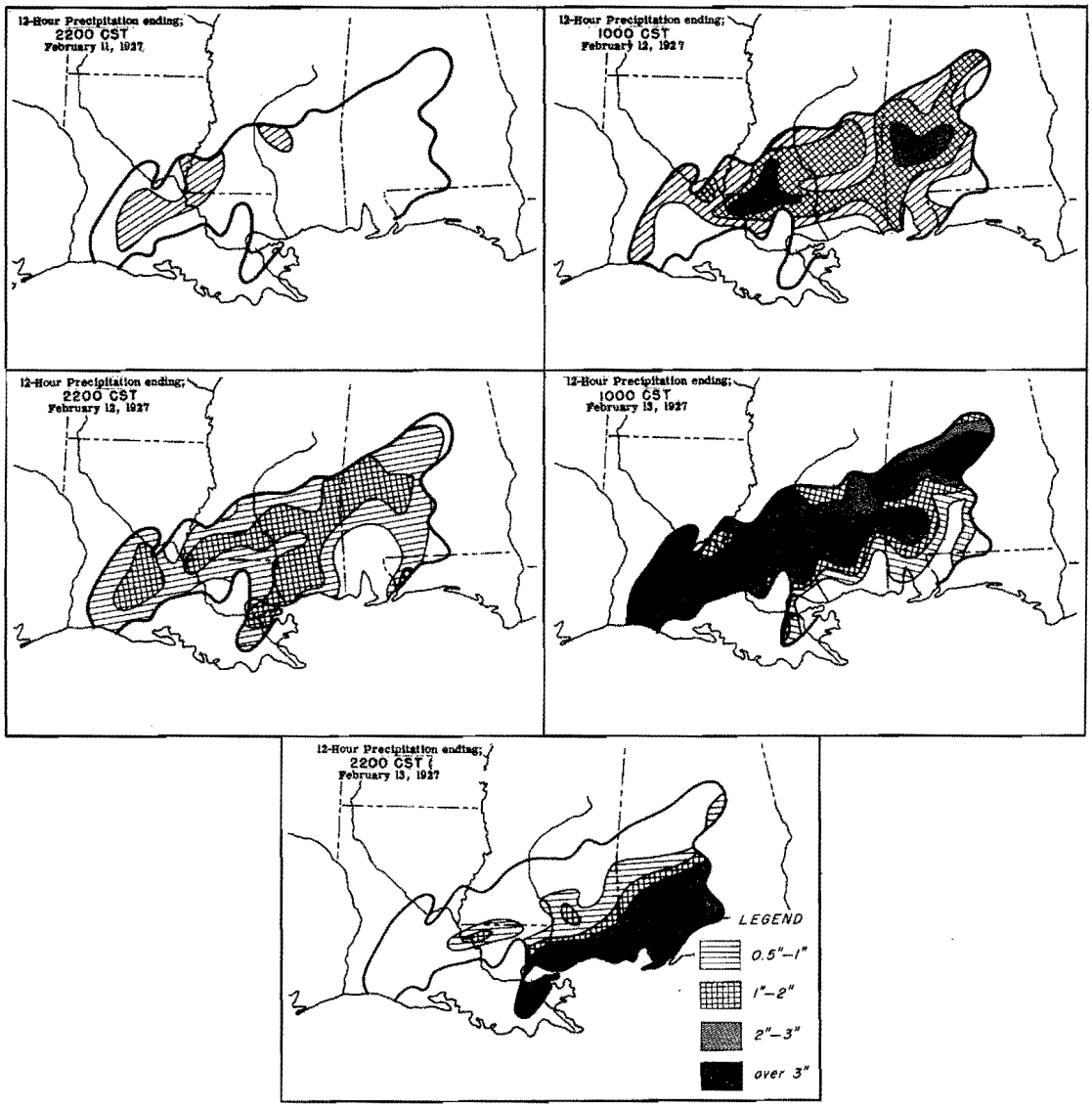

Figure 68. Incremental Isohyetal Patterns

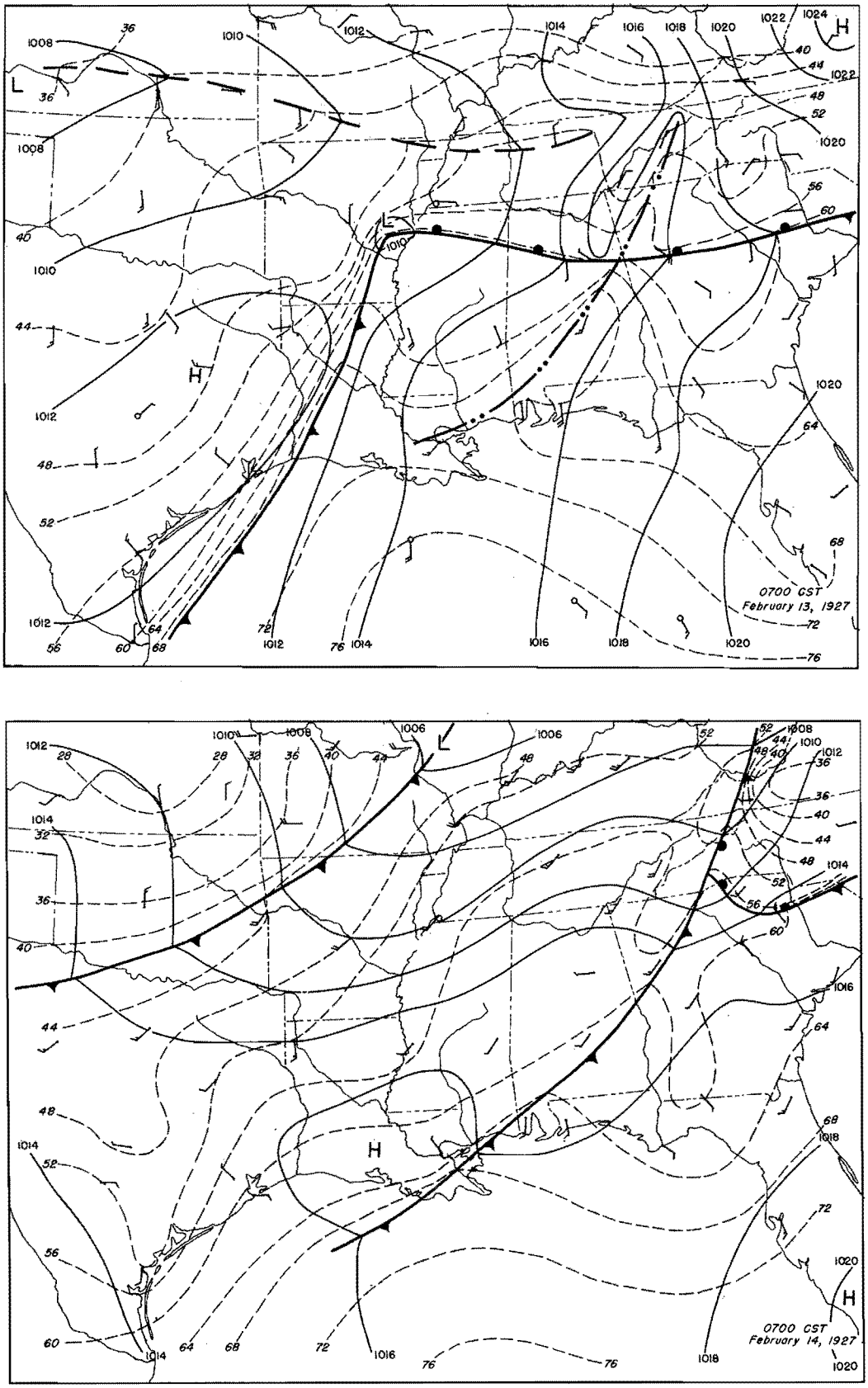

Figure 69. Detailed Surface Weather Maps

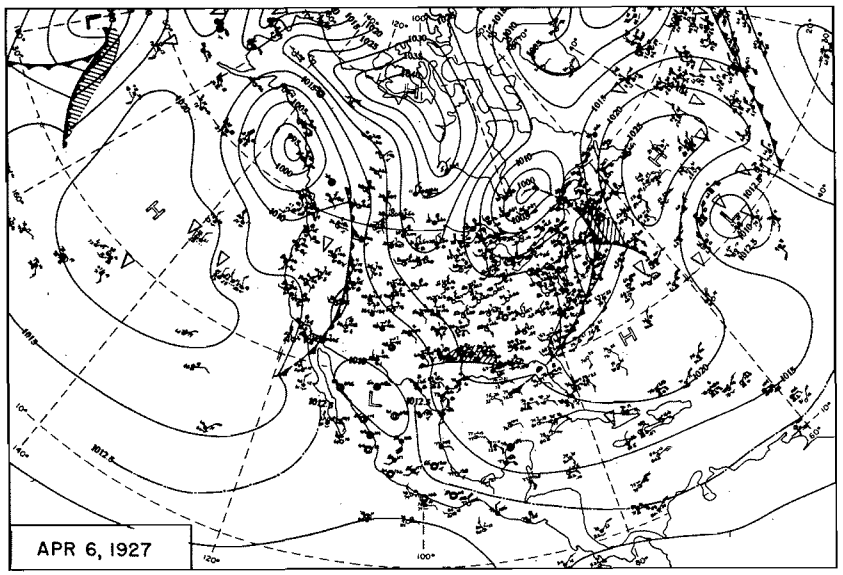

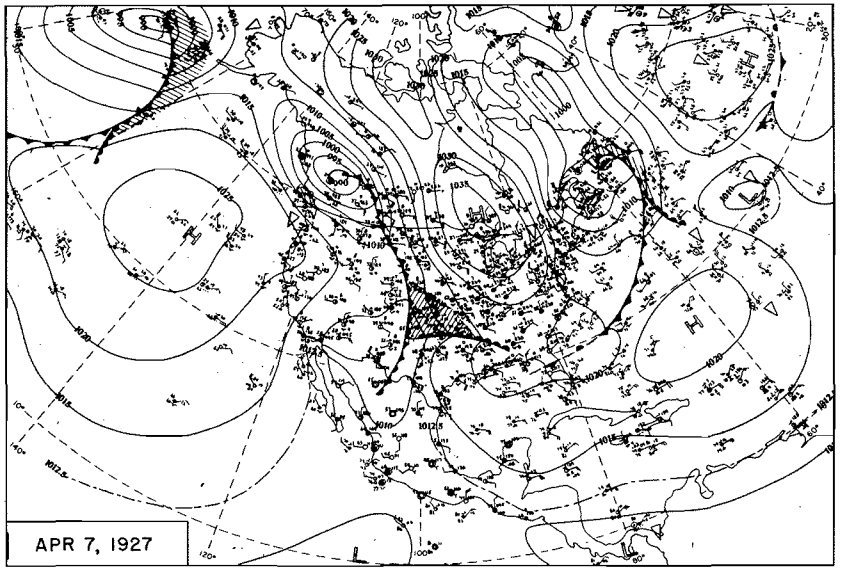

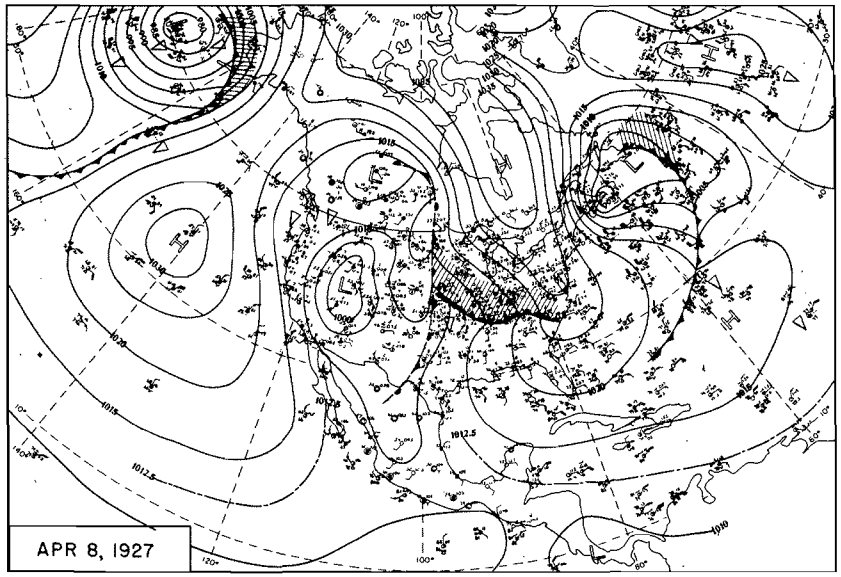

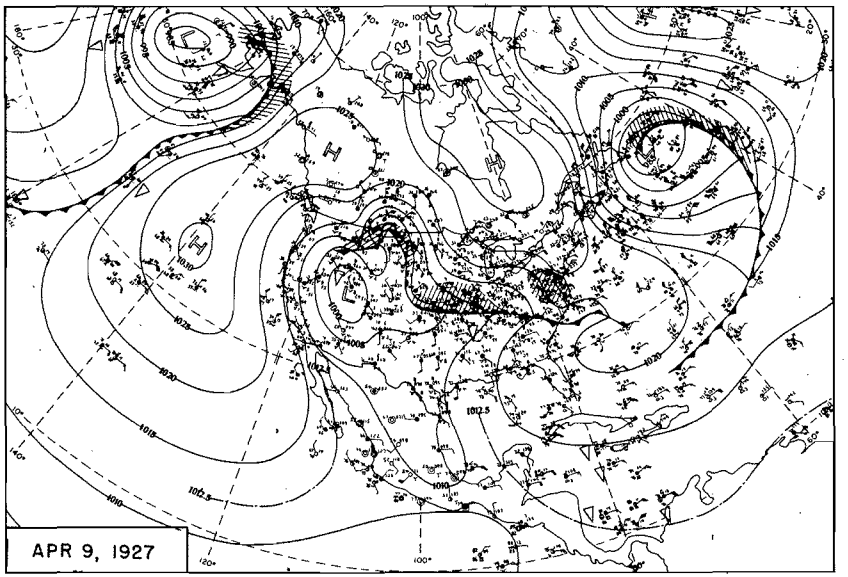

Figure 70. 0700 CST Northern Hemisphere Sea-Level Maps

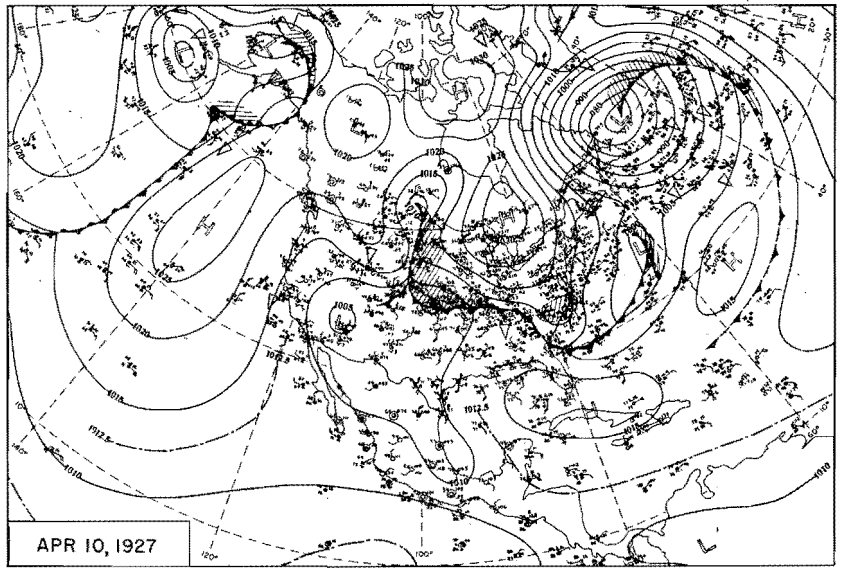

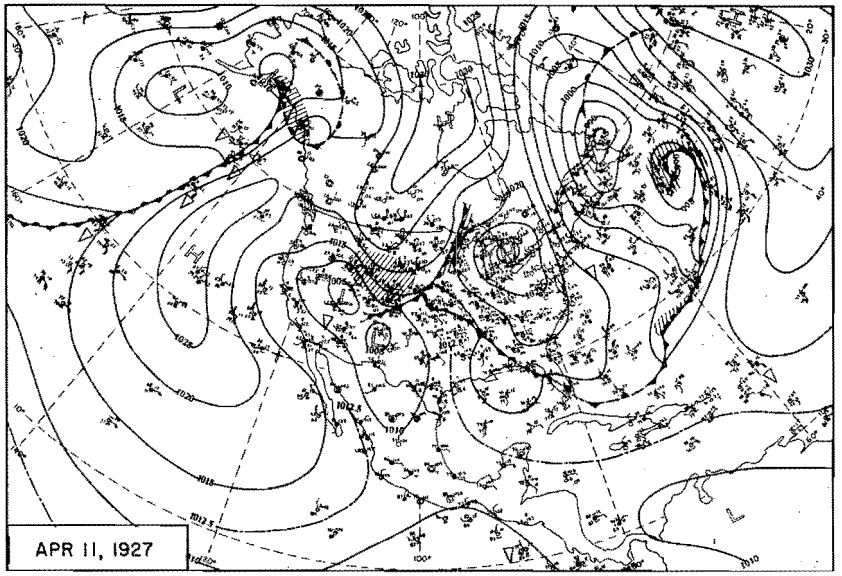

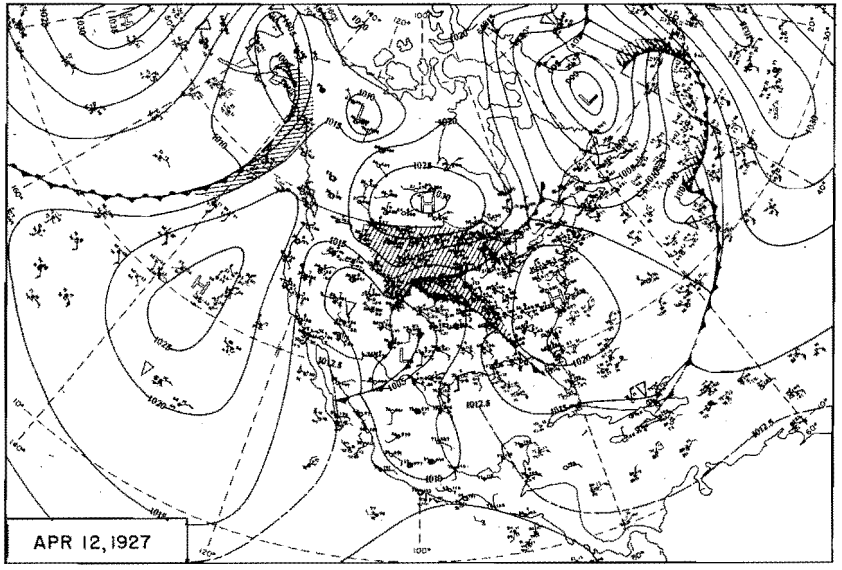

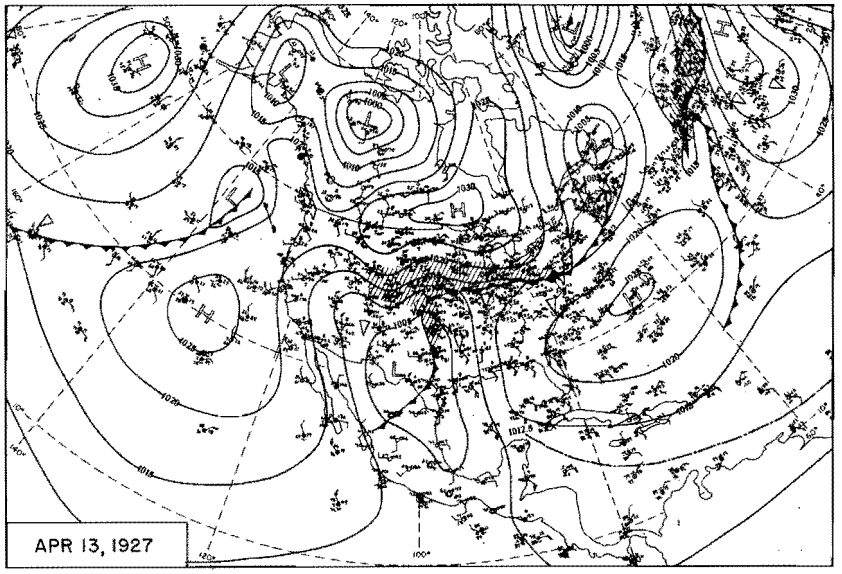

Figure 71. 0700 CST Northern Hemisphere Sea-Level Maps

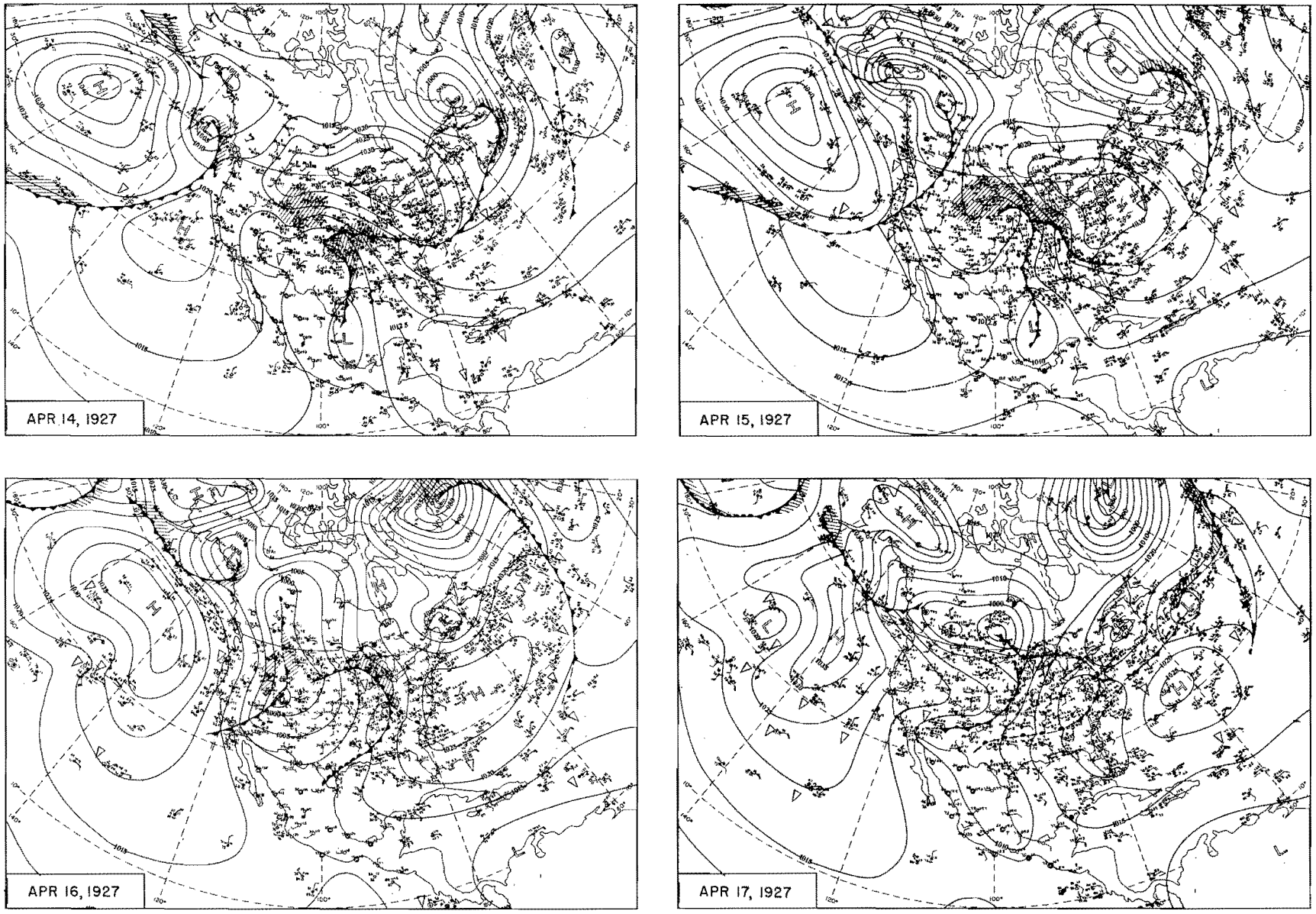

Figure 72. 0700 CST Northern Hemisphere Sea—Level Maps

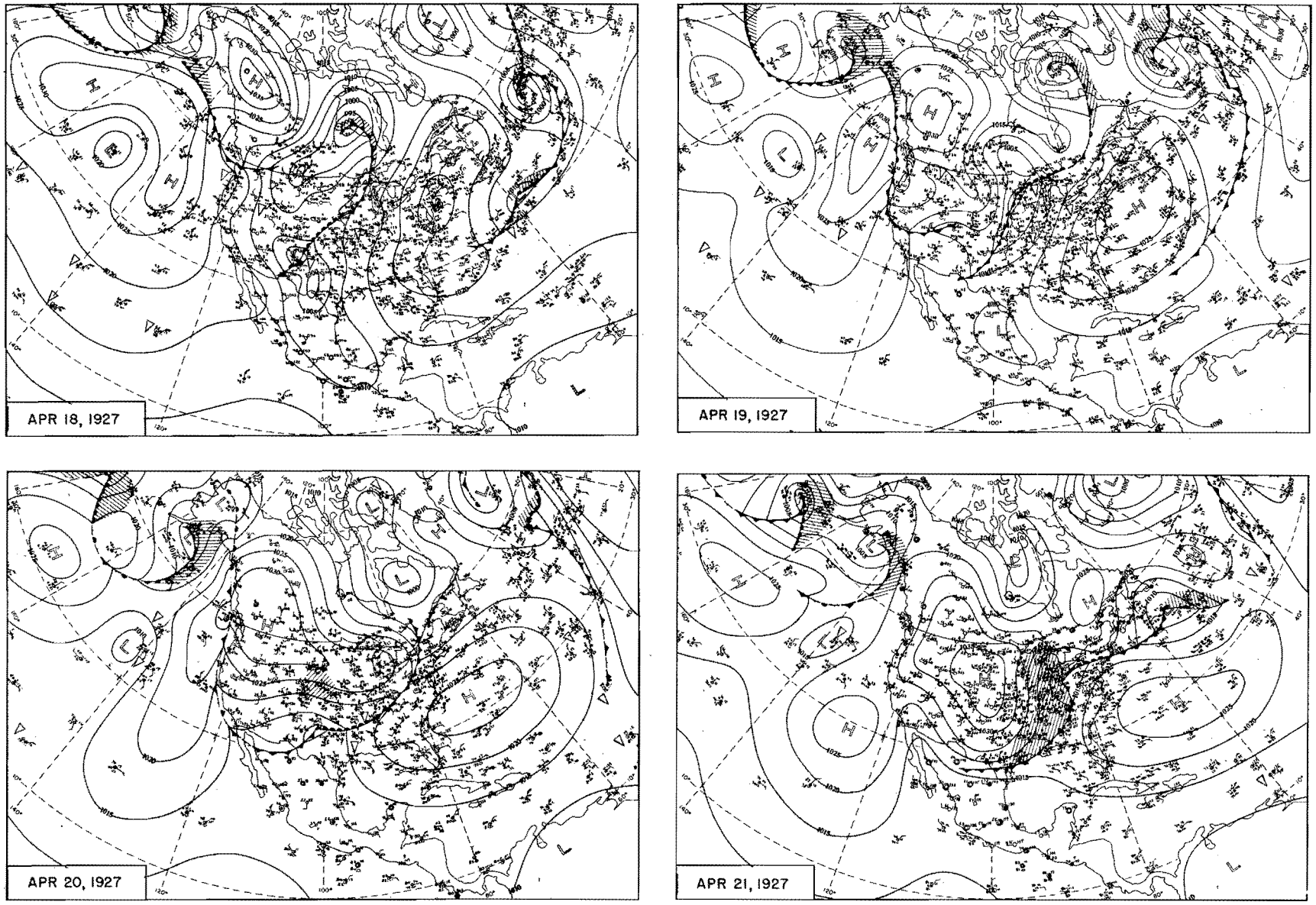

Figure 73. 0700 CST Northern Hemisphere Sea-Level Maps

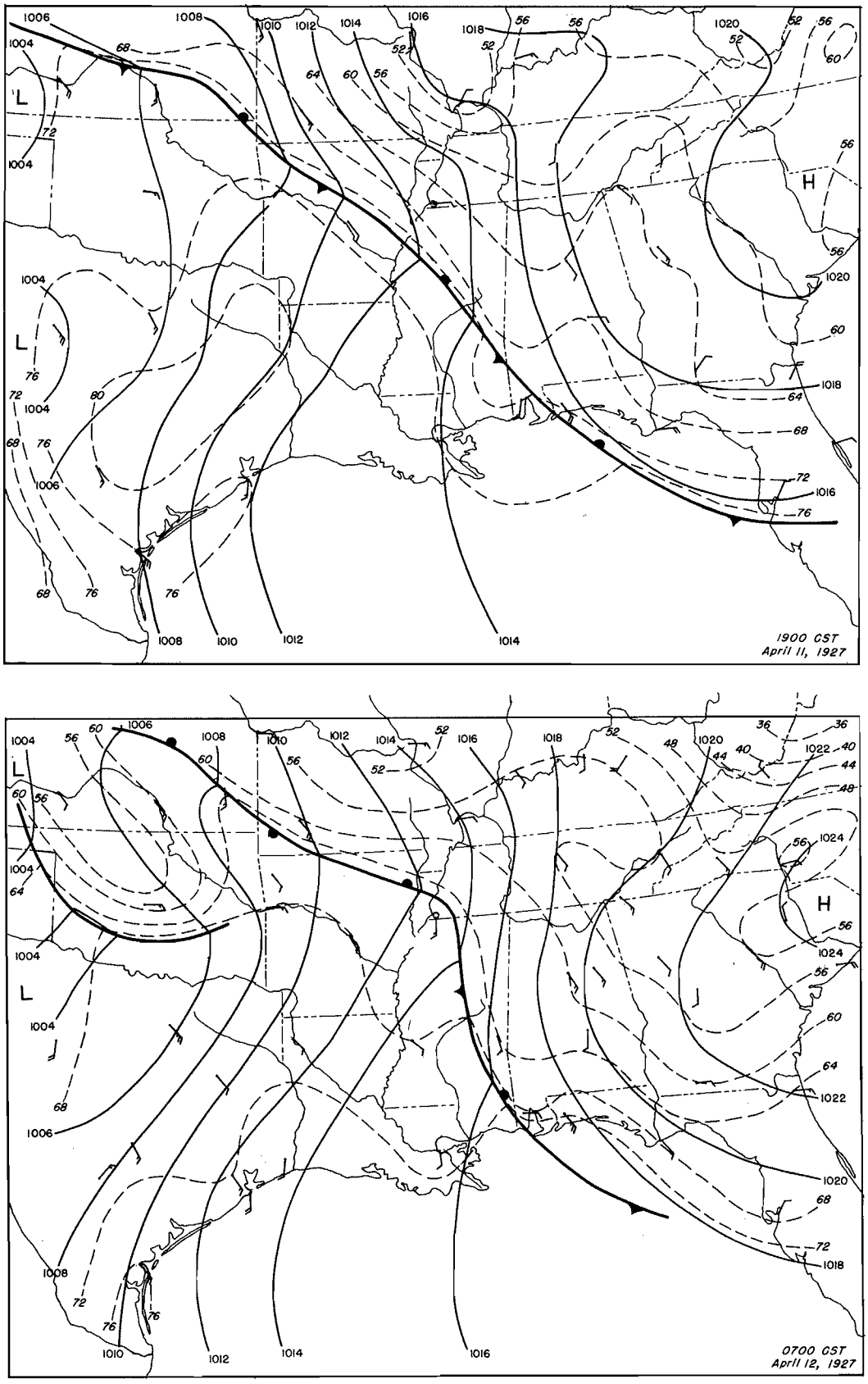

Figure 74. Detailed Surface Weather Maps

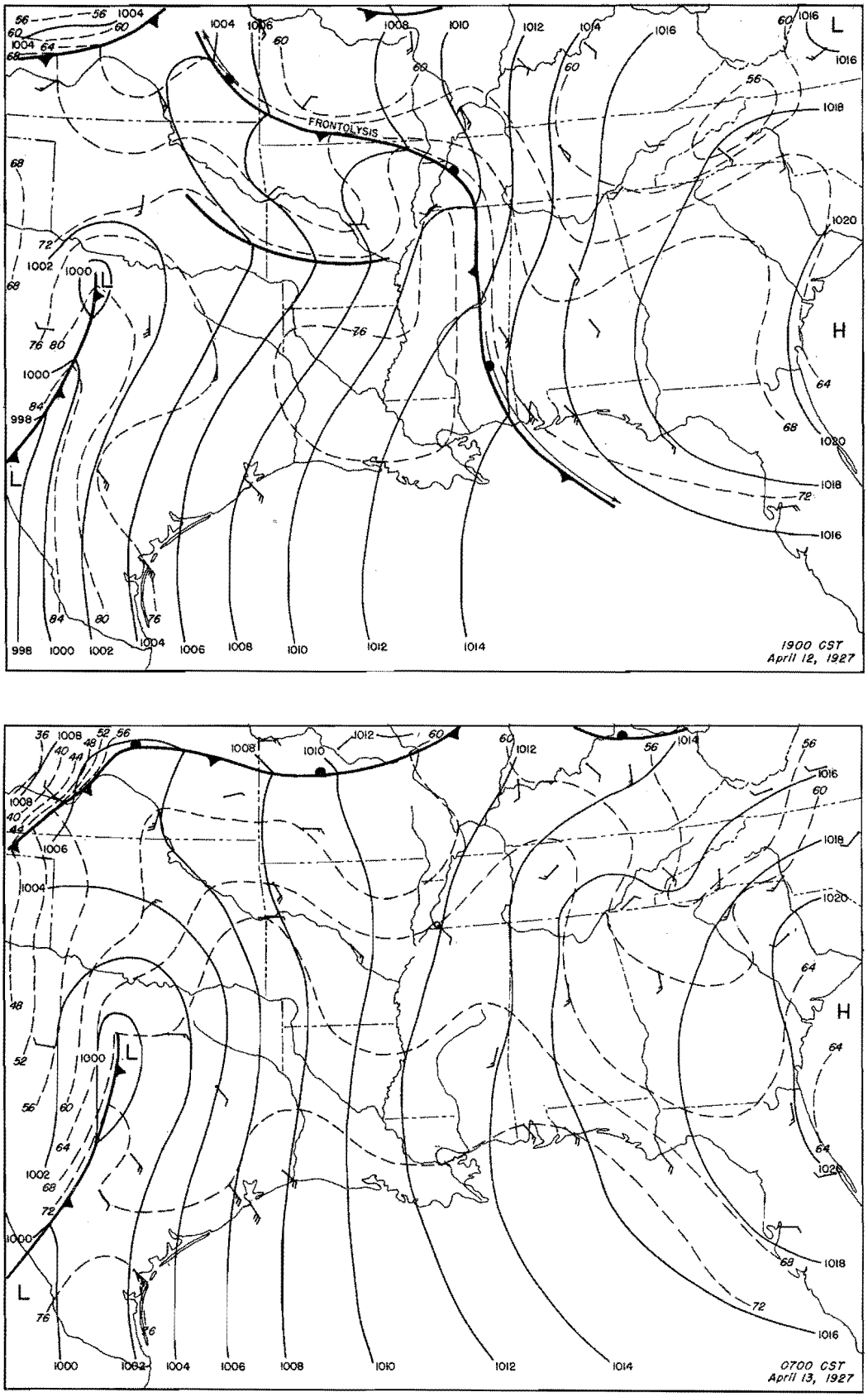

Figure 75. Detailed Surface Weather Maps

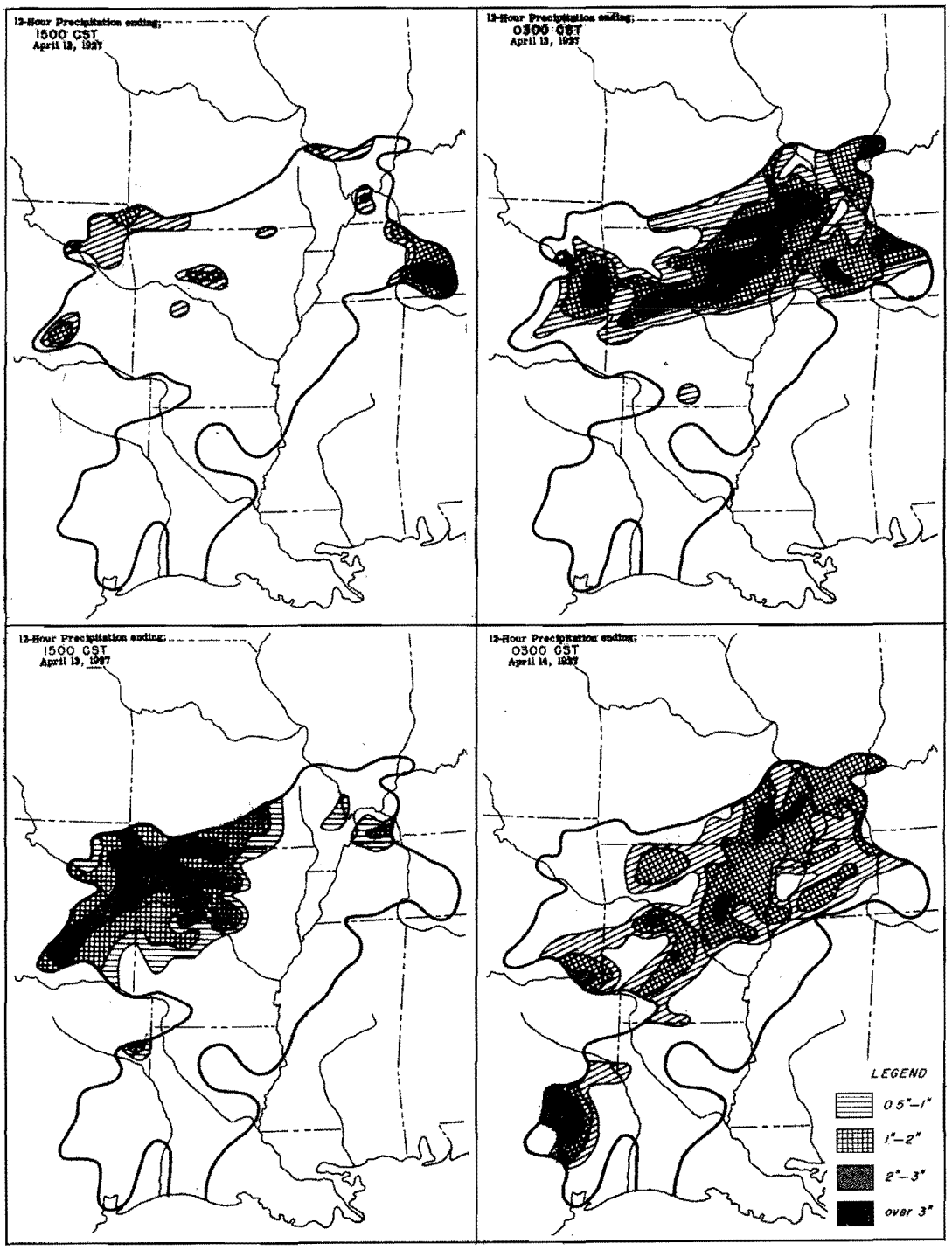

Figure 76. Incremental Isohyetal Patterns

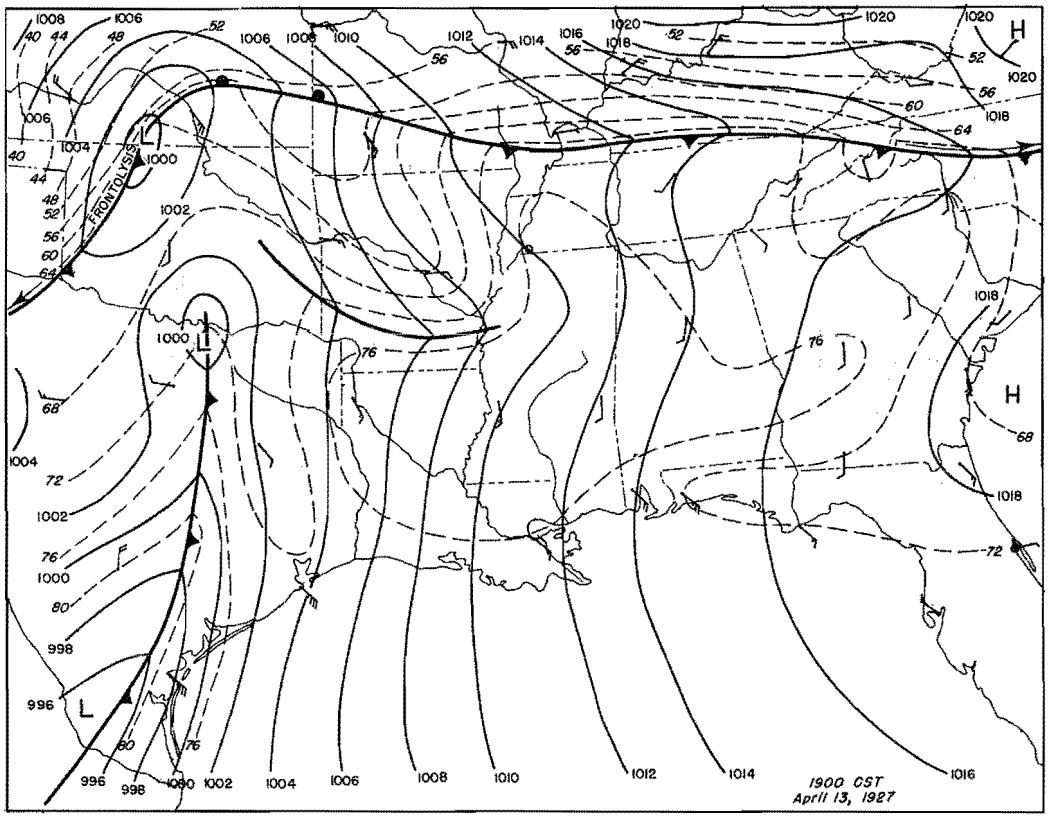

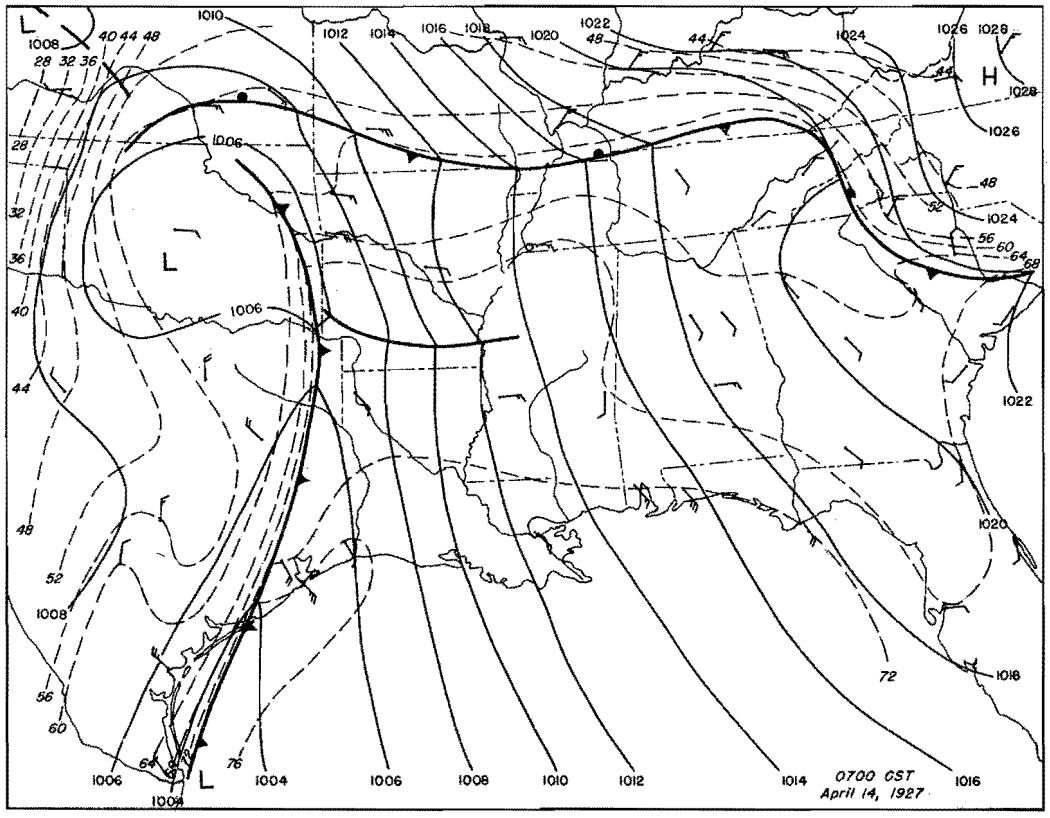

Figure 77. Detailed Surface Weather Maps

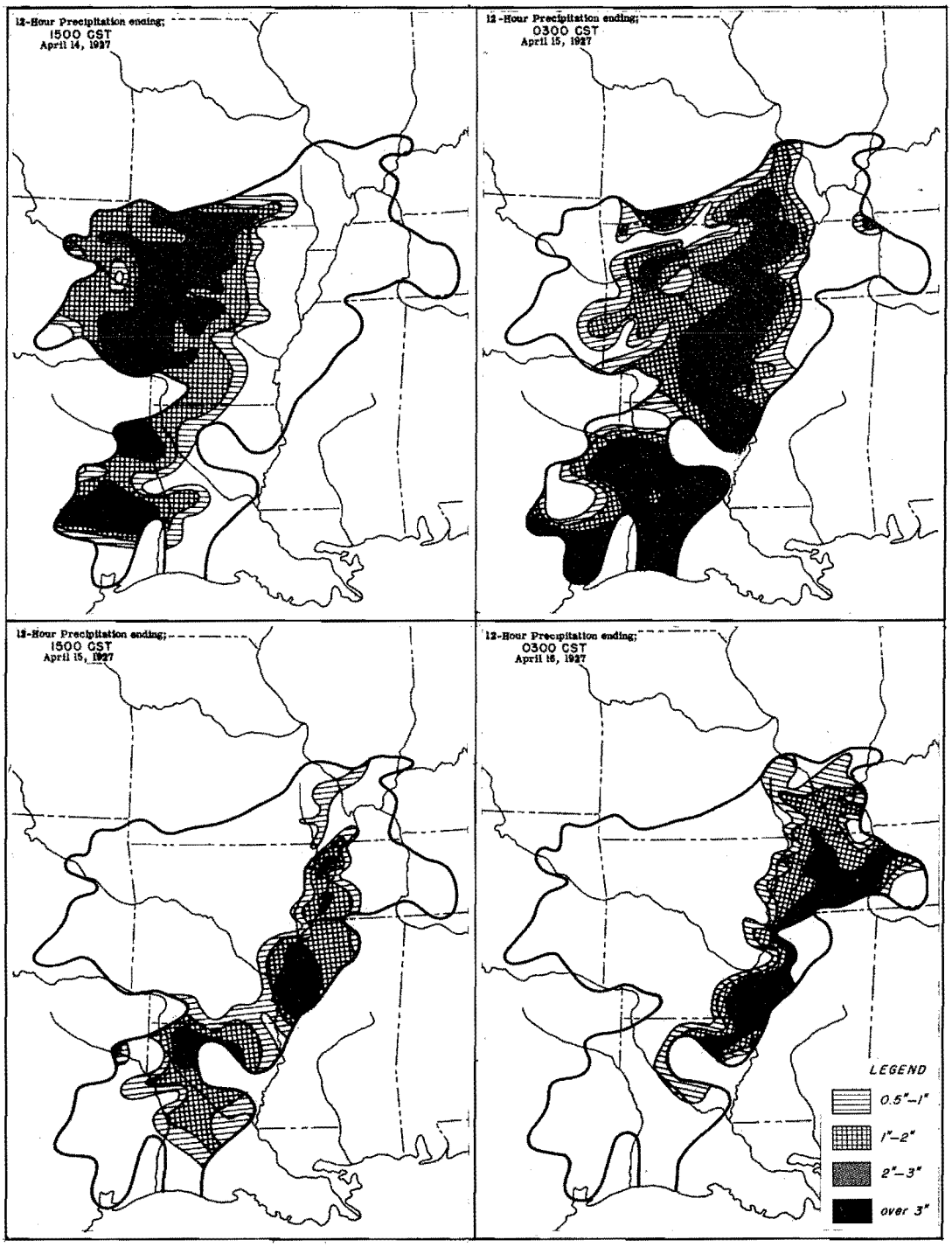

Figure 78. Incremental Isohyetal Patterns

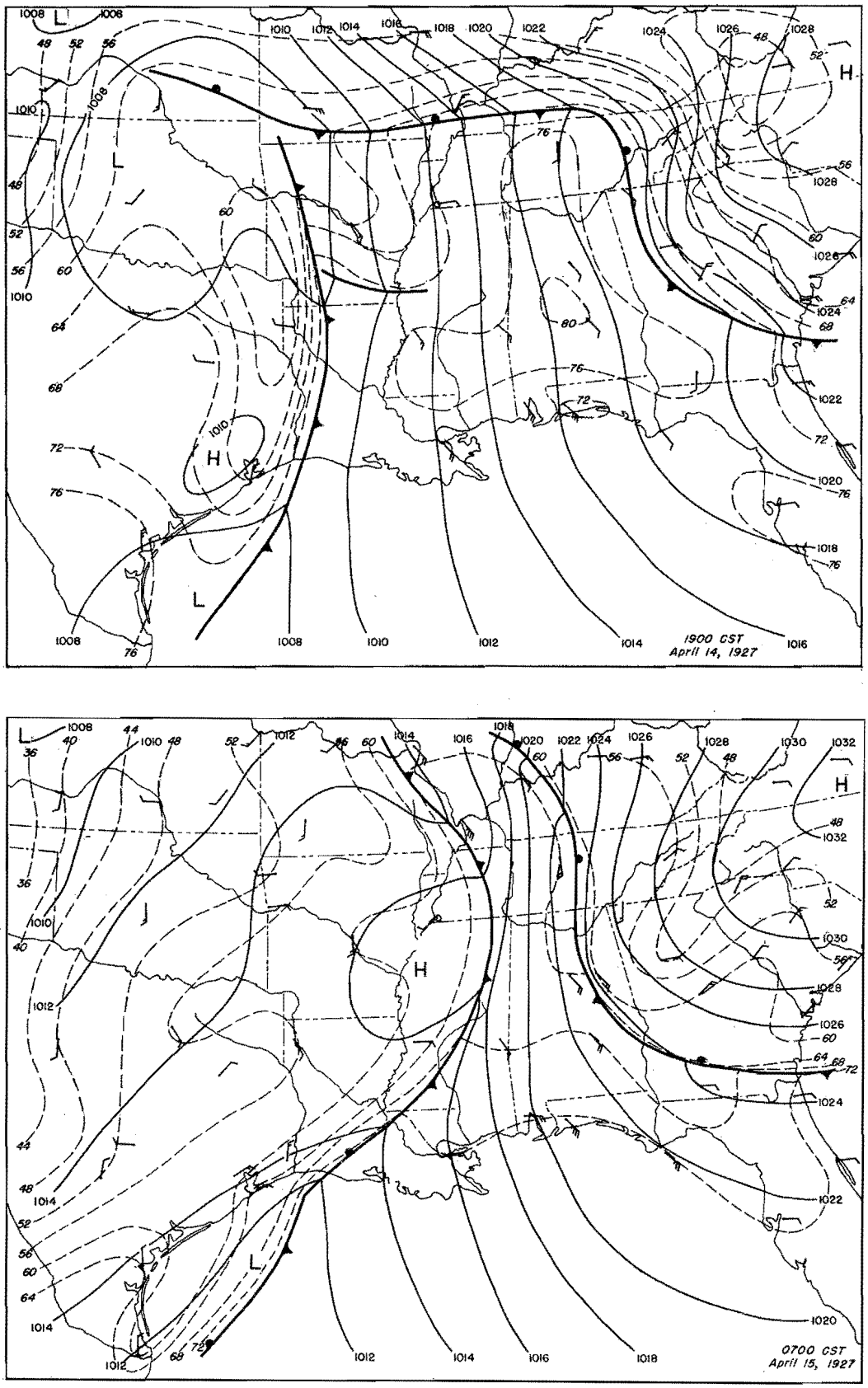

Figure 79. Detailed Surface Weather Maps

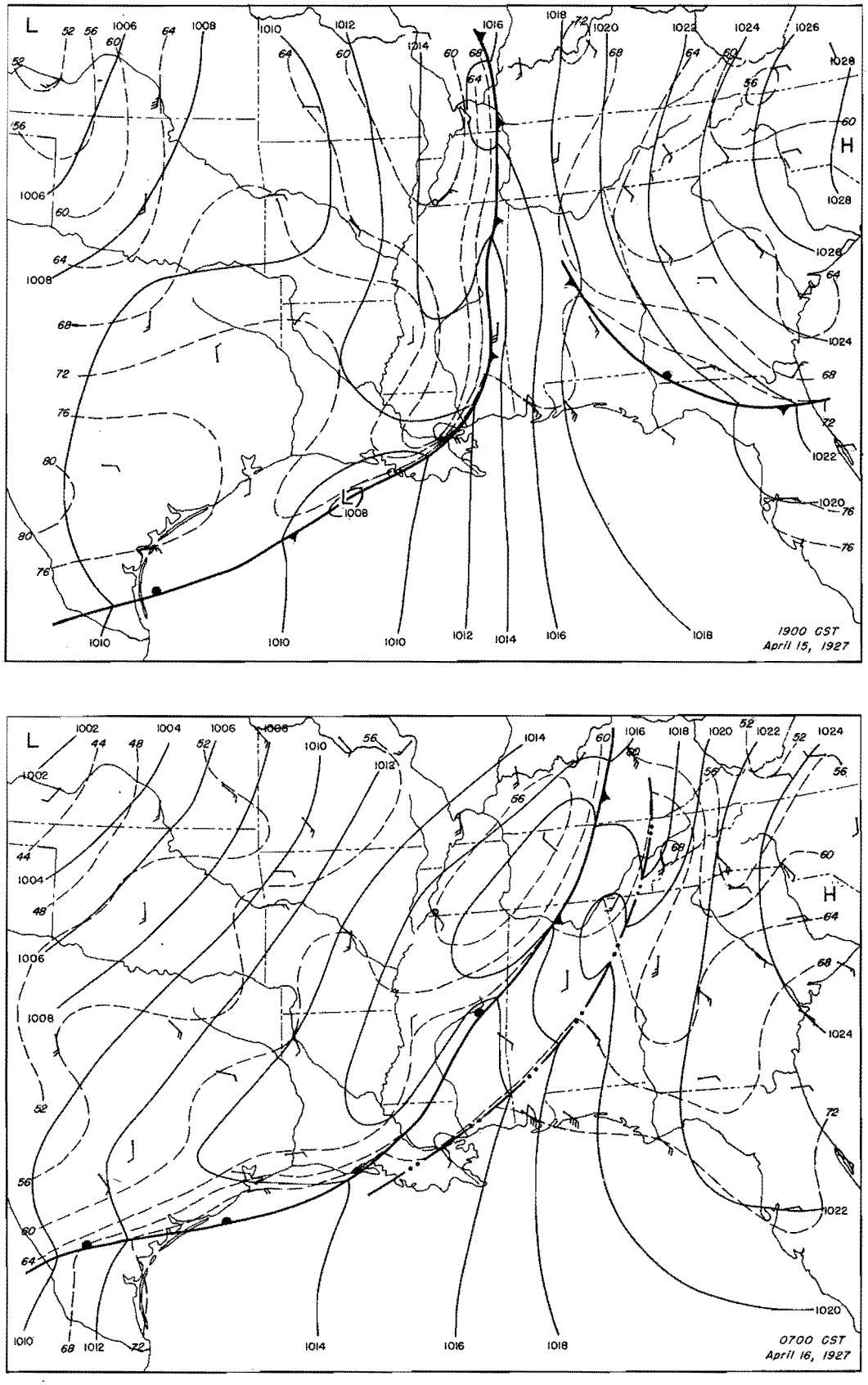

Figure 80. Detailed Surface Weather Maps

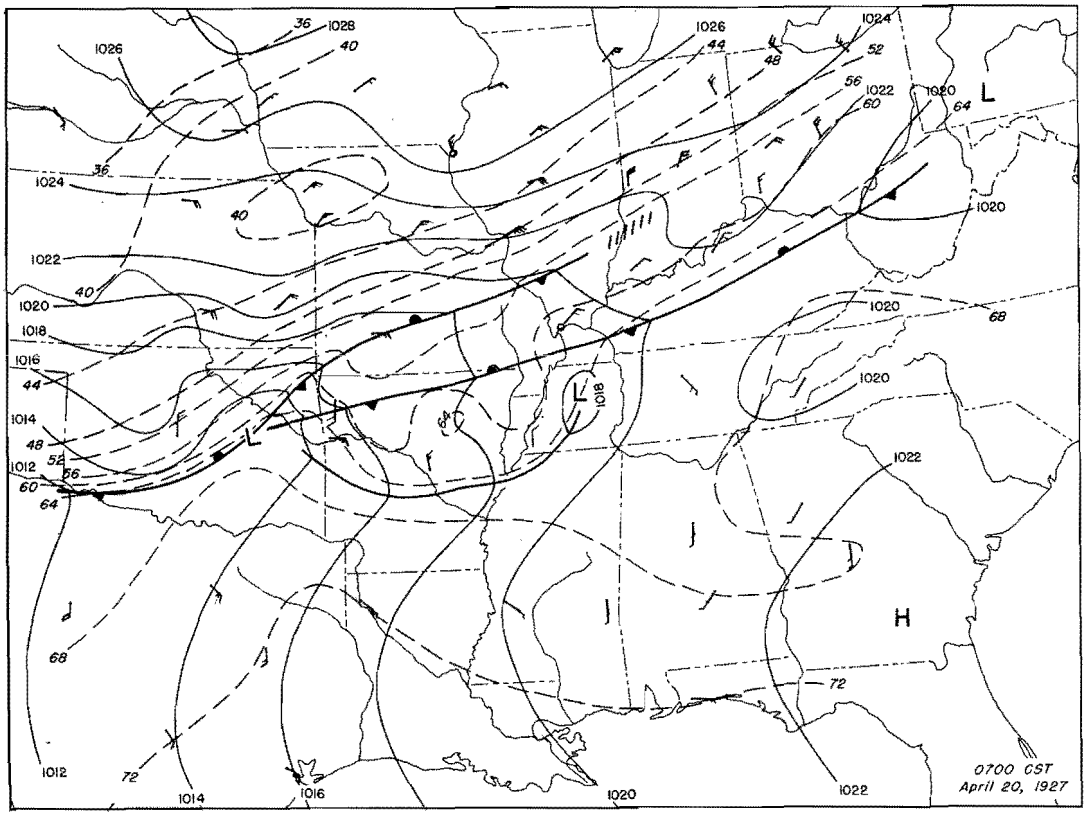

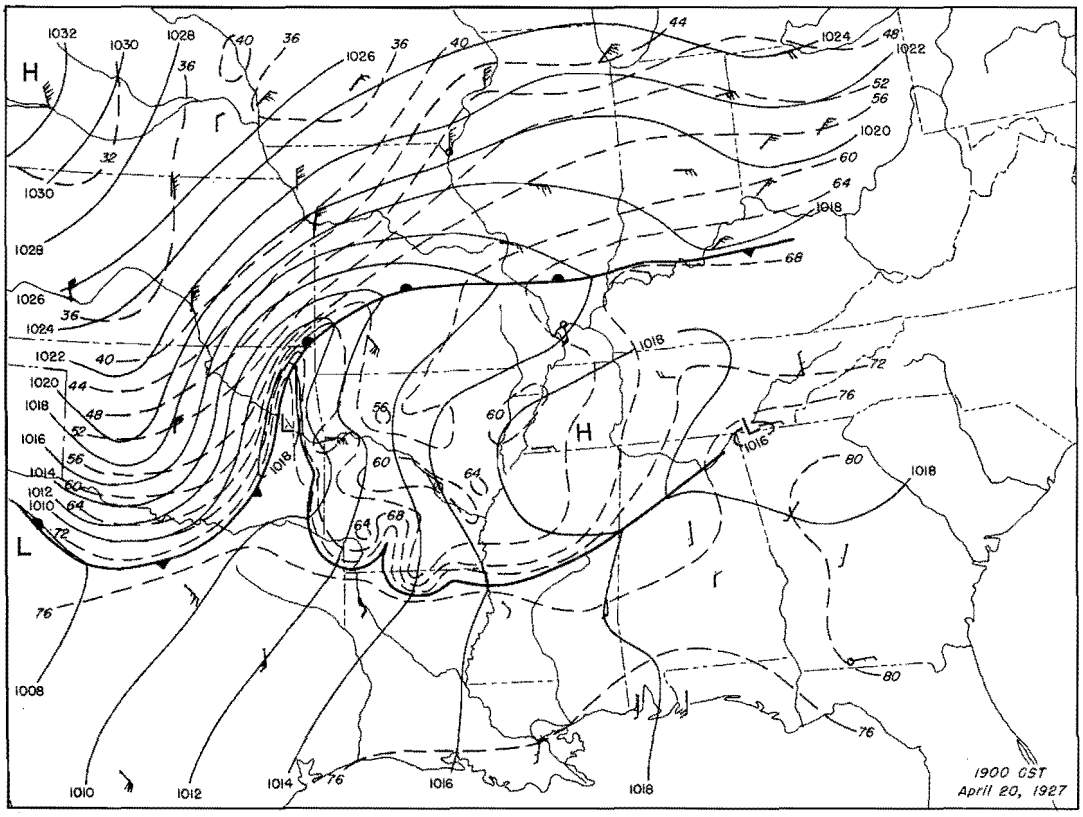

Figure 81. Detailed Surface Weather Maps

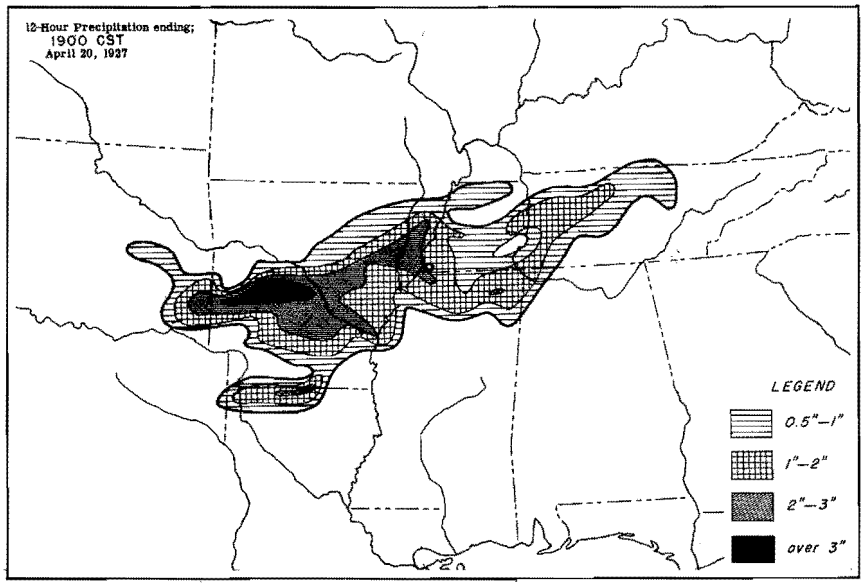

Figure 82. Incremental Isohyetal Patterns

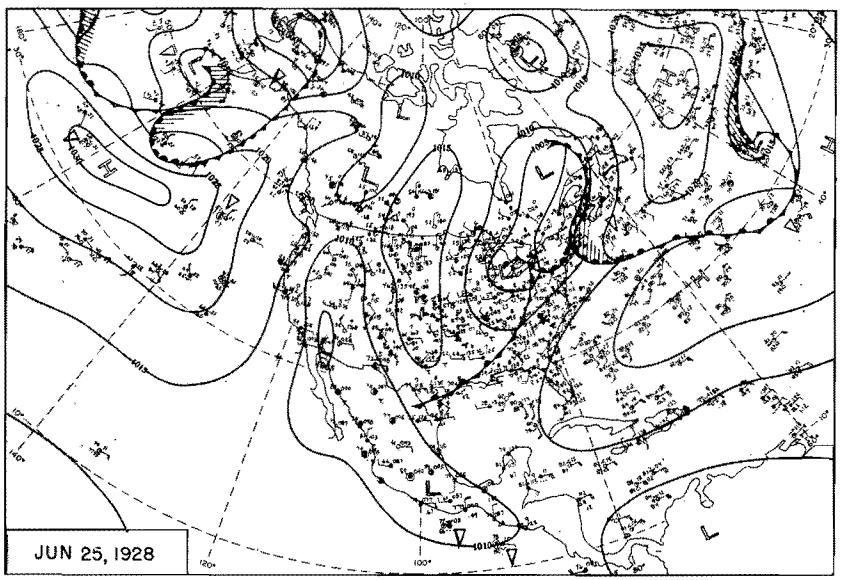

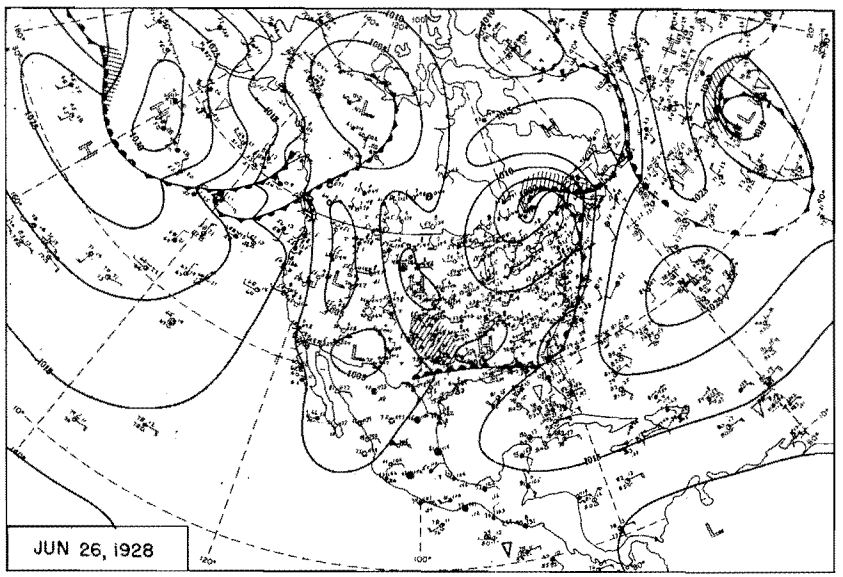

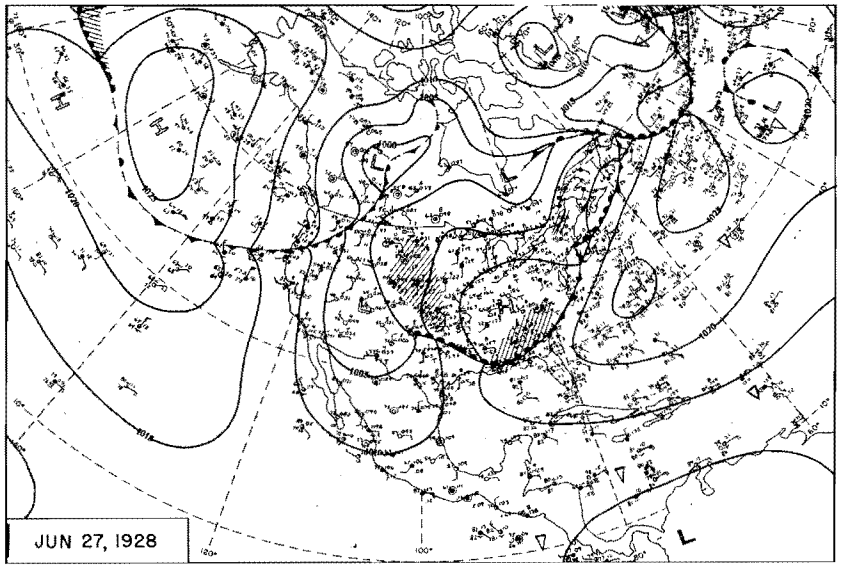

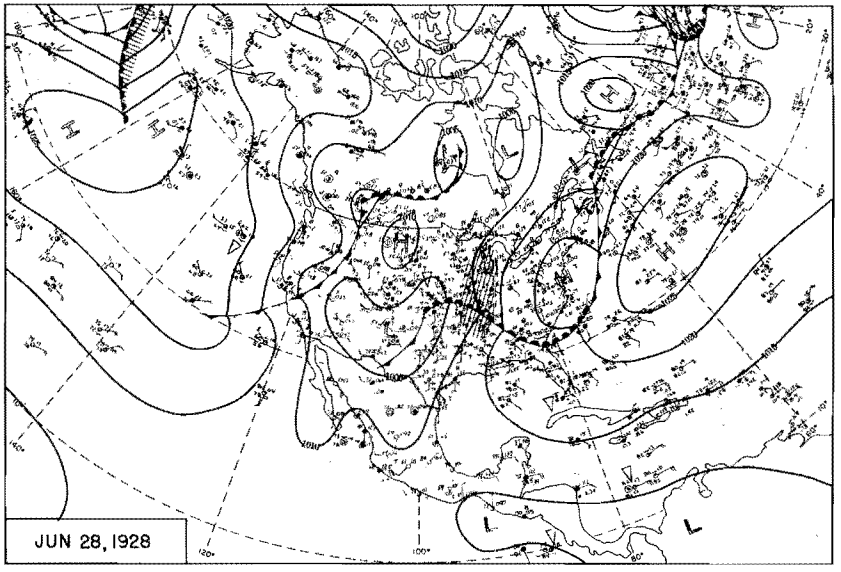

Figure 83. 0700 CST Northern Hemisphere Sea--Level Maps

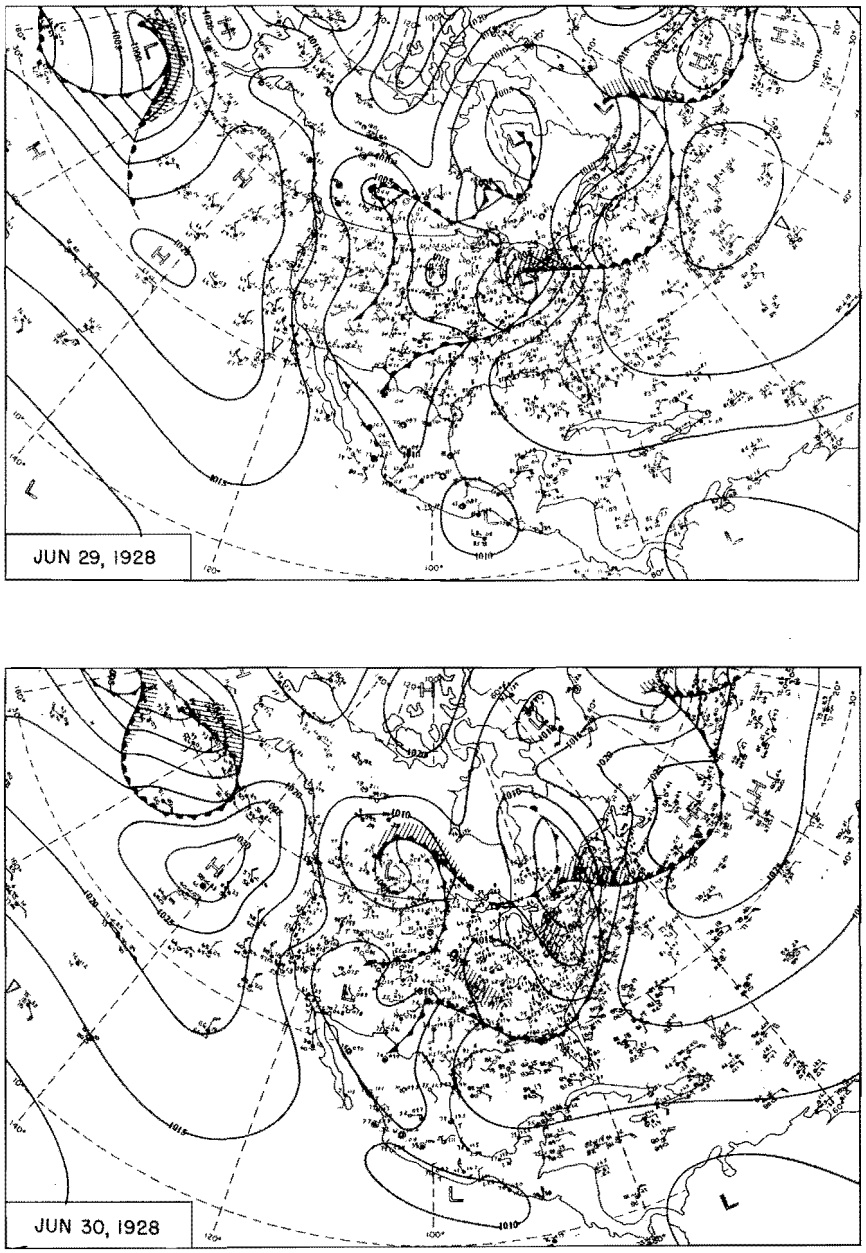

Figure 84. 0700 CST Northern Hemisphere Sea—Level Maps

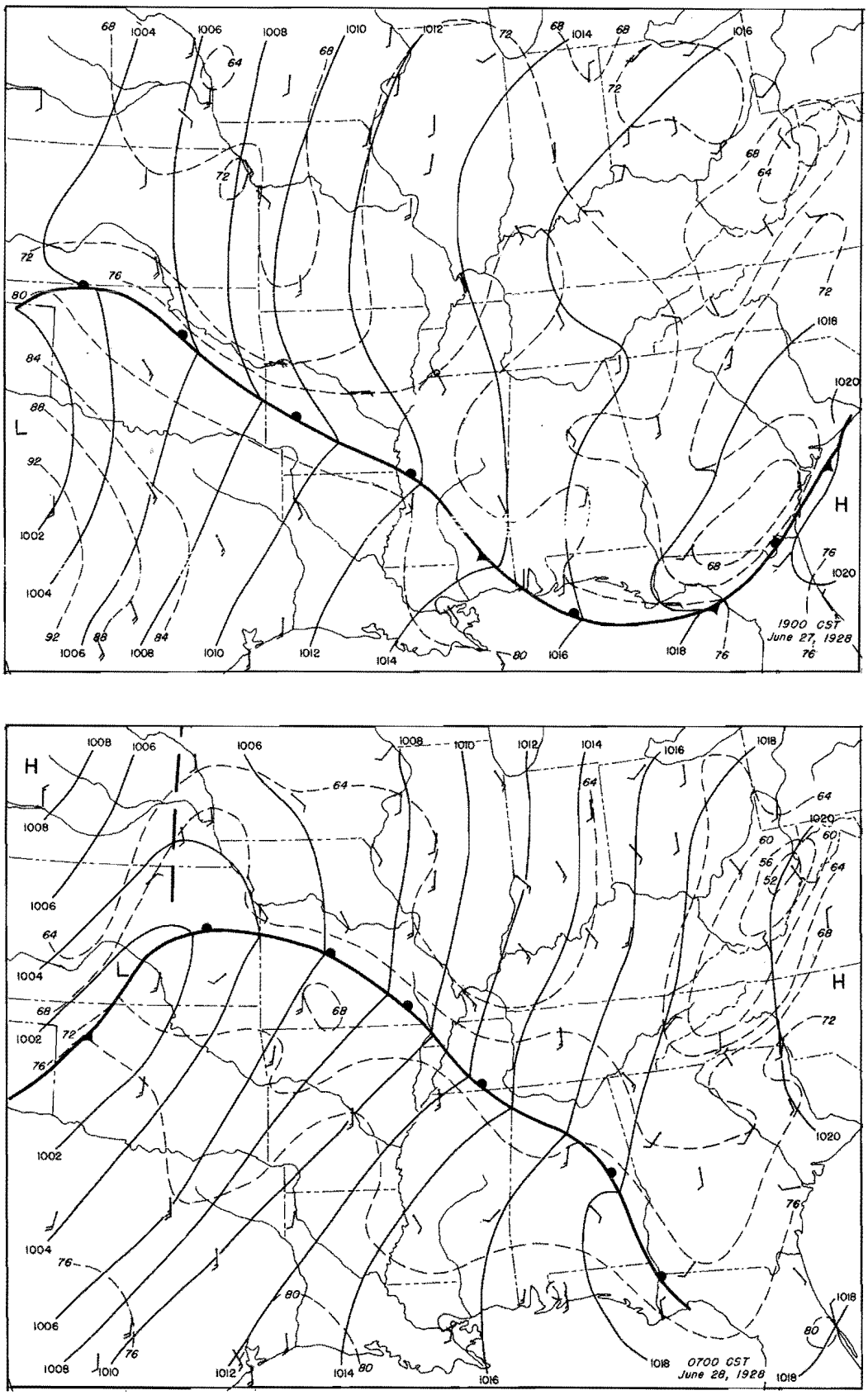

Figure 85. Detailed Surface Weather Maps

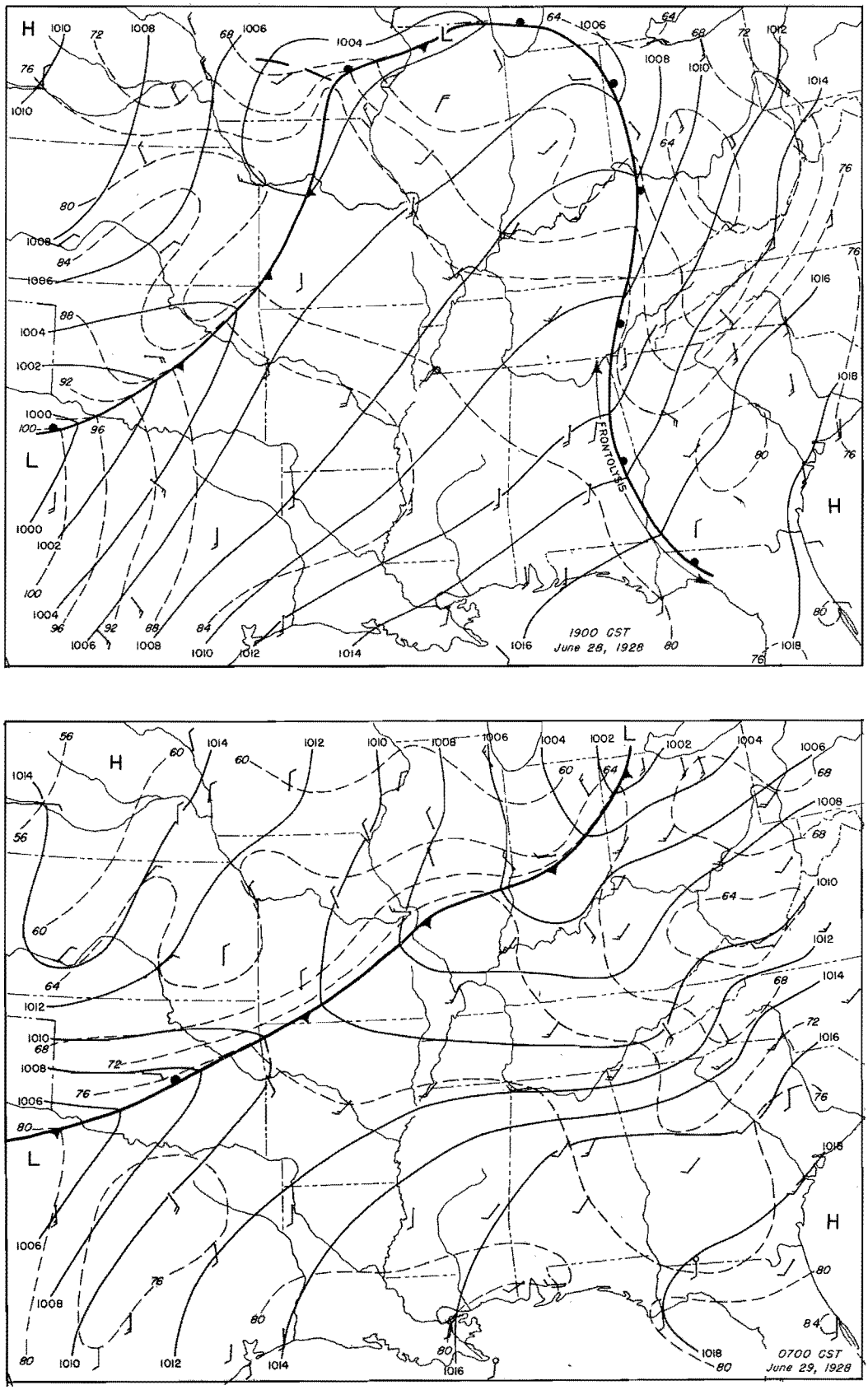

Figure 86. Detailed Surface Weather Maps

OR 7-10 36°06 84°08

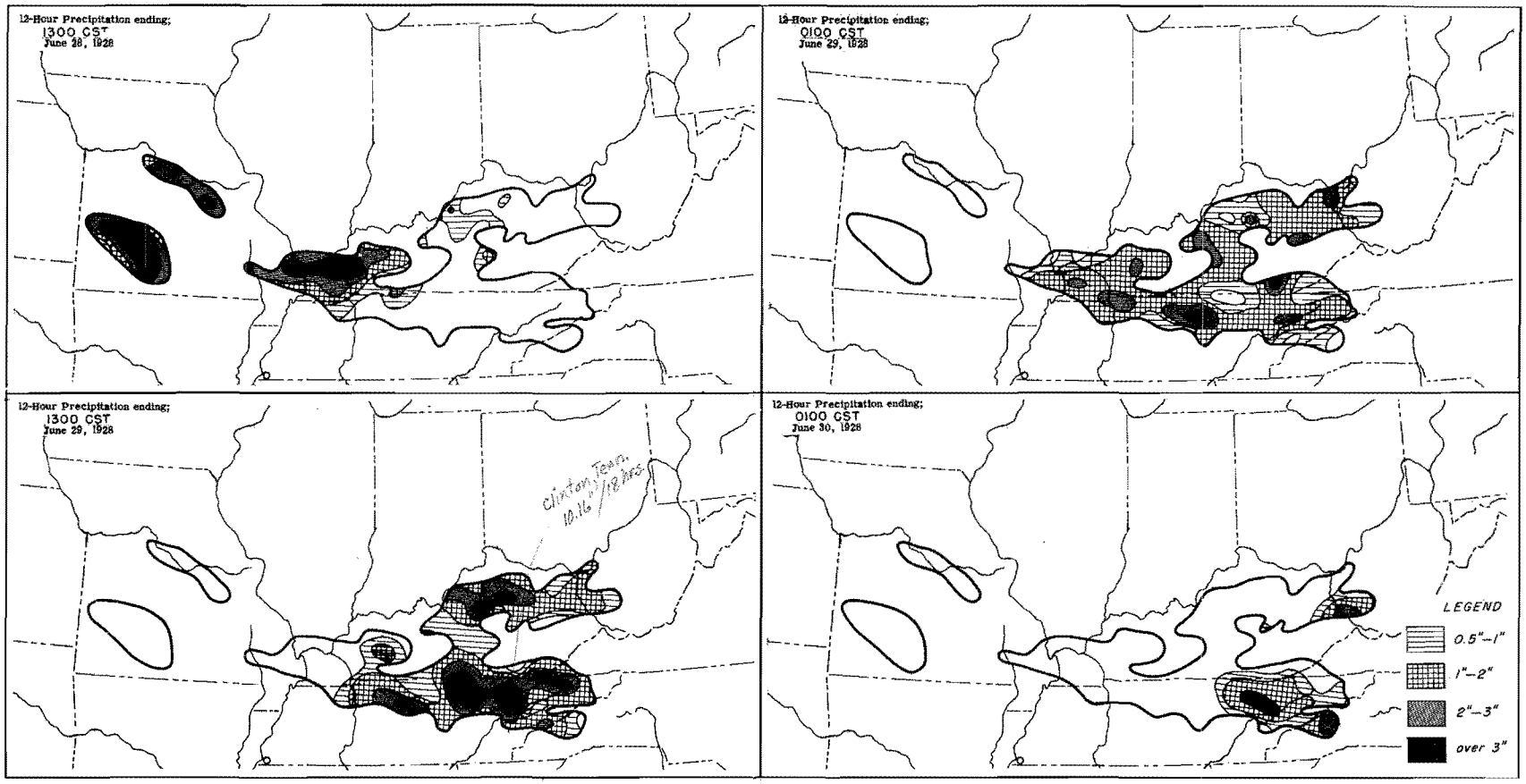

Figure 87. Incremental Isohyetal Pattern

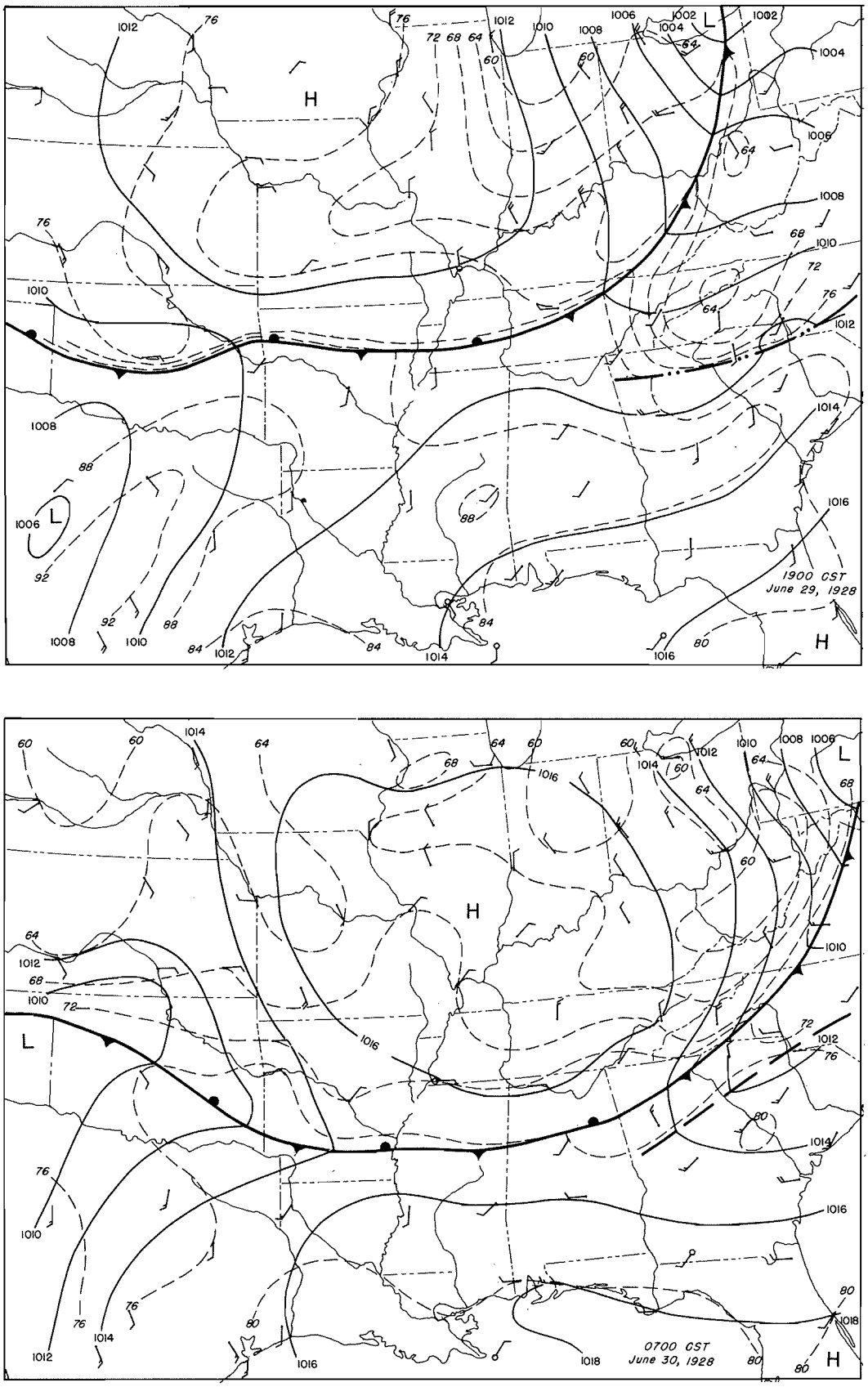

Figure 88. Detailed Surface Weather Maps

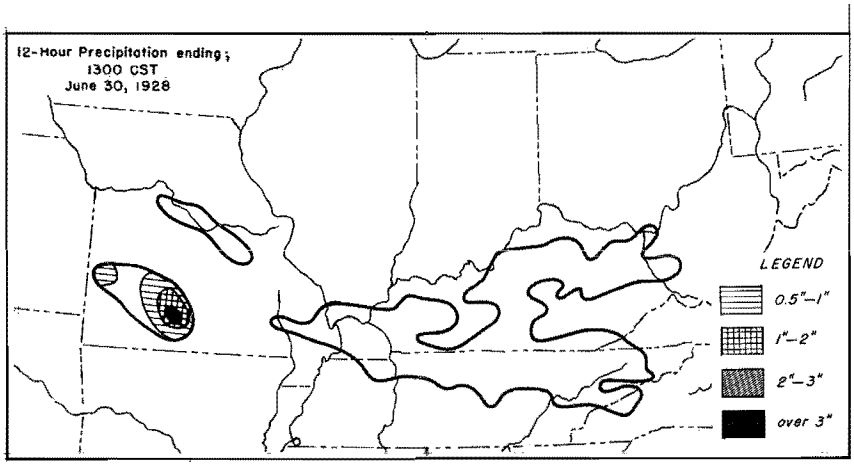

Figure 89. Incremental Isohyetal Patterns

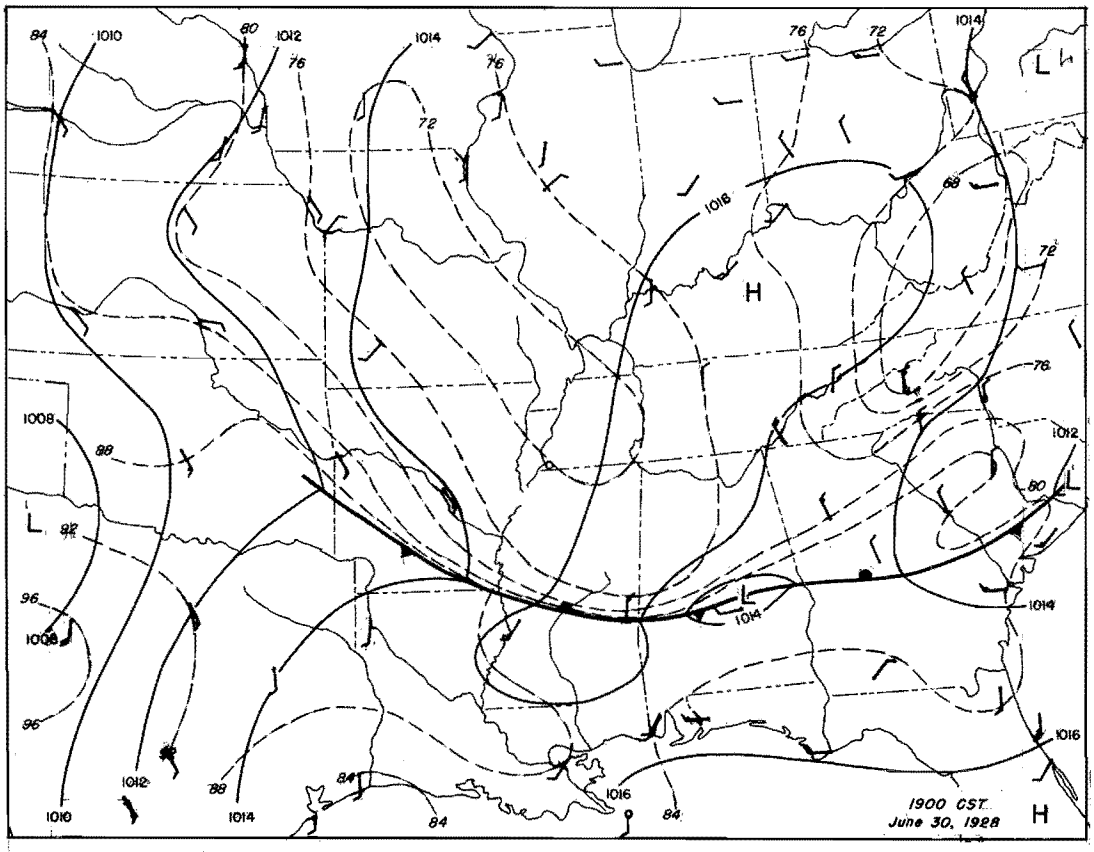

Figure 90. Detailed Surface Weather Map

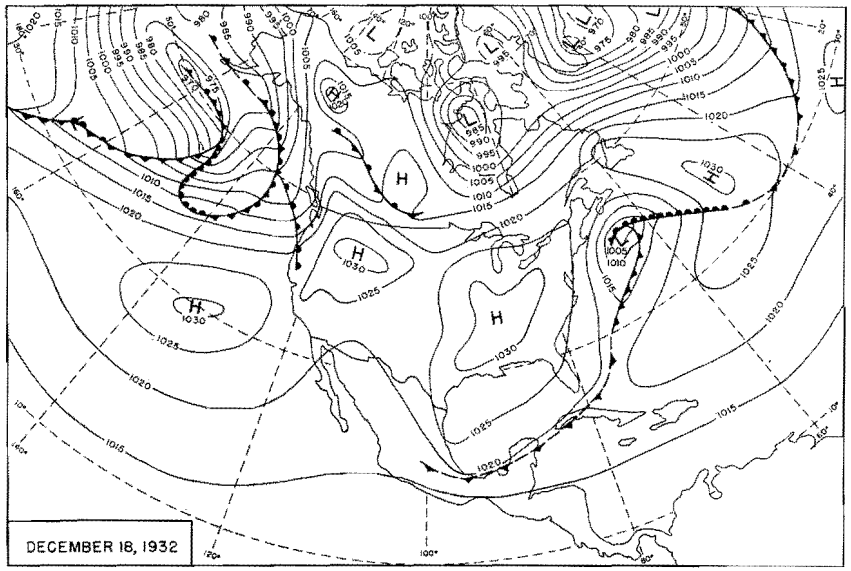

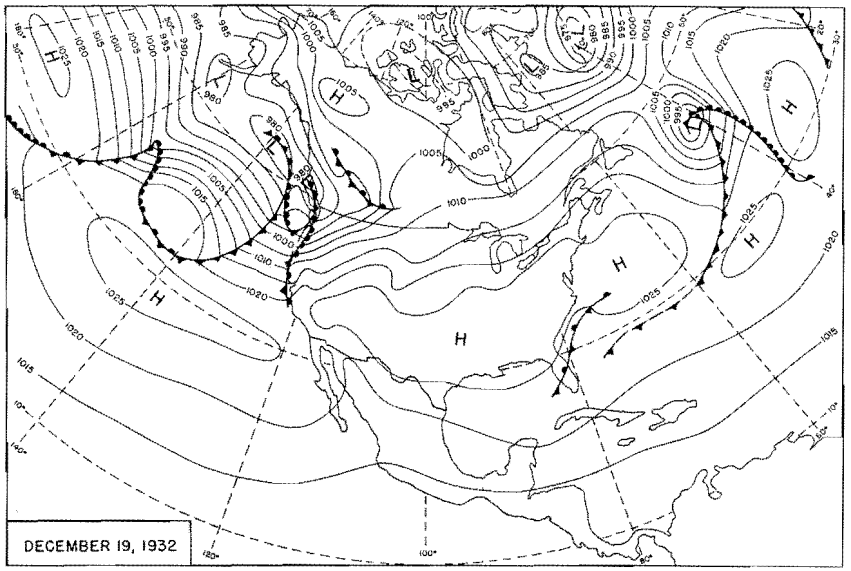

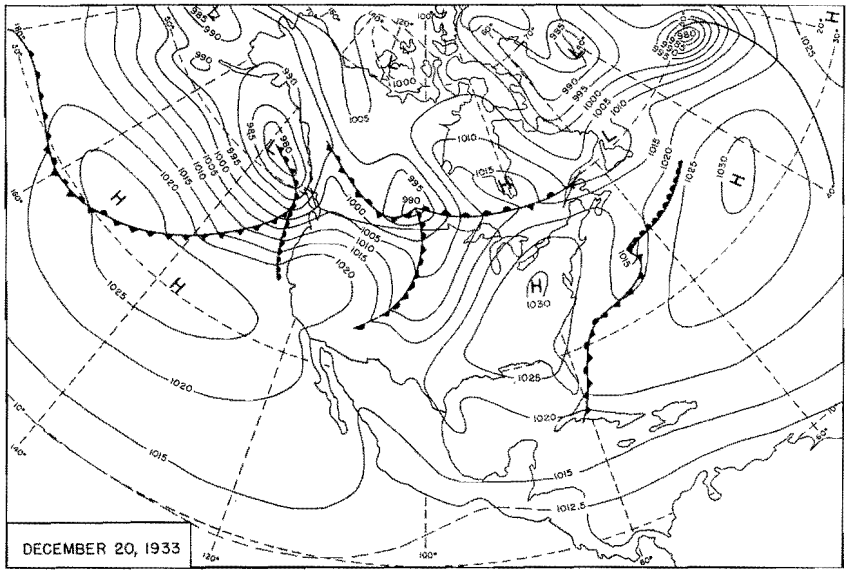

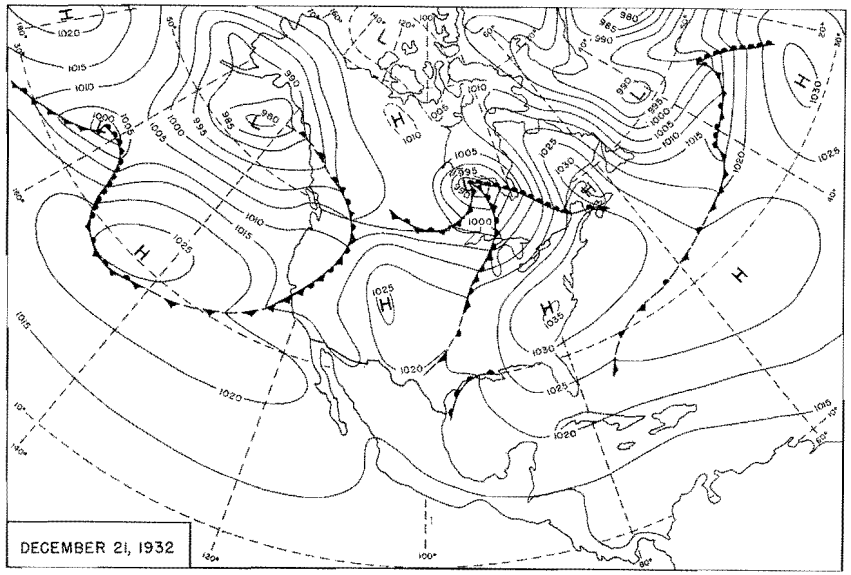

Figure 91. 0700 CST Northern Hemisphere Sea-Level Maps

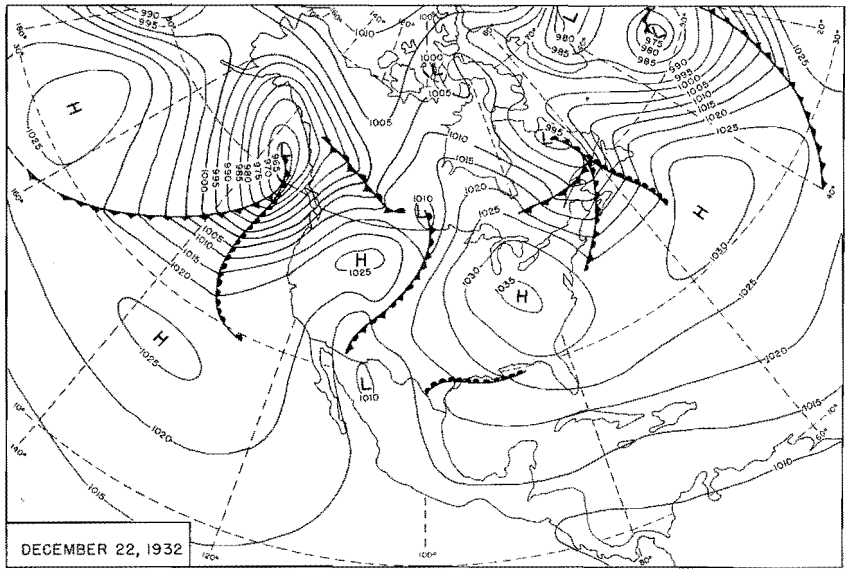

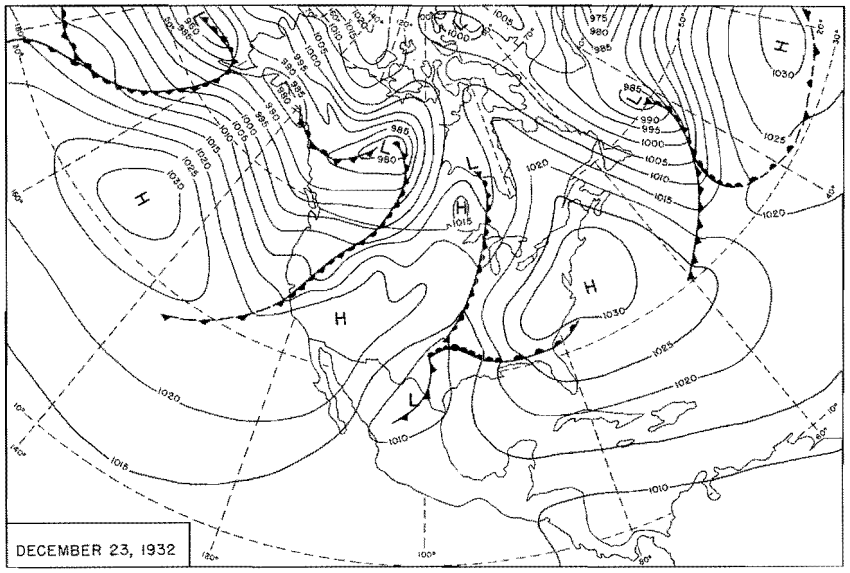

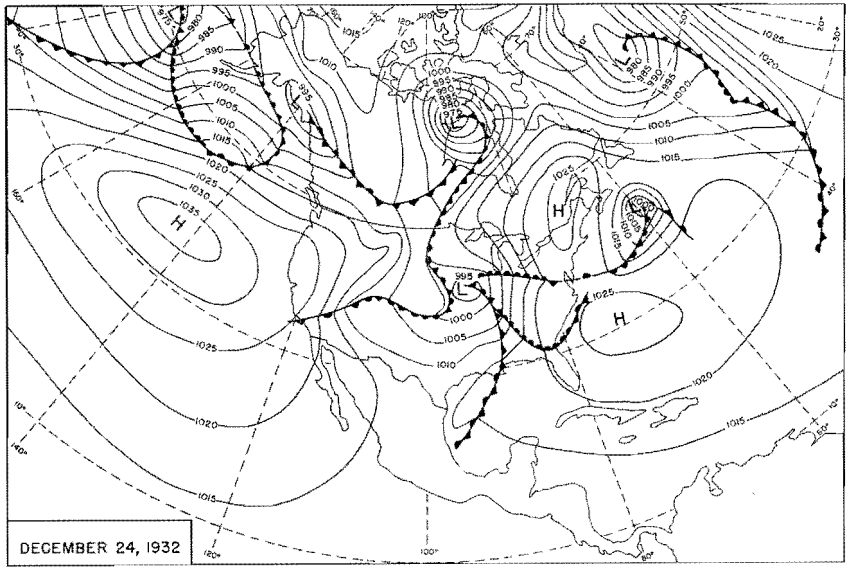

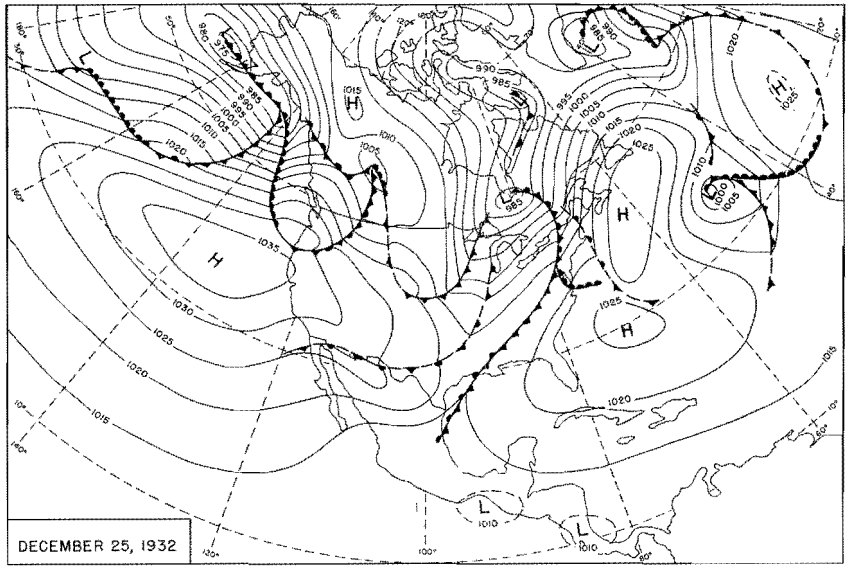

Figure 92. 0700 CST Northern Hemisphere Sea-Level Maps

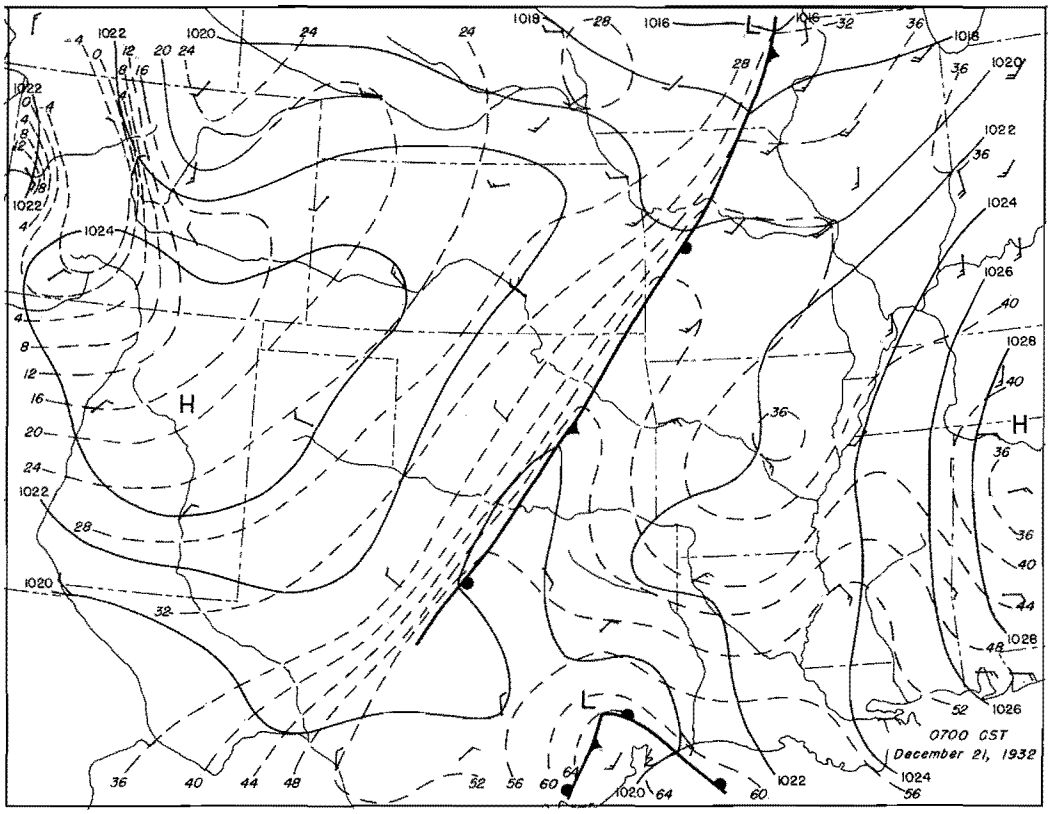

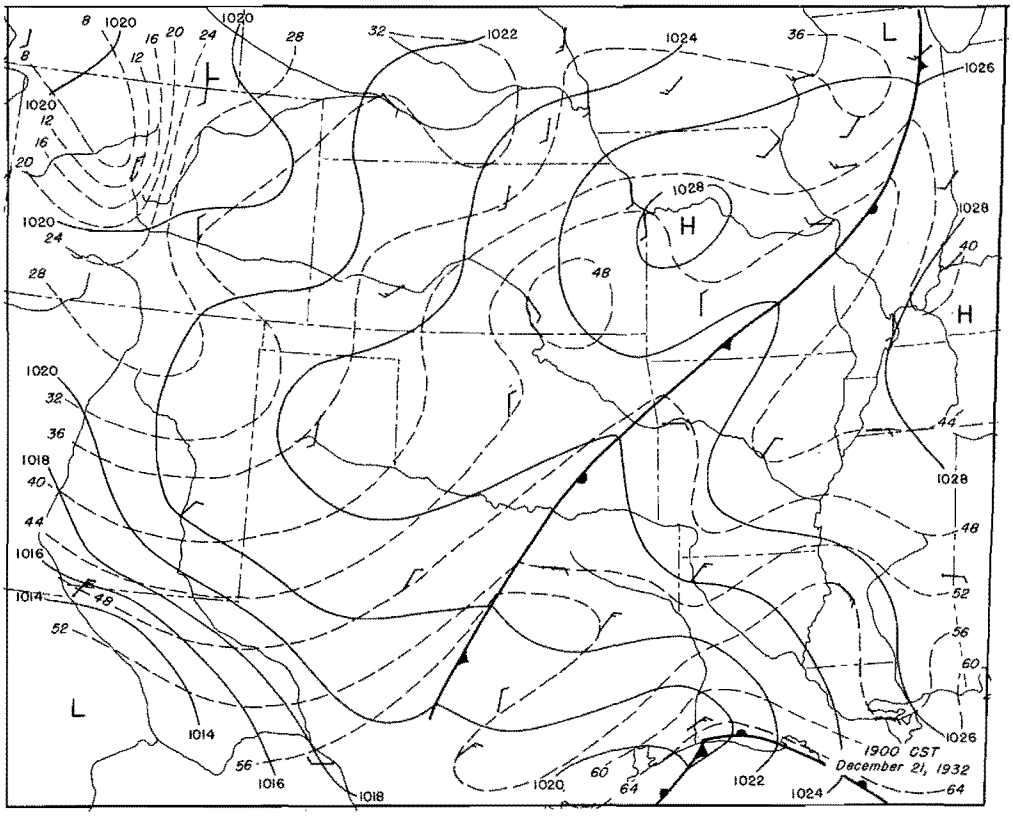

Figure 93. Detailed Surface Weather Maps

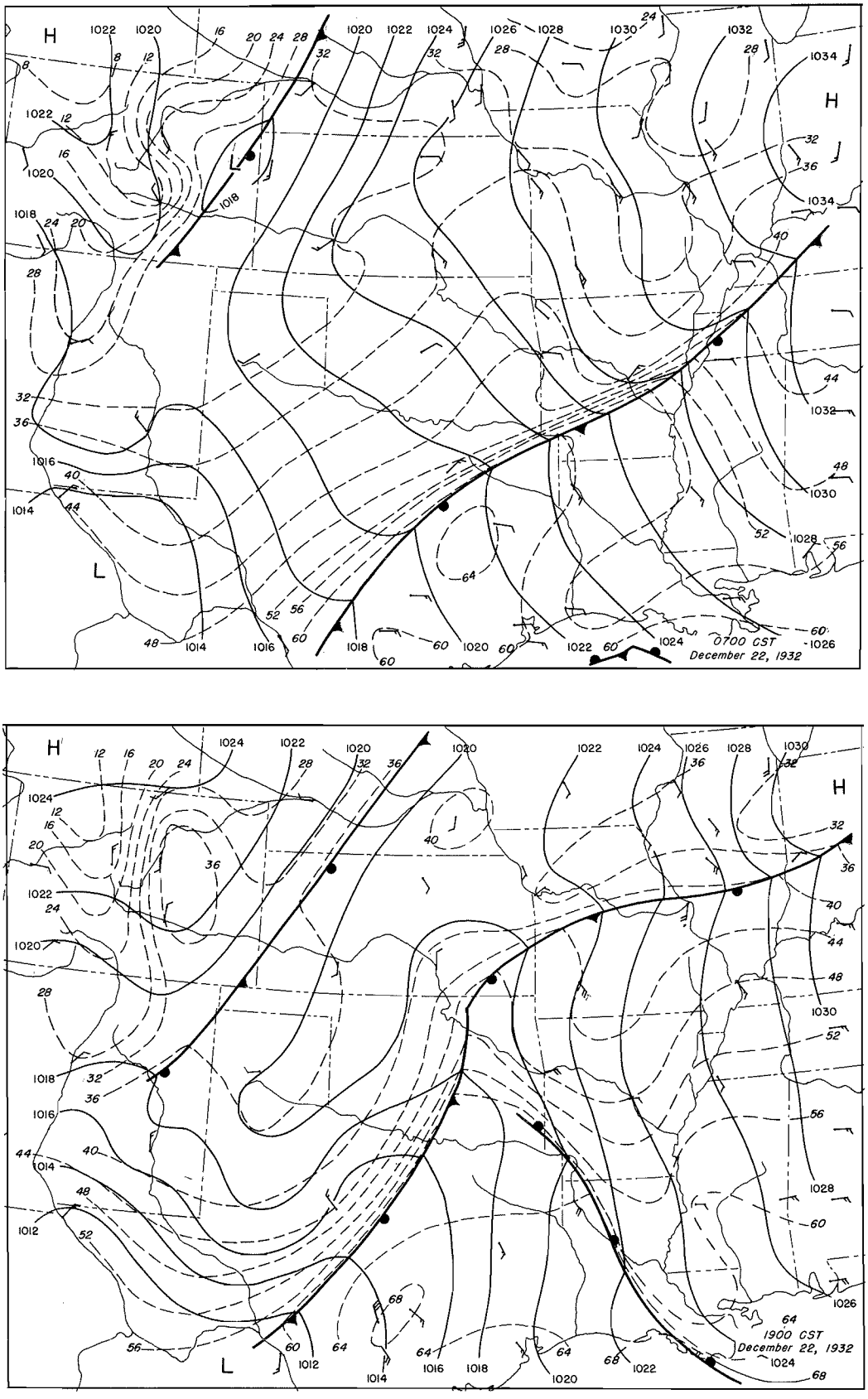

Figure 94. Detailed Surface Weather Maps

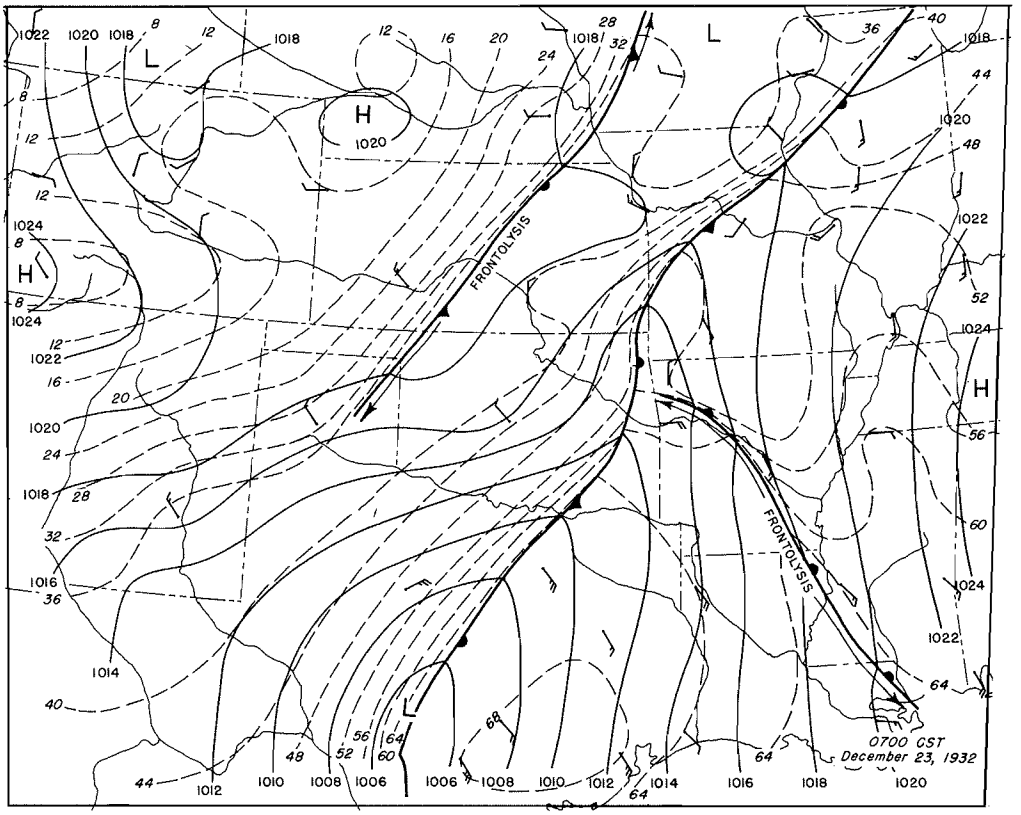

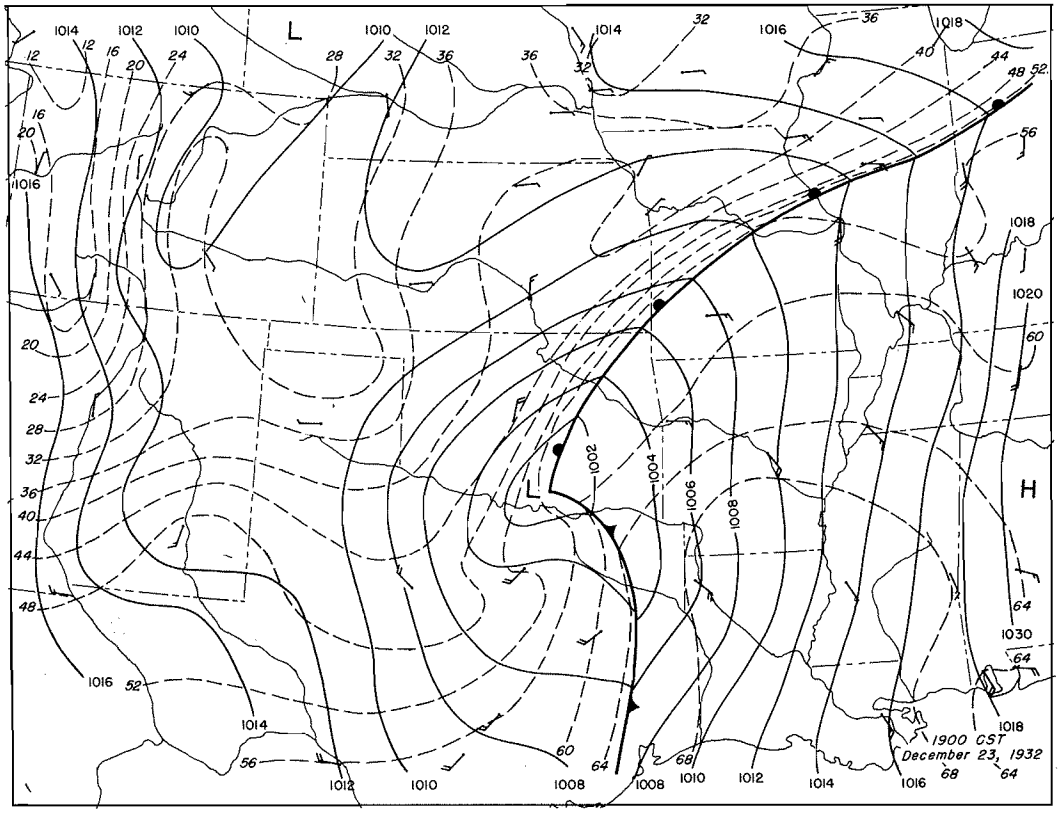

Figure 95. Detailed Surface Weather Maps

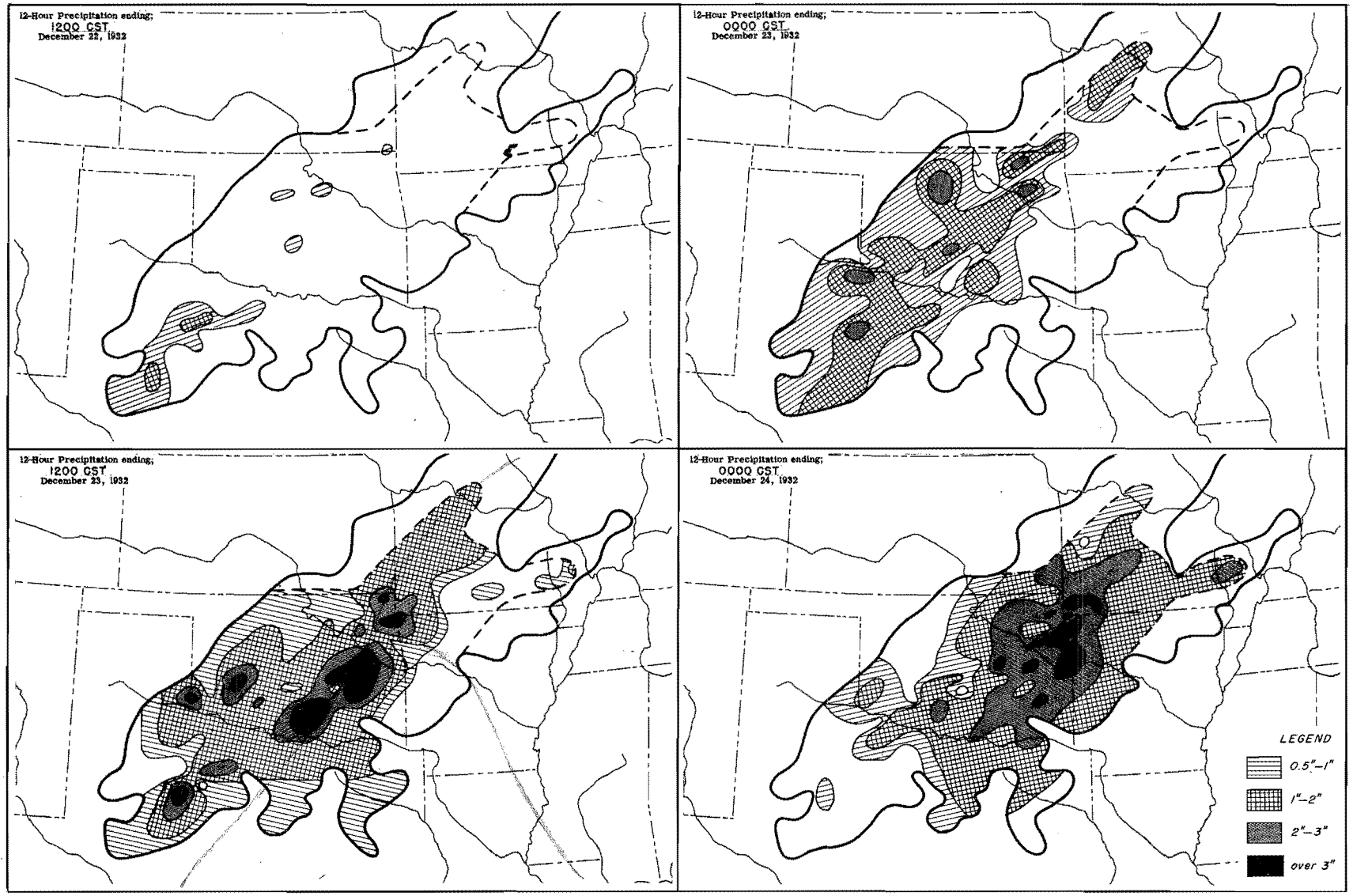

0700 CST '23

Figure 96. Incremental Isohyetal Patterns

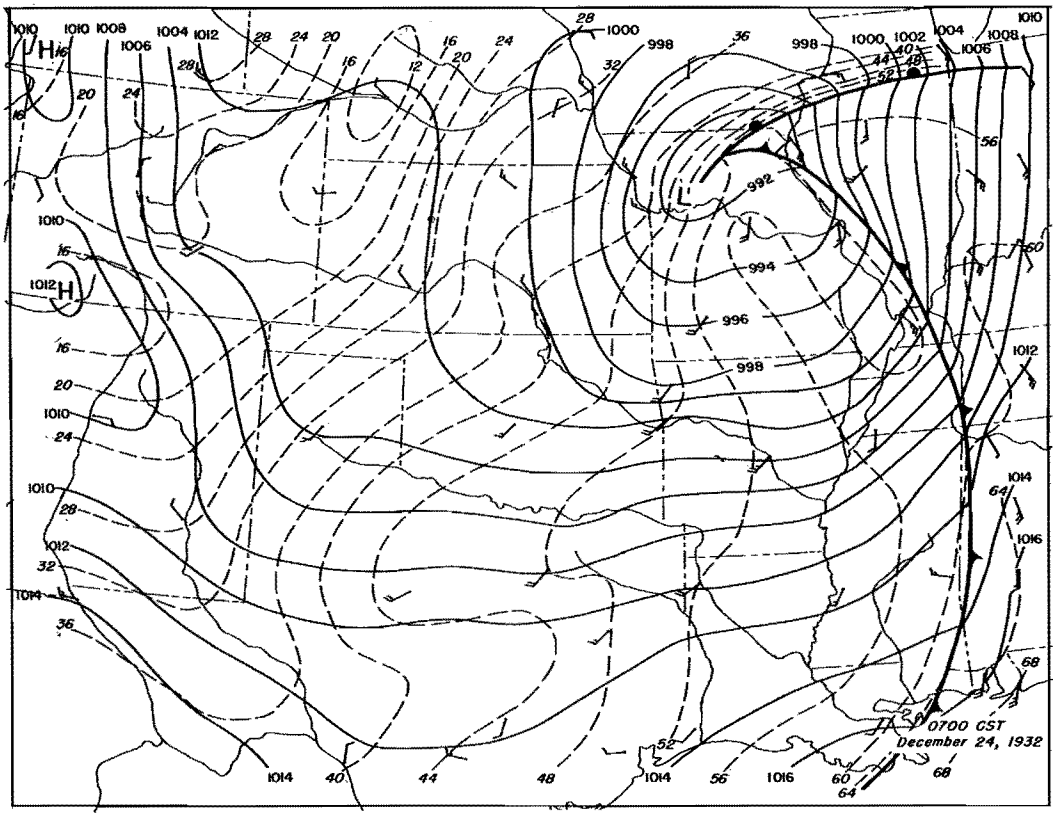

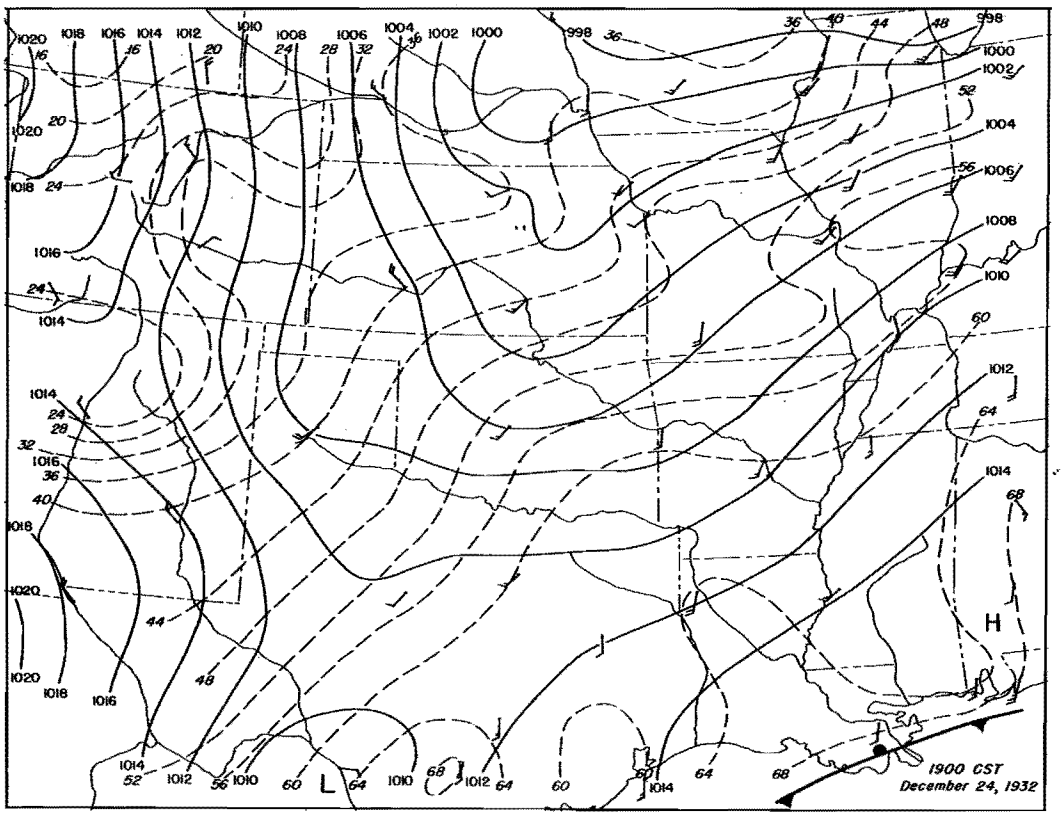

Figure 97. Detailed Surface Weather Maps

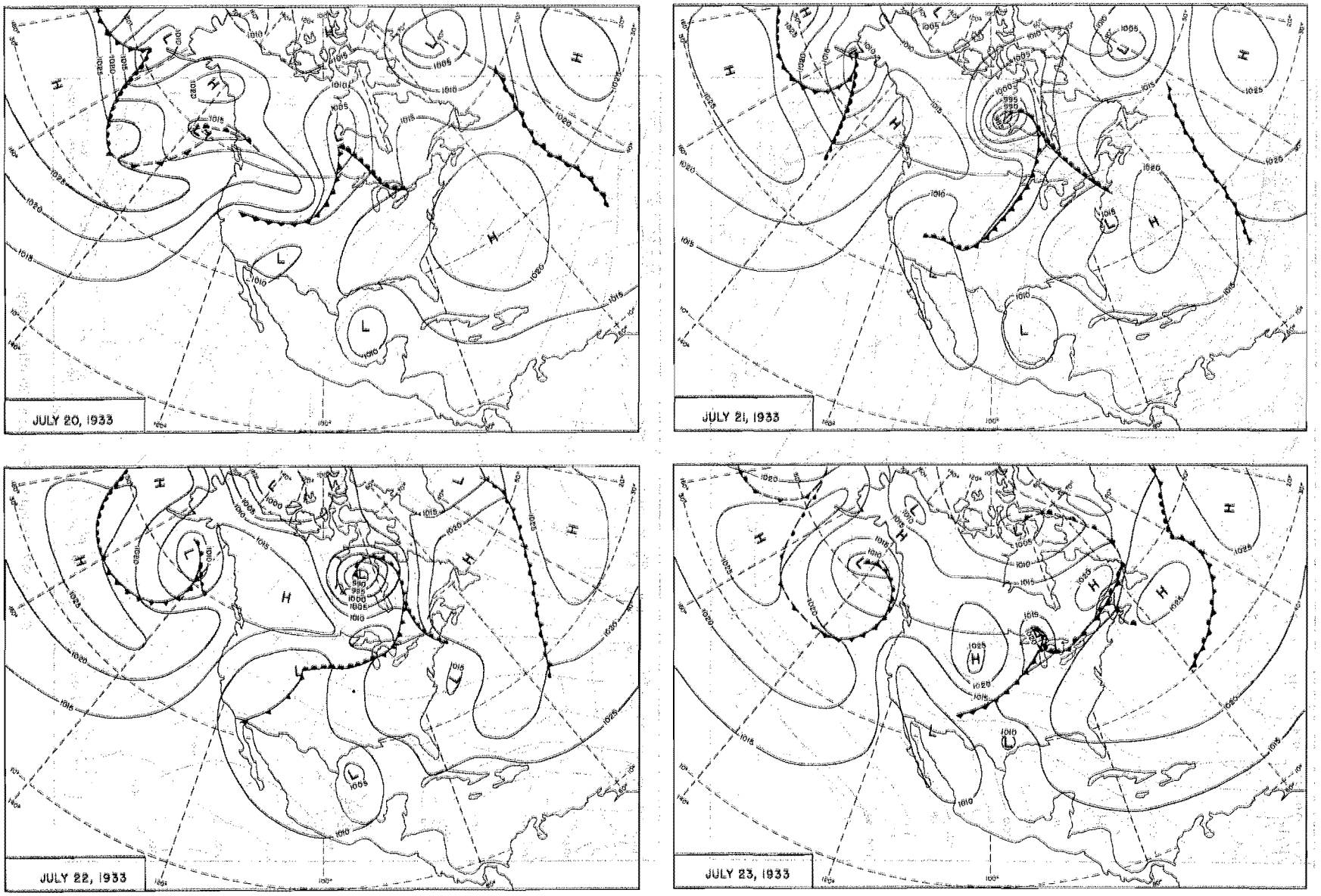

Figure 98. 0700 CST Northern Hemisphere Sea-Level Maps

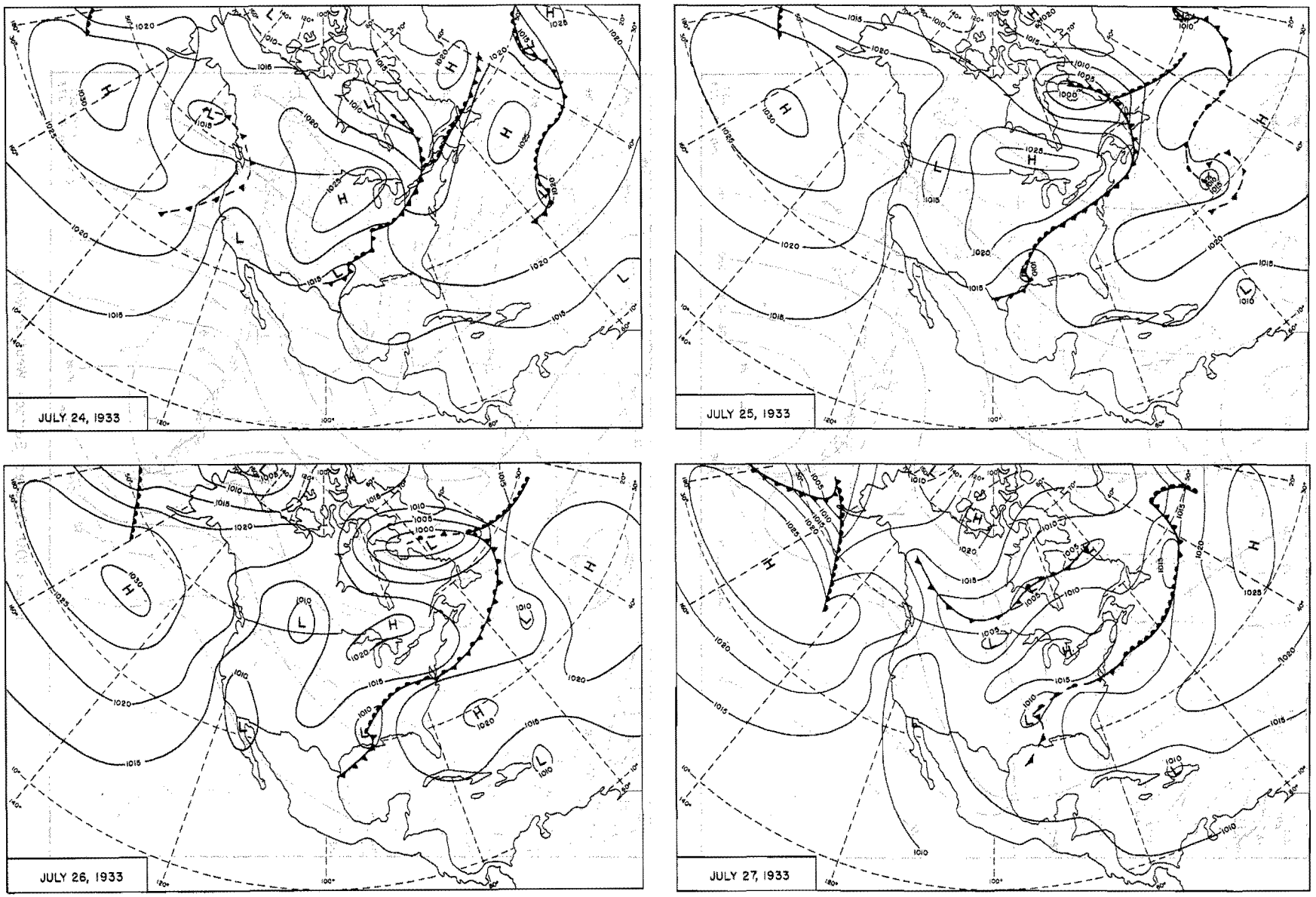

Figure 99. 0700 CST Northern Hemisphere Sea-Level Maps

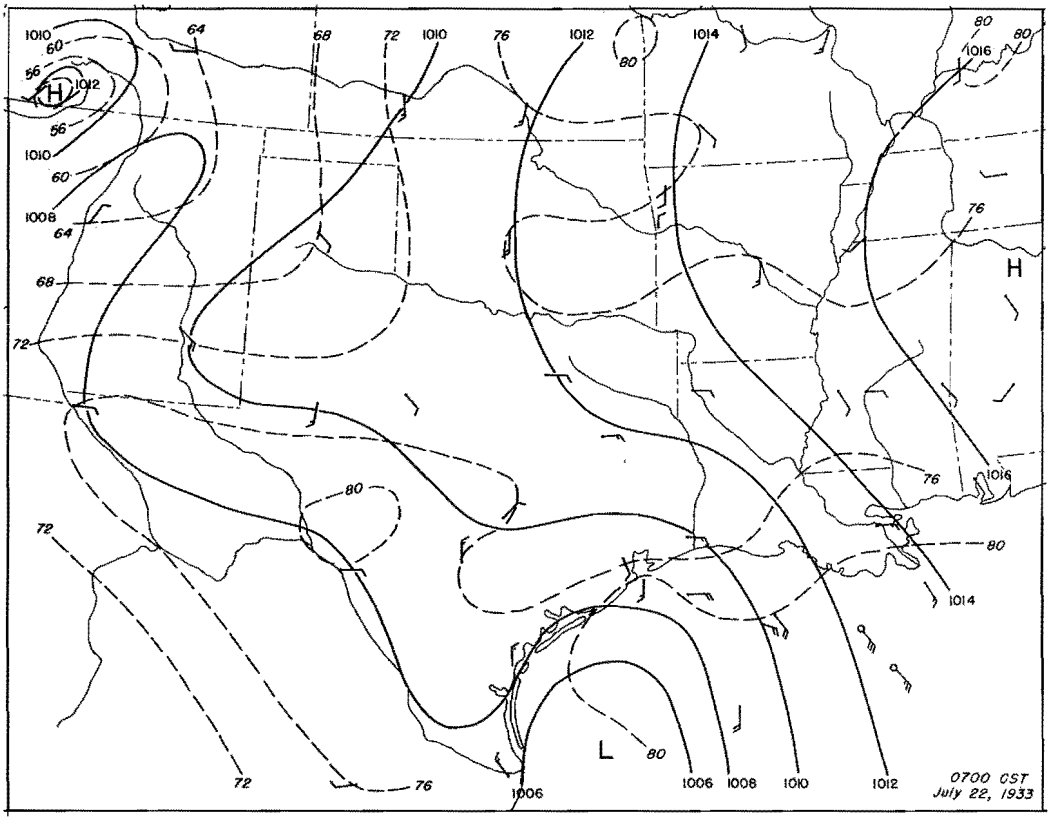

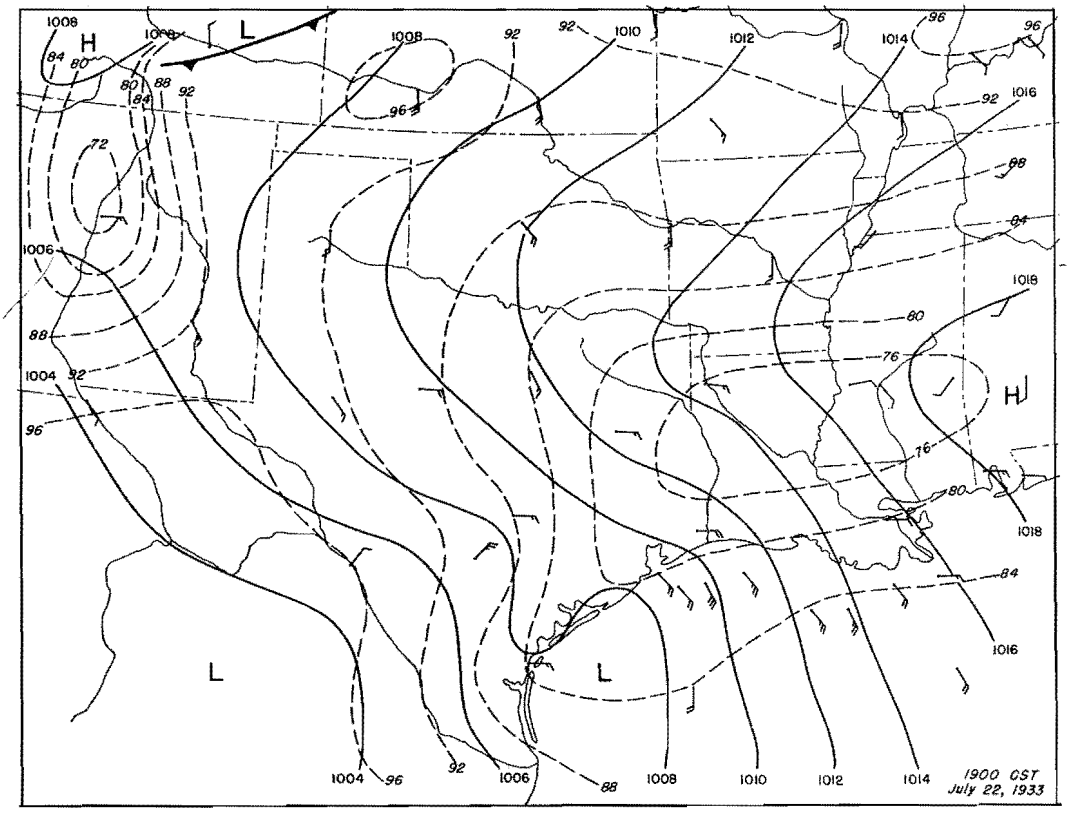

Figure 100. Detailed Surface Weather Maps

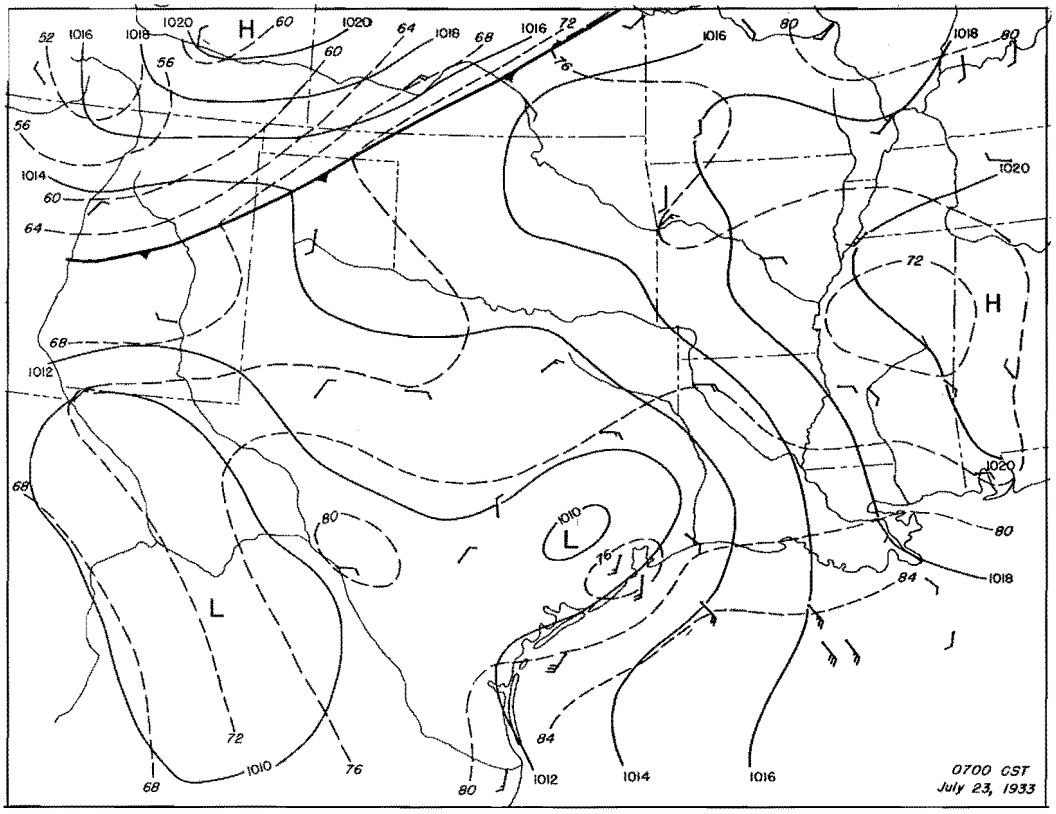

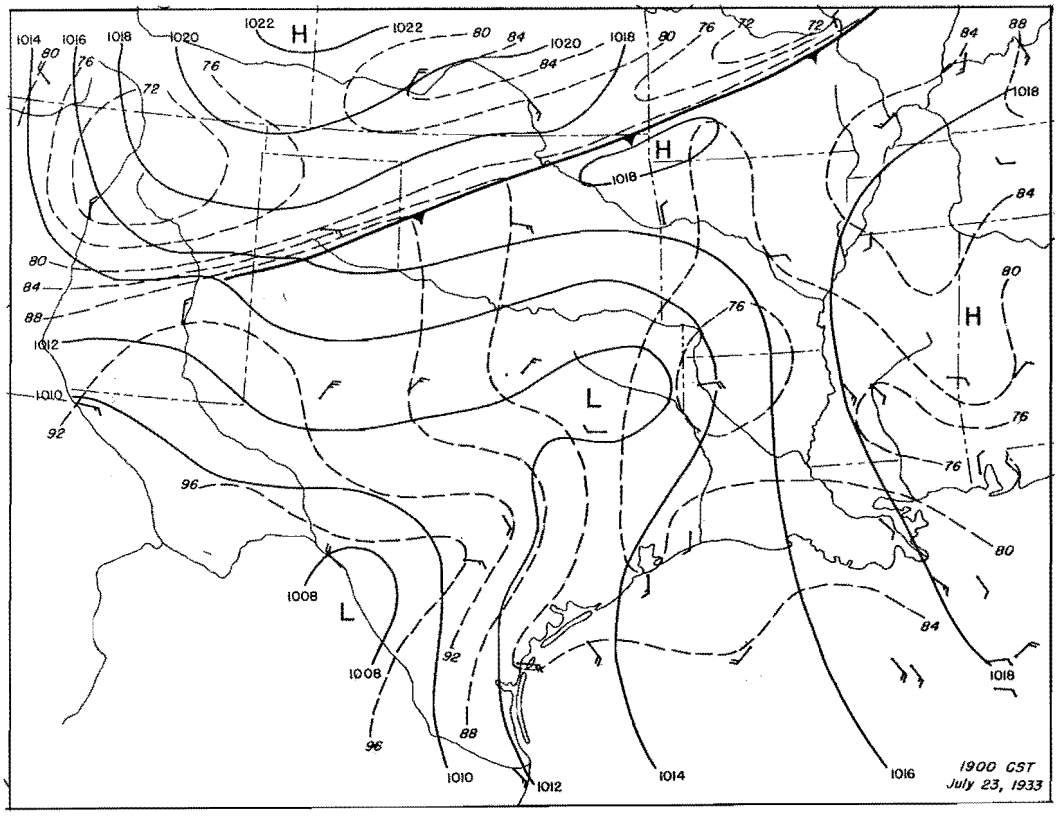

Figure 101. Detailed Surface Weather Maps

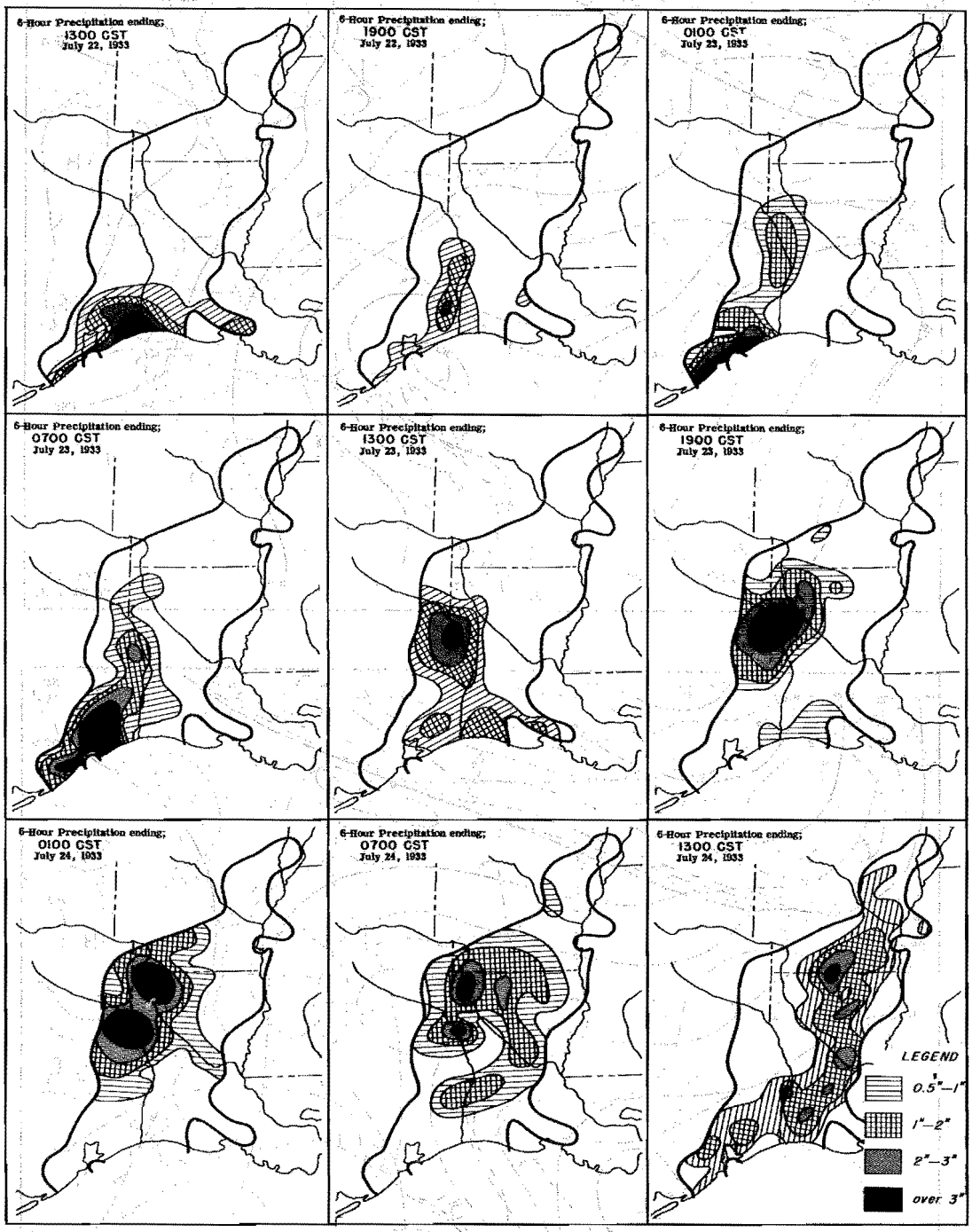

Figure 102. Incremental Isohyetal Patterns

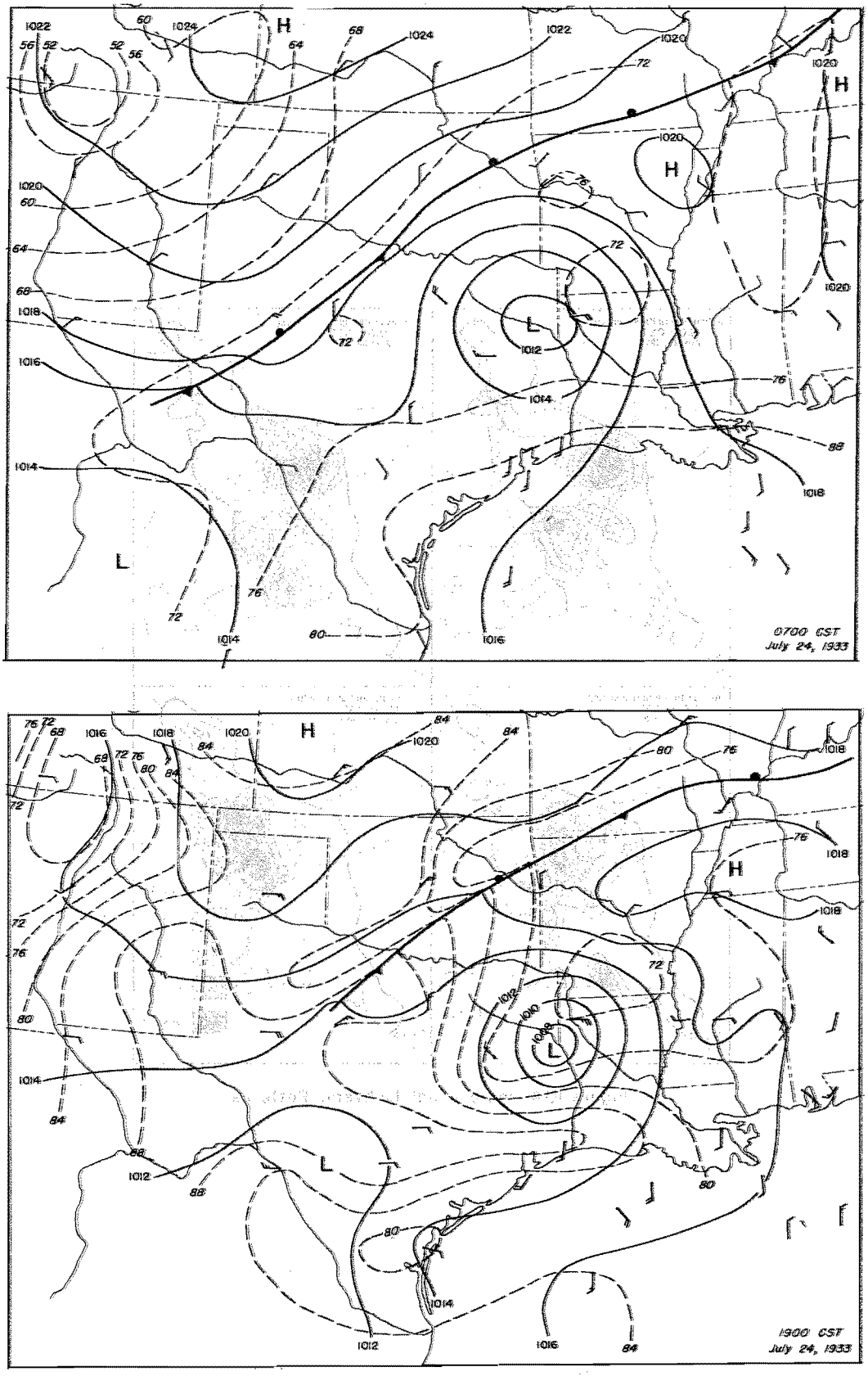

Figure 103. Detailed Surface Weather Maps

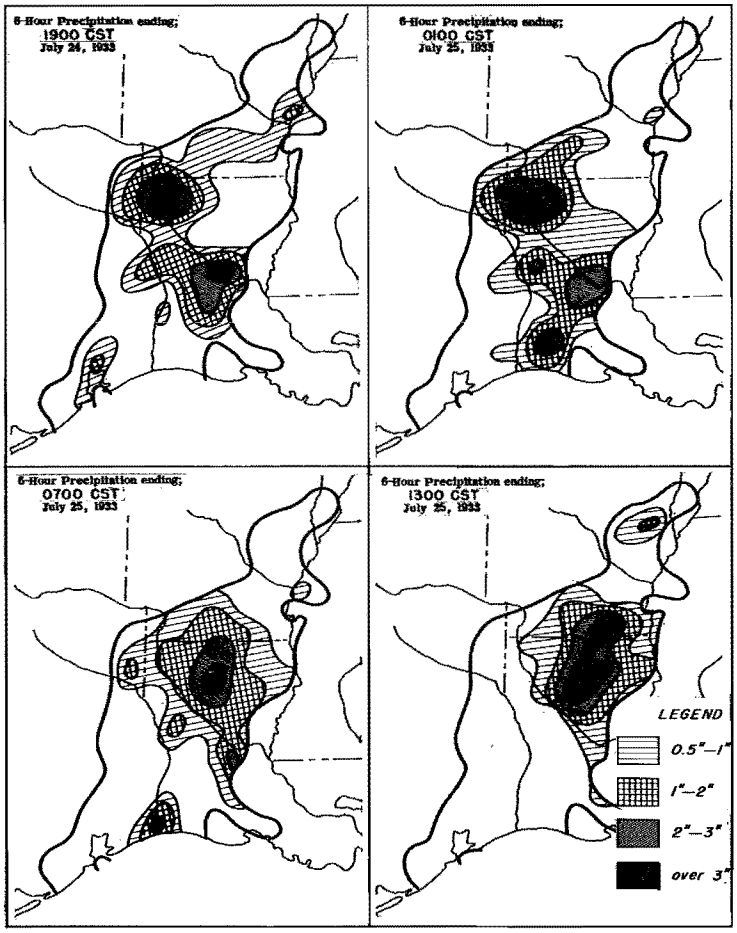

Figure 104. Incremental Isohyetal Patterns

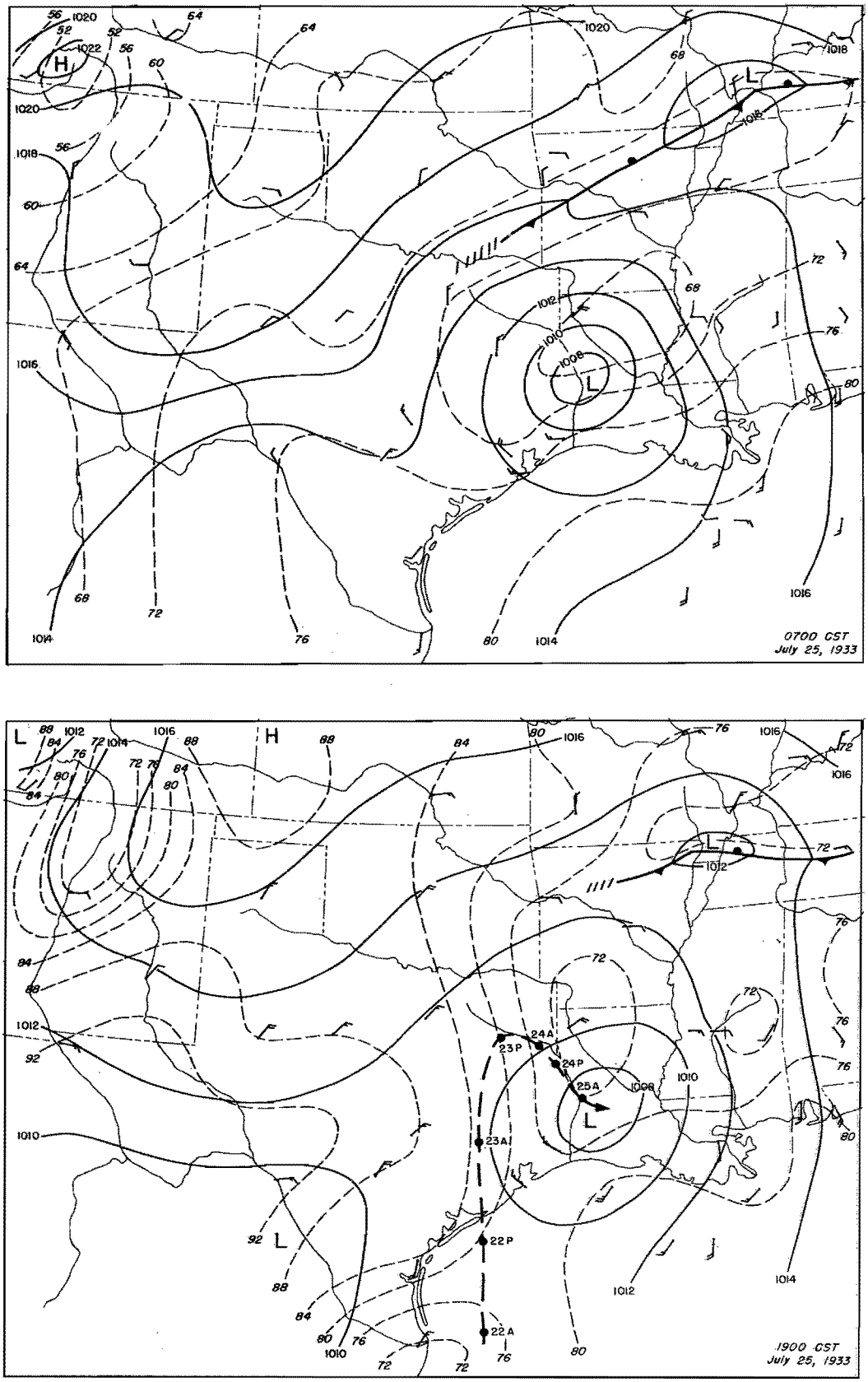

Figure 105. Detailed Surface Weather Maps

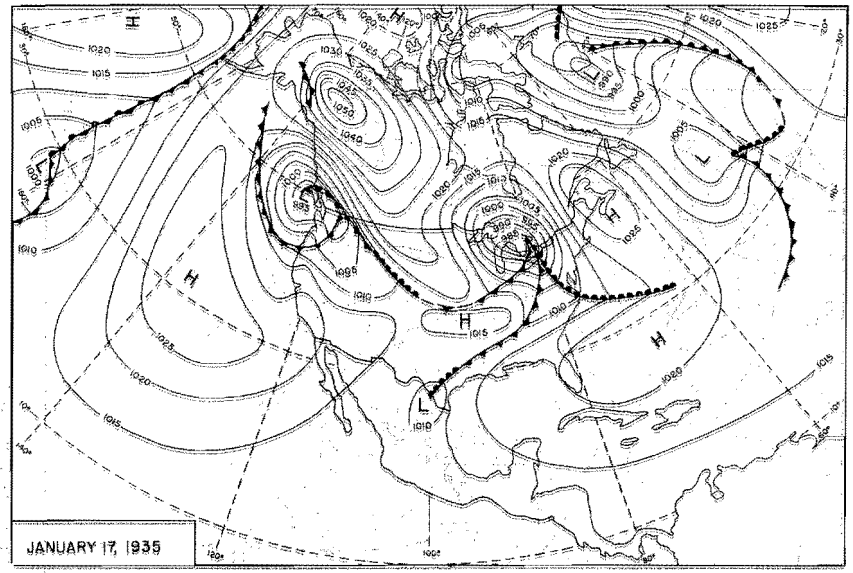

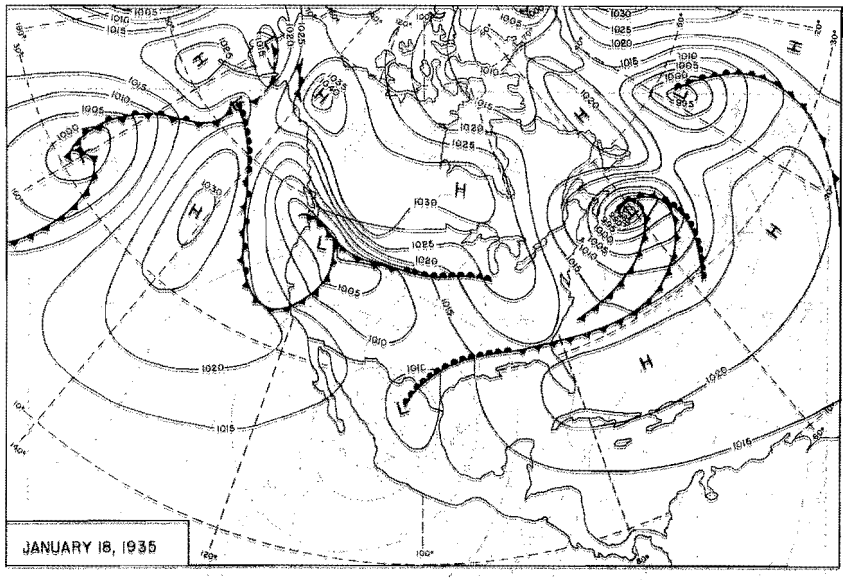

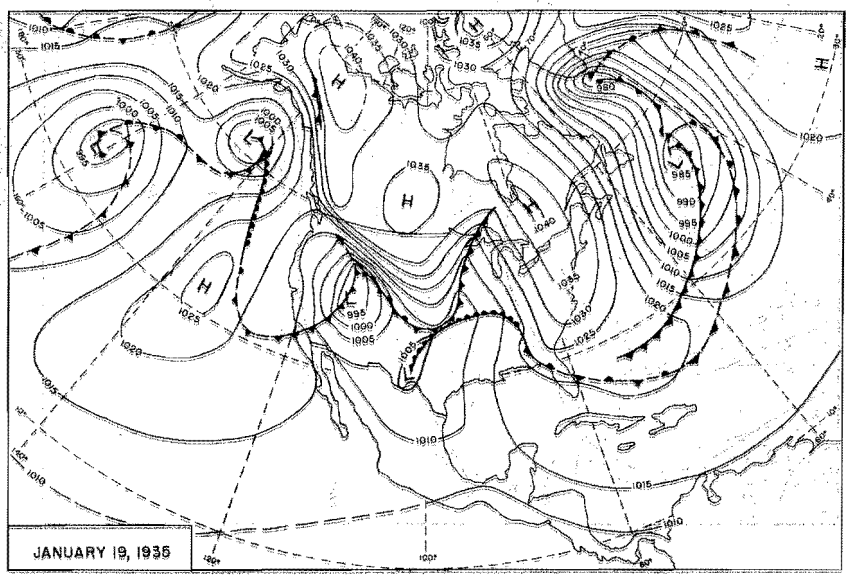

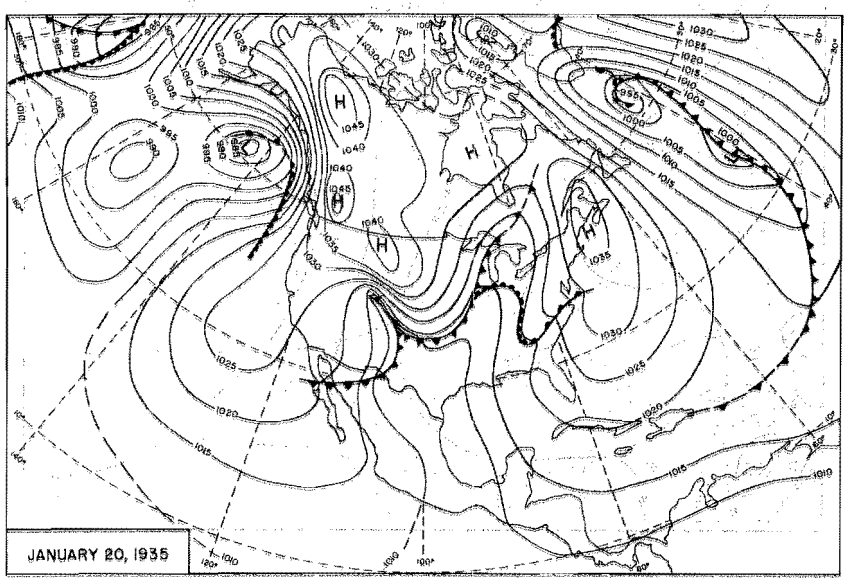

Figure 106. 0700 CST Northern Hemisphere Sea-Level Maps

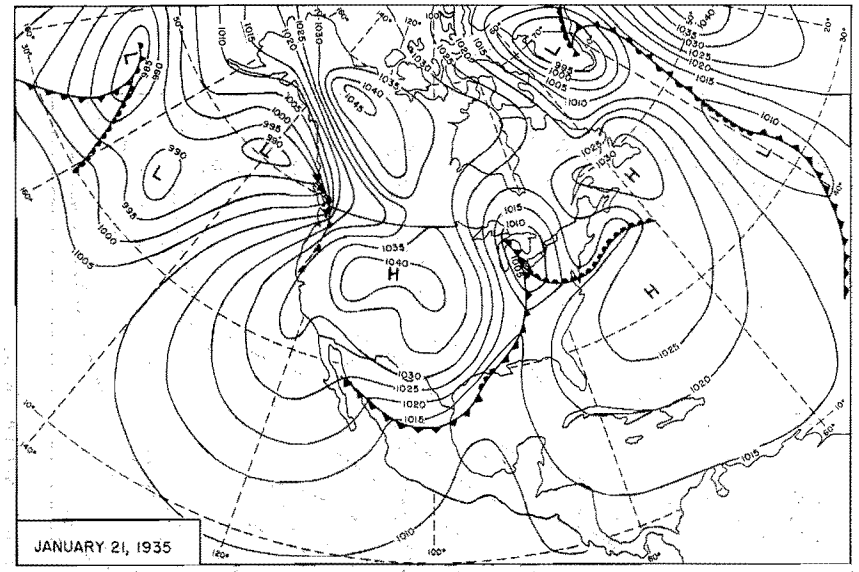

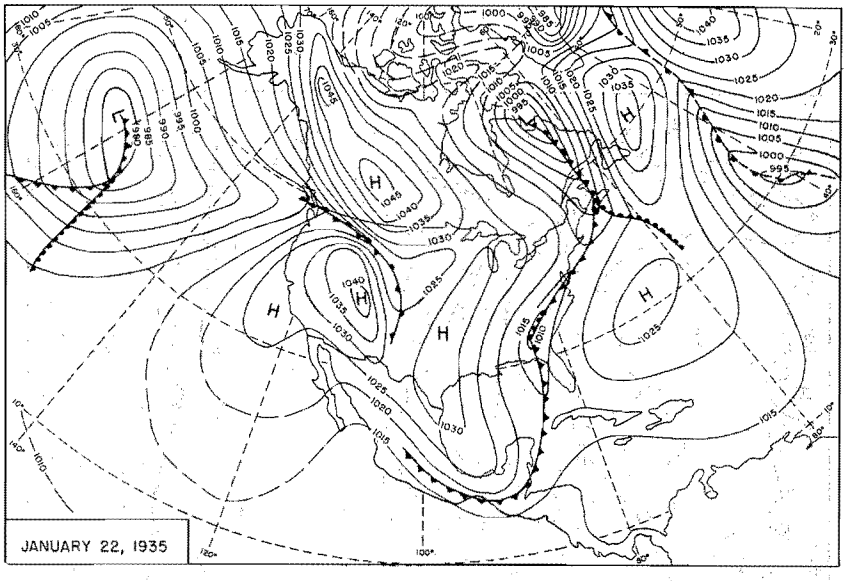

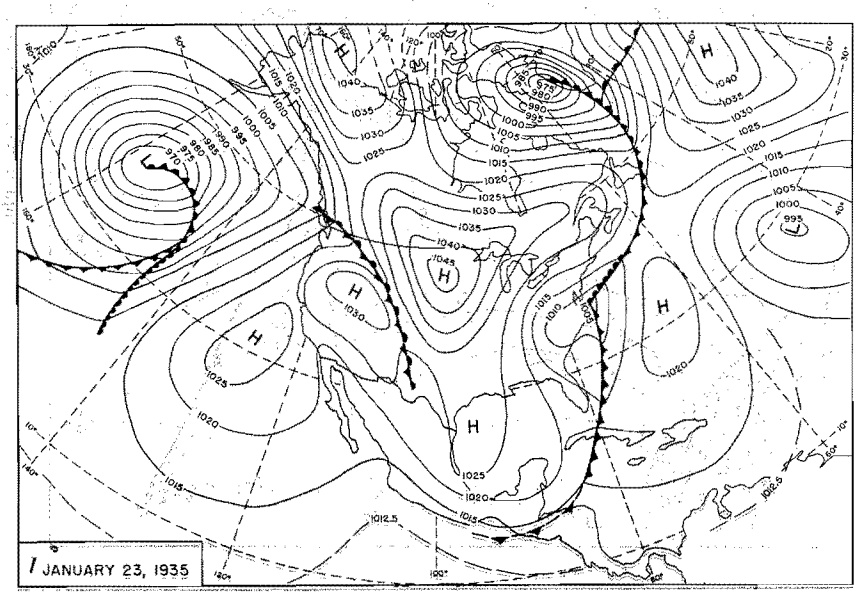

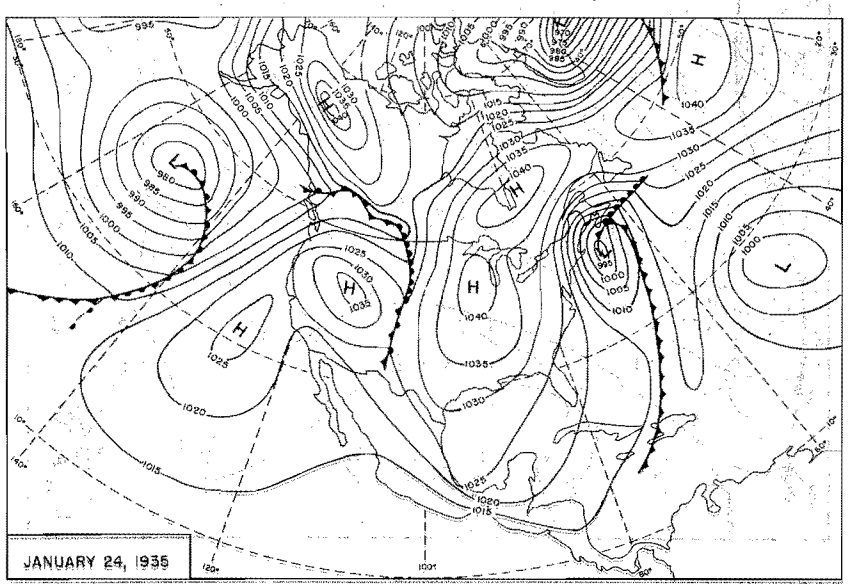

Figure 107. 0700 CST Northern Hemisphere Sea-Level Maps

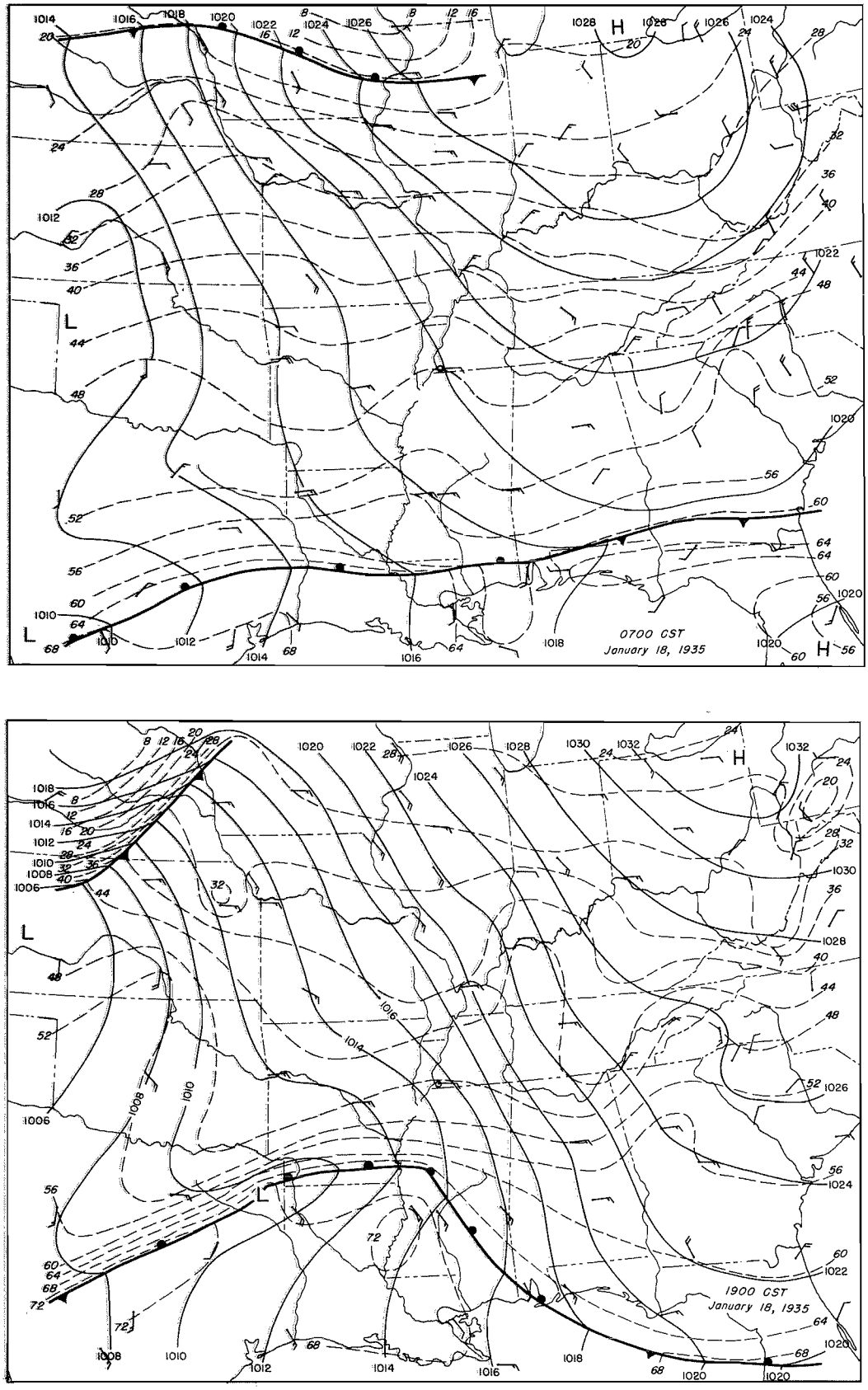

Figure 108. Detailed Surface Weather Maps

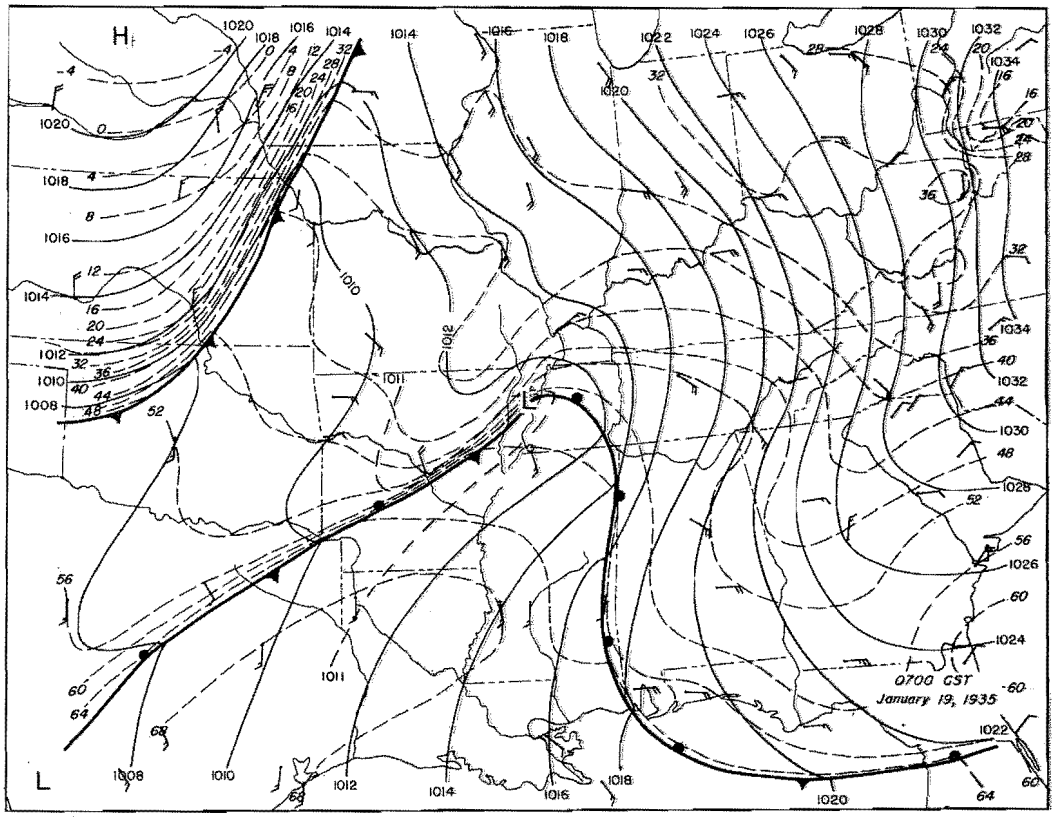

Figure 109. Detailed Surface Weather Maps

3" total storm isohyet

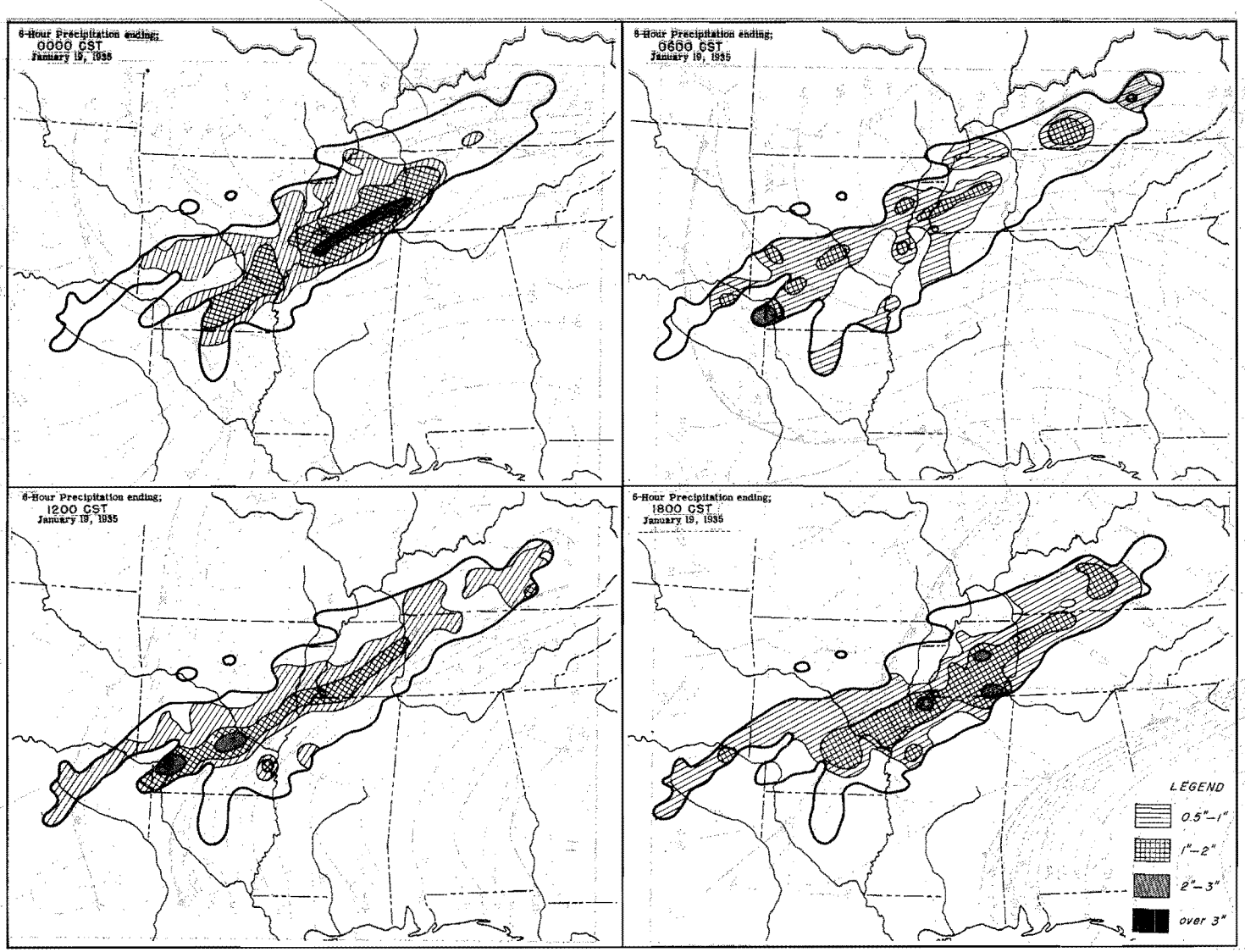

Figure 110. Incremental Isohyetal Patterns

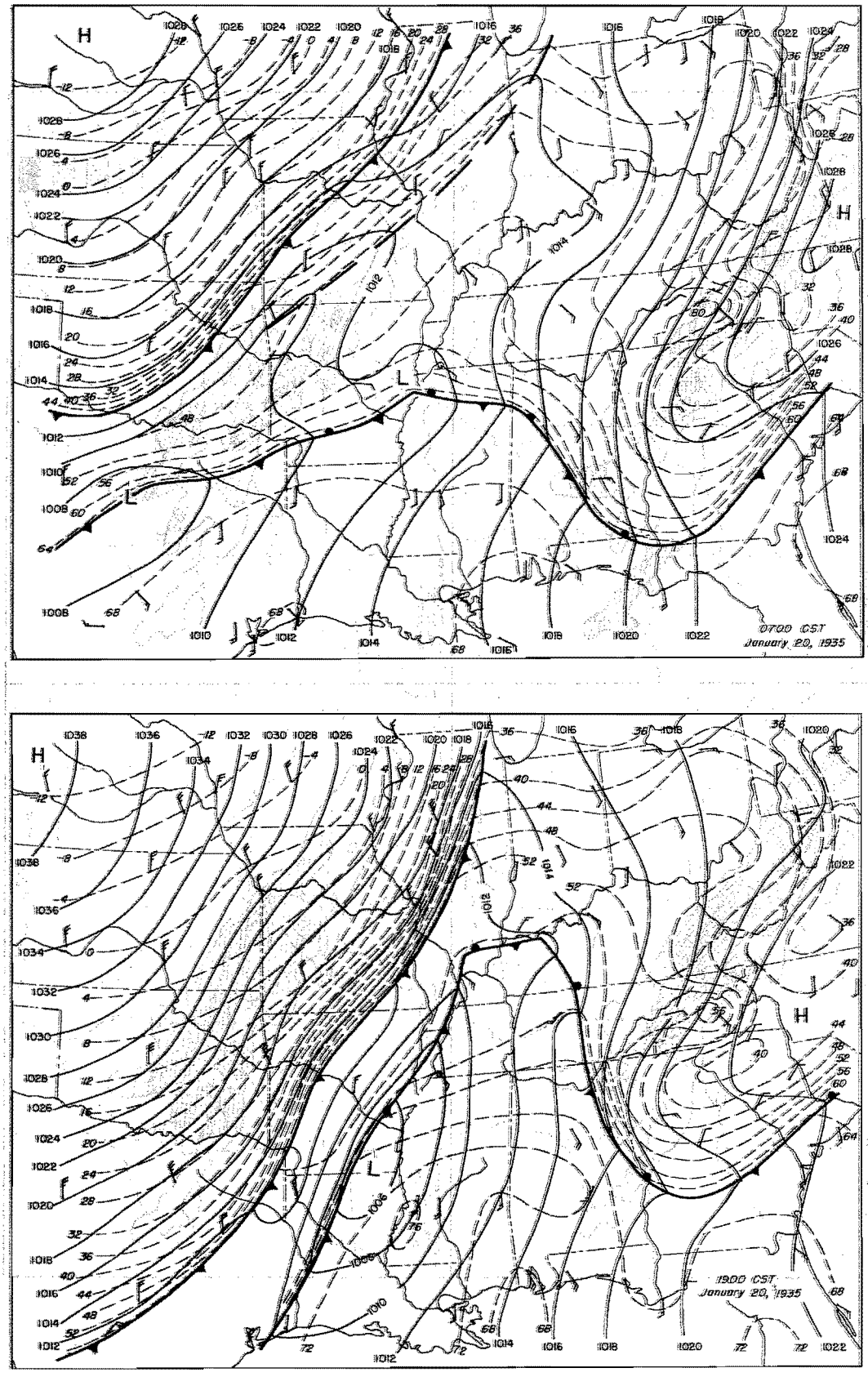

Figure III. Detailed Surface Weather Maps

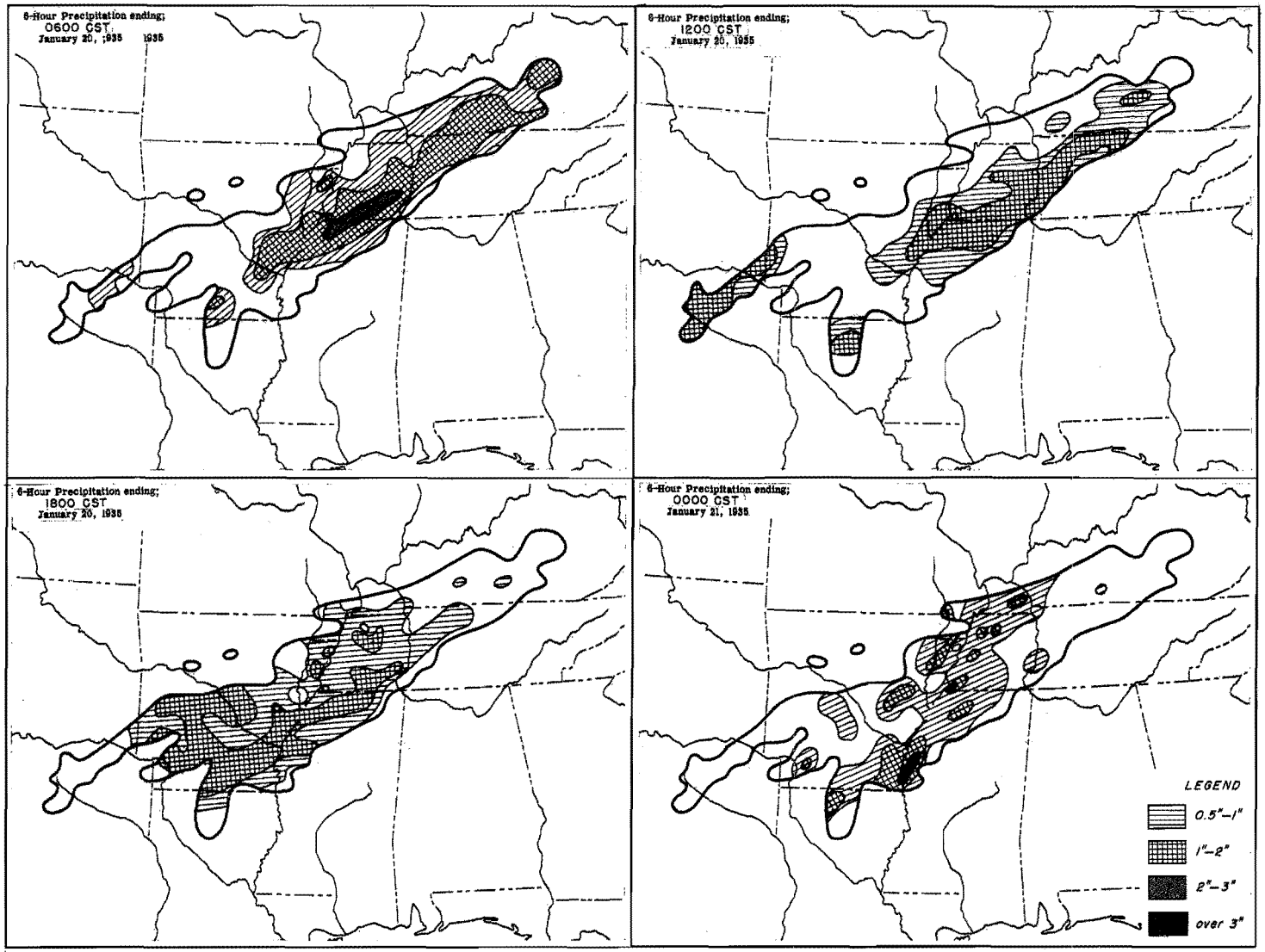

Figure 112. Incremental Isohyetal Patterns

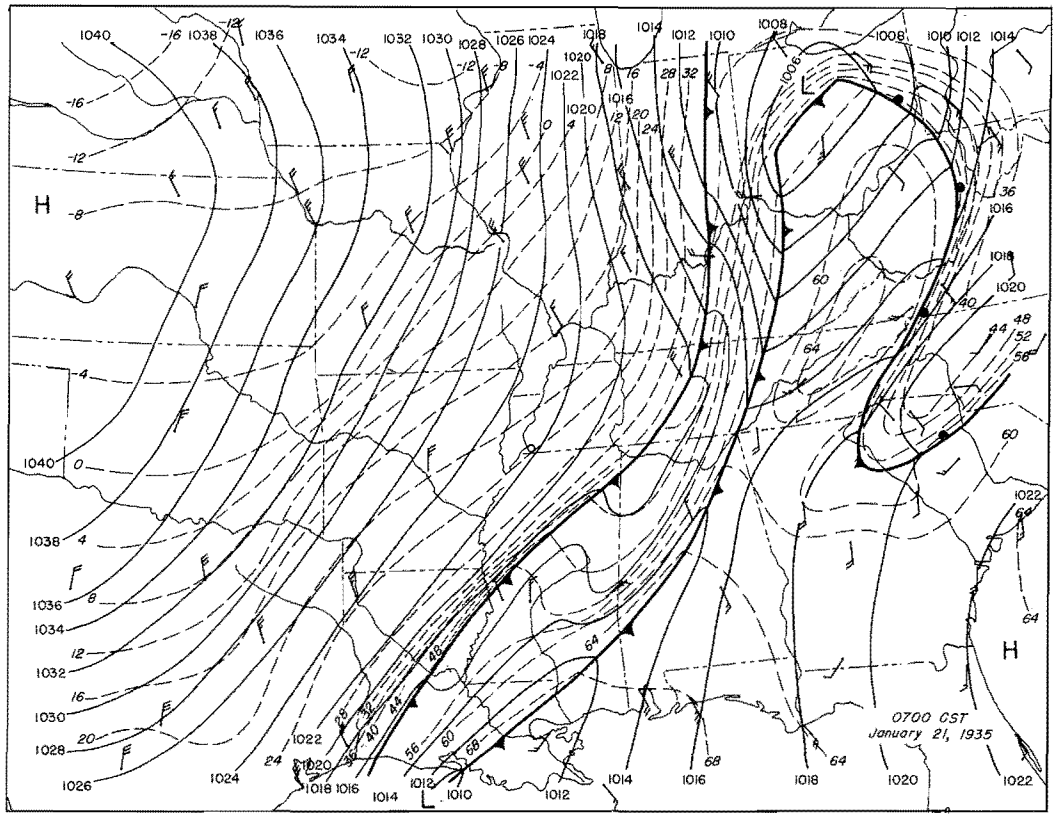

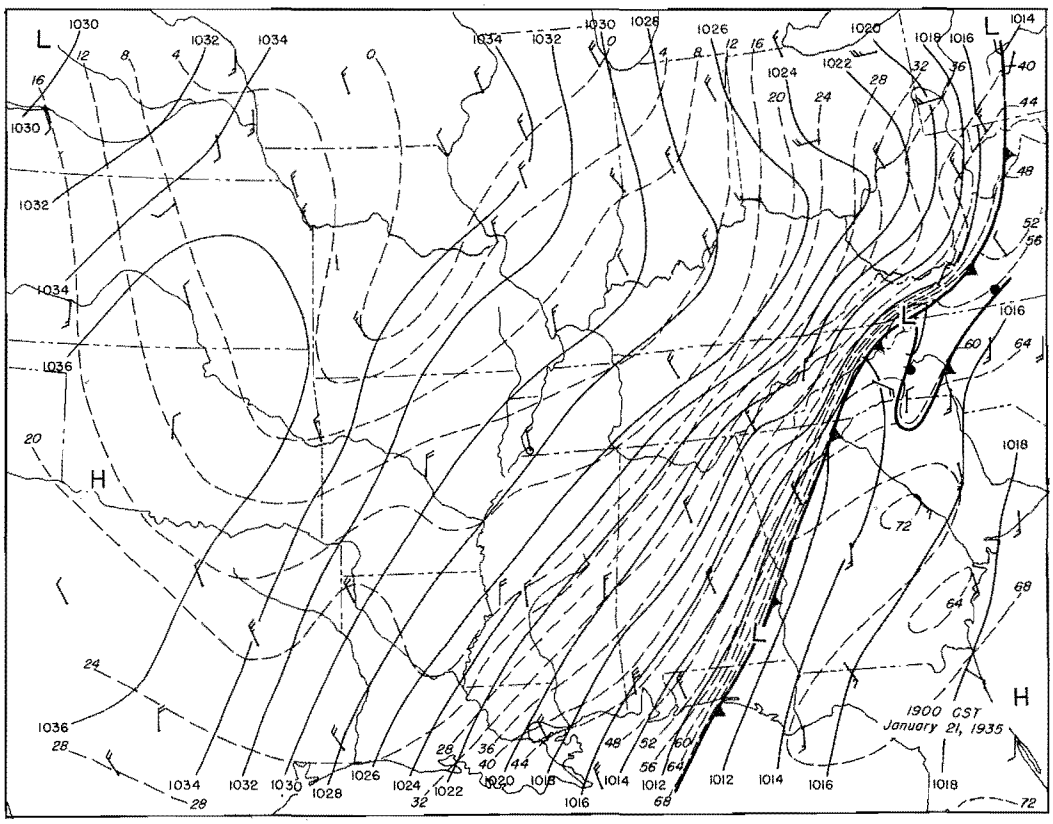

Figure 113. Detailed Surface Weather Maps

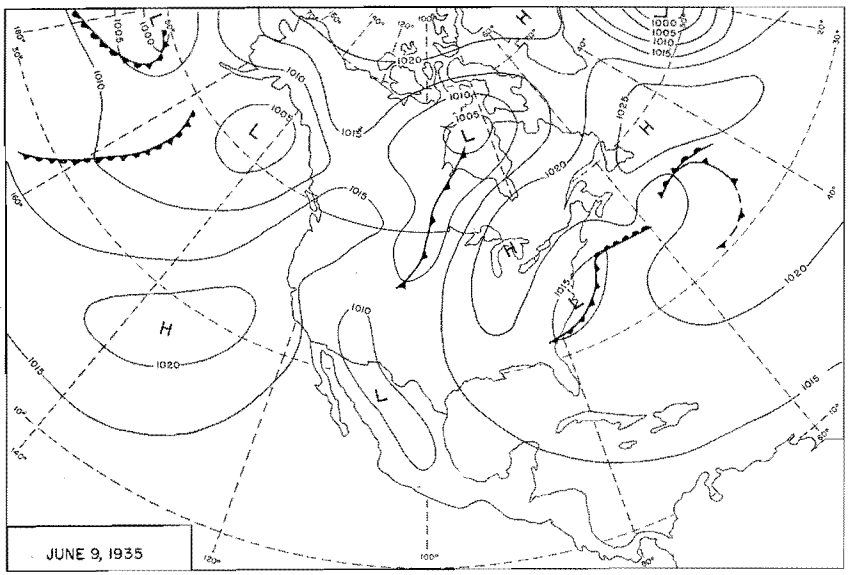

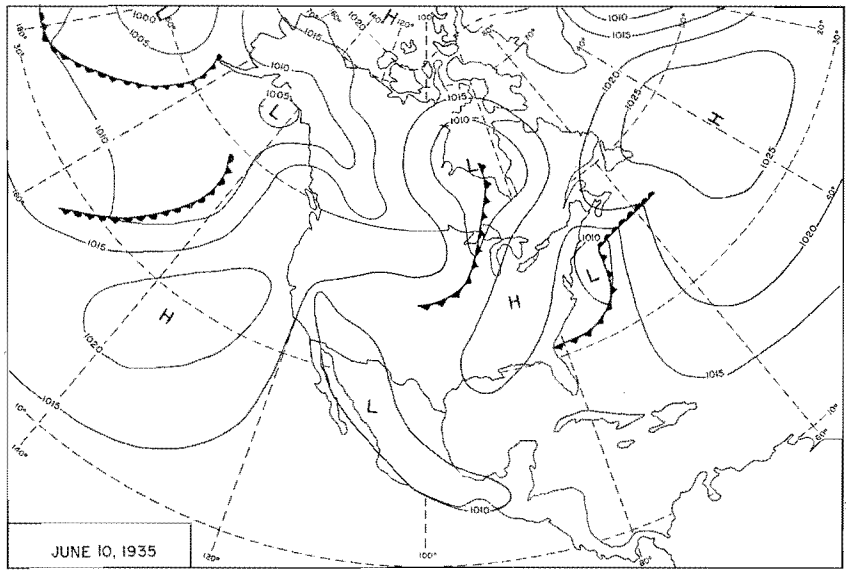

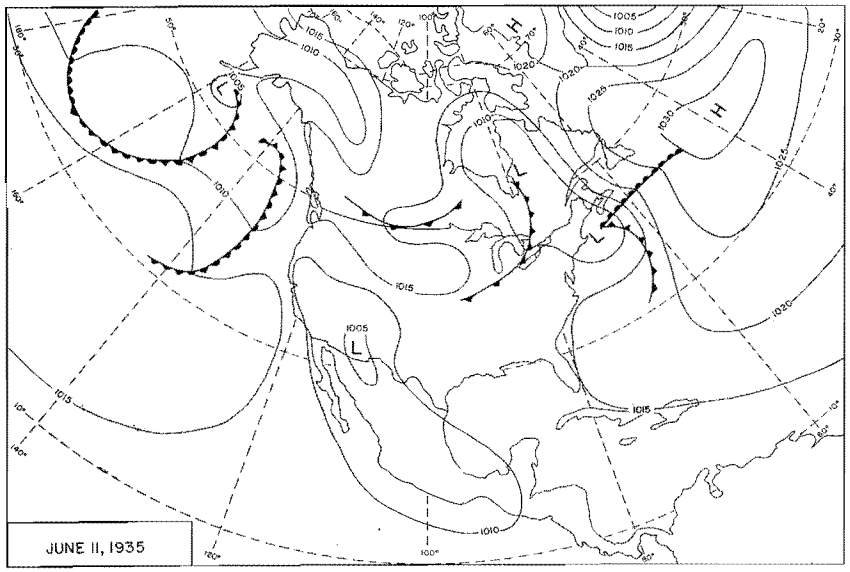

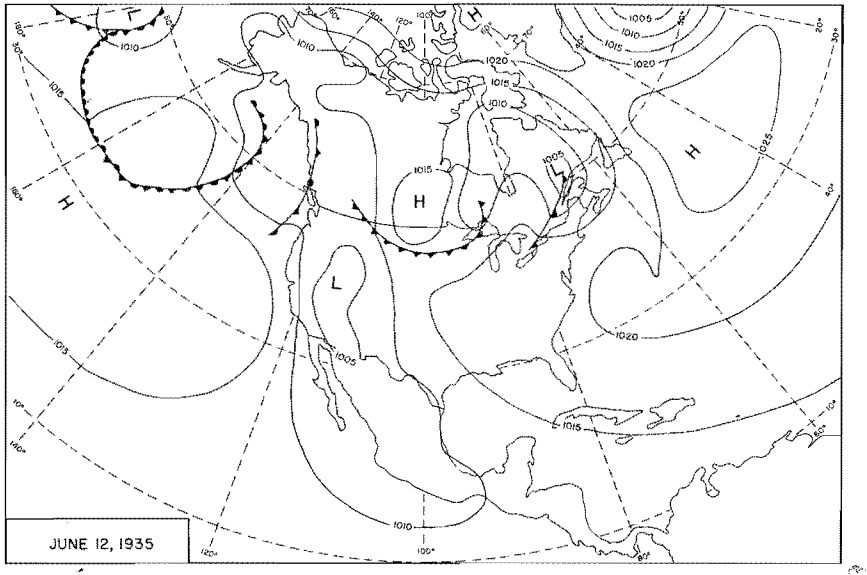

Figure 114. 0700 CST Northern Hemisphere Sea-Level Maps

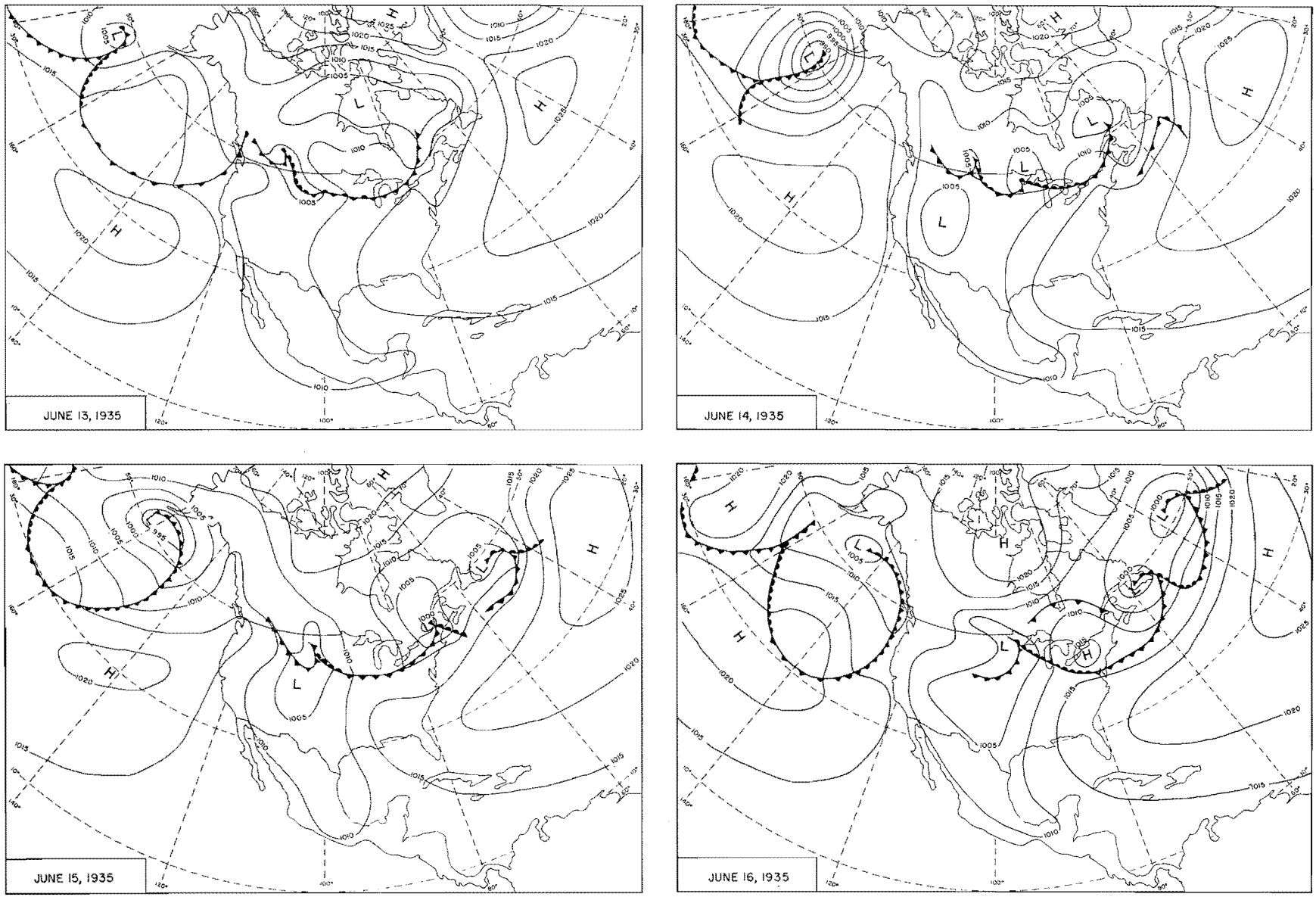

Figure 115. 0700 CST Northern Hemisphere Sea–Level Maps

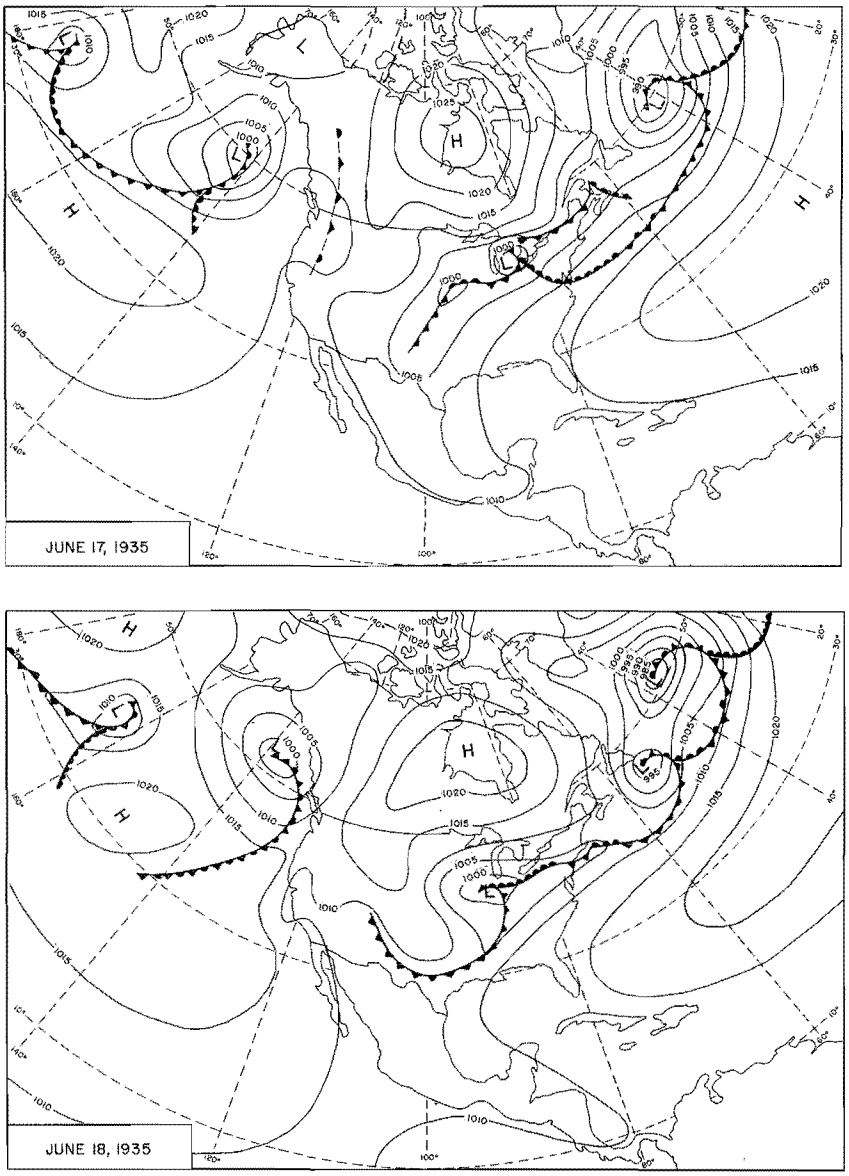

Figure 116 0700 CST Northern Hemisphere Sea–Level Maps

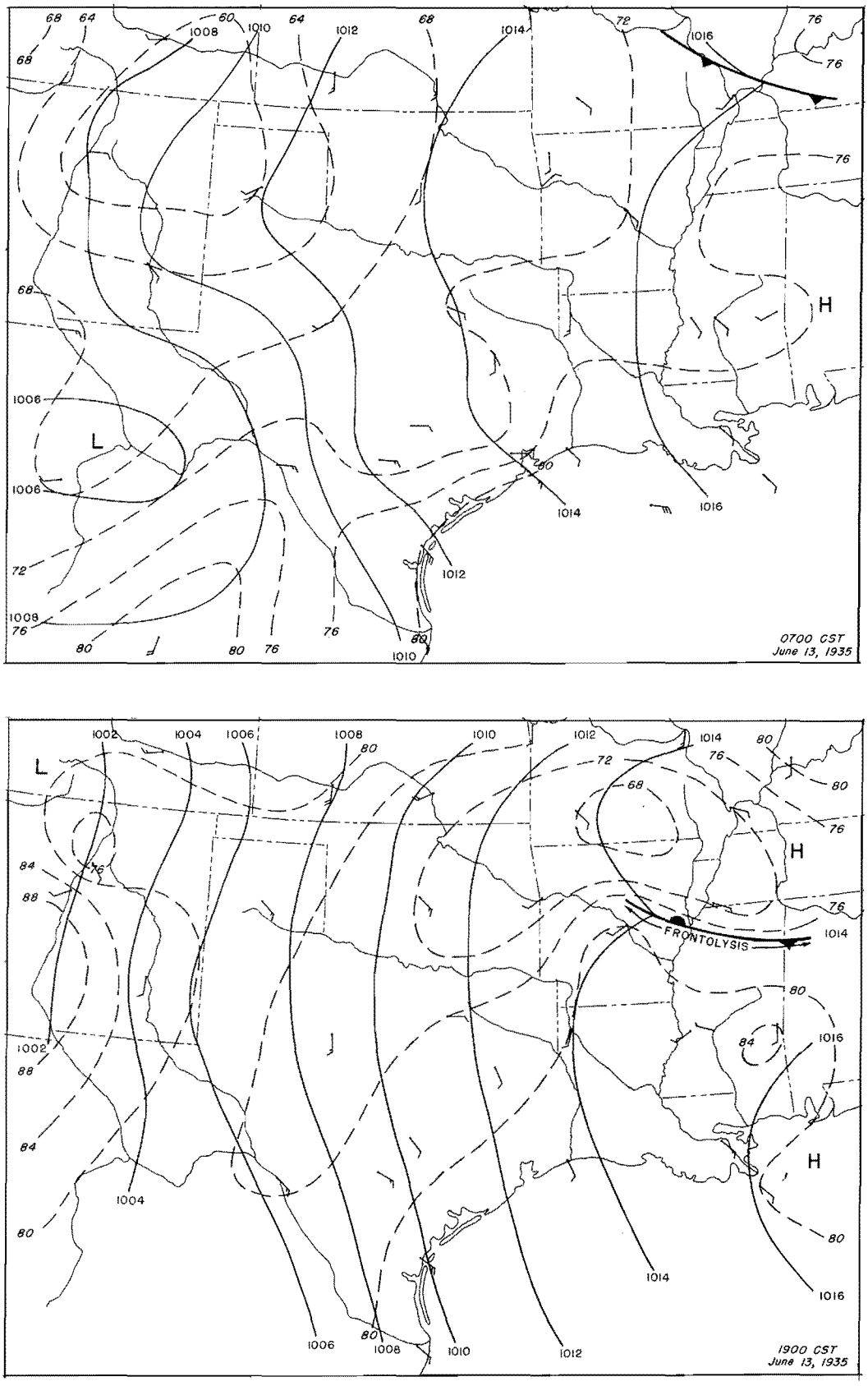

Figure 117. Detailed Surface Weather Maps

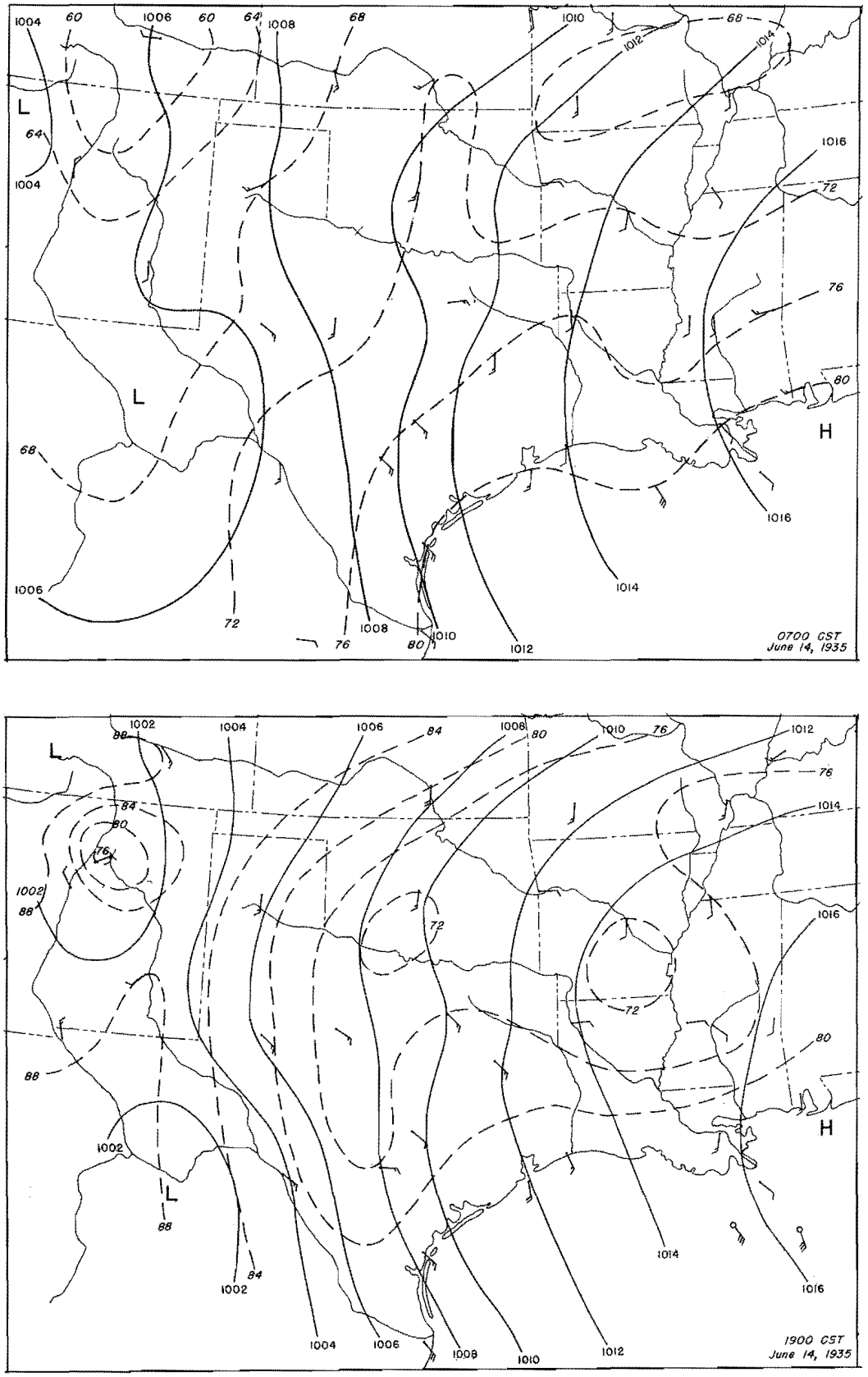

Figure 118. Detailed Surface Weather Maps

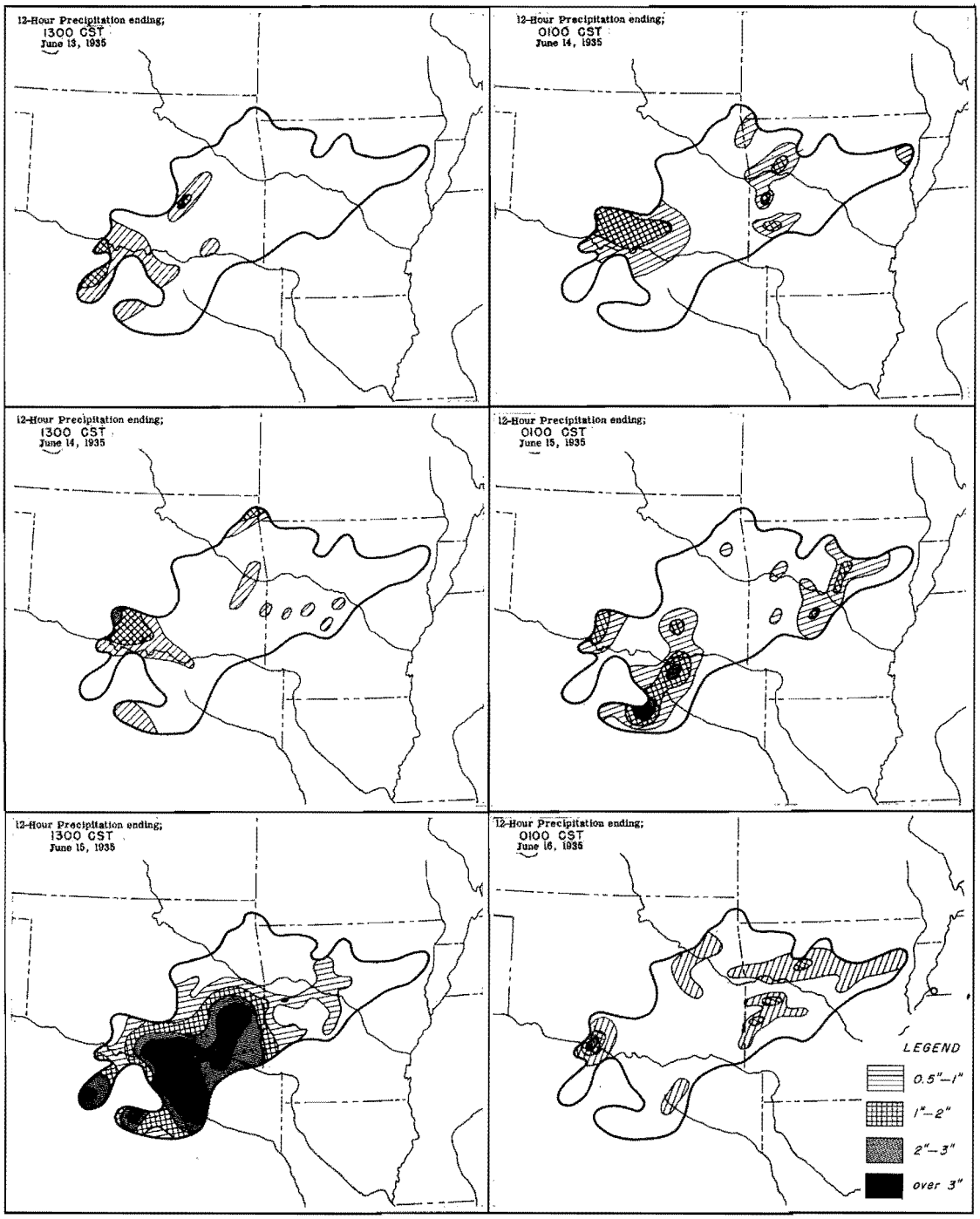

Figure 119. Incremental Isohyetal Patterns

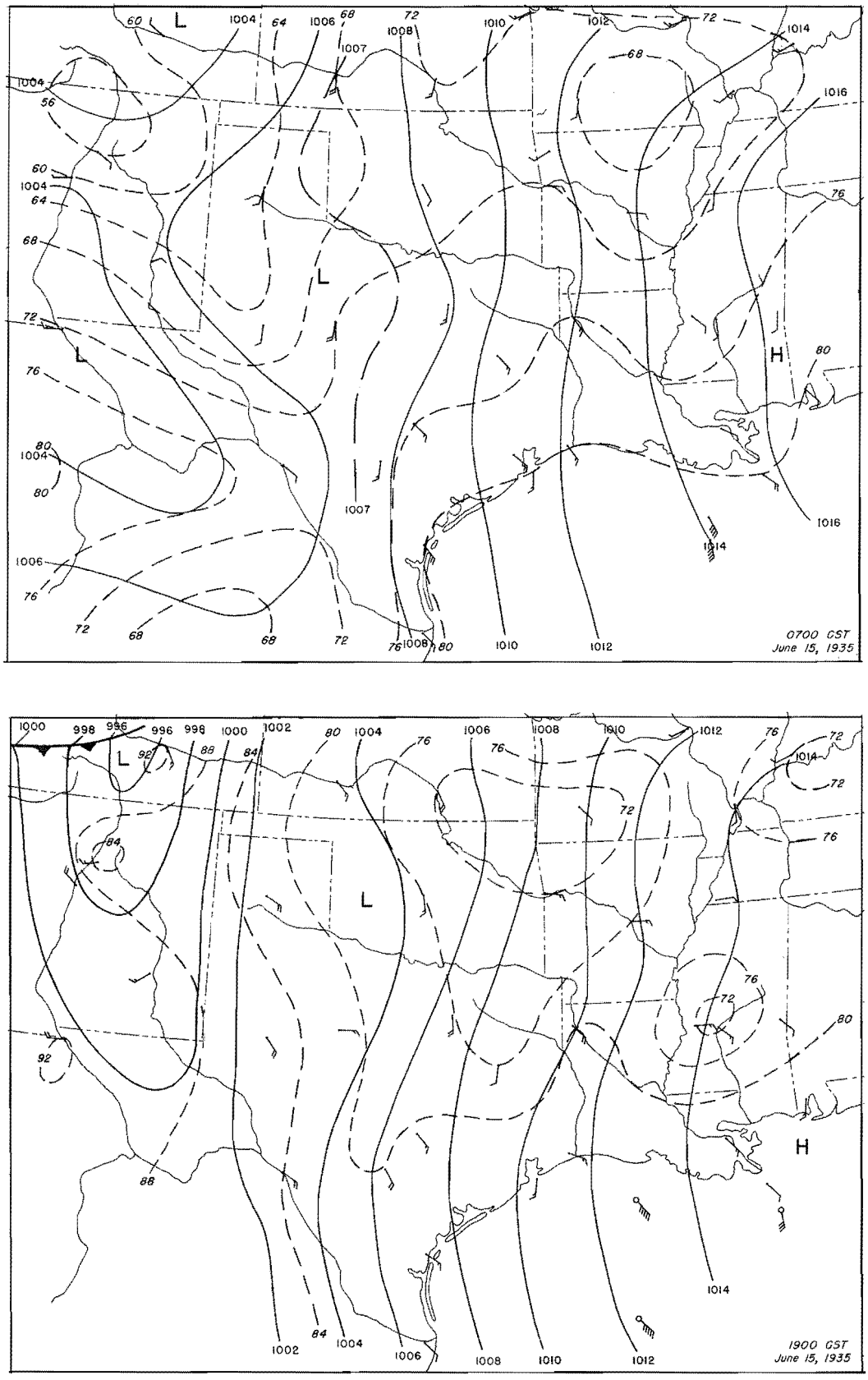

Figure 120. Detailed Surface Weather Maps

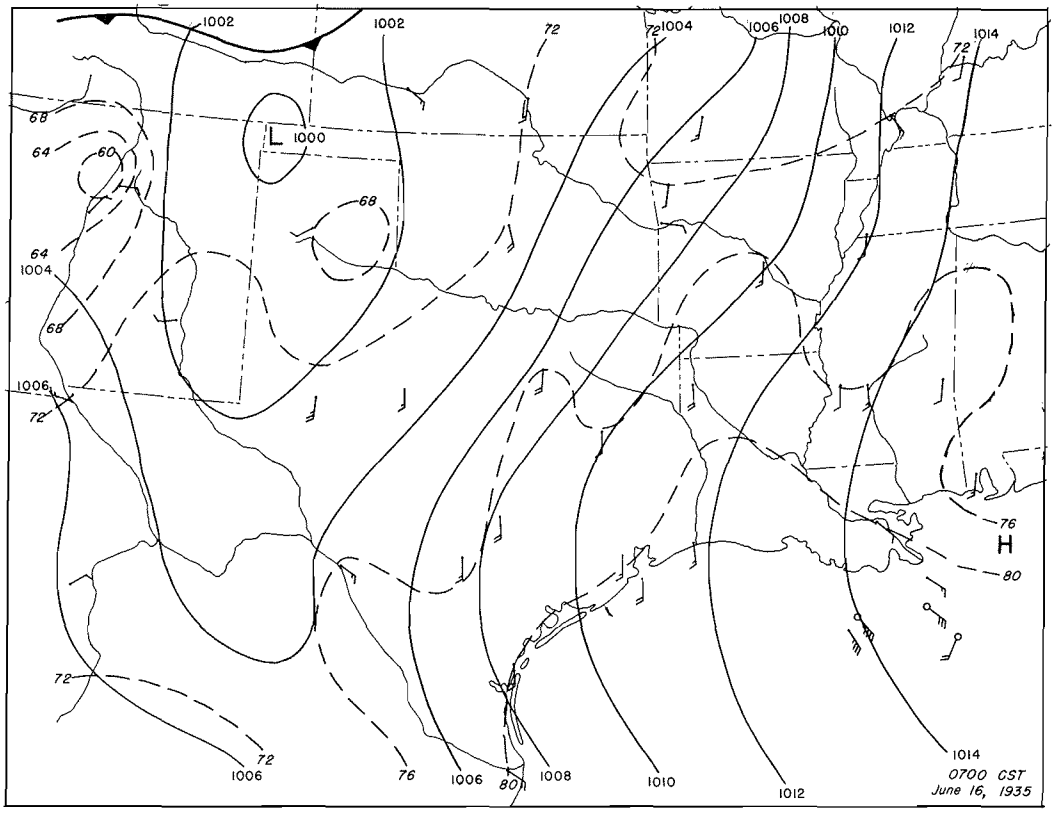

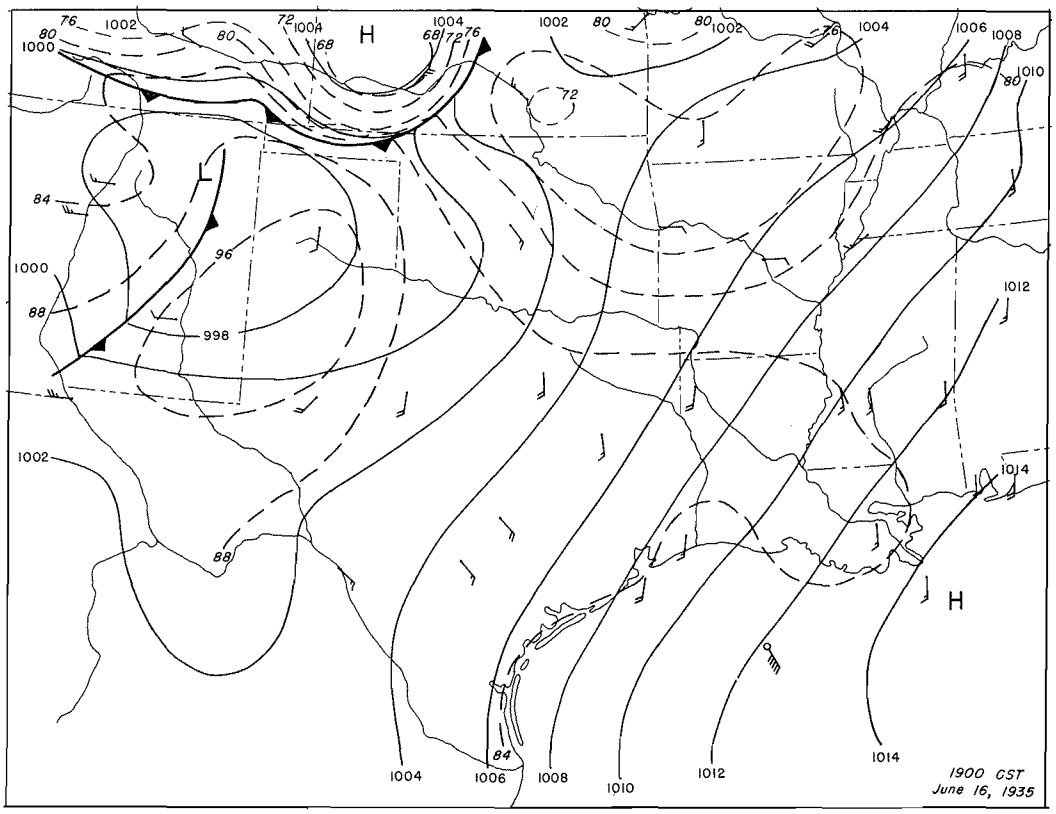

Figure 121. Detailed Surface Weather Maps

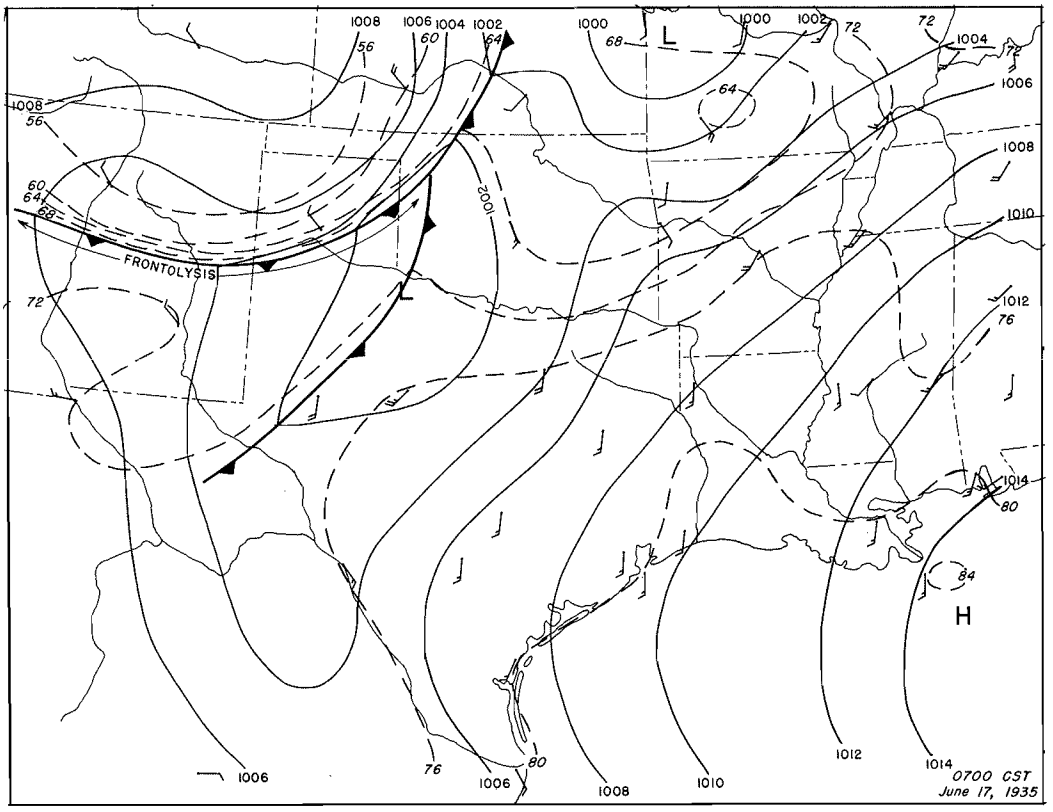

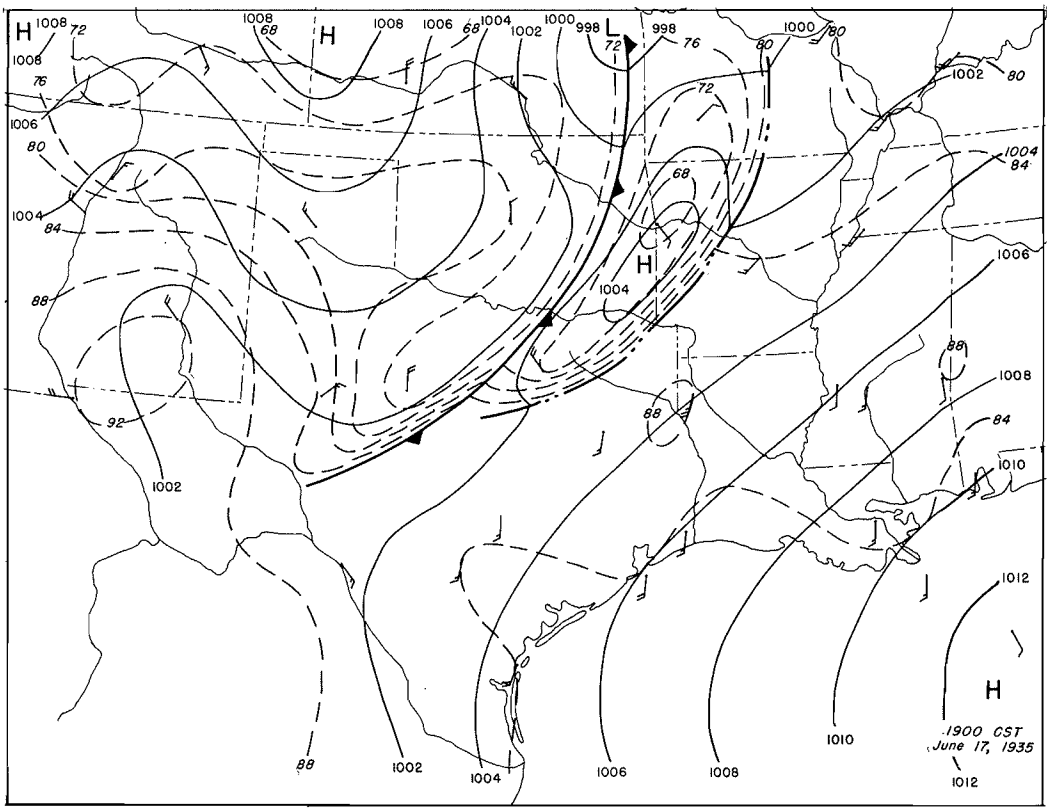

Figure 122. Detailed Surface Weather Maps.

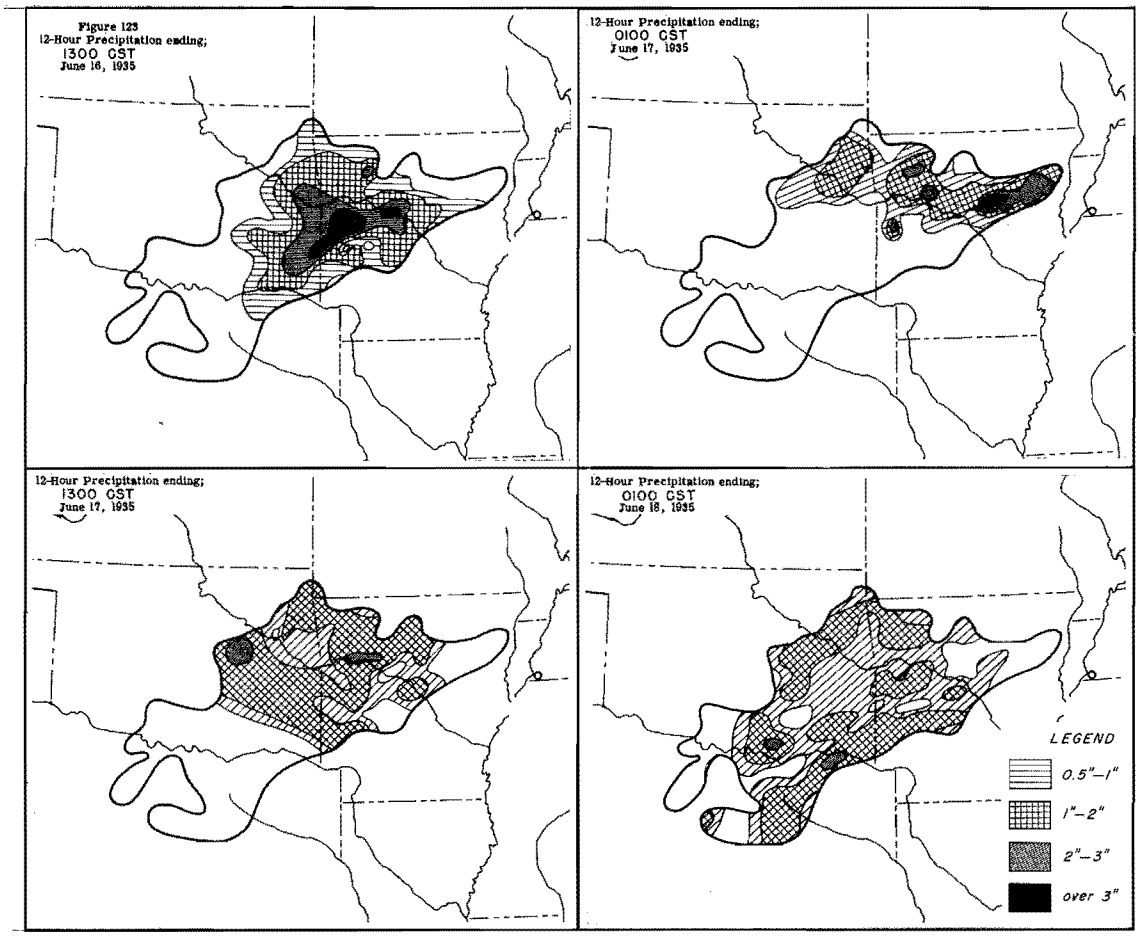

Figure 123. Incremental Isohyetal Patterns

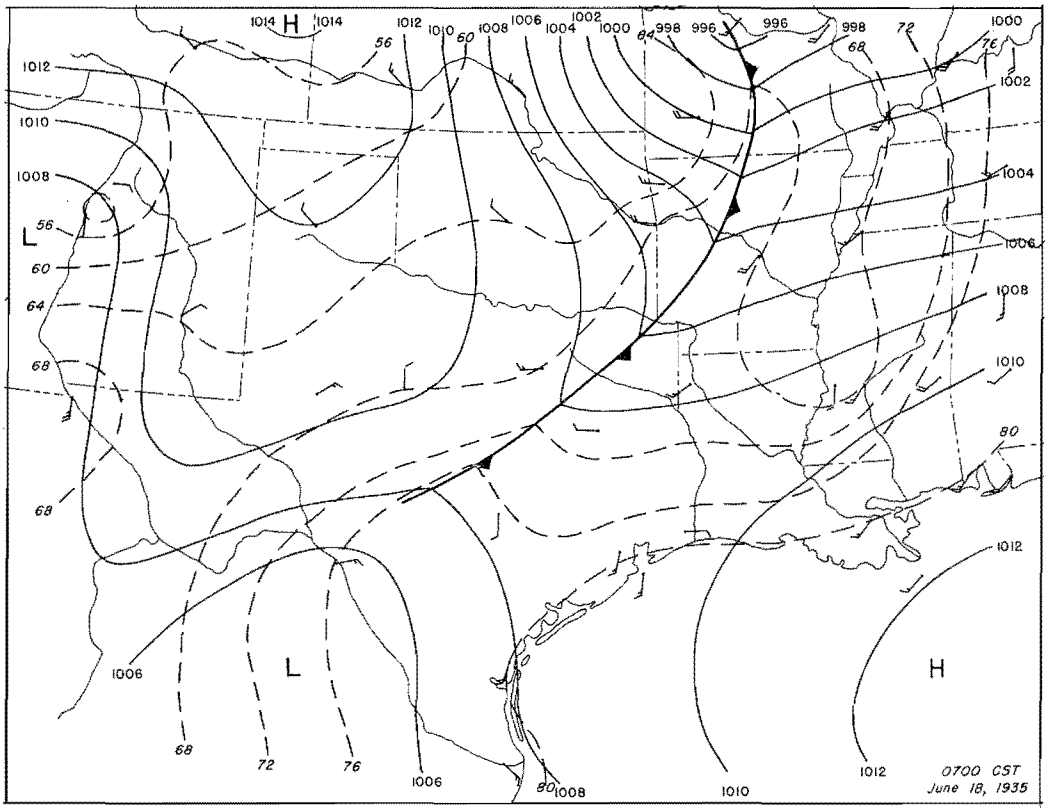

Figure 124. Detailed Surface Weather Map

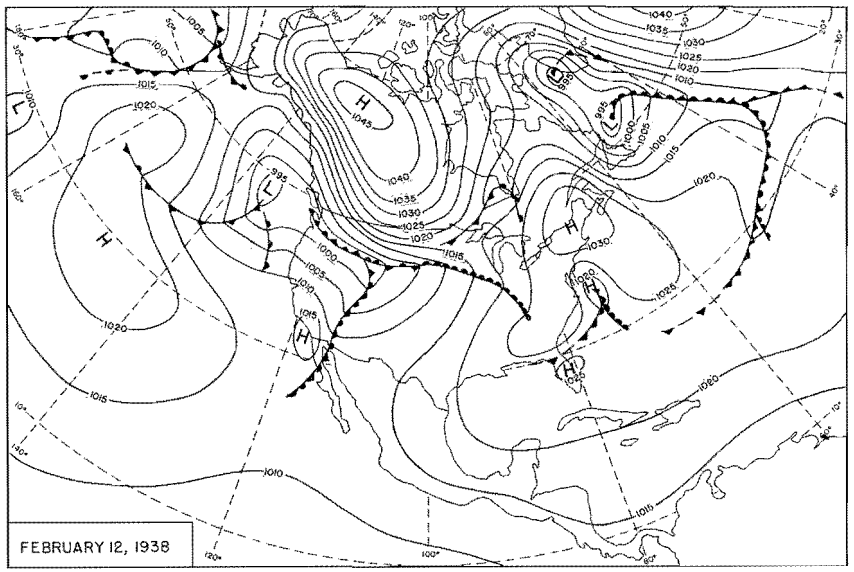

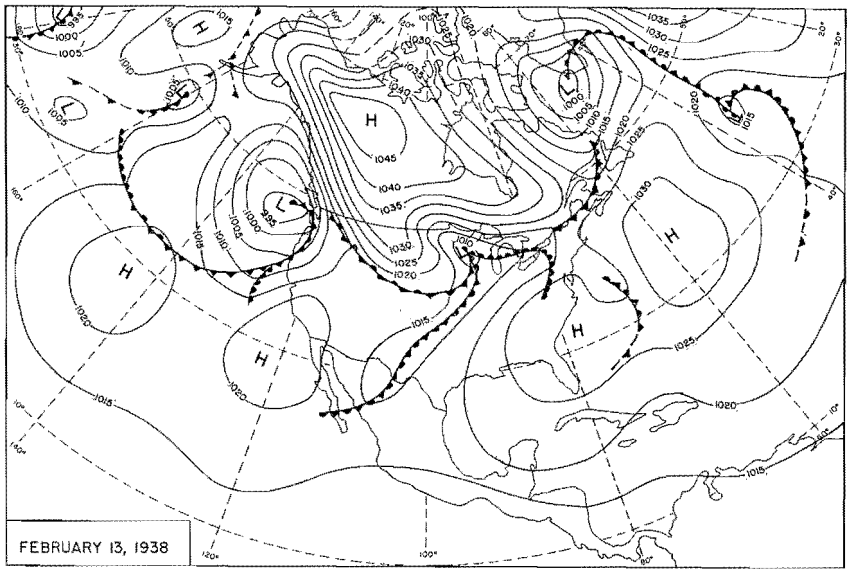

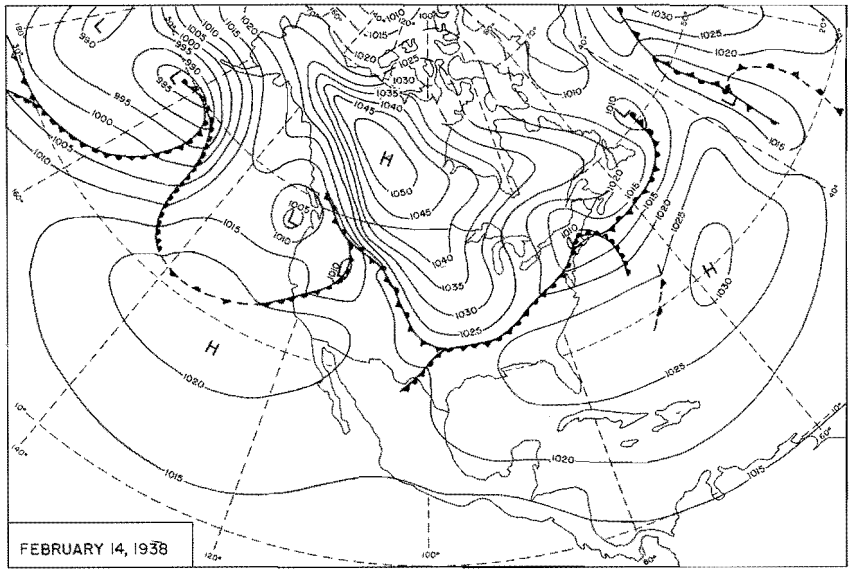

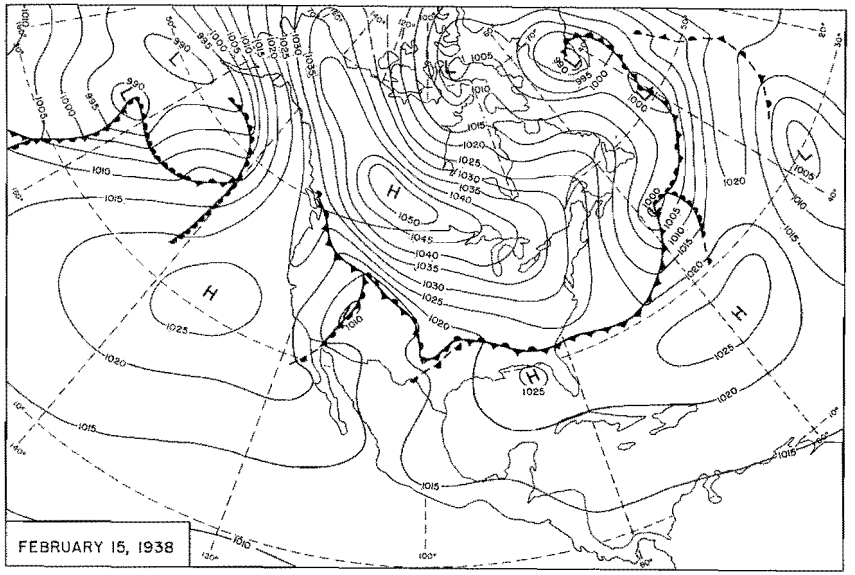

Figure 125 0700 CST Northern Hemisphere Sea-Level Maps

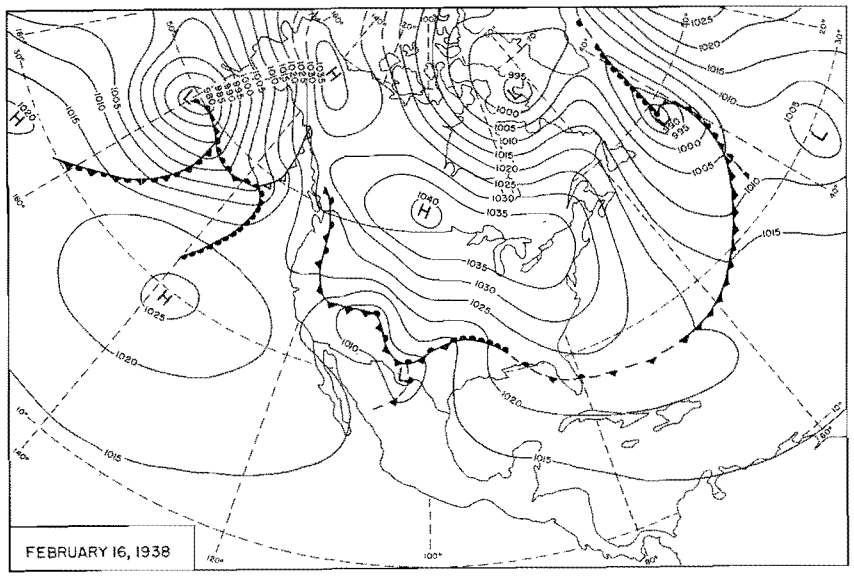

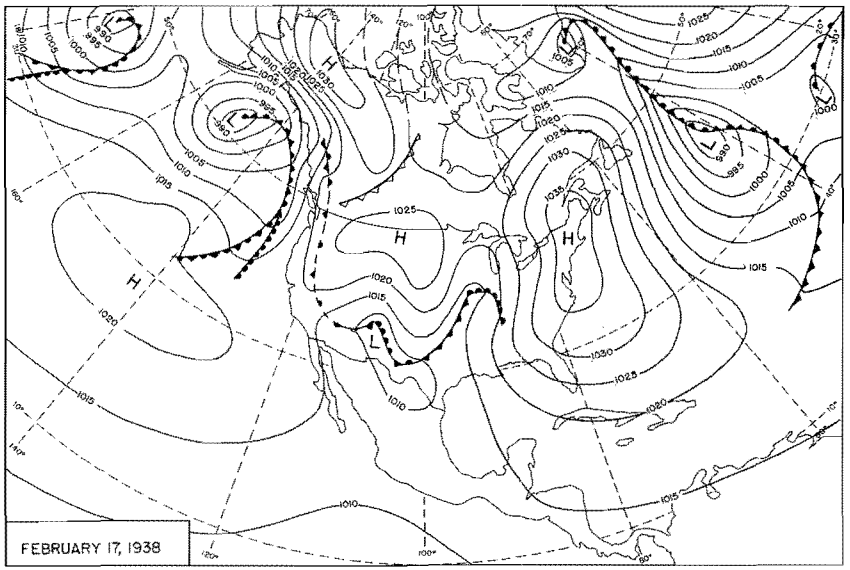

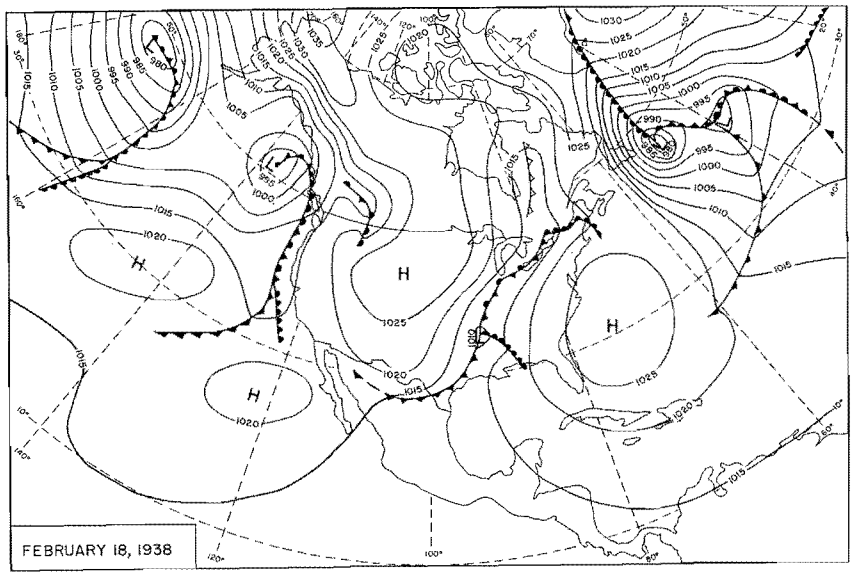

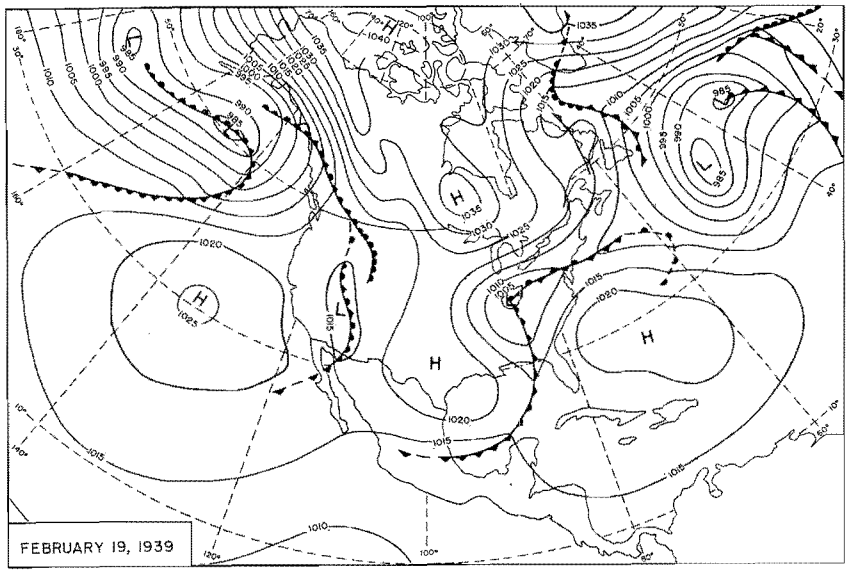

Figure 126. 0700 CST Northern Hemisphere Sea-Level Maps

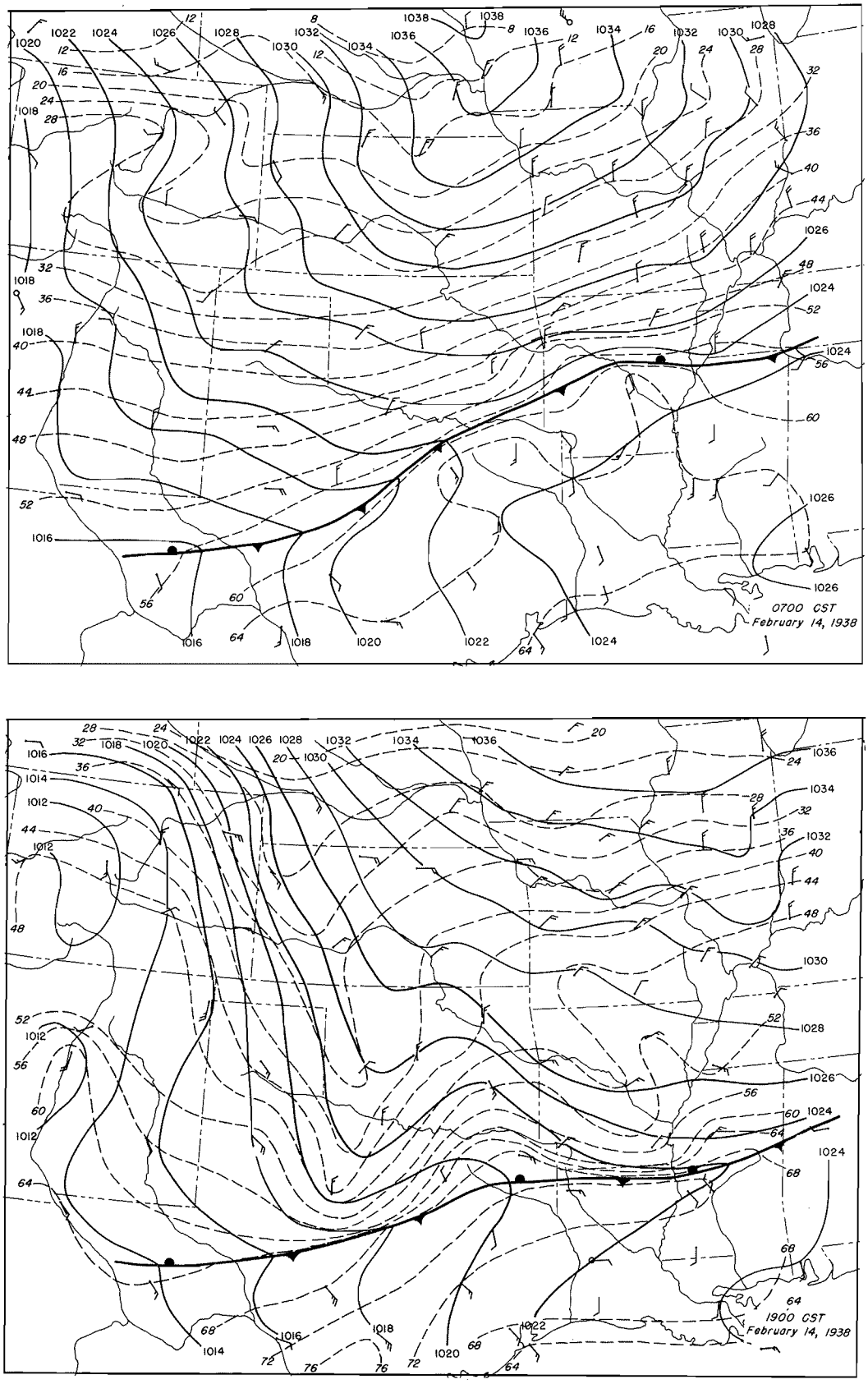

Figure 127. Detailed Surface Weather Maps

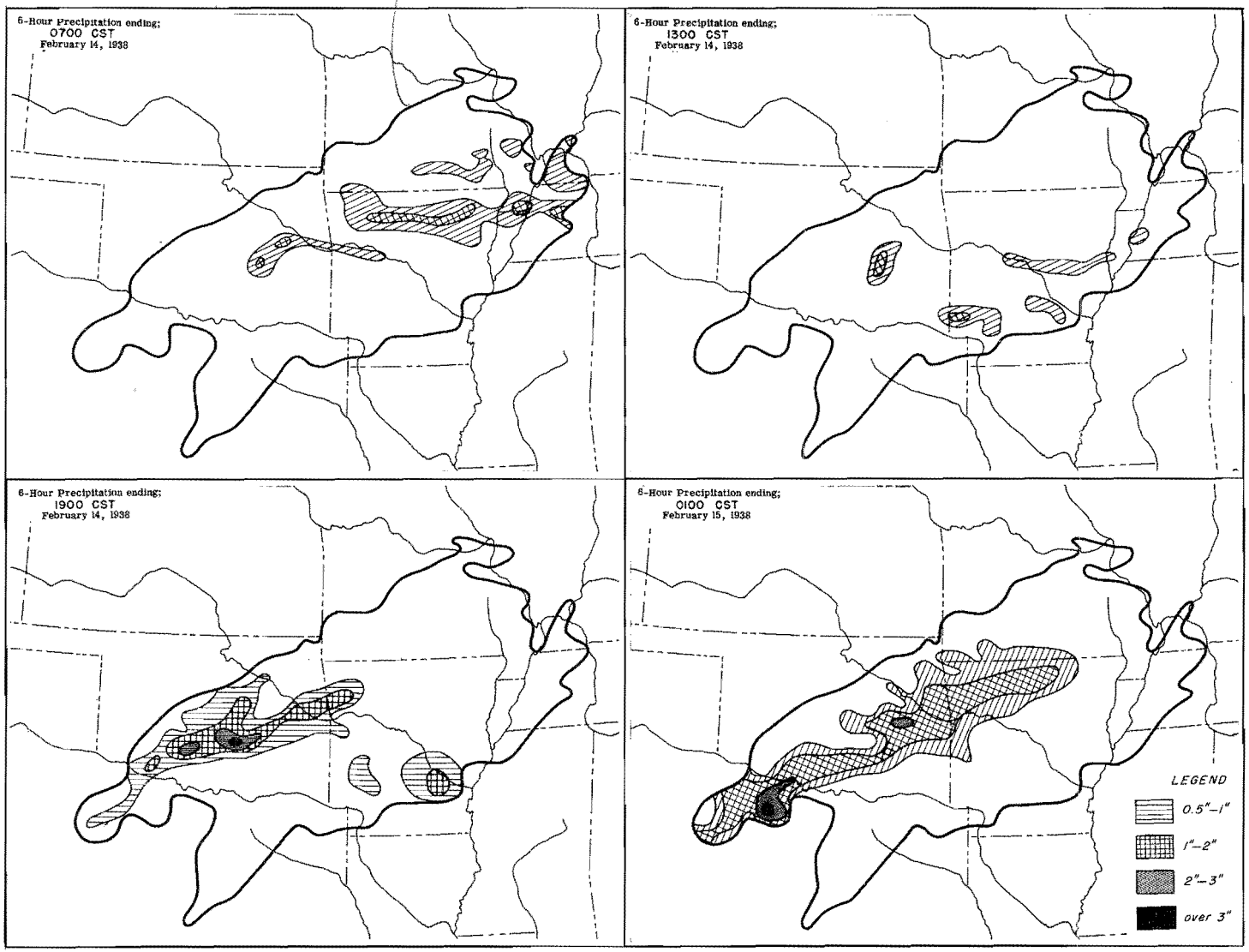

Figure 128. Incremental Isohyetal Patterns

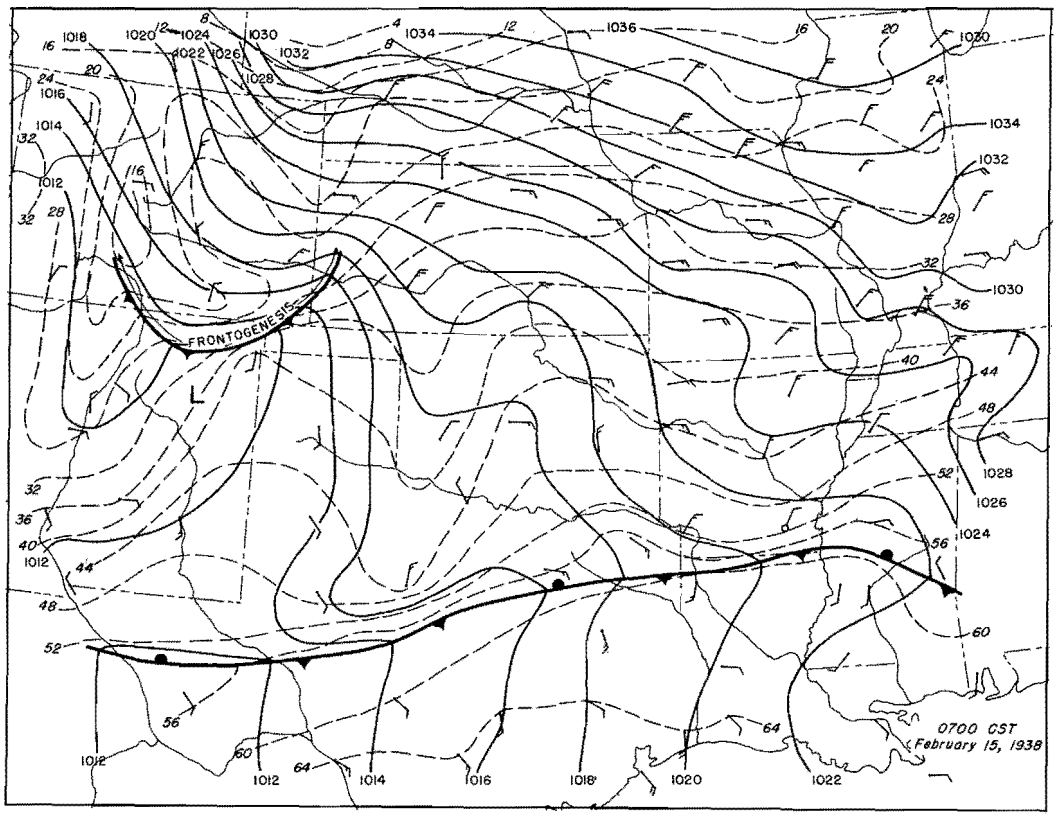

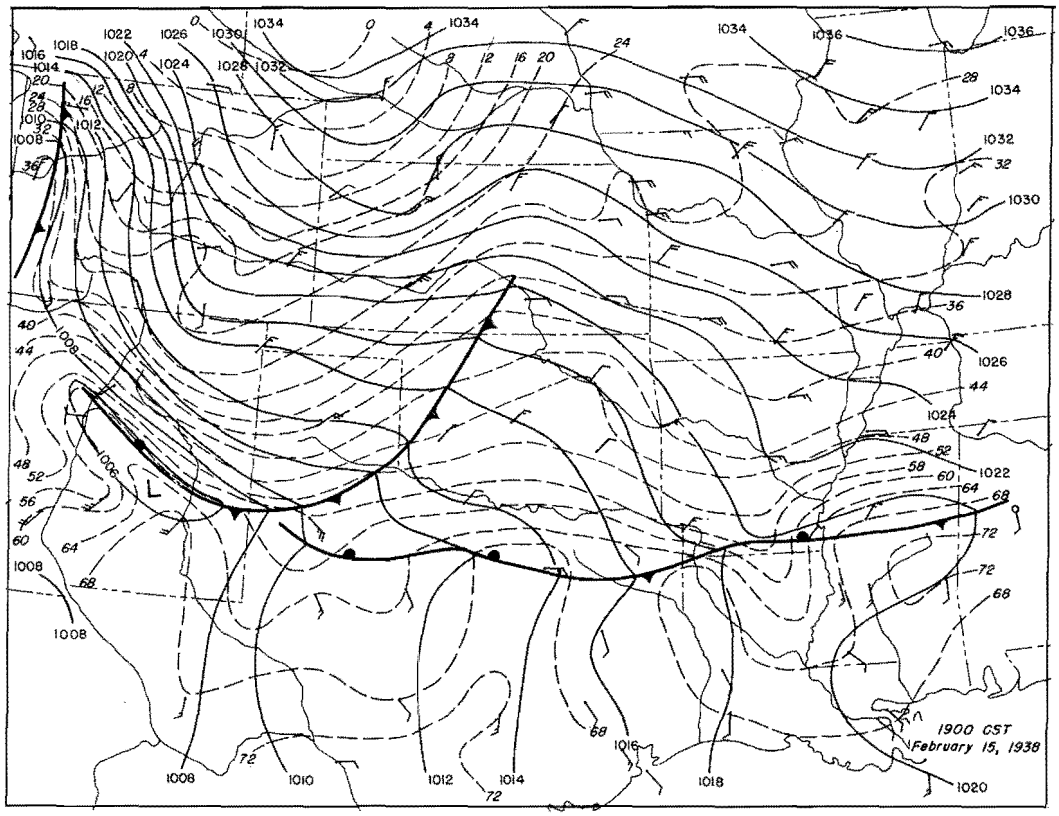

Figure 129. Detailed Surface Weather Maps

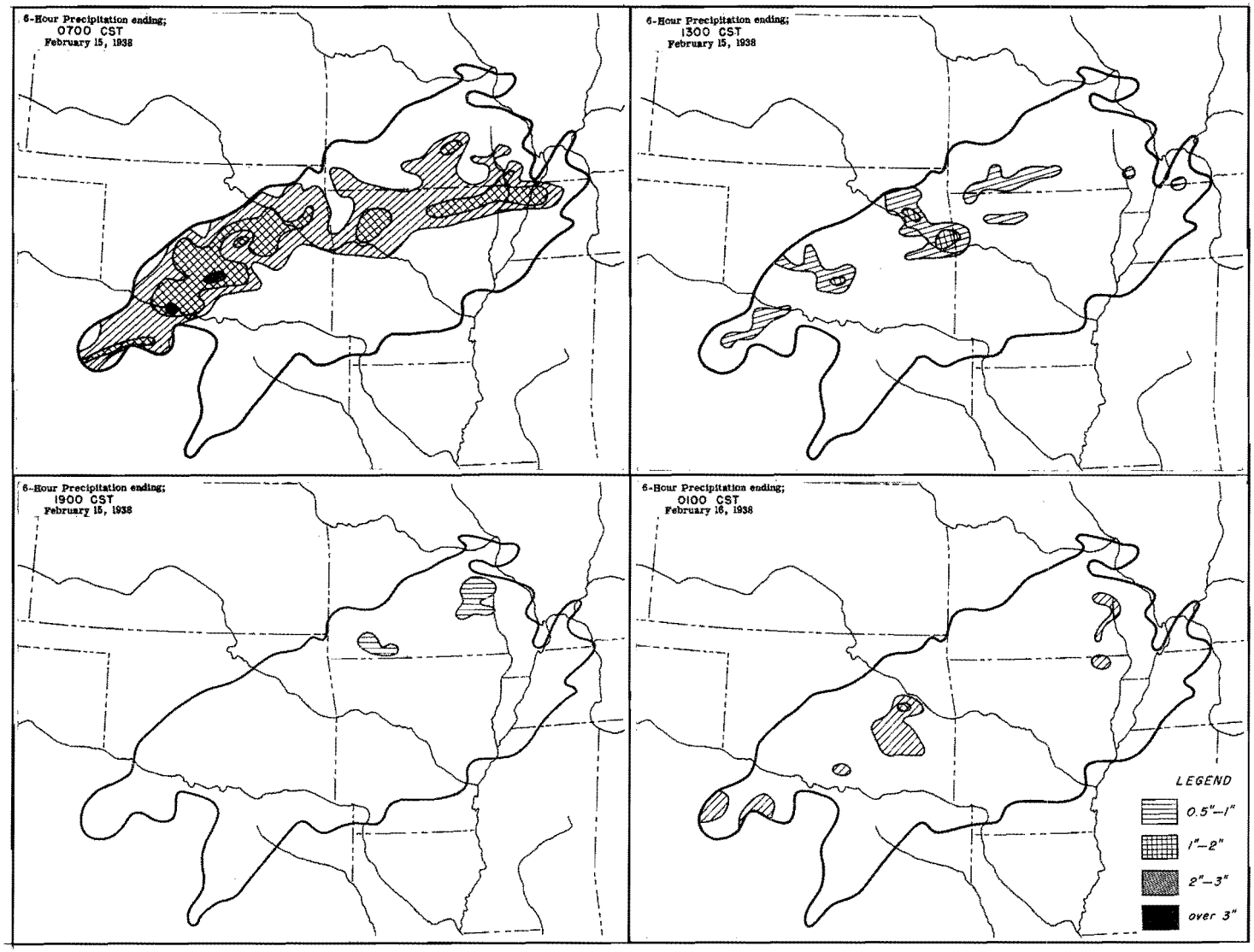

Figure 130. Incremental Isohyetal Patterns

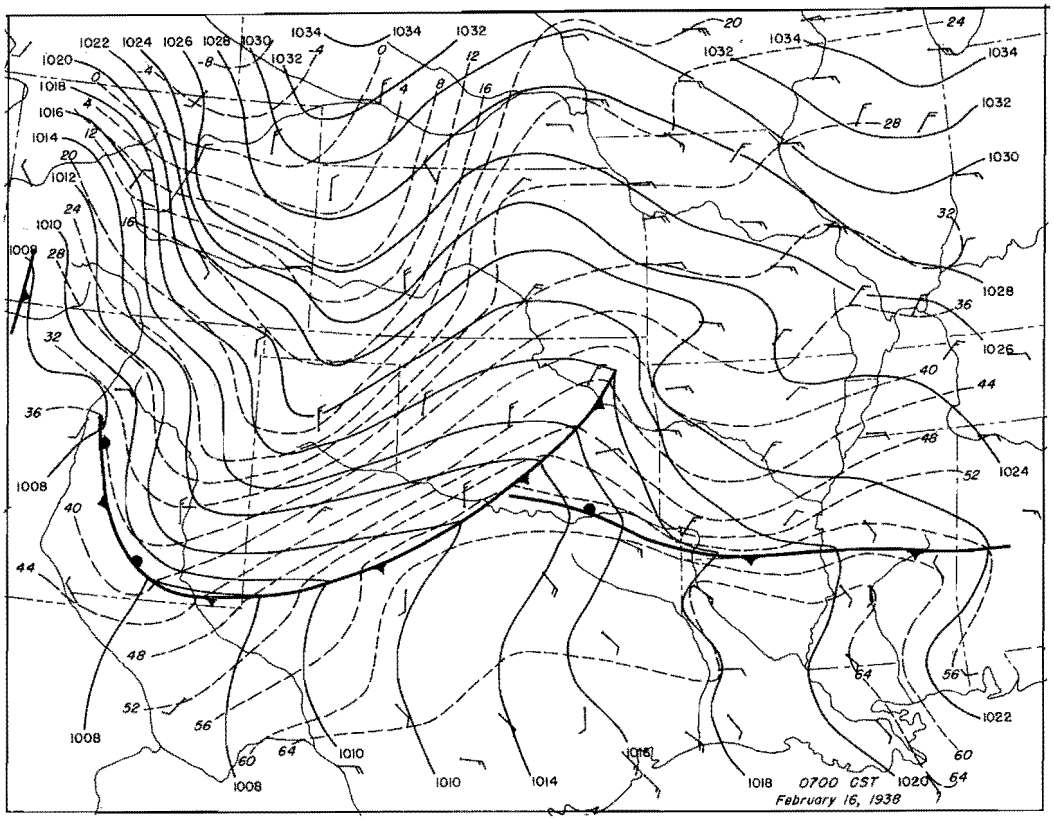

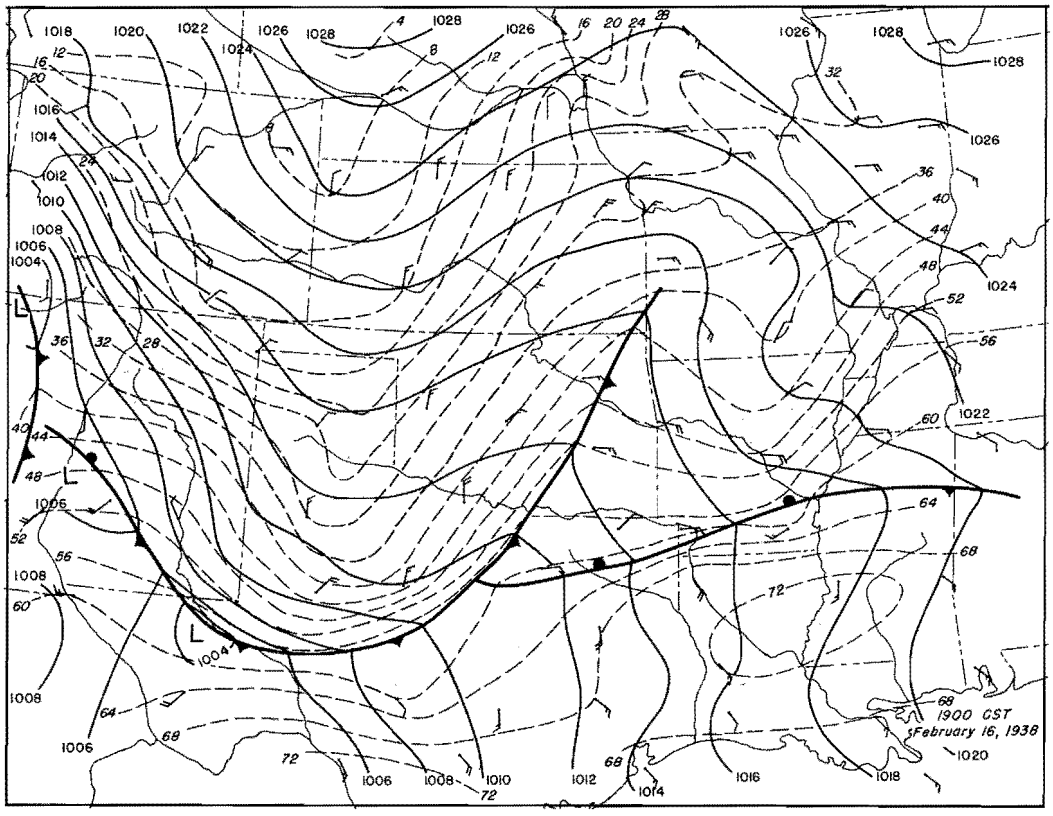

Figure 131. Detailed Surface Weather Maps

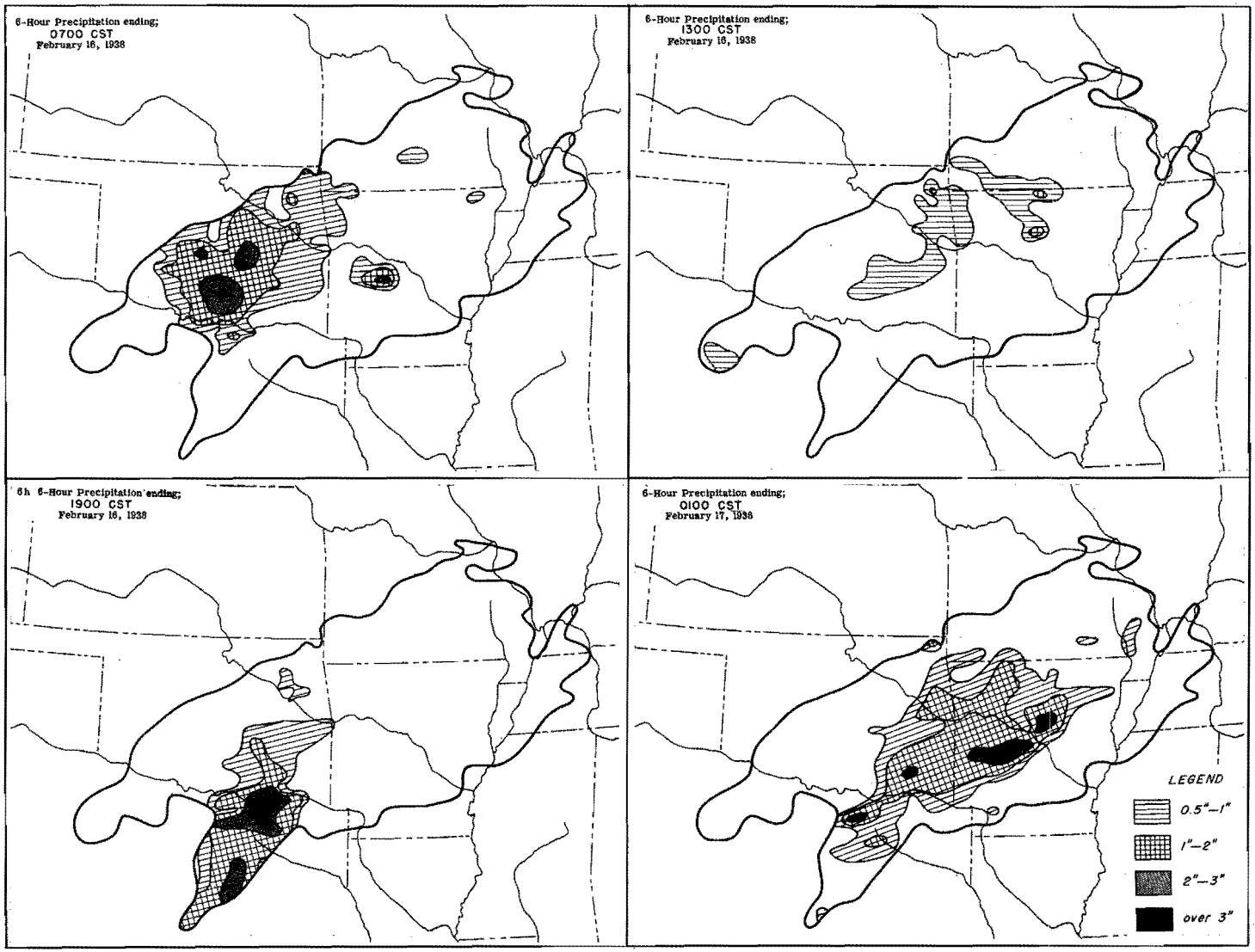

Figure 132. Incremental Isohyetal Patterns

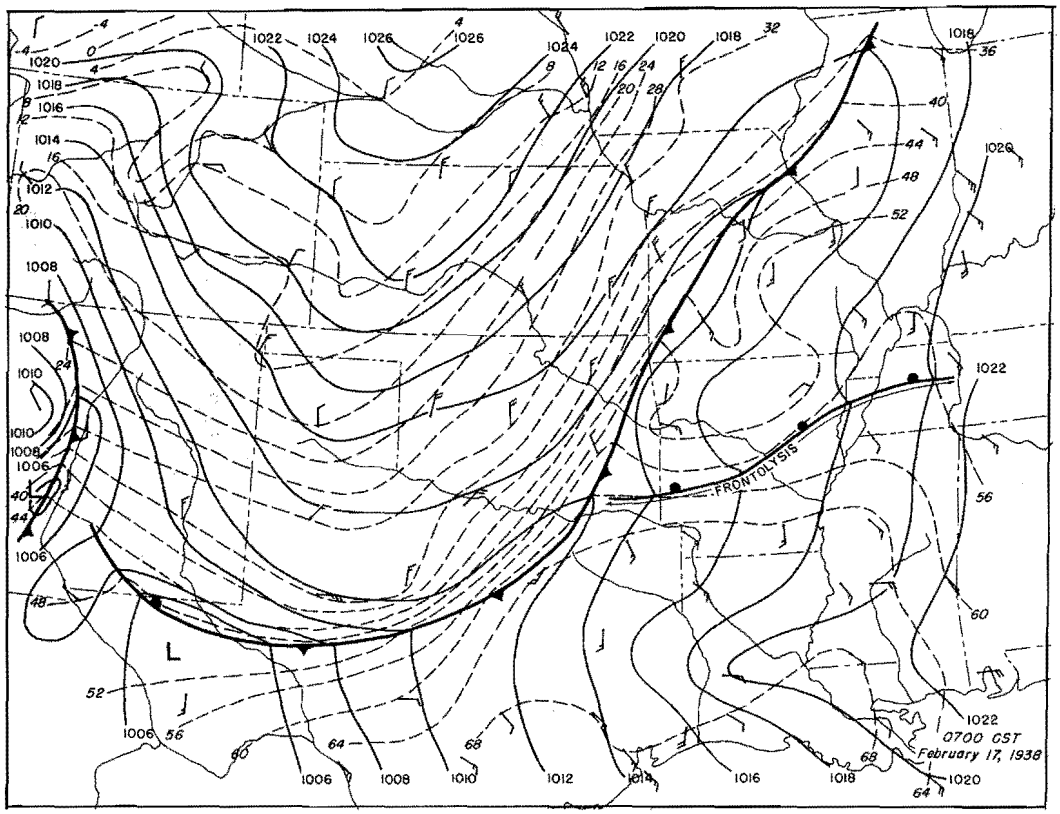

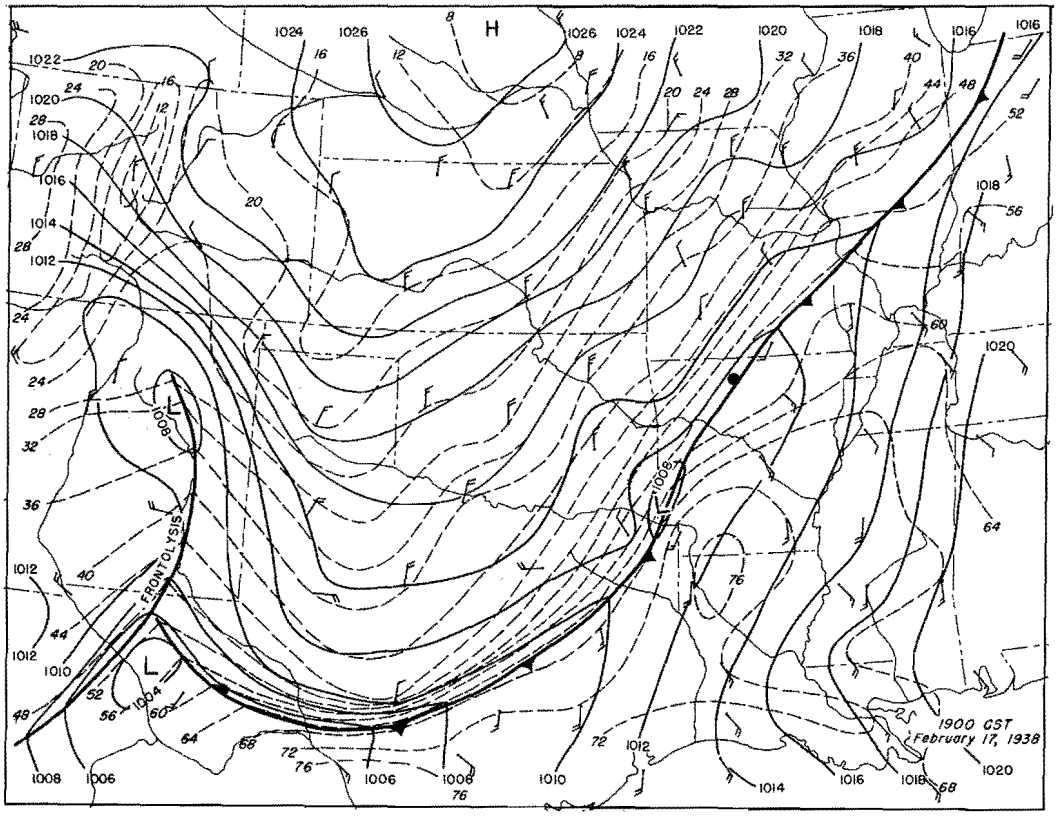

Figure 133. Detailed Surface Weather Maps

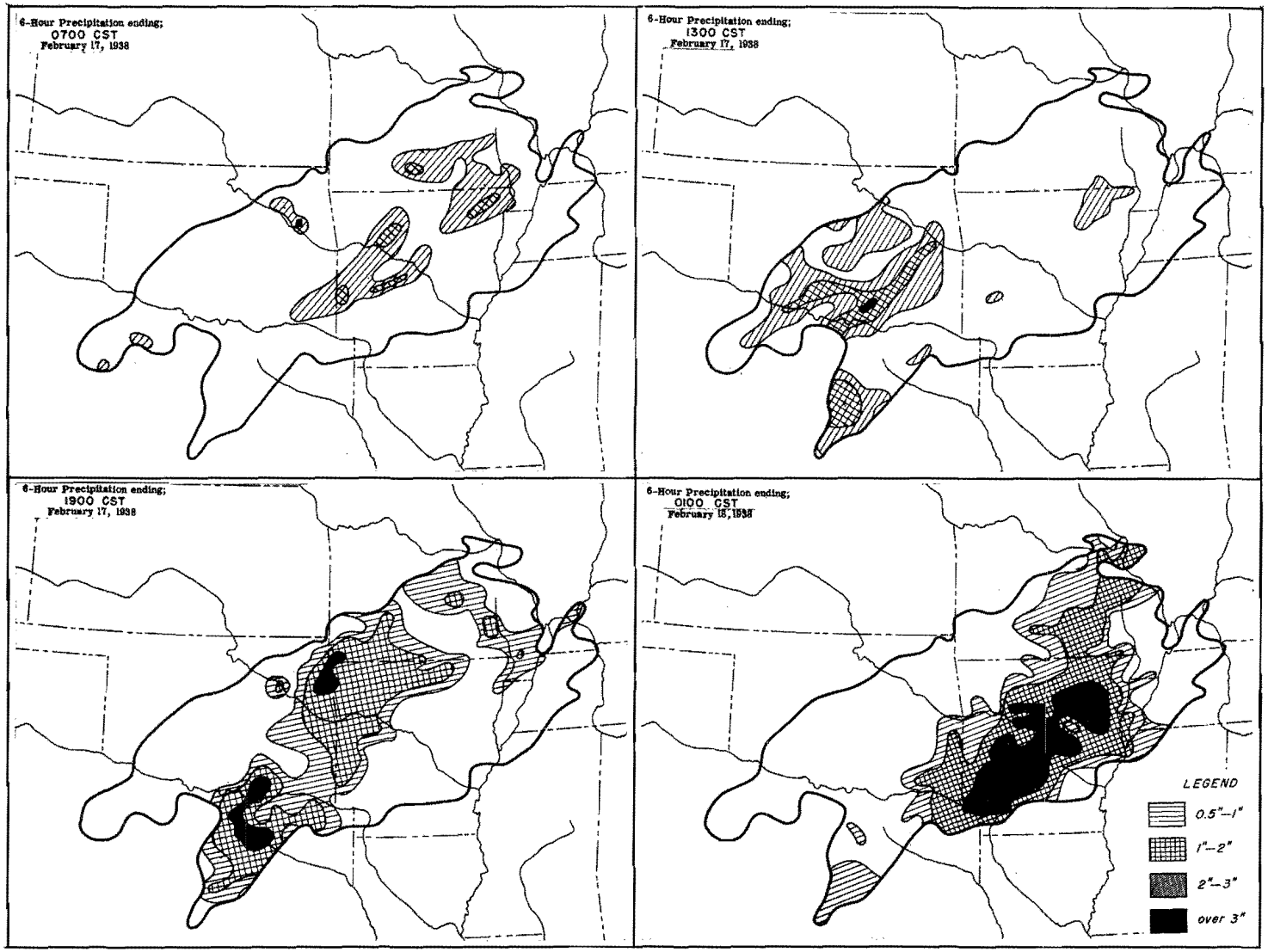

Figure 134. Incremental Isohyetal Patterns

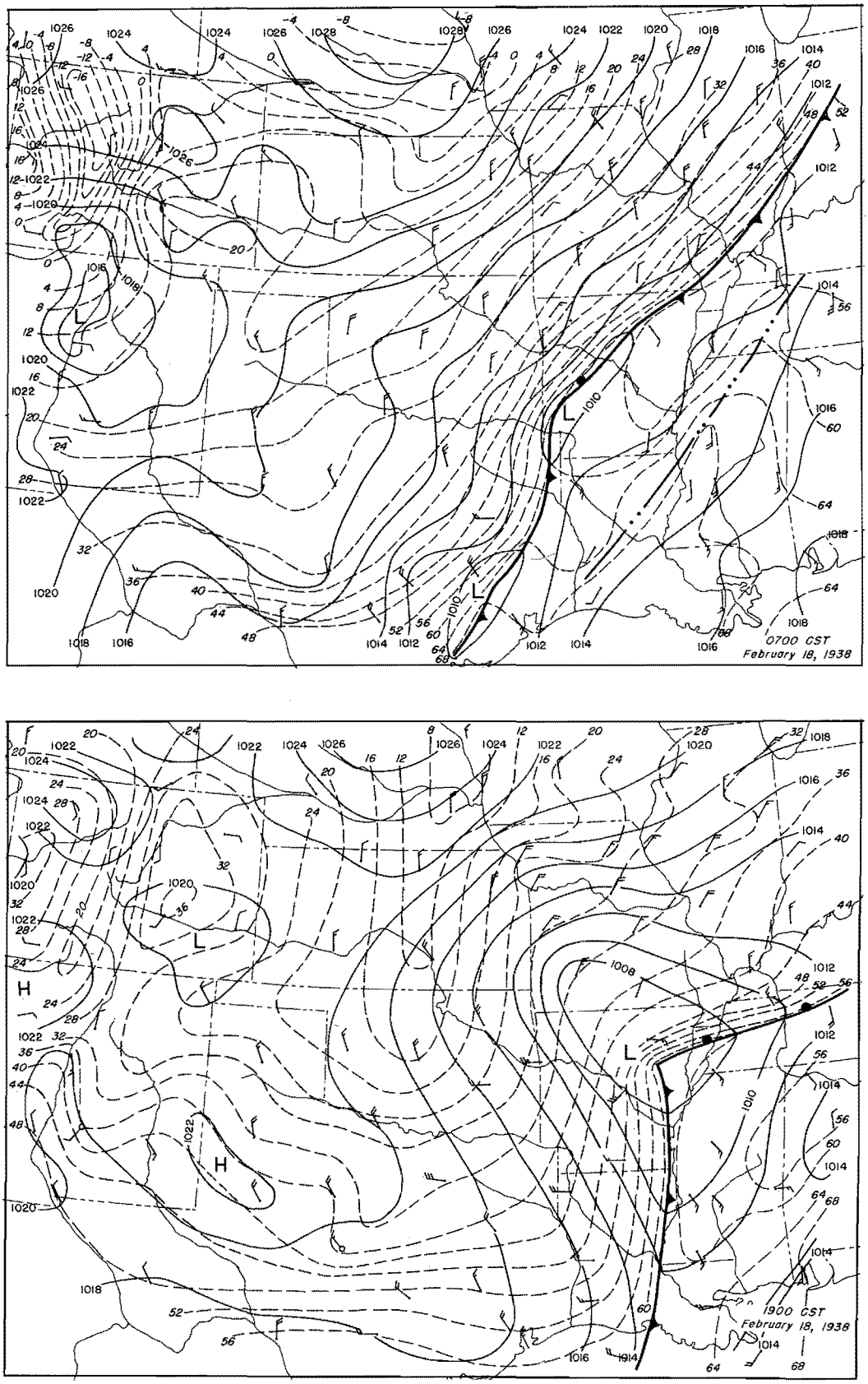

Figure 135 Detailed Surface Weather Maps

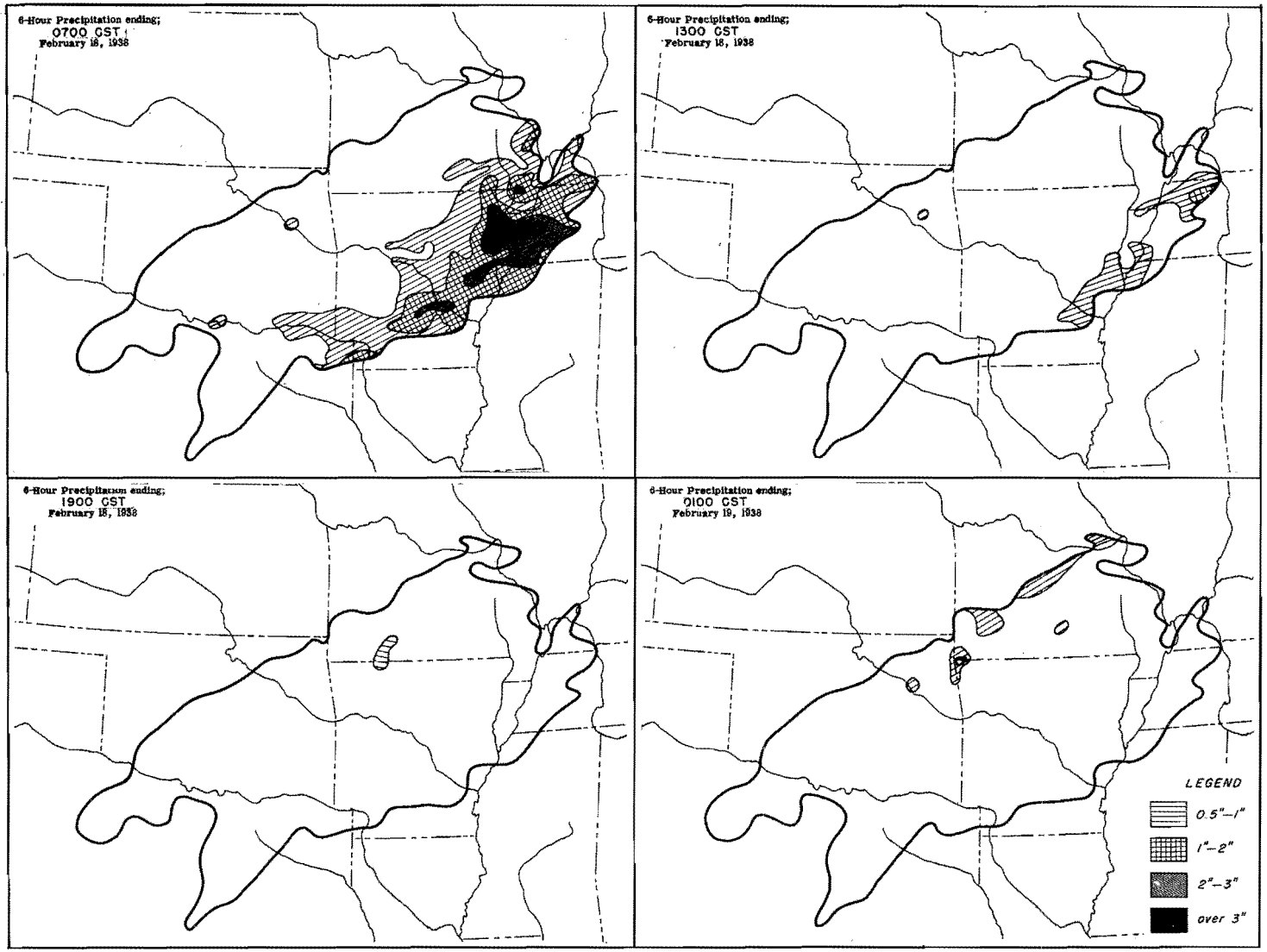

Figure 136. Incremental Isohyetal Patterns

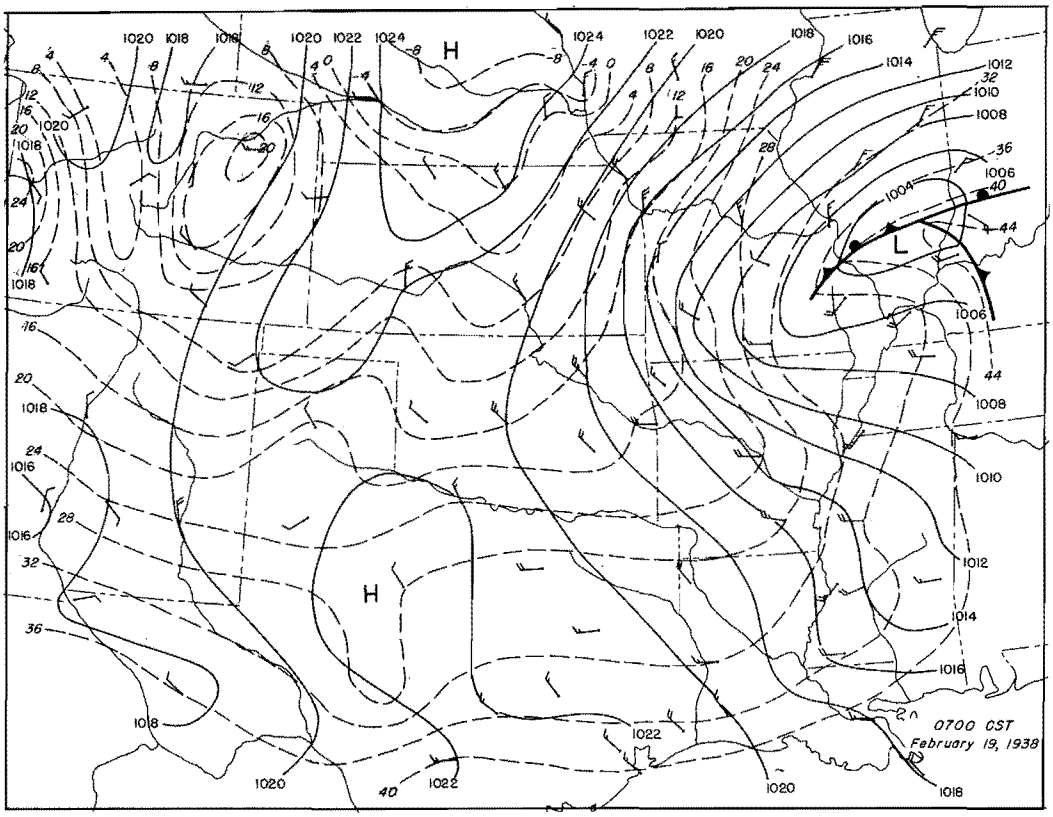

Figure 137. Detailed Surface Weather Map

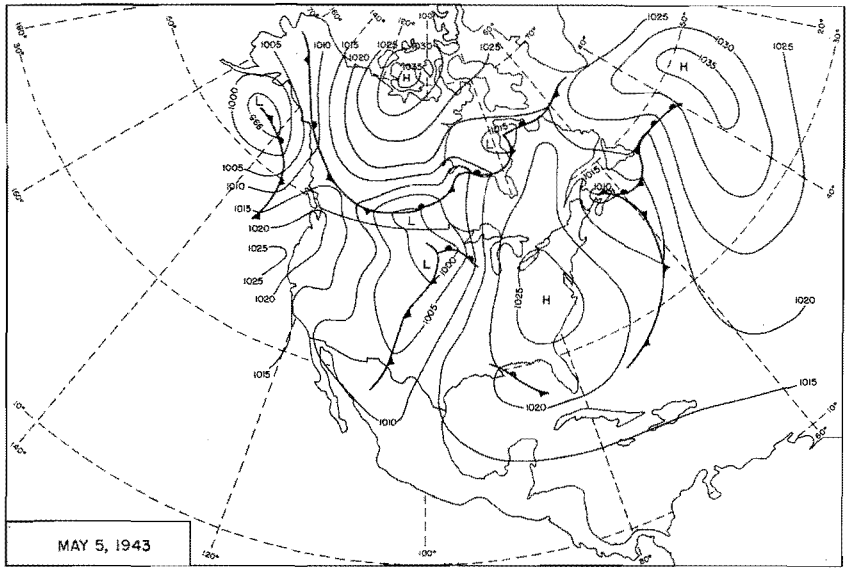

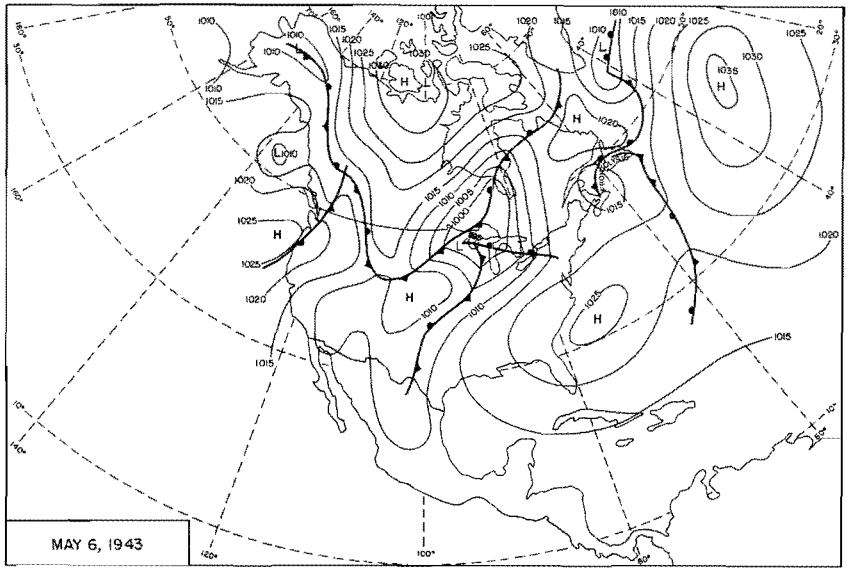

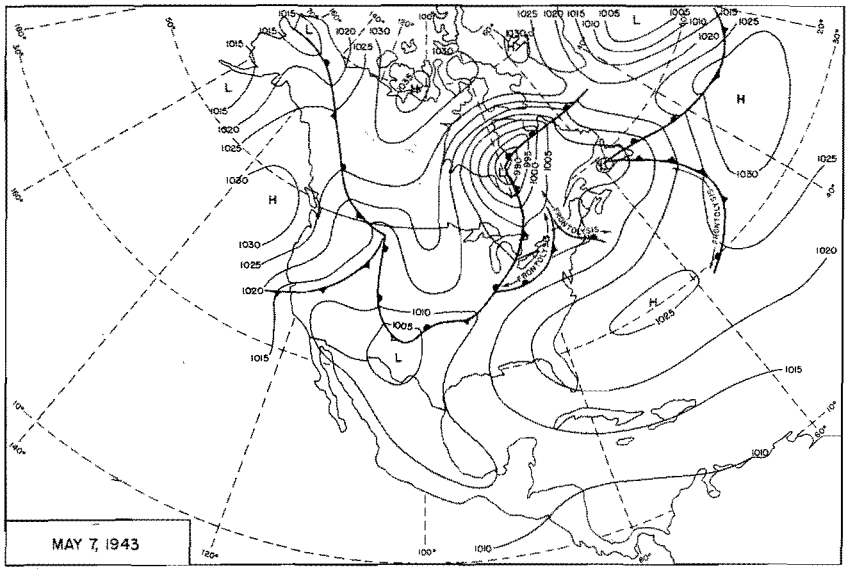

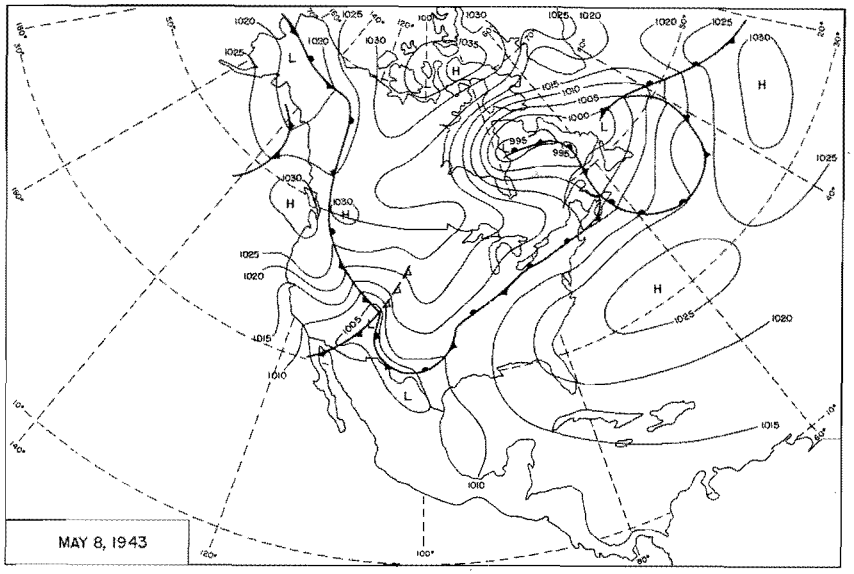

Figure 138. 0700 CST Northern Hemisphere Sea-Level Maps

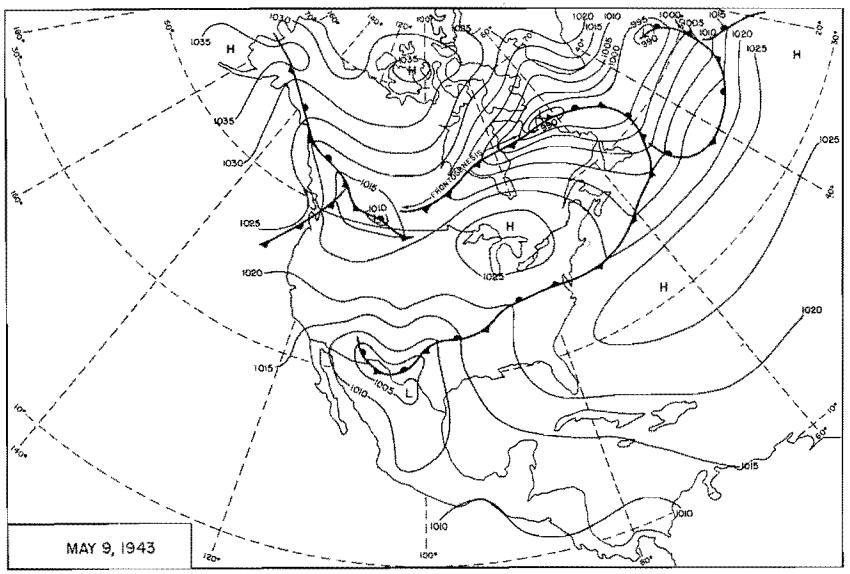

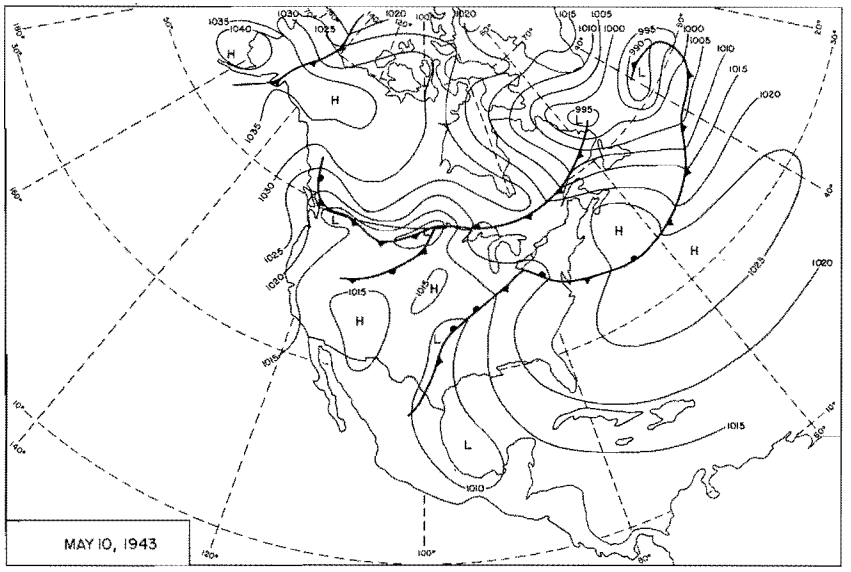

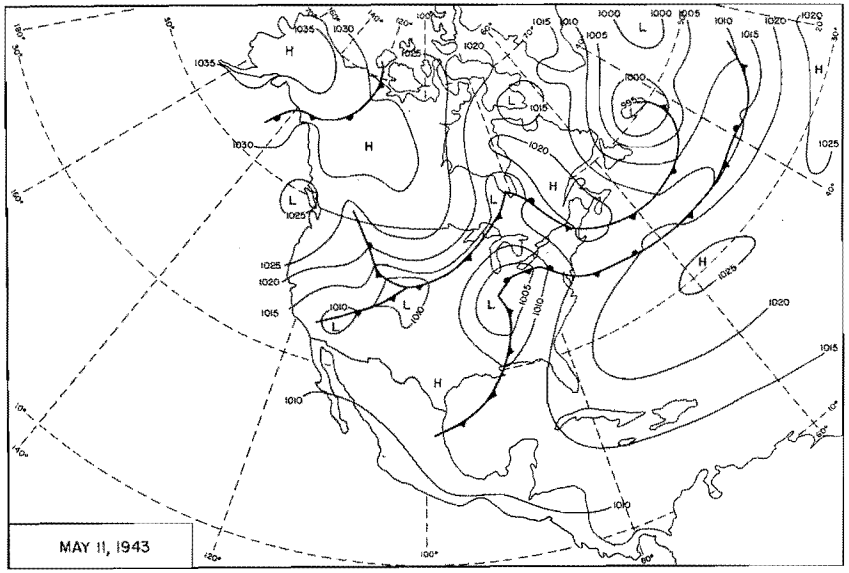

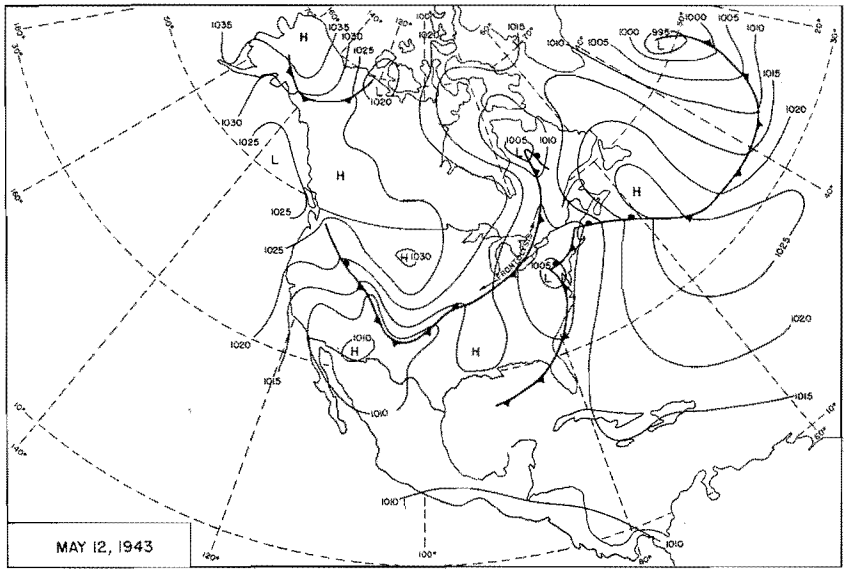

Figure 139. 0700 CST Northern Hemisphere Sea-Level Maps

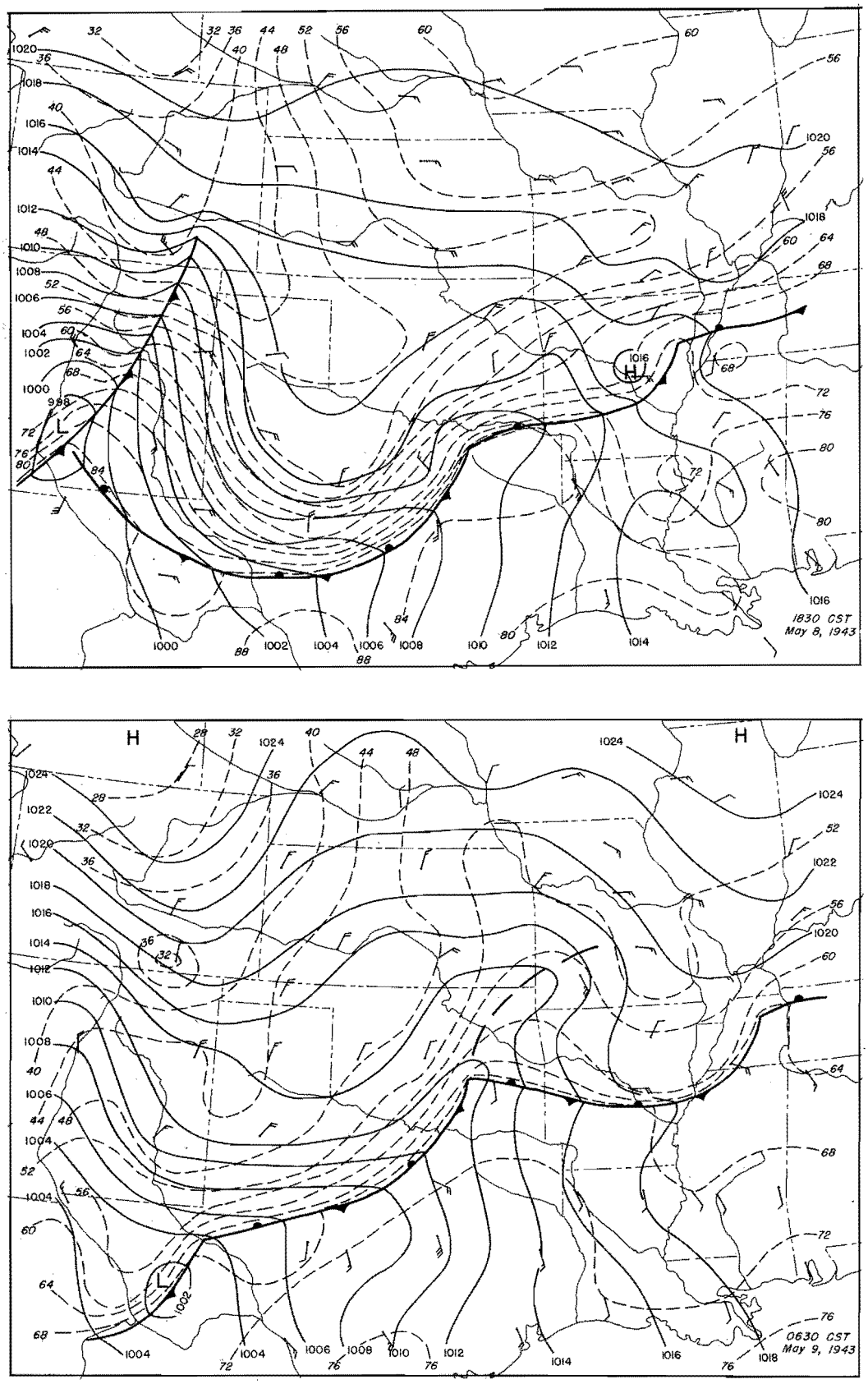

Figure 140. Detailed Surface Weather Maps

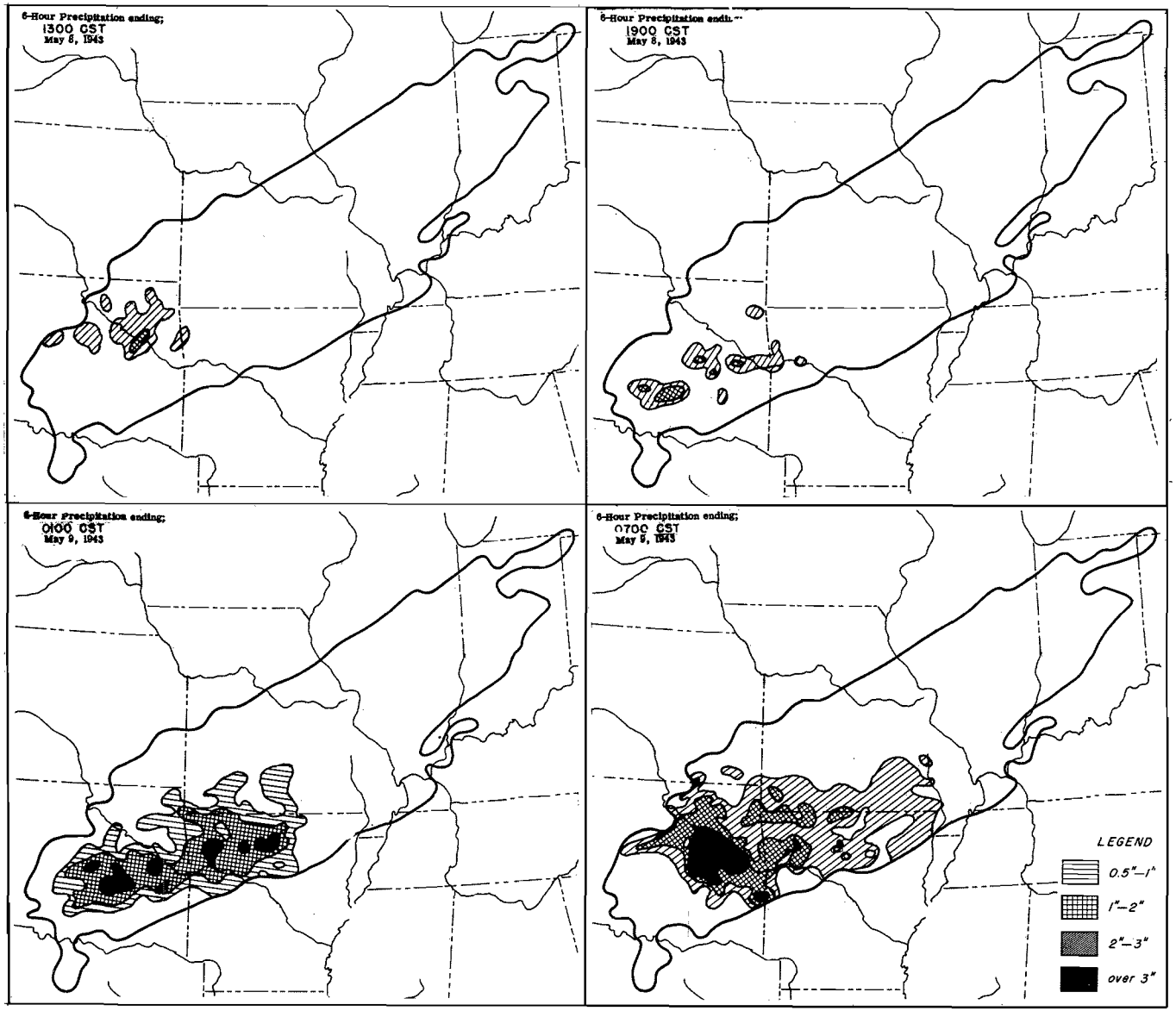

Figure 141. Incremental Isohyetal Patterns

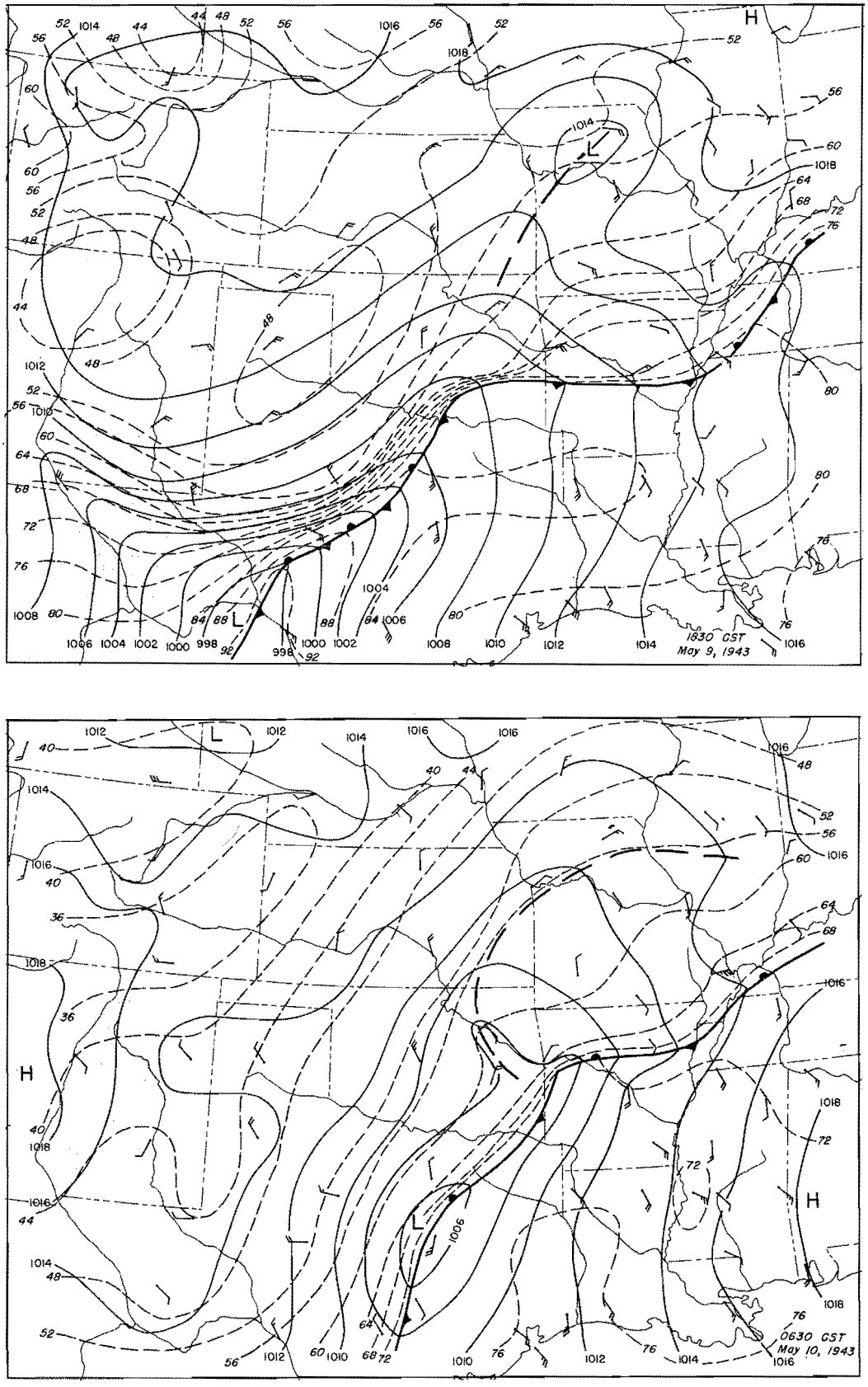

Figure 142. Detailed Surface Weather Maps

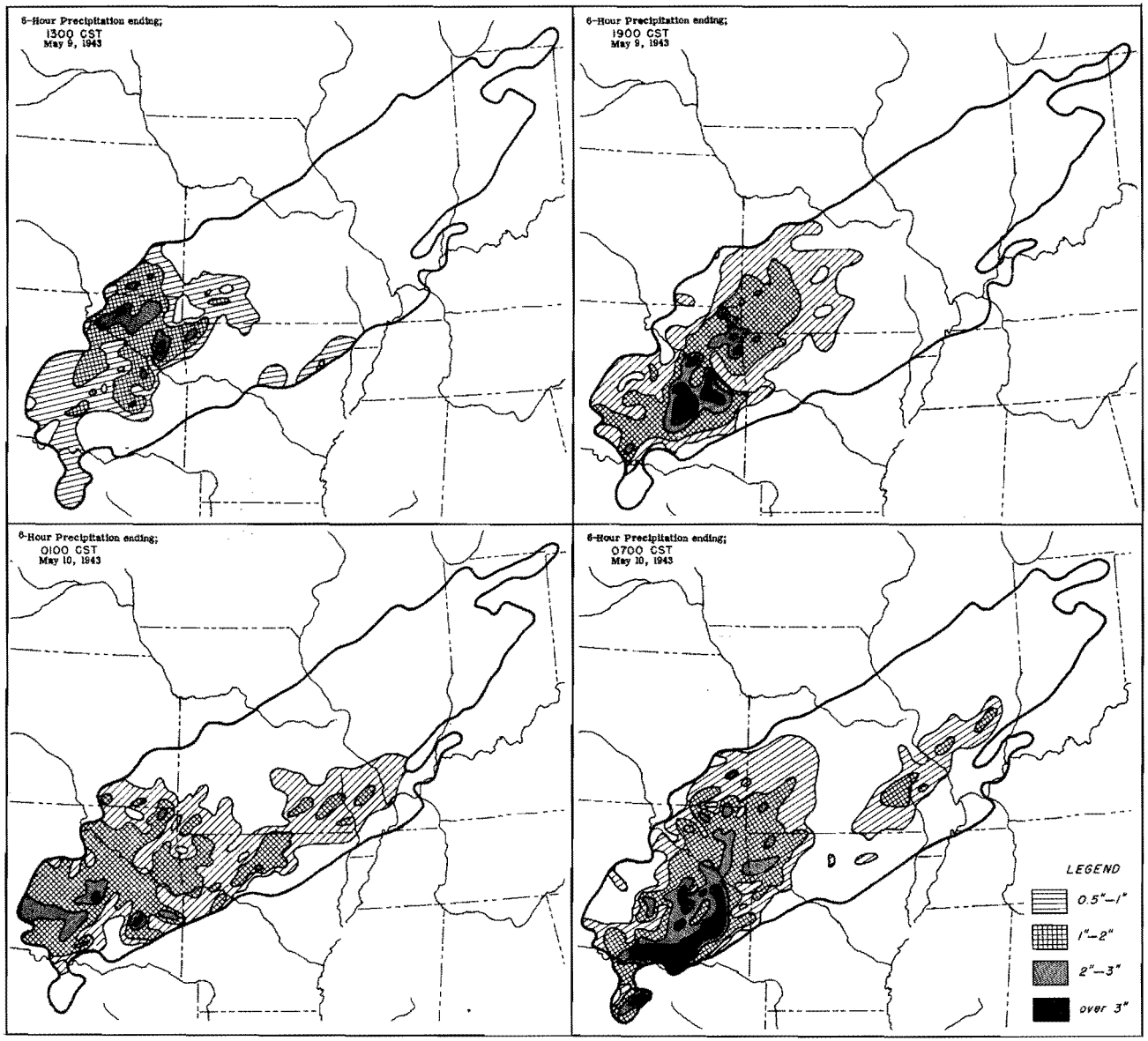

Figure 143. Incremental Isohyetal Patterns

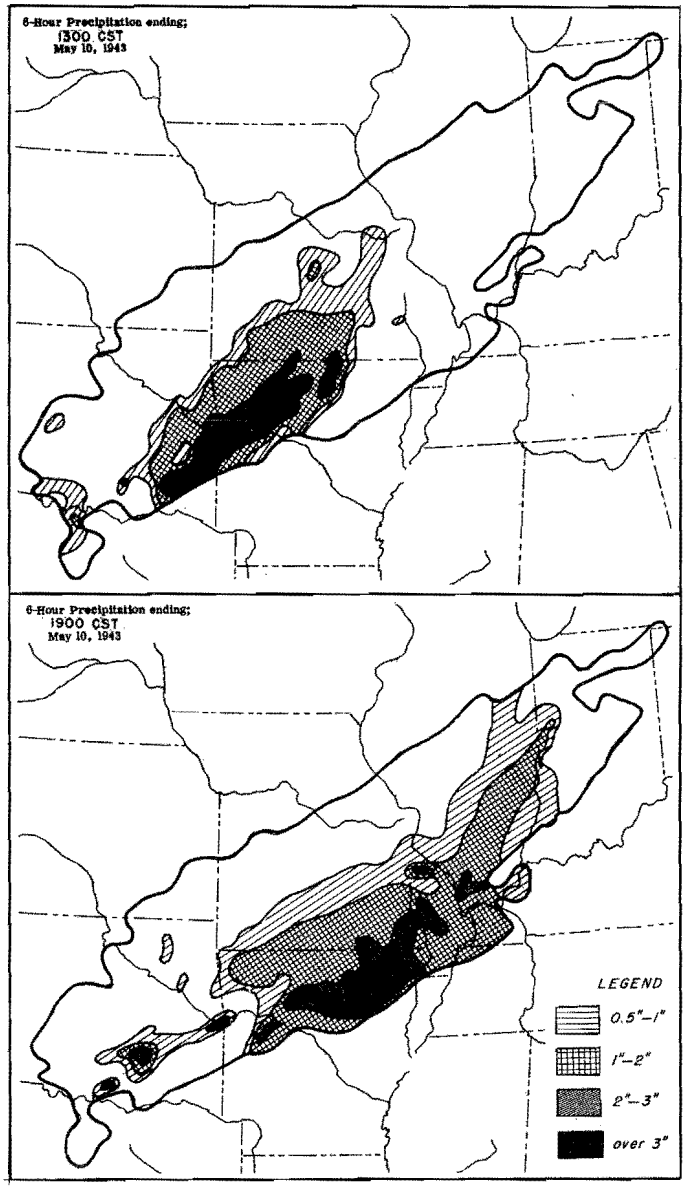

Figure 144. Incremental Isohyetal Patterns

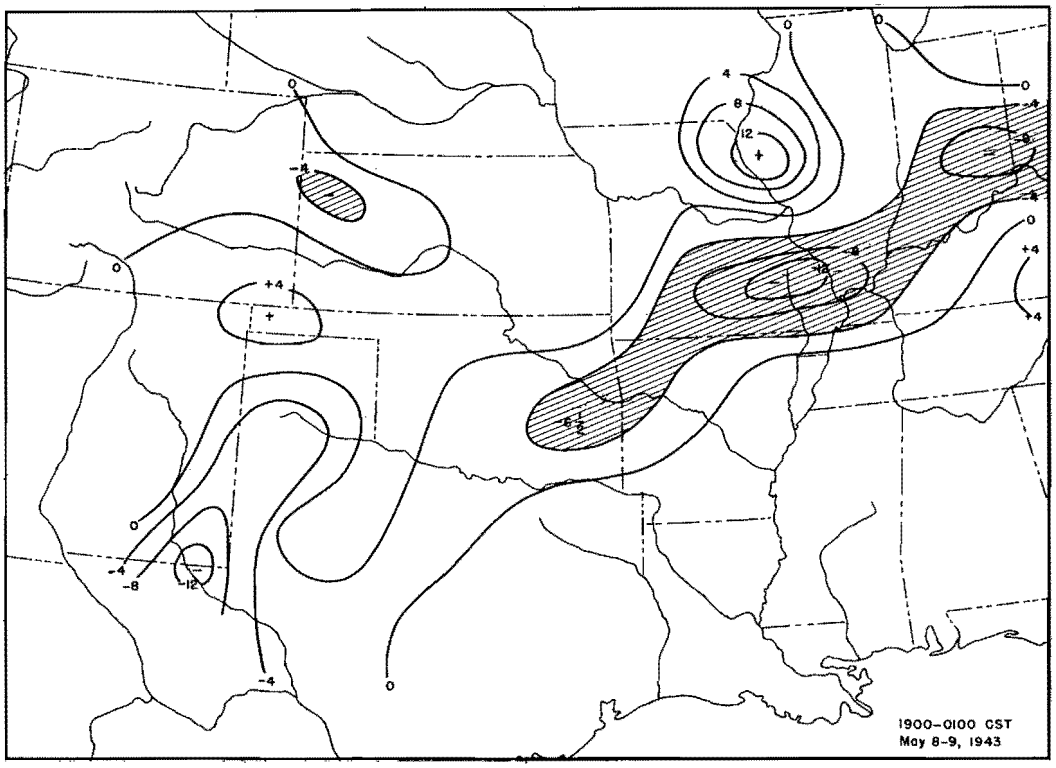

Figure 145. Differential Advection at 5000 feet

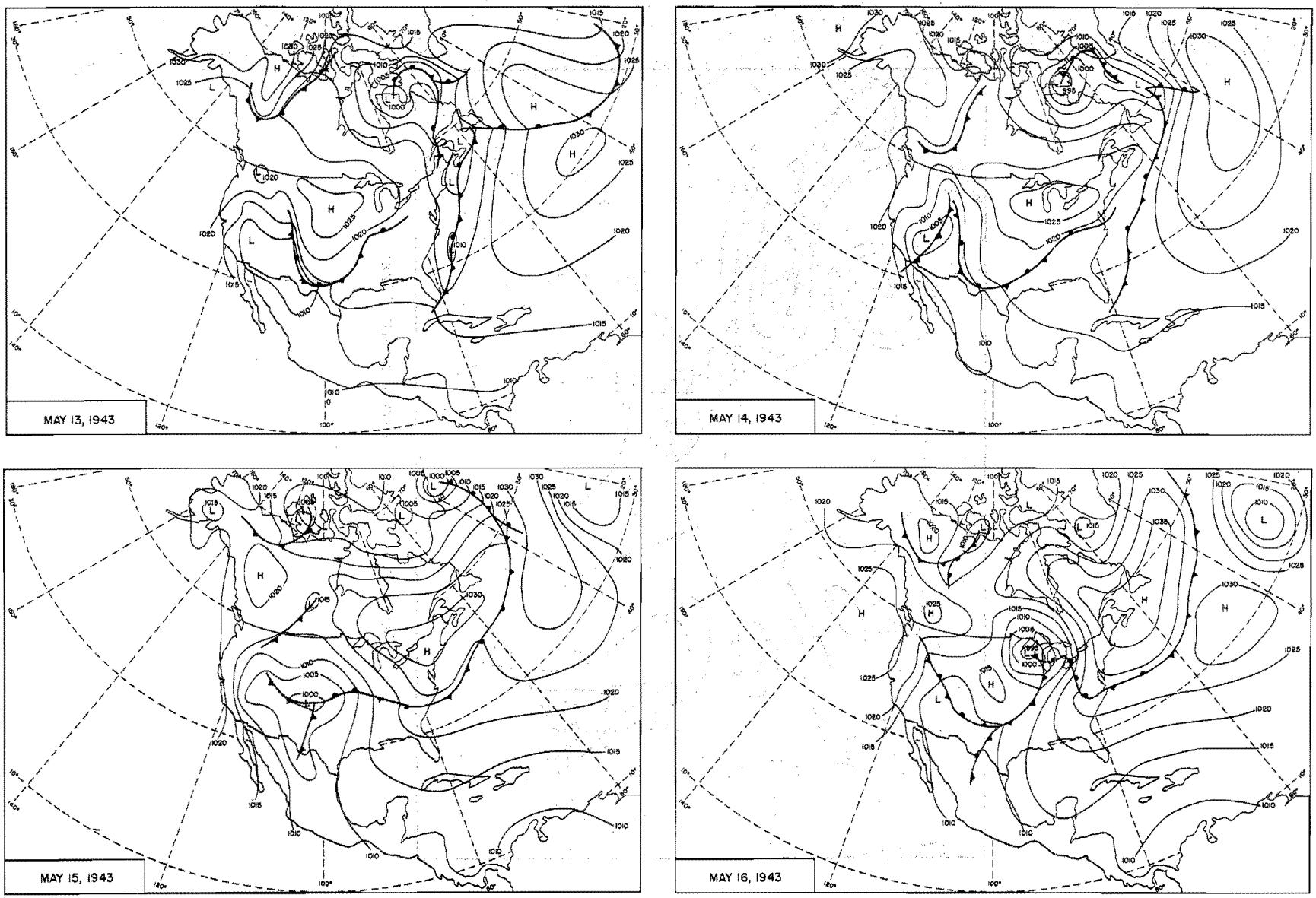

Figure 146. 0700 CST Northern Hemisphere Sea-Level Maps

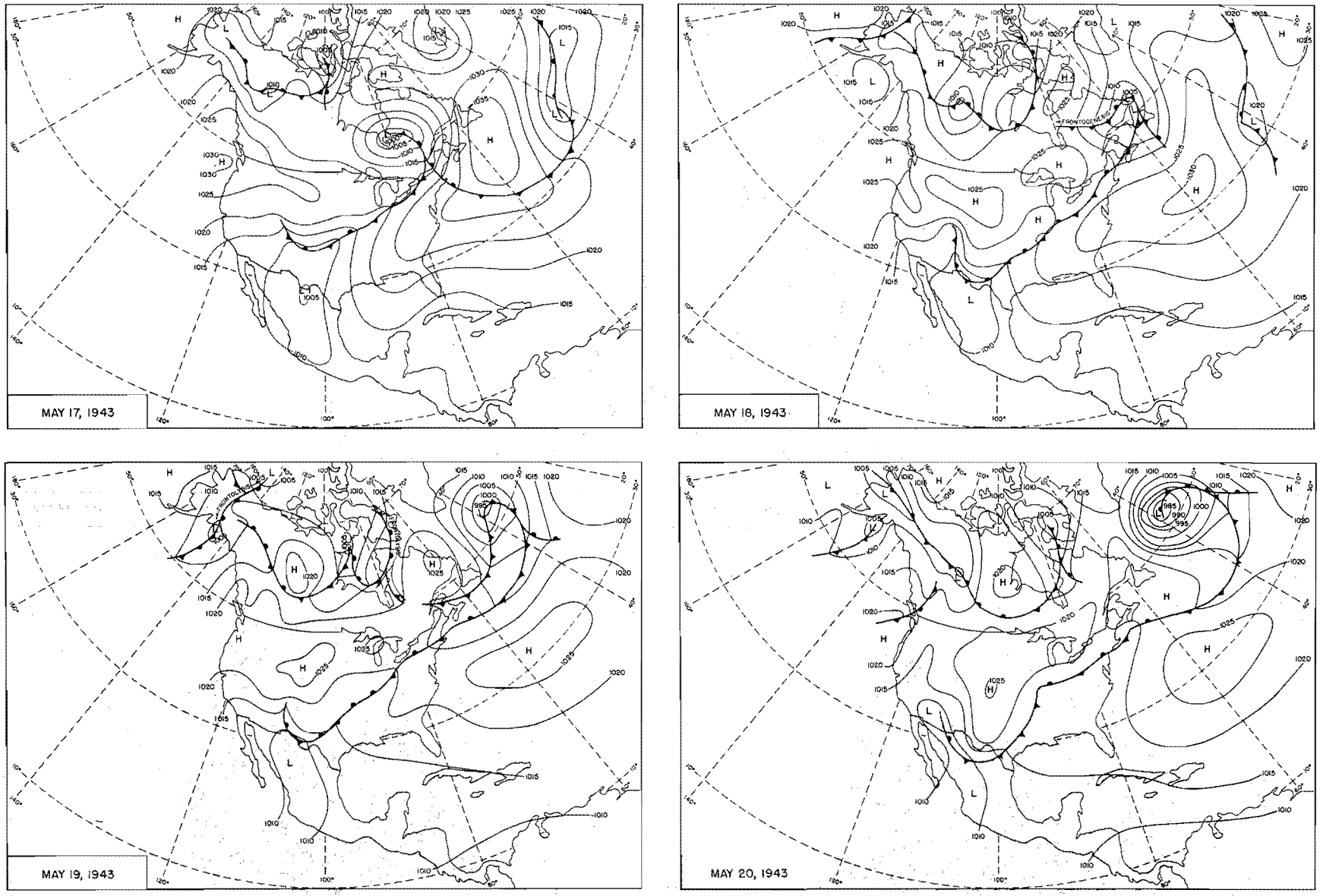

Figure 147. 0700 CST Northern Hemisphere Sea-Level Maps

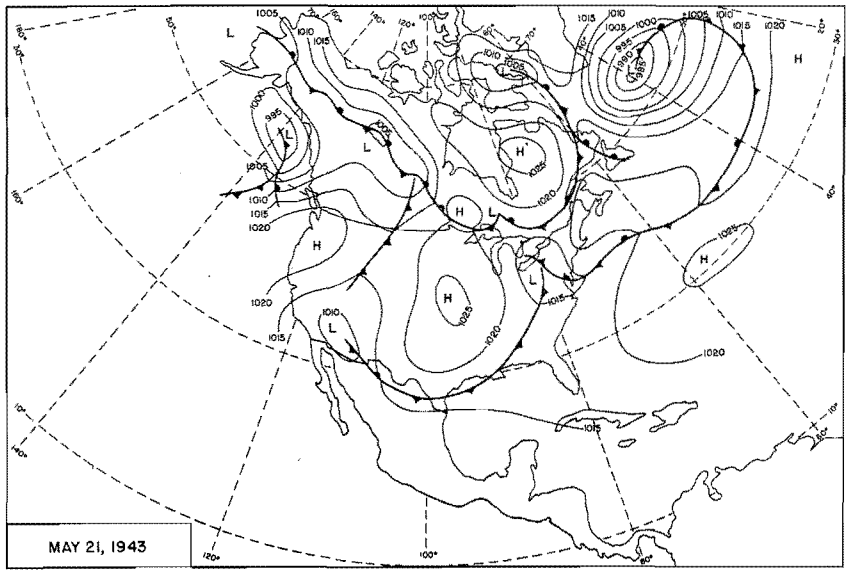

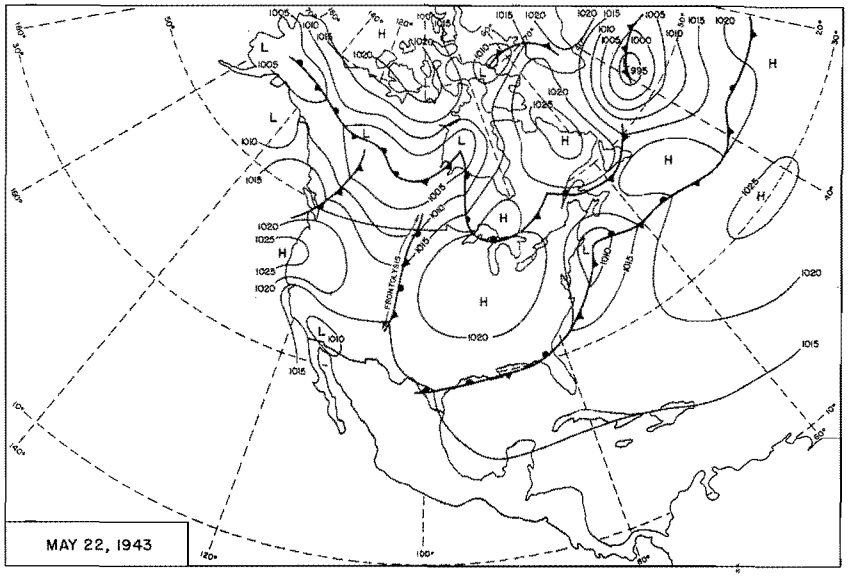

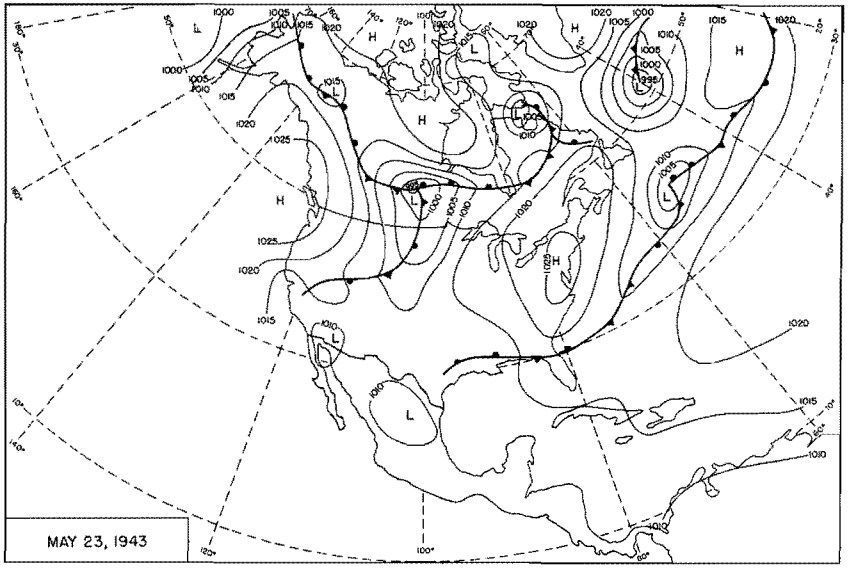

Figure 148. 0700 CST Northern Hemisphere Sea-Level Maps

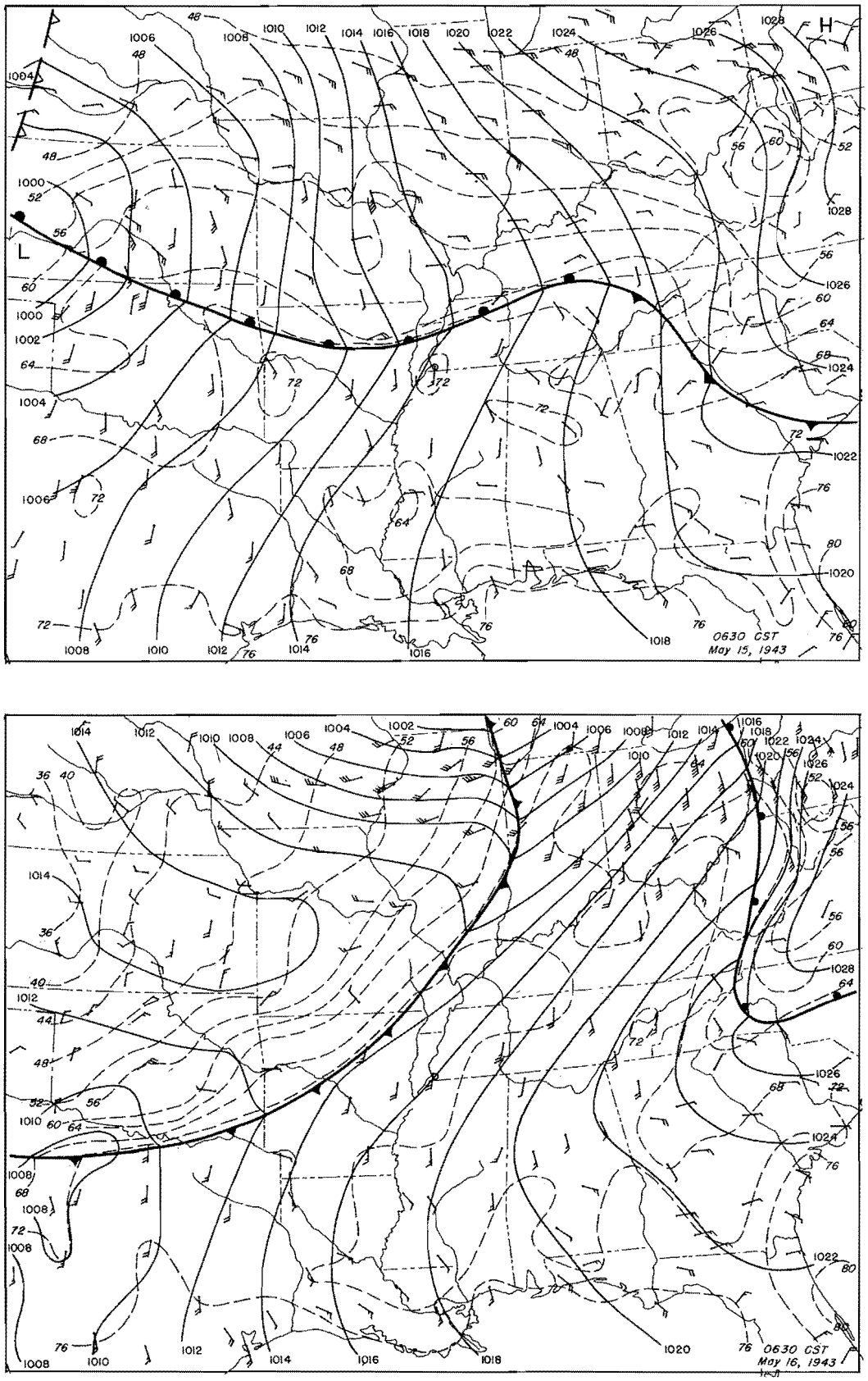

Figure 149. Detailed Surface Weather Maps

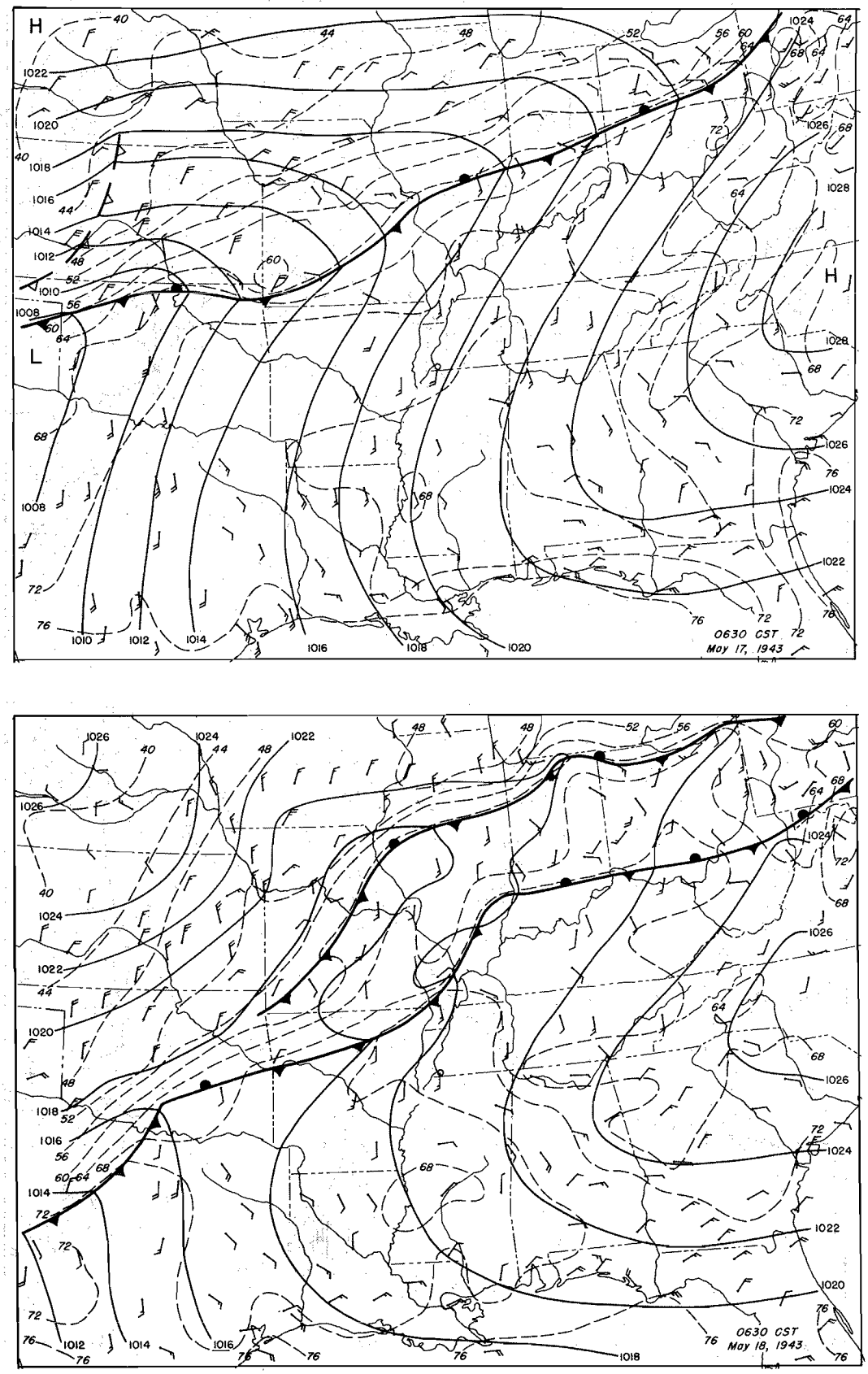

Figure 150. Detailed Surface Weather Maps

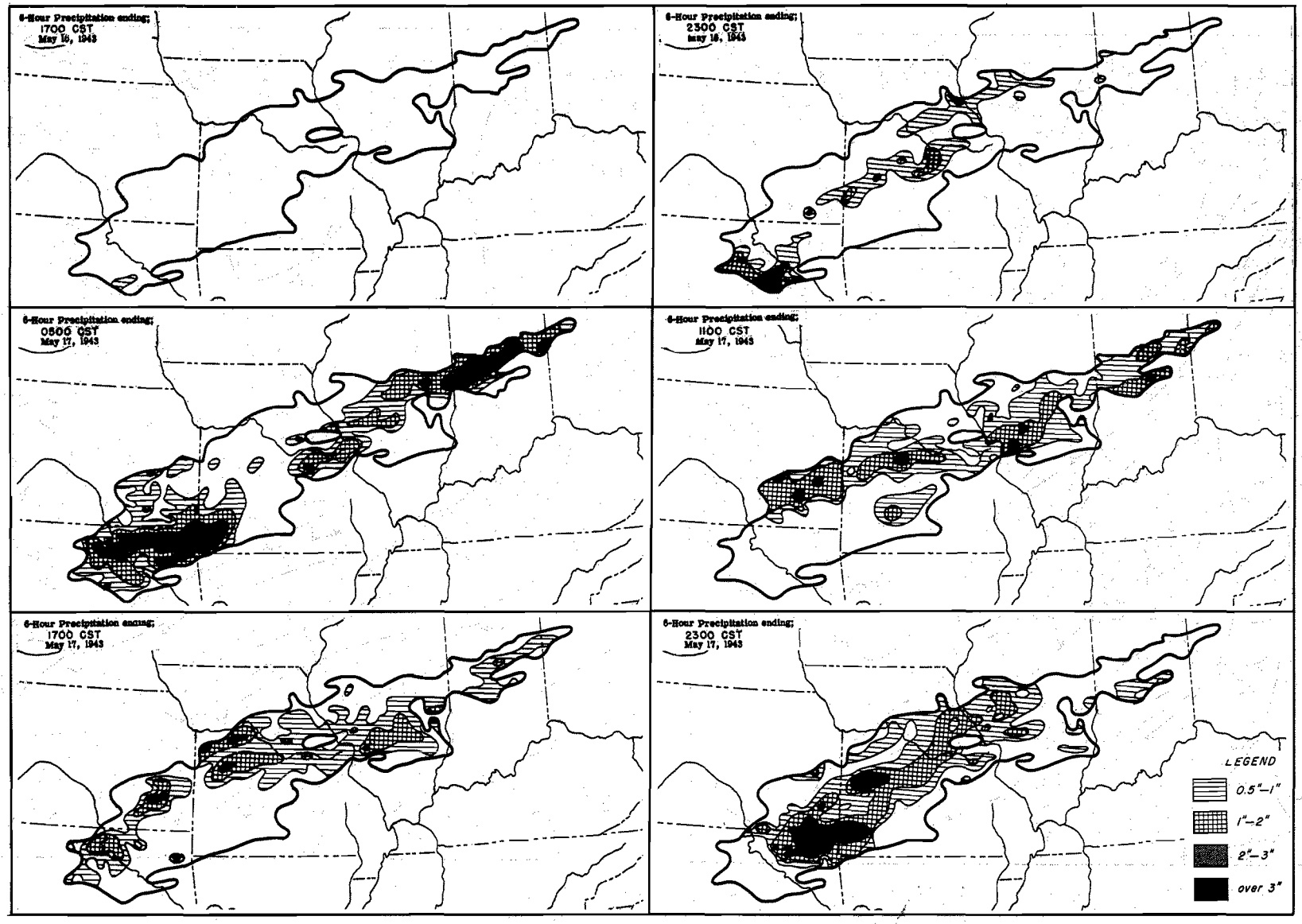

Figure 151. Incremental Isohyetal Patterns

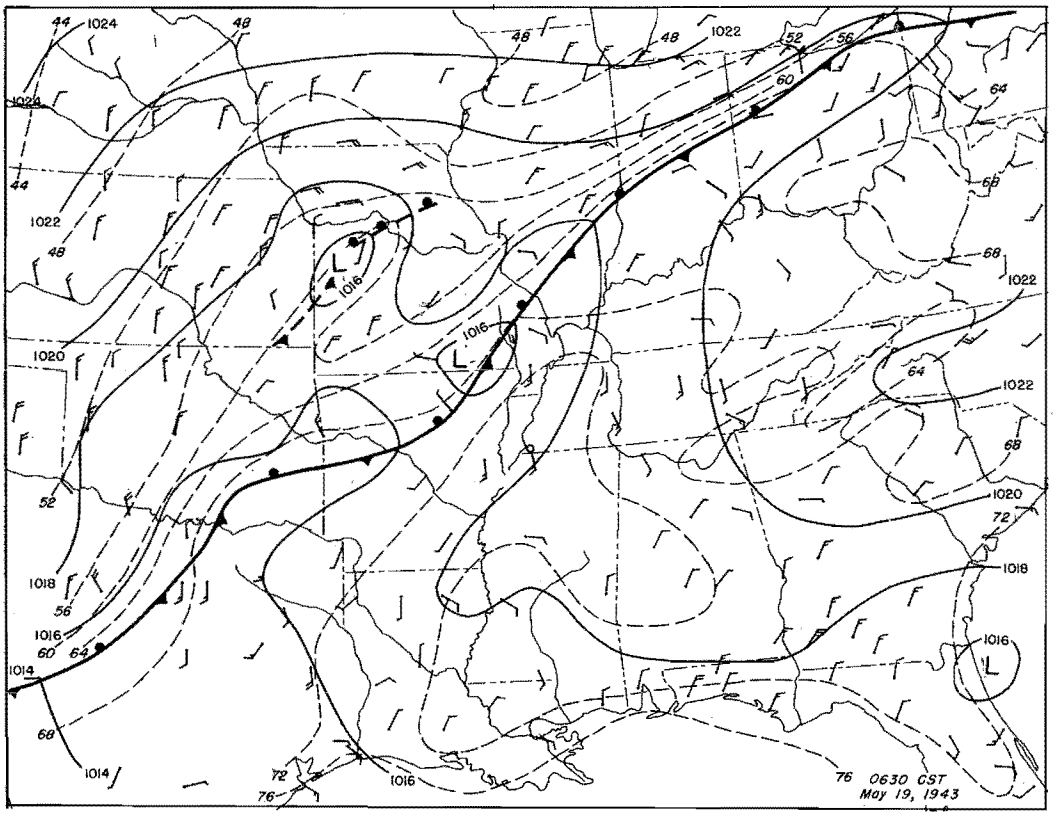

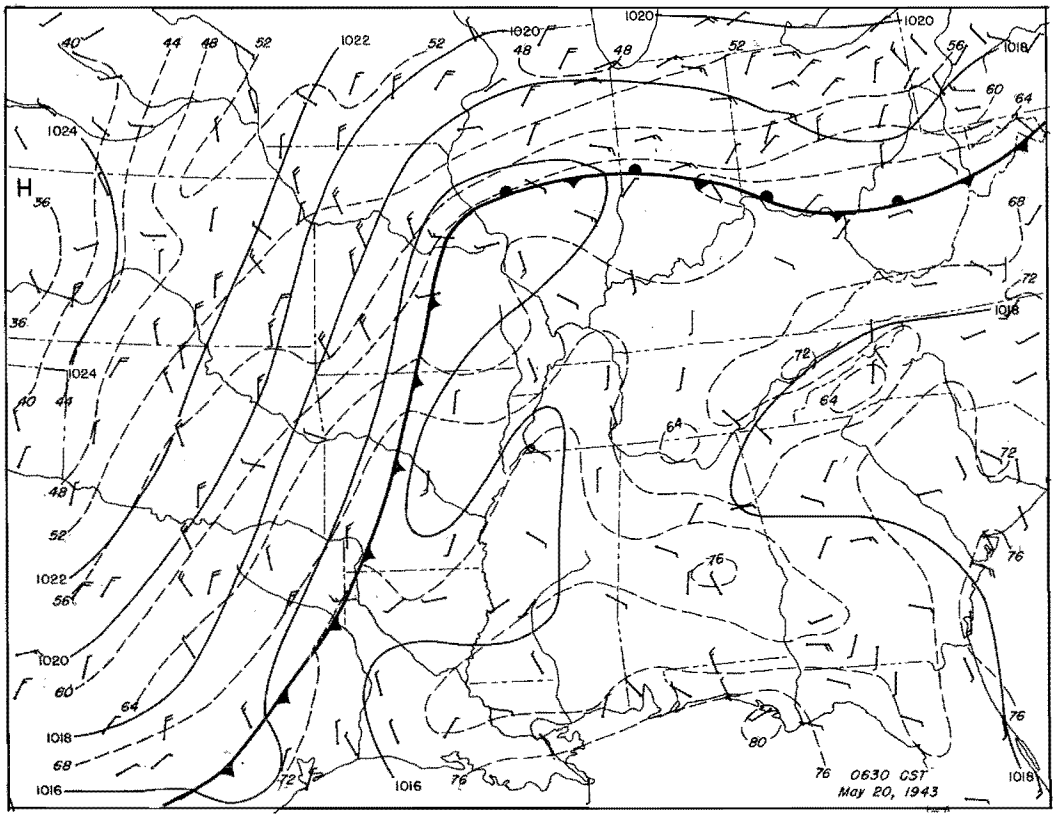

Figure 152. Detailed Surface Weather Maps

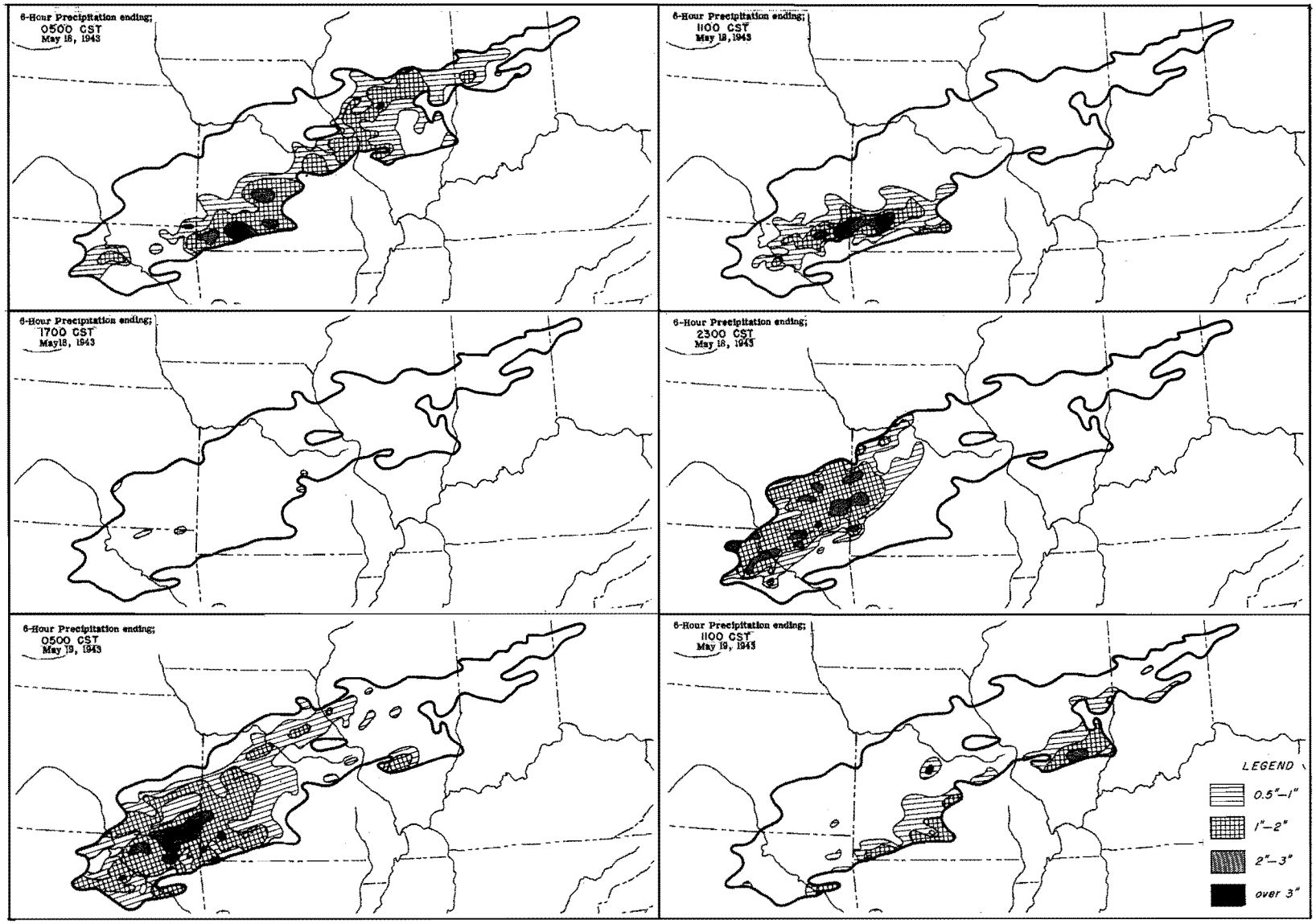

Figure 153. Incremental Isohyetal Patterns

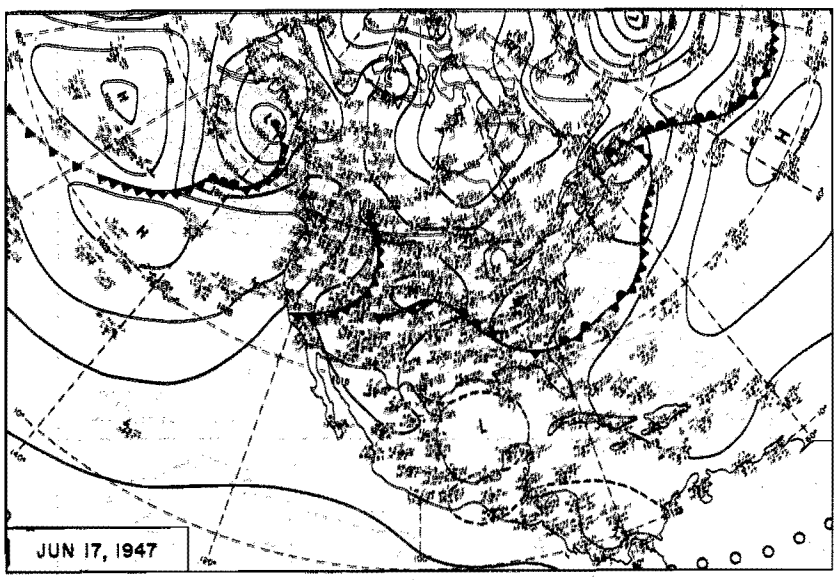

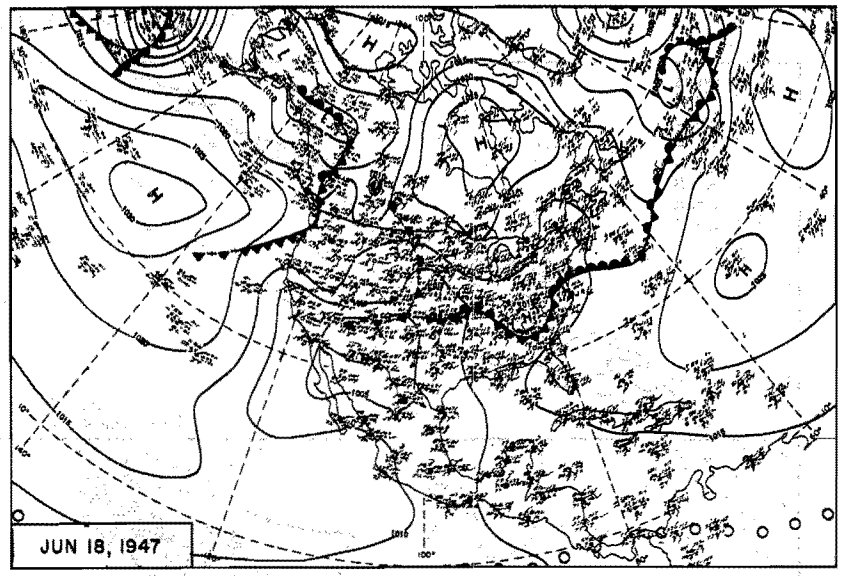

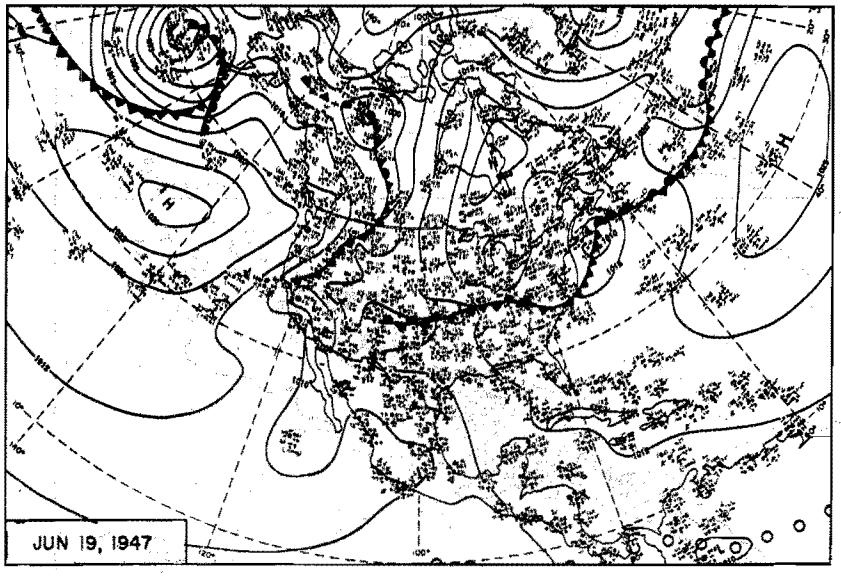

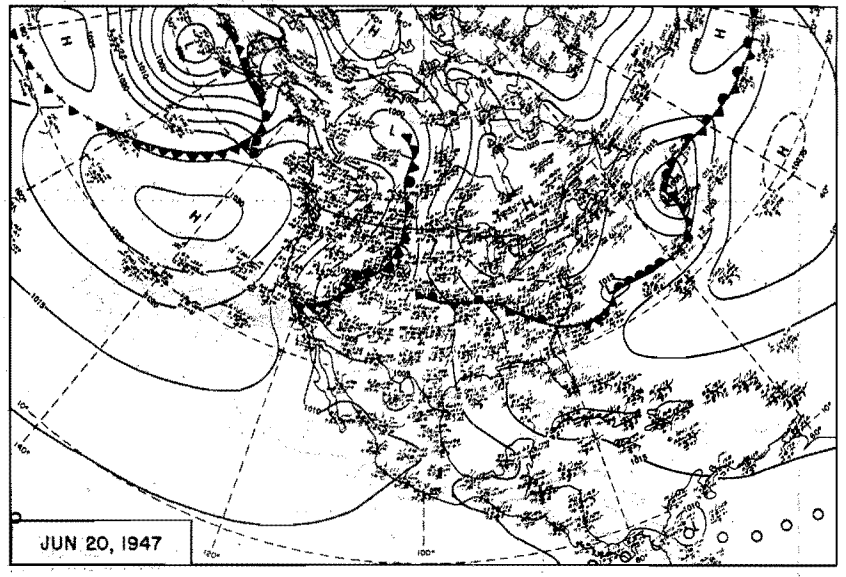

Figure 154. 0700 CST Northern Hemisphere Sea—Level Maps

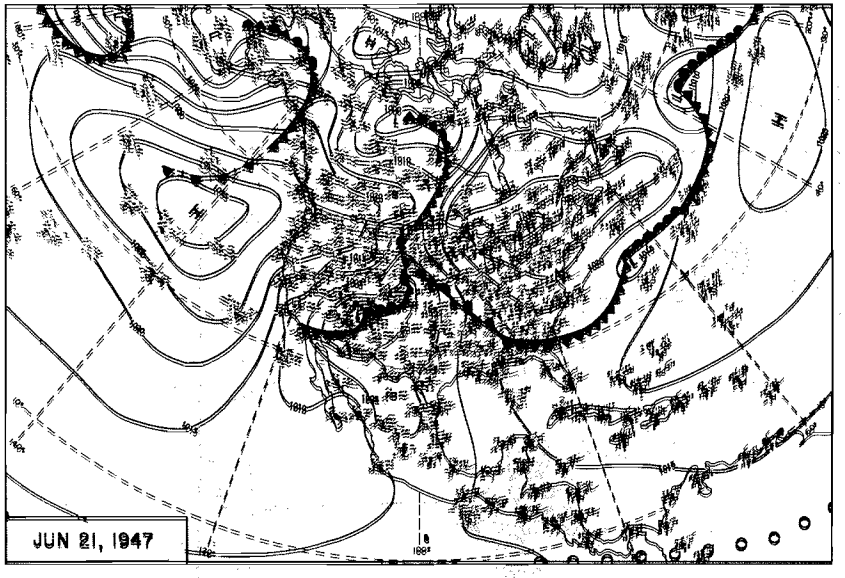

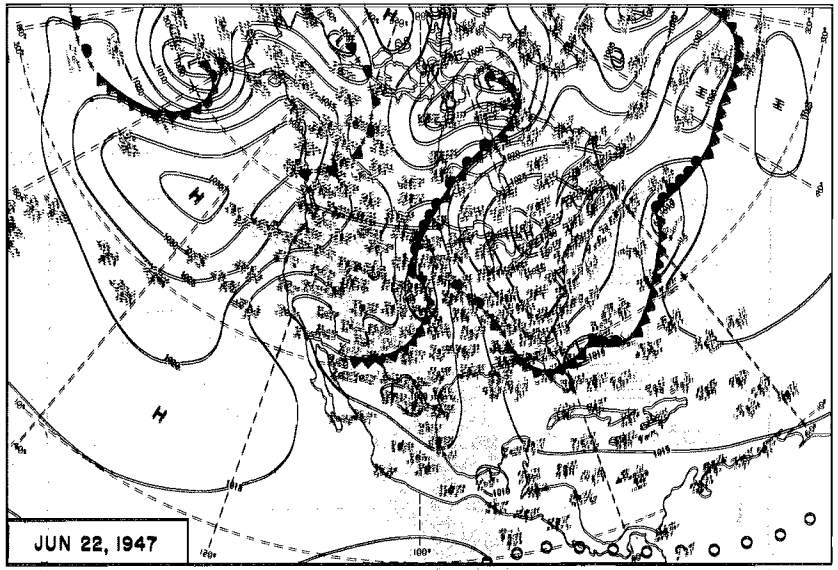

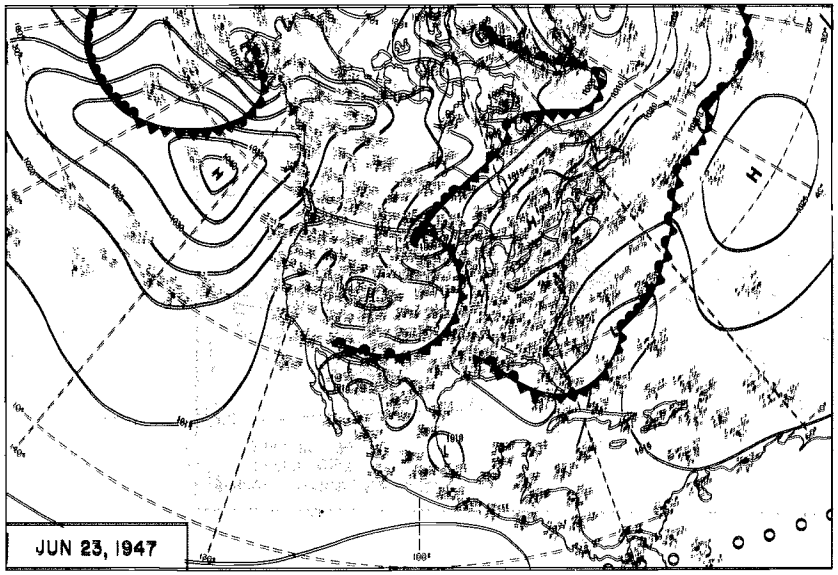

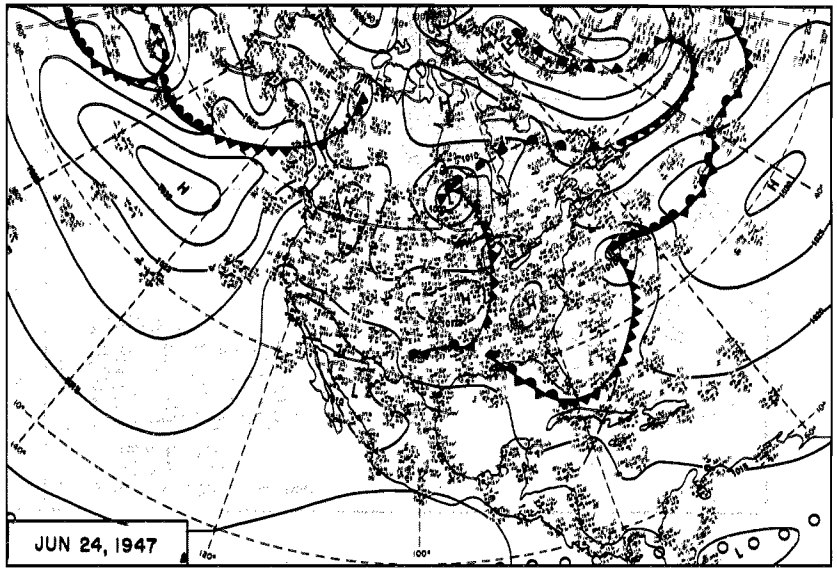

Figure 155. 0700 CST Northern Hemisphere Sea-Level Maps

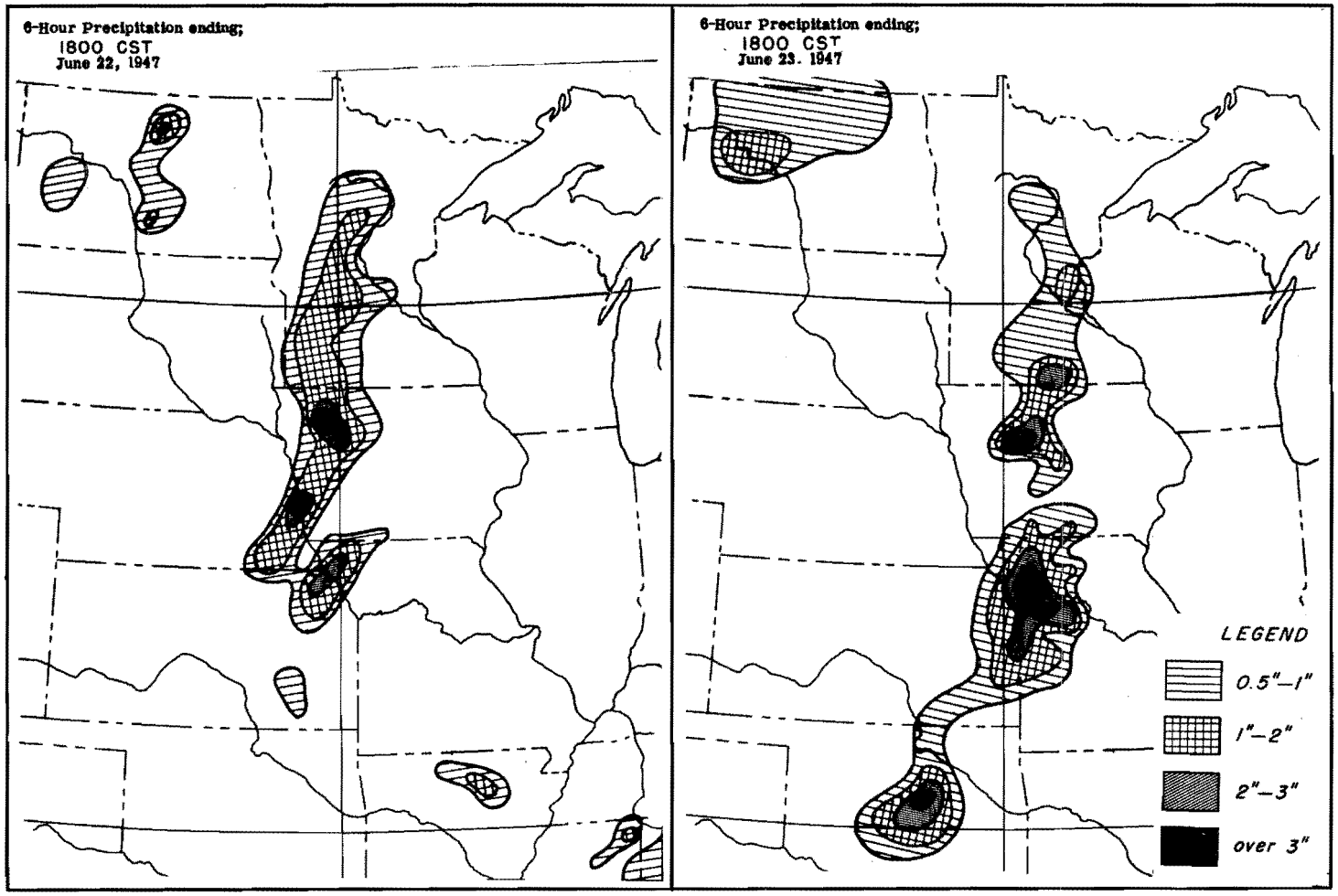

Figure 156. Incremental Isohyetal Patterns

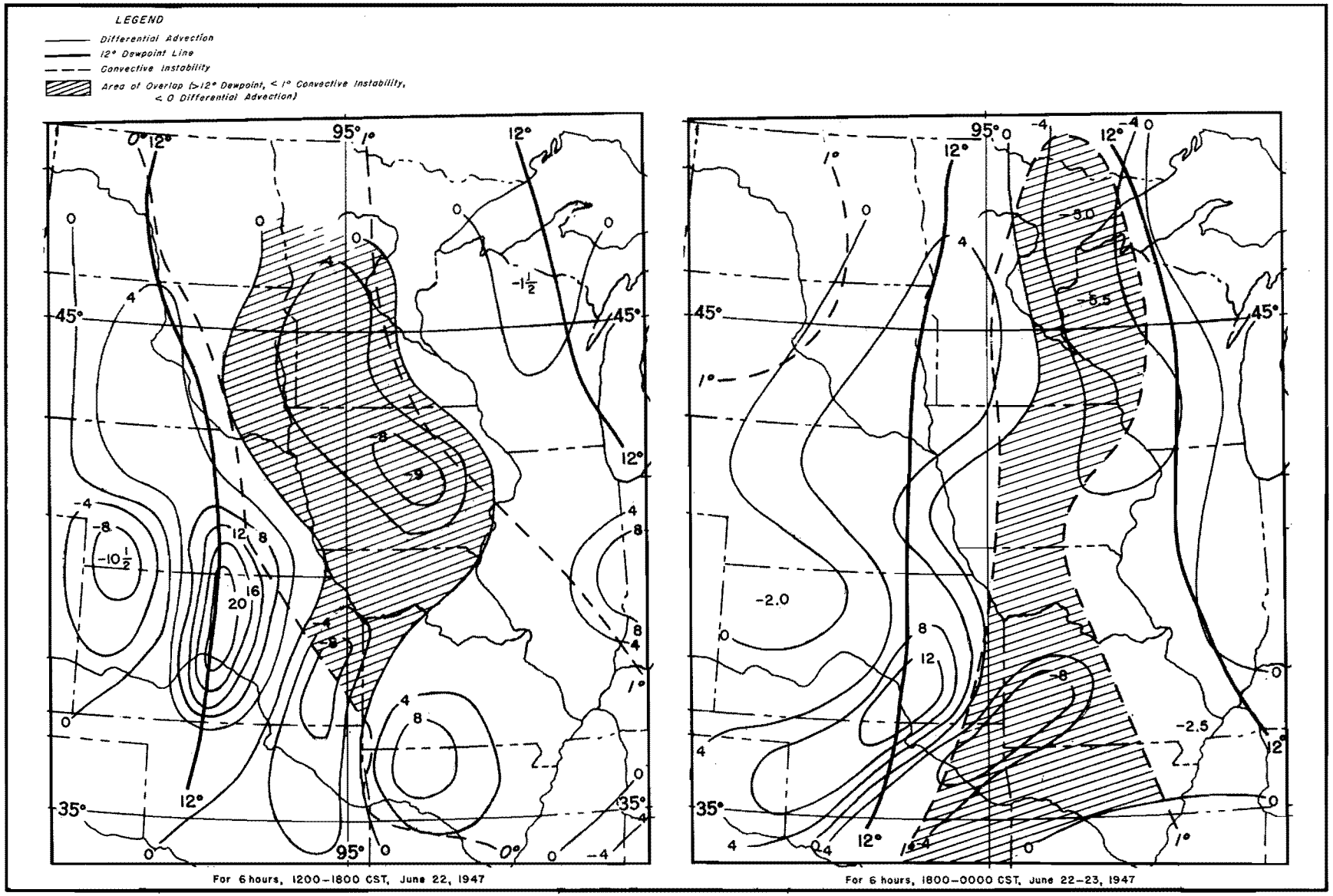

FIGURE 157. FORECAST DIFFERERENTIAL ADVECTION, 12° DEWPOINT LINE, AND CONVECTIVE INSTABILITY FOR 850 MBS

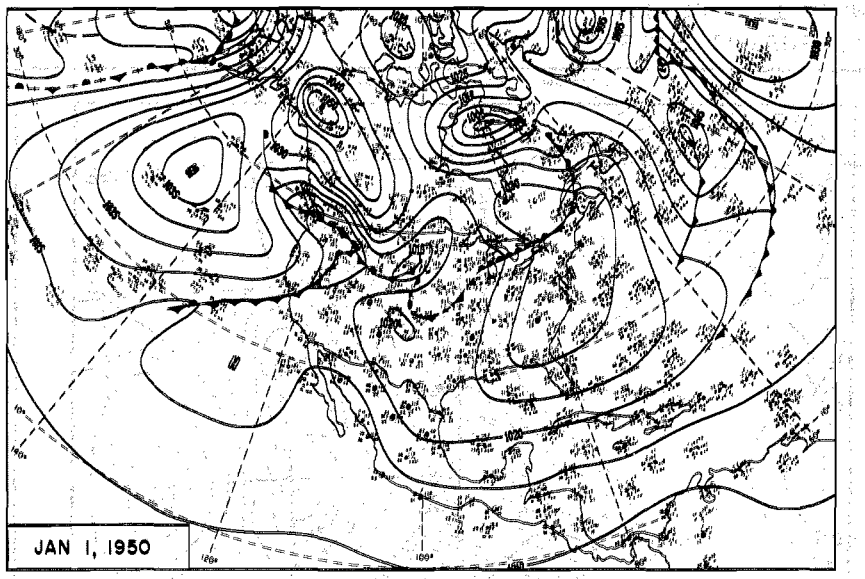

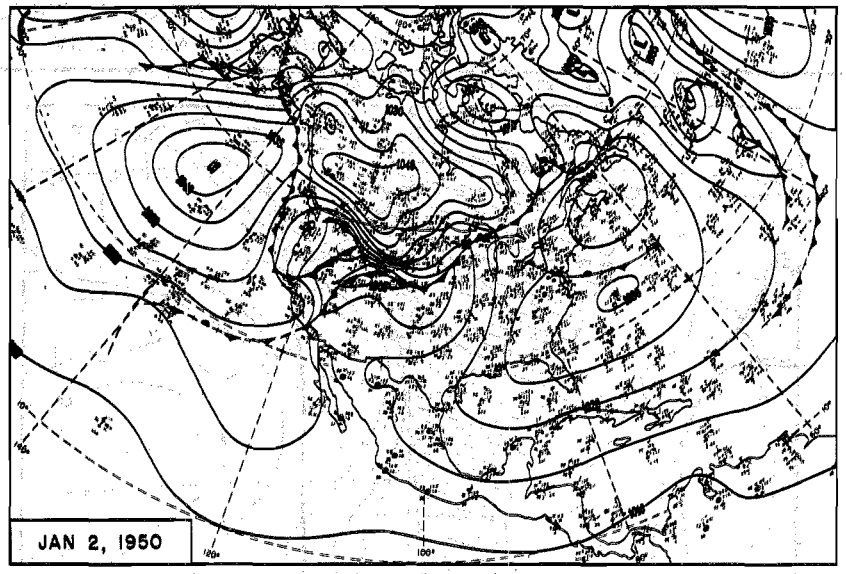

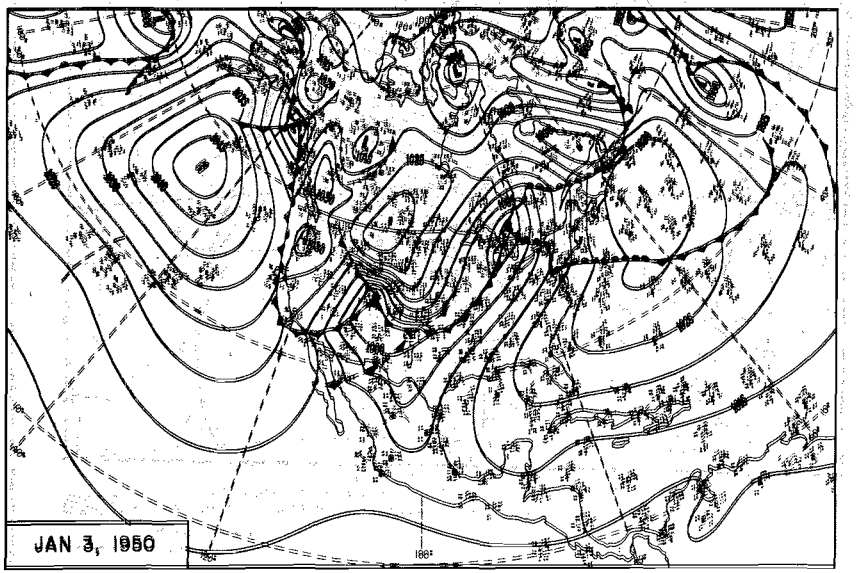

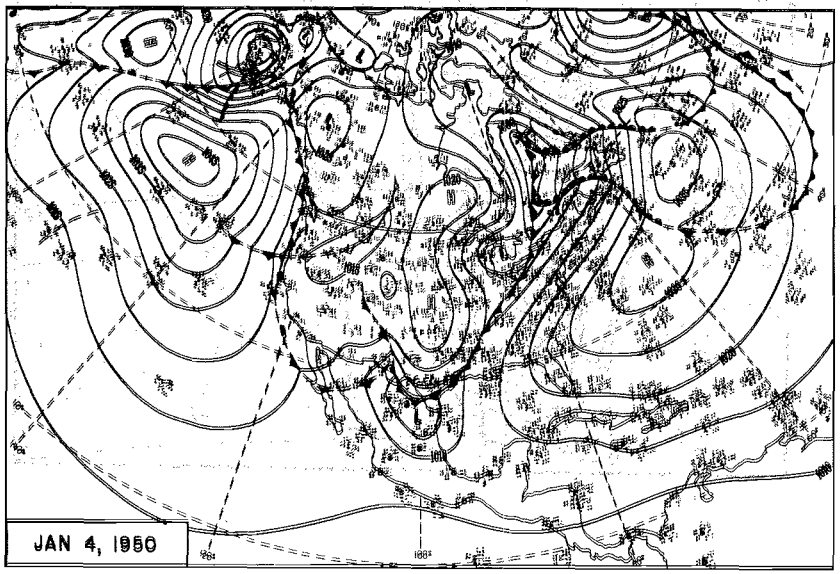

Figure 158. 0700 GST Northern Hemisphere Sea-Level Maps

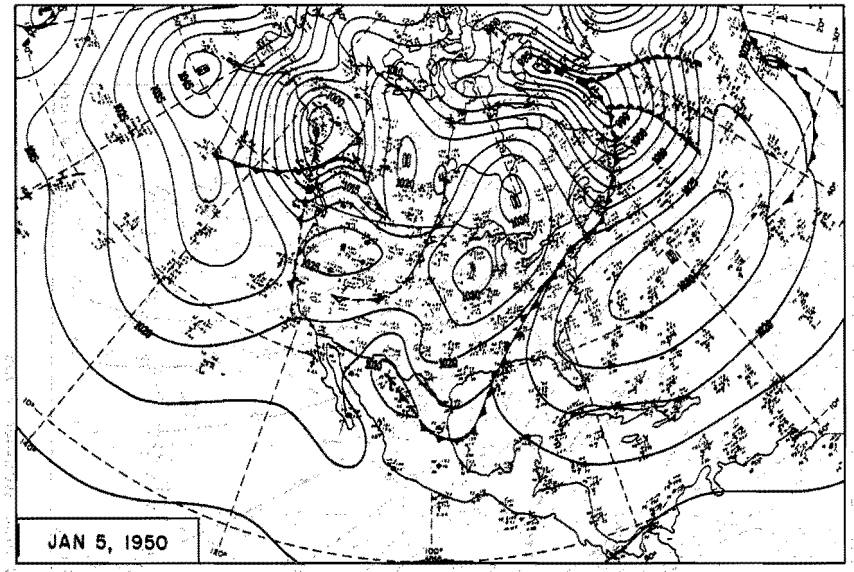

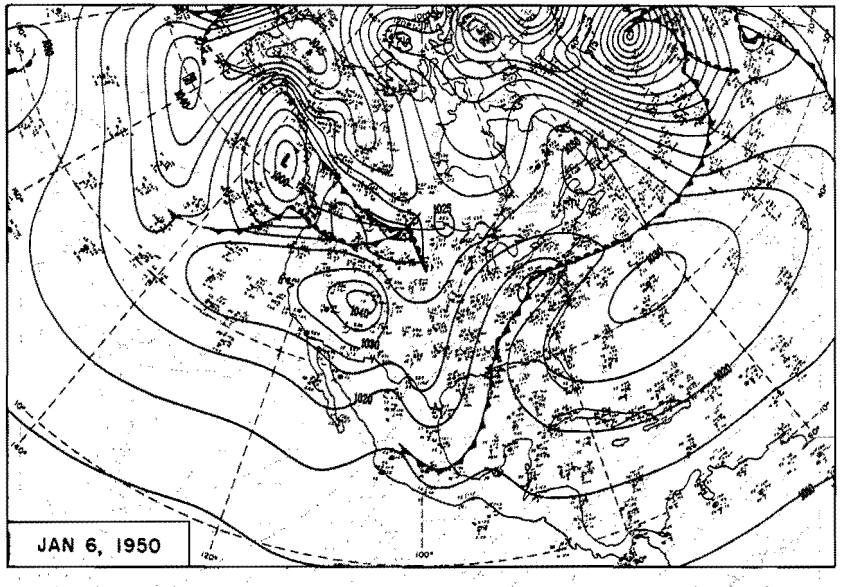

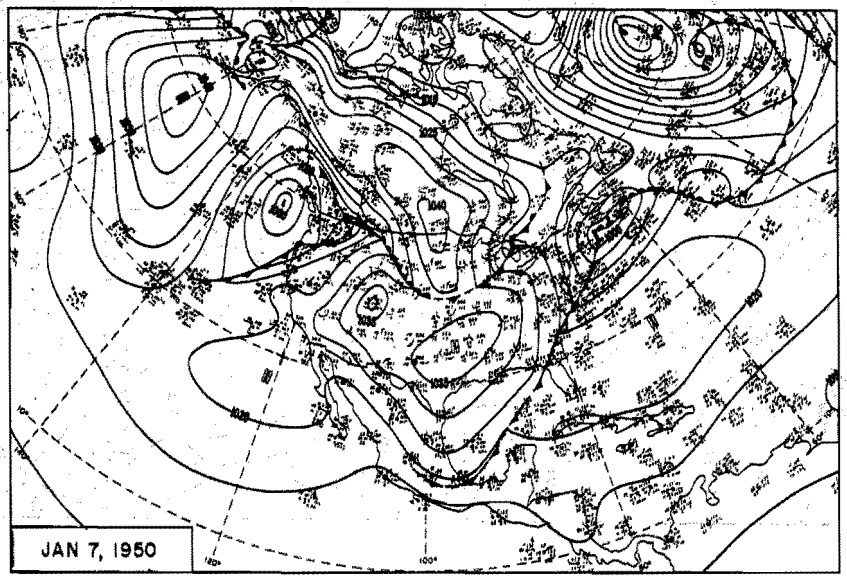

Figure 159. 0700 CST Northern Hemisphere Sea—Level Maps

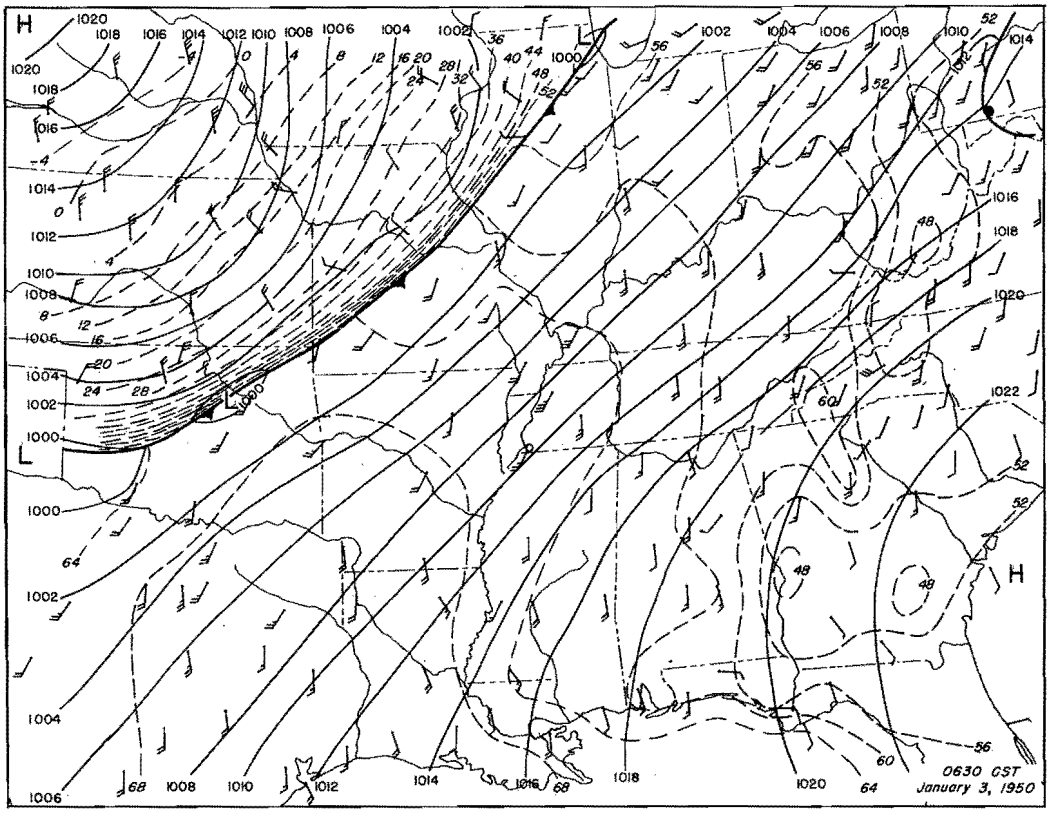

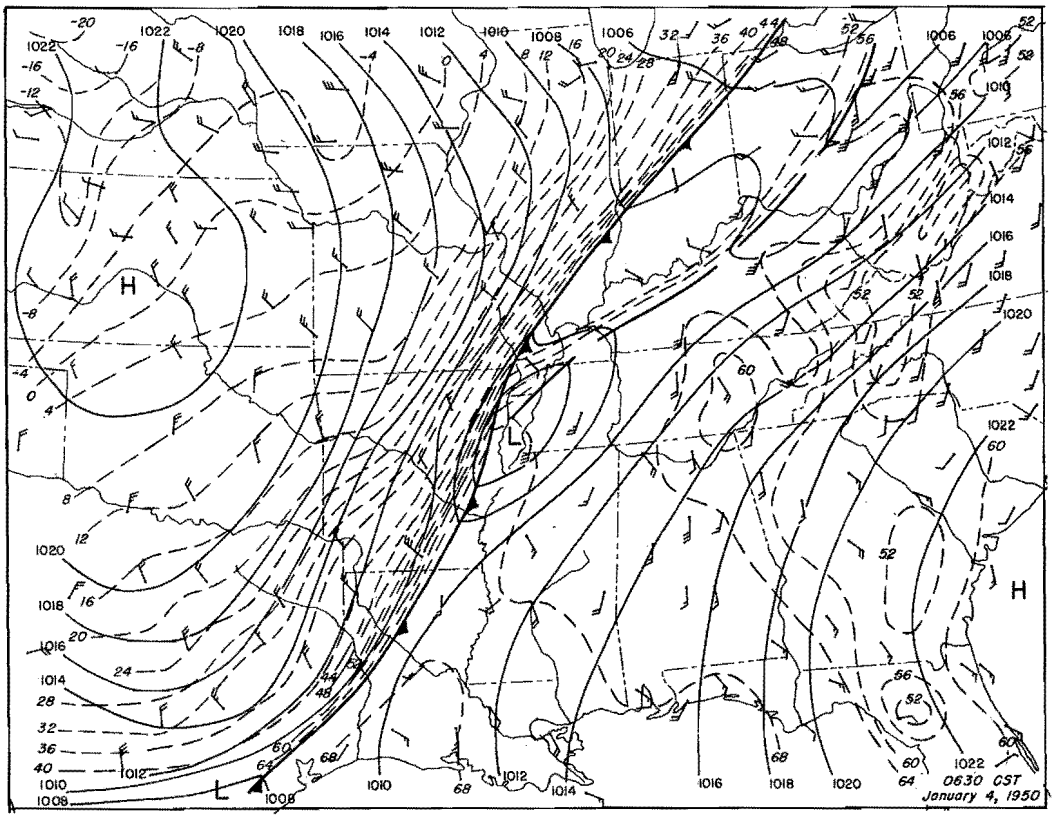

Figure 160. Detailed Surface Weather Maps.

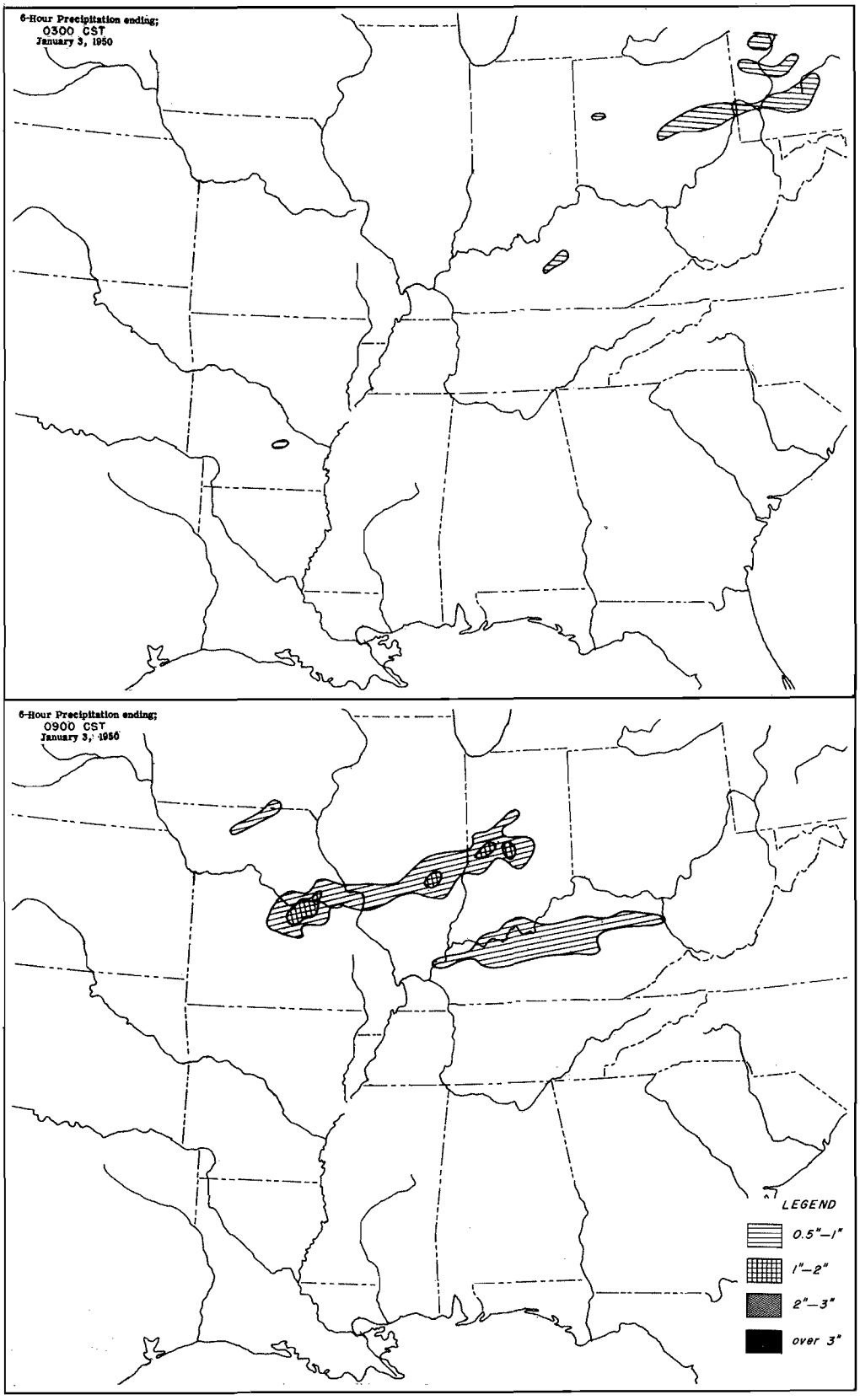

Figure 161. Incremental Isohyetal Patterns

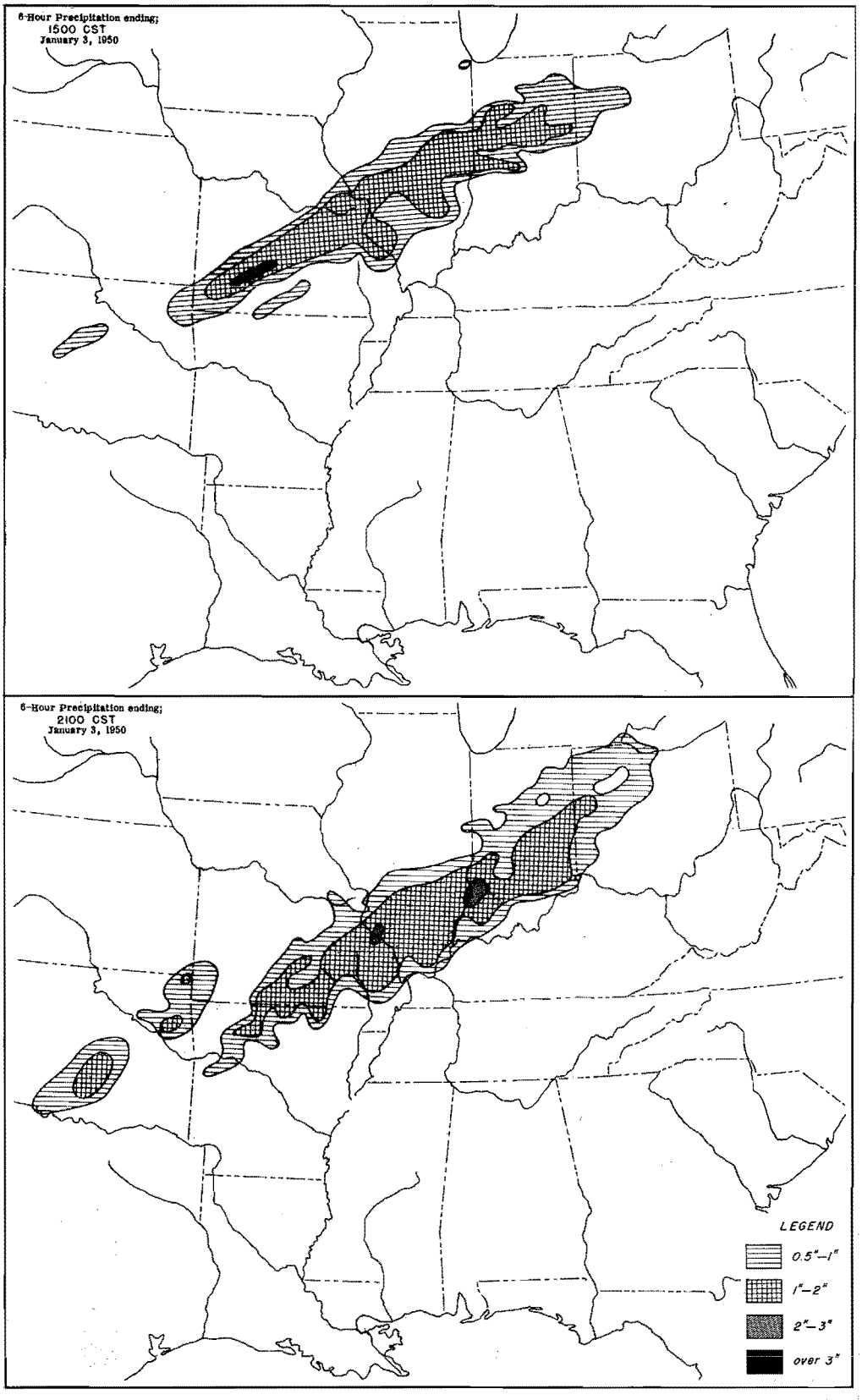

Figure 162. Incremental Isohyetal Patterns

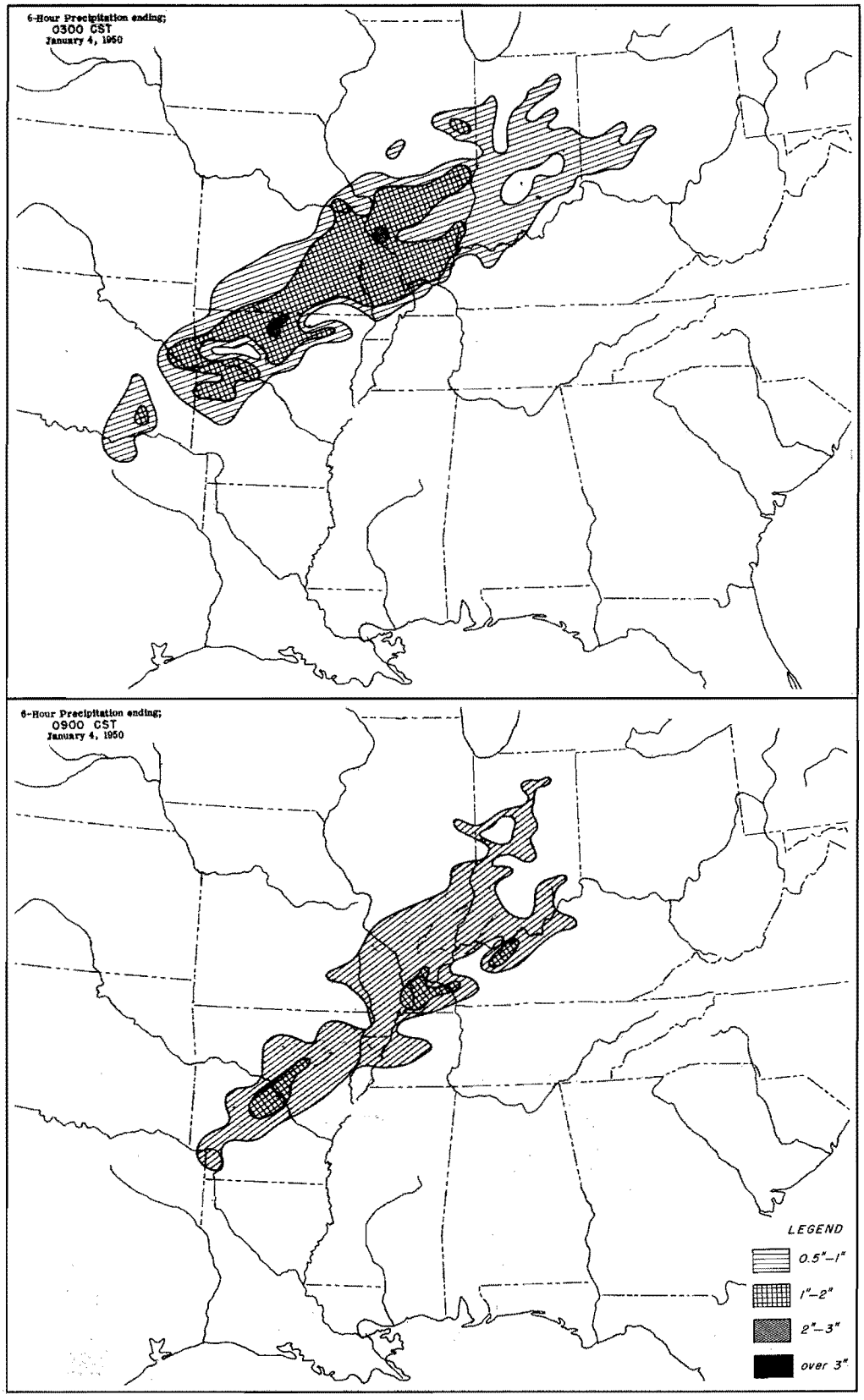

Figure 163. Incremental Isohyetal Patterns

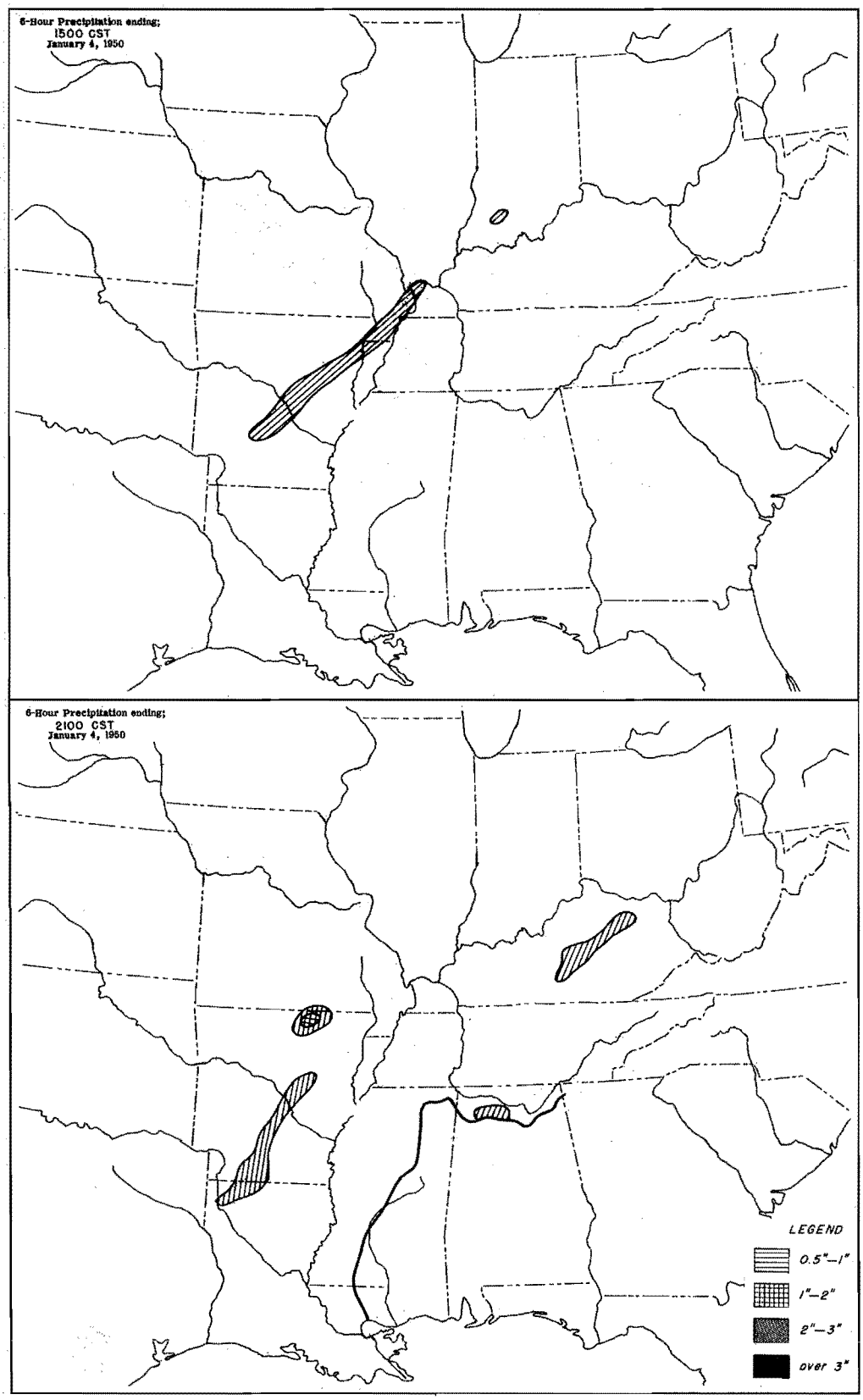

Figure 164. Incremental Isohyetal Patterns

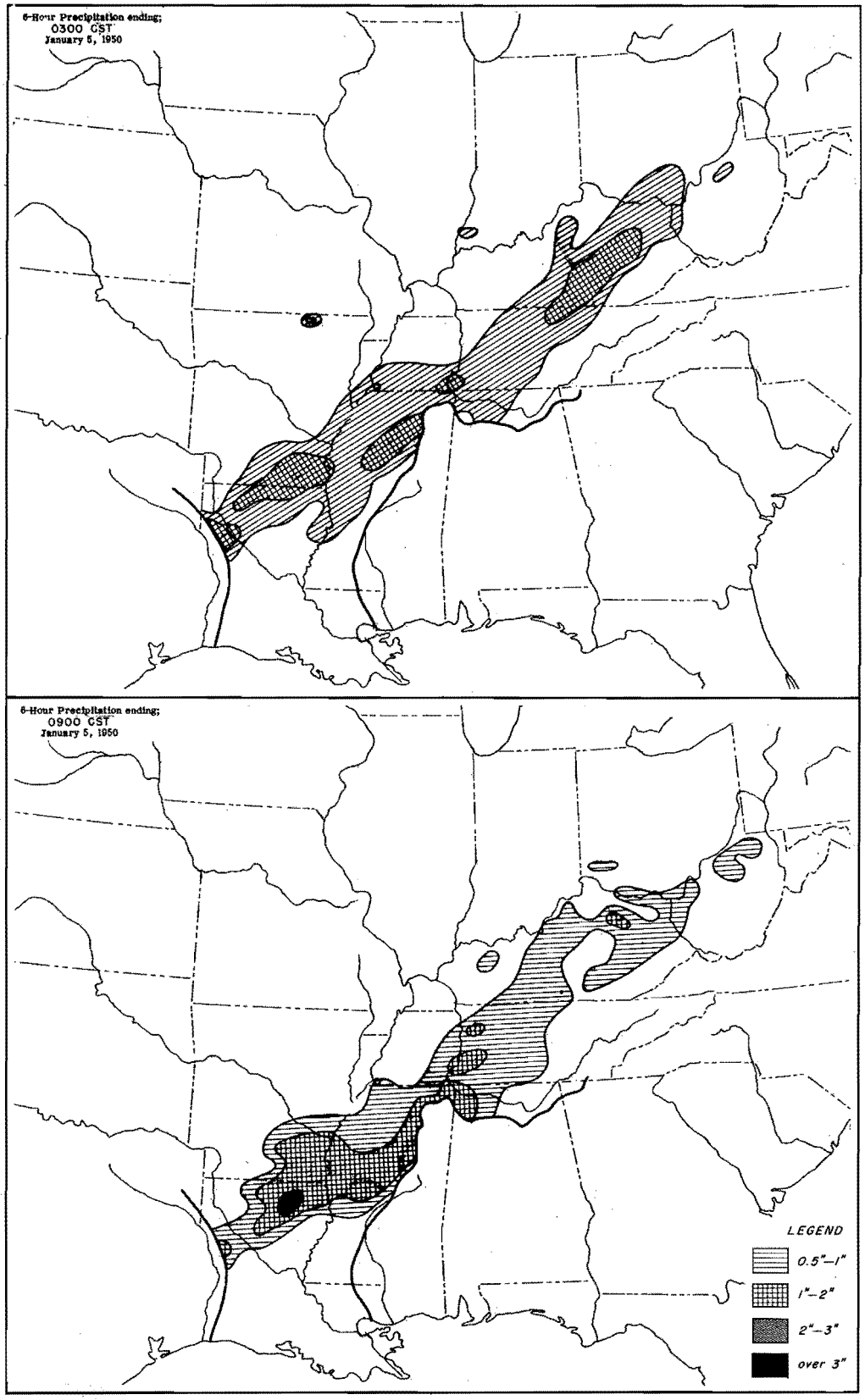

Figure 165. Incremental Isohyetal Patterns

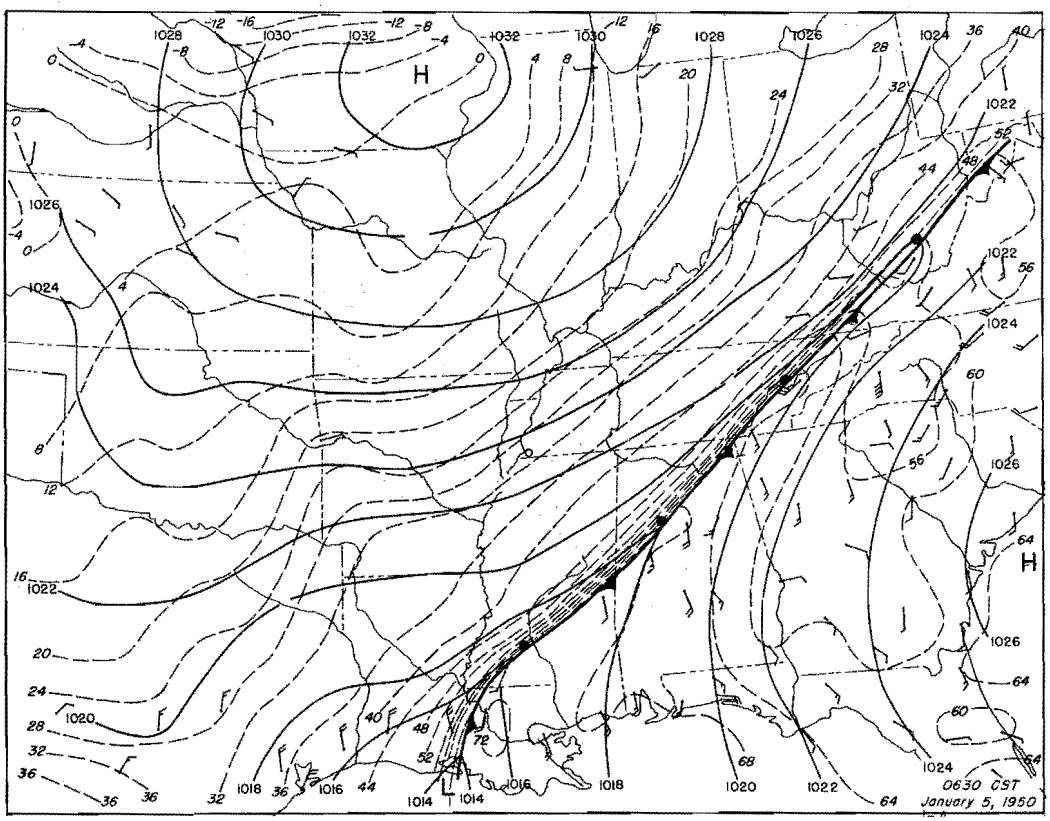

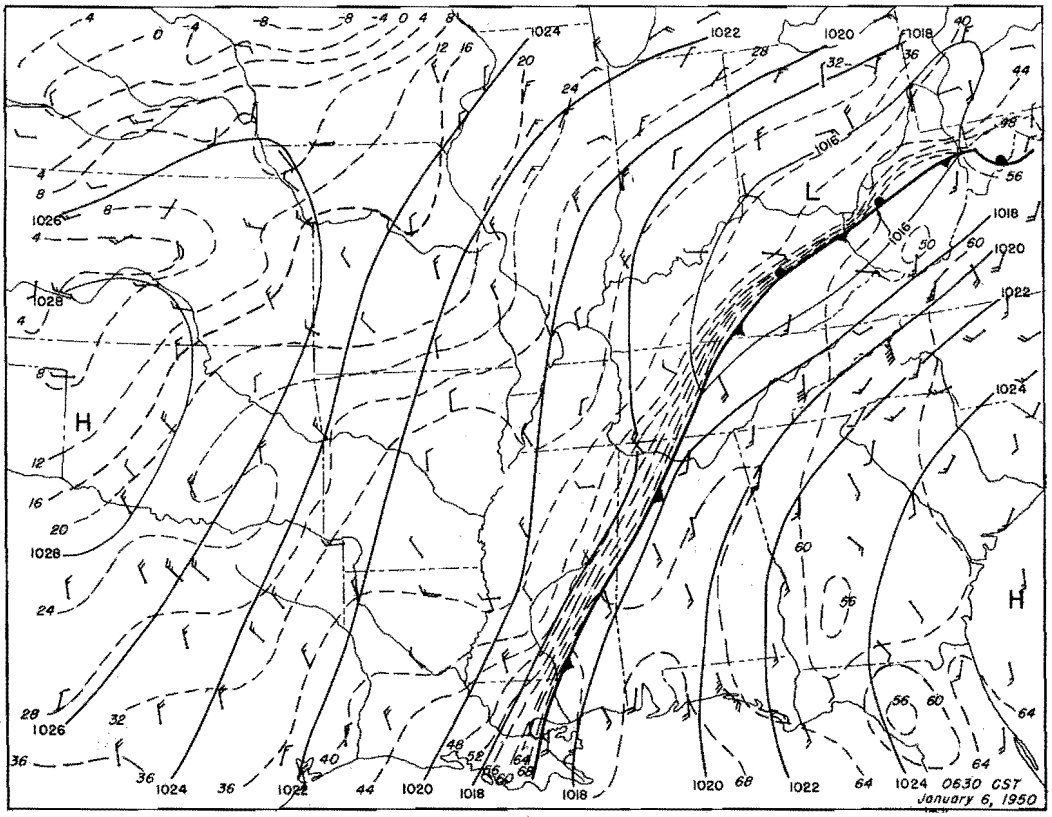

Figure 166. Detailed Surface Weather Maps

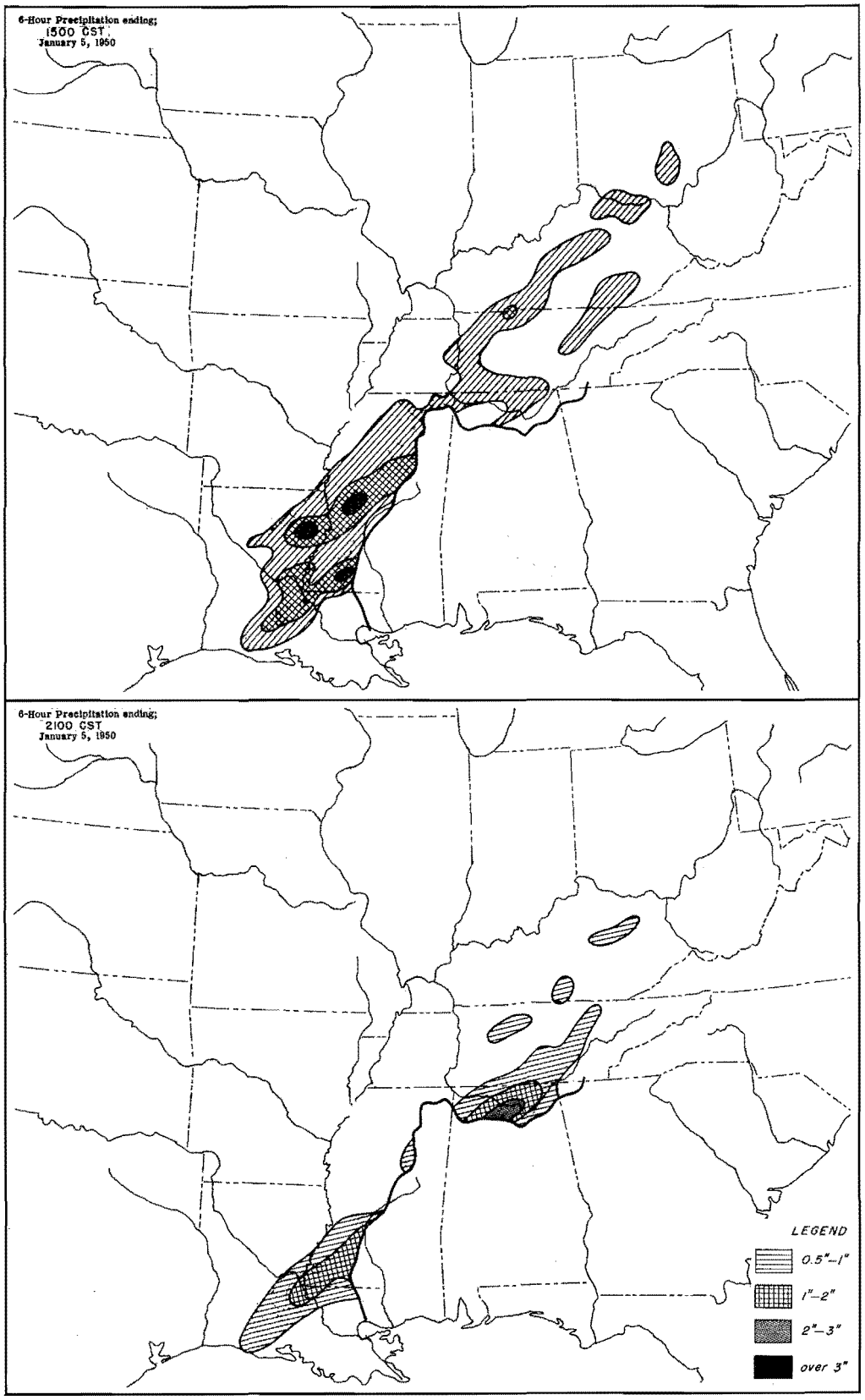

Figure 167. Incremental Isohyetal Patterns

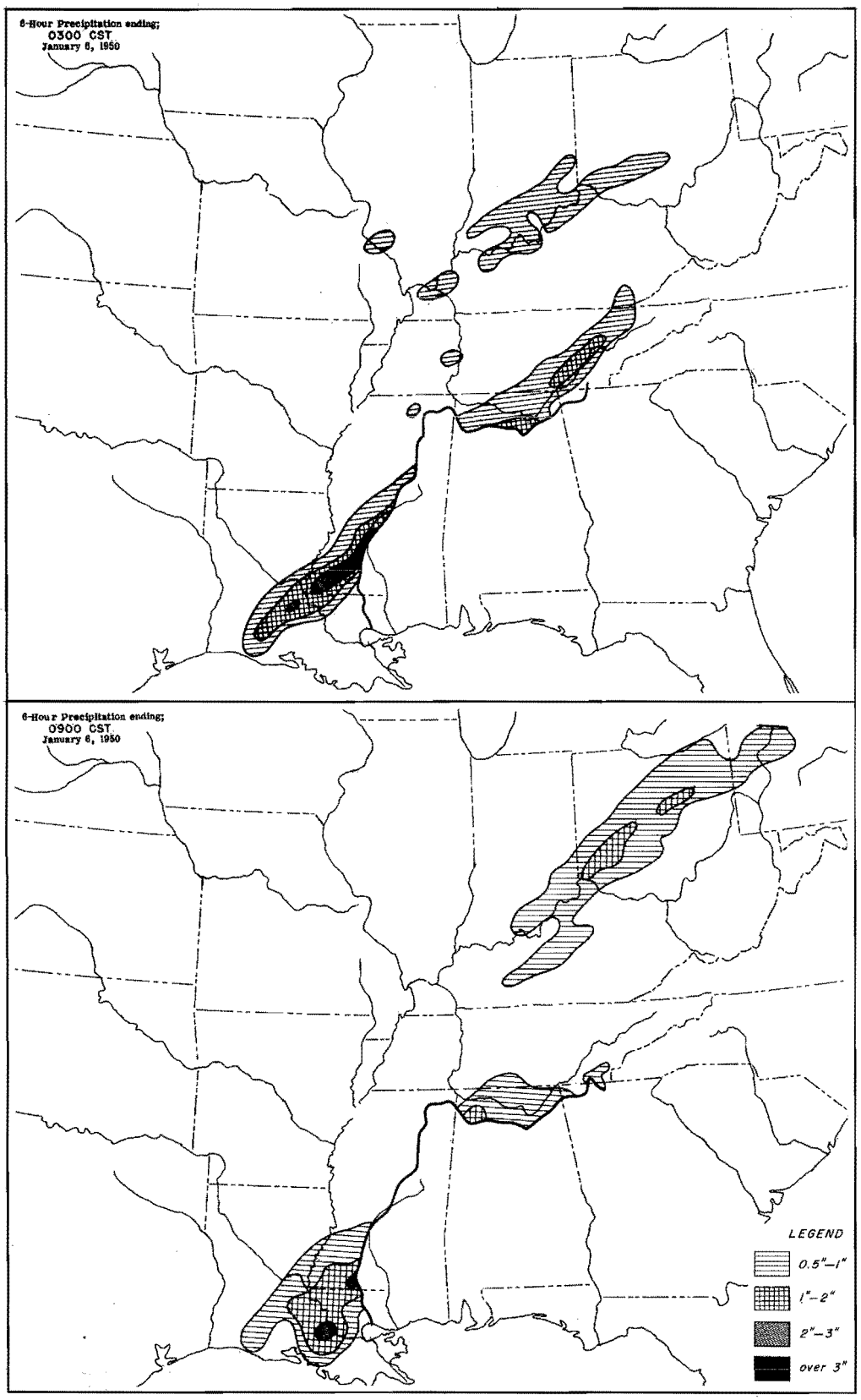

Figure 168. Incremental Isohyetal Patterns

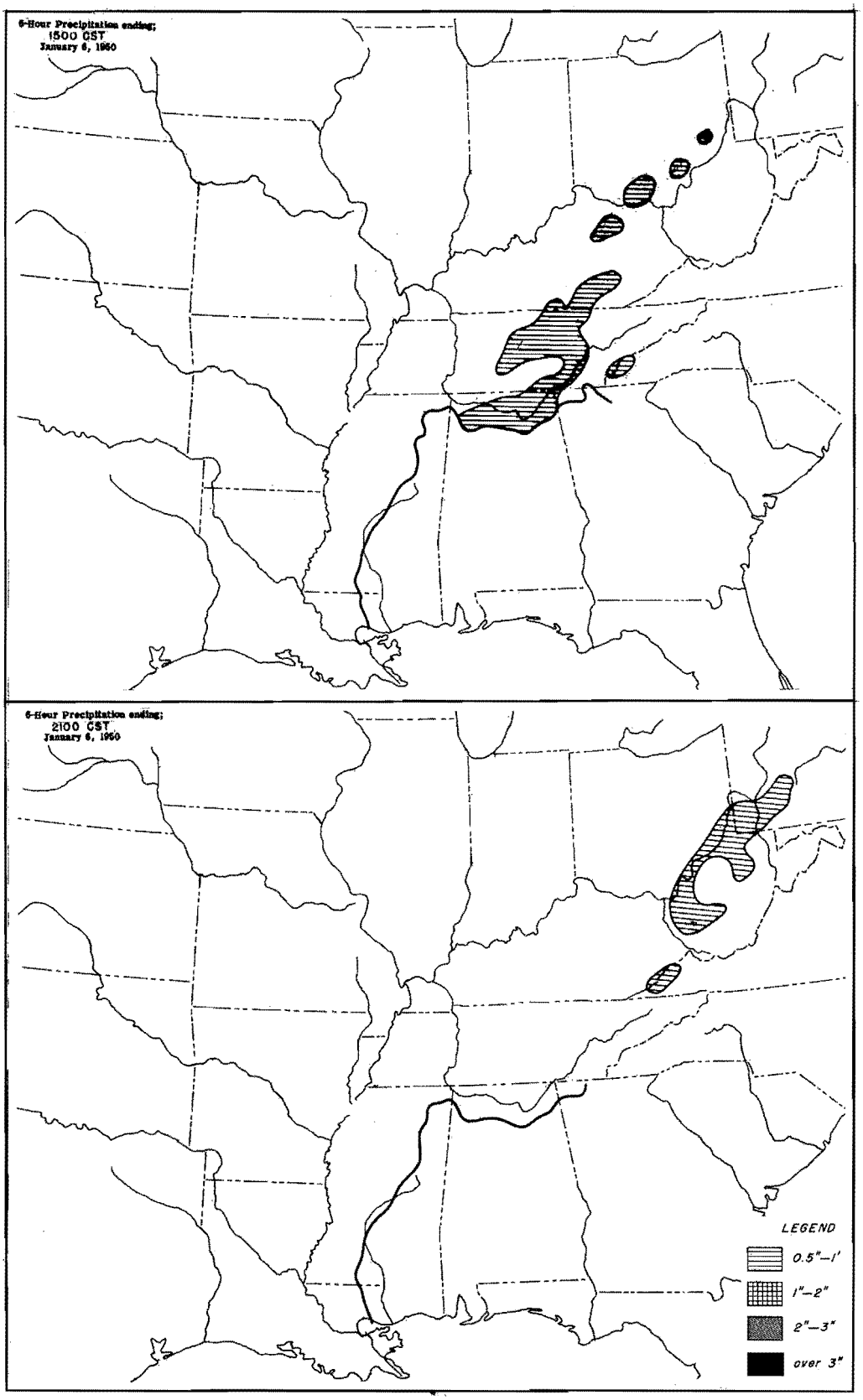

Figure 169. Incremental Isohyetal Patterns

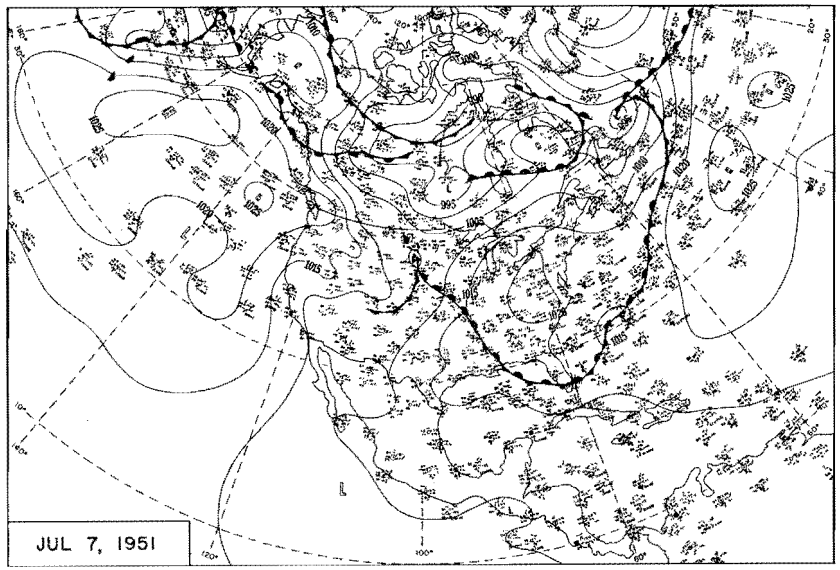

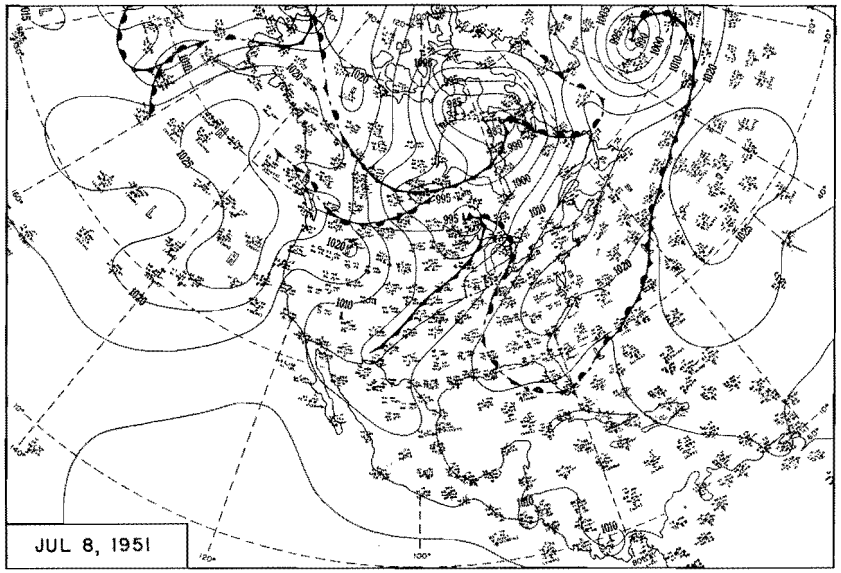

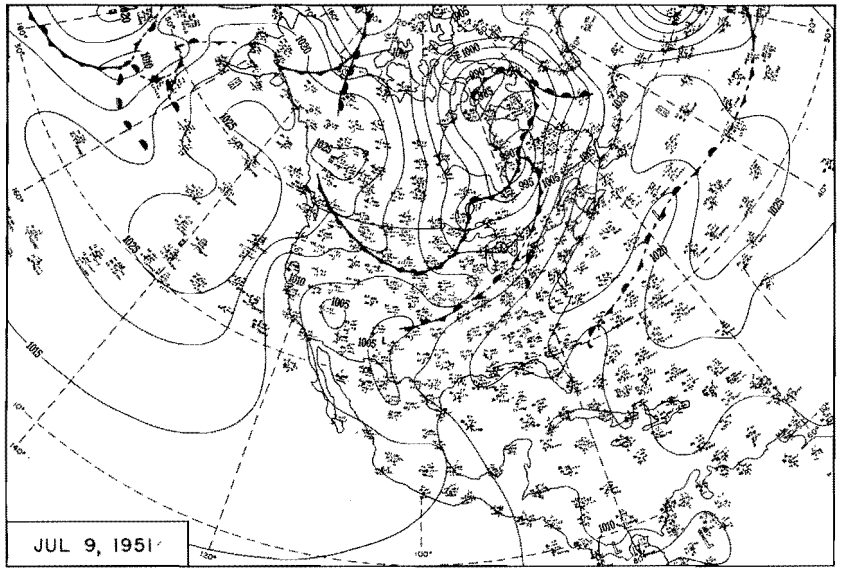

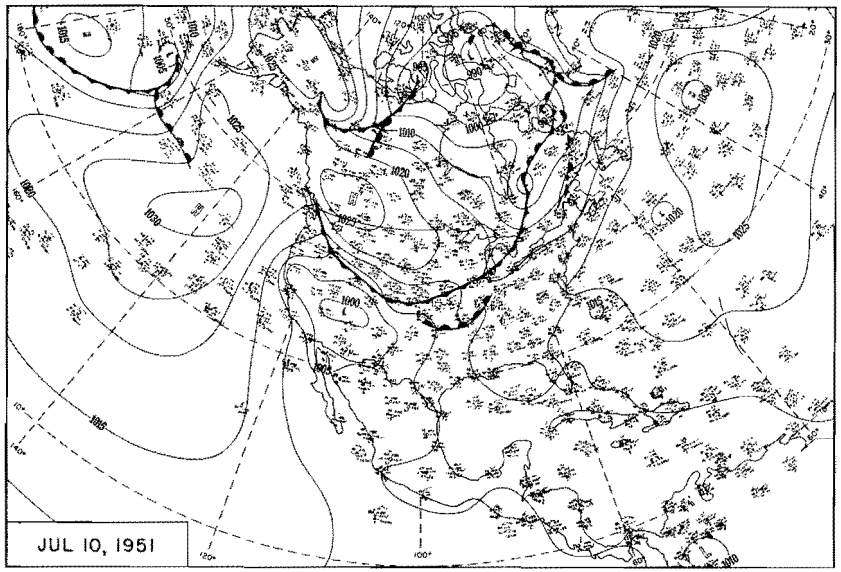

Figure 170. 0700 CST Northern Hemisphere Sea-Level Maps

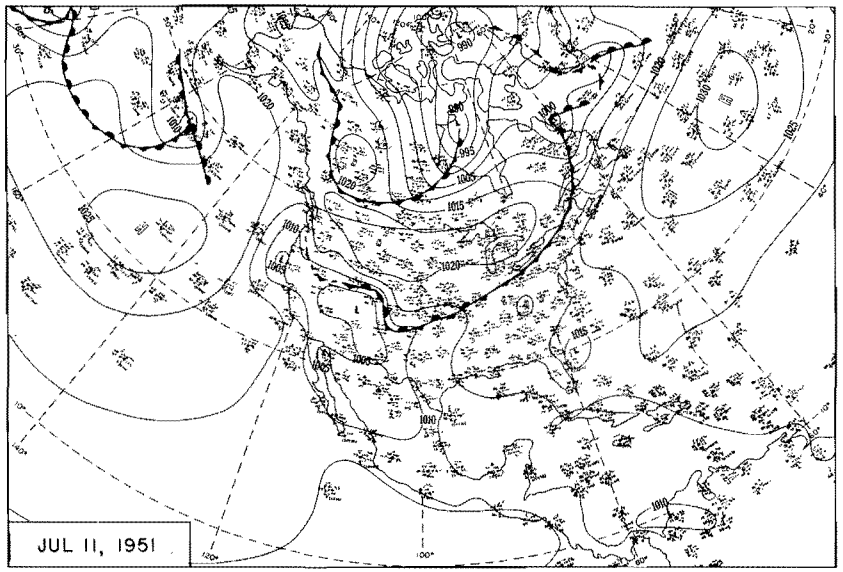

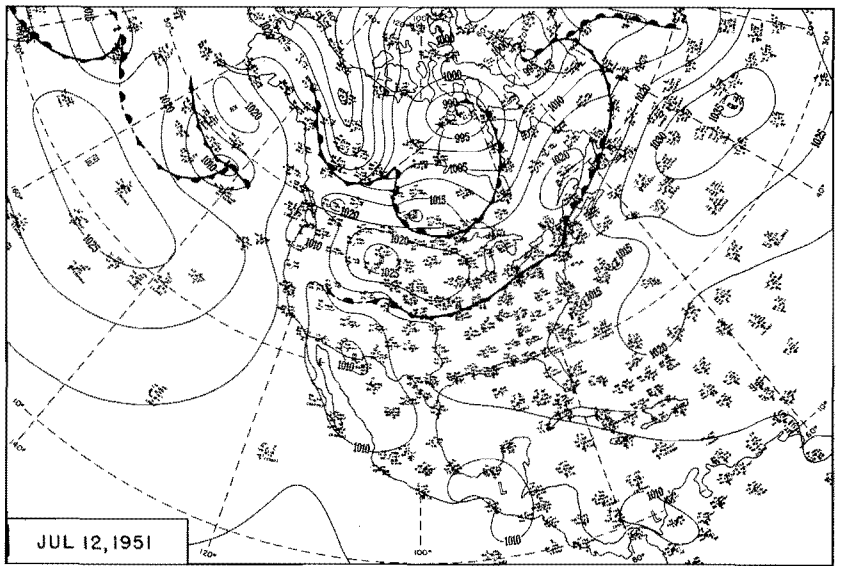

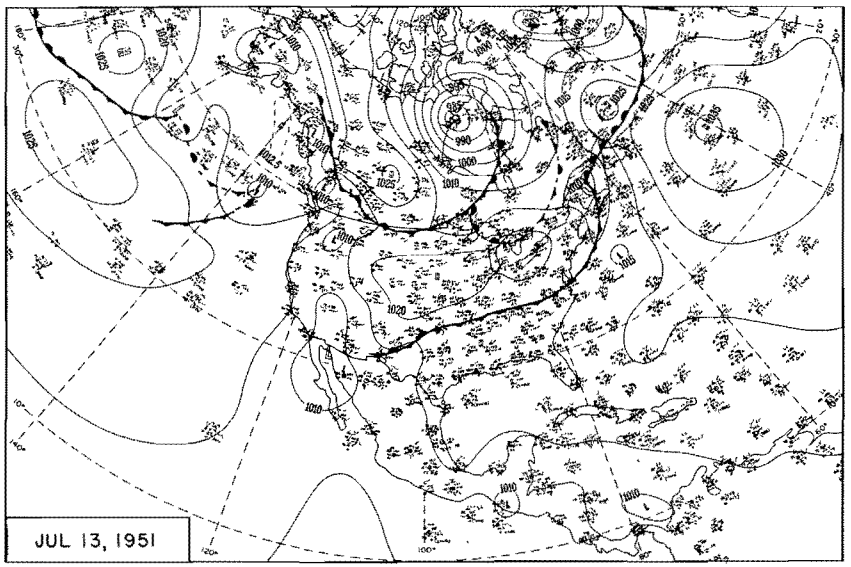

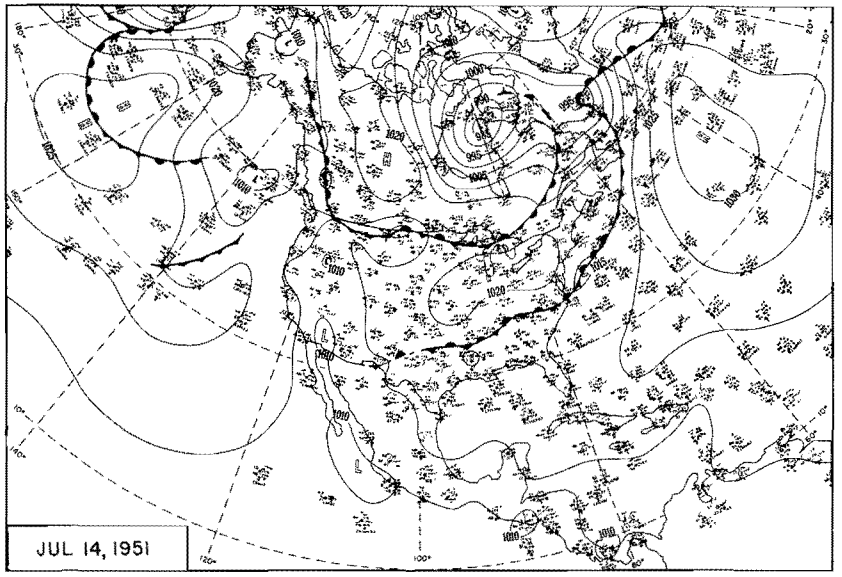

Figure 171. 0700 CST Northern Hemisphere Sea—Level Maps

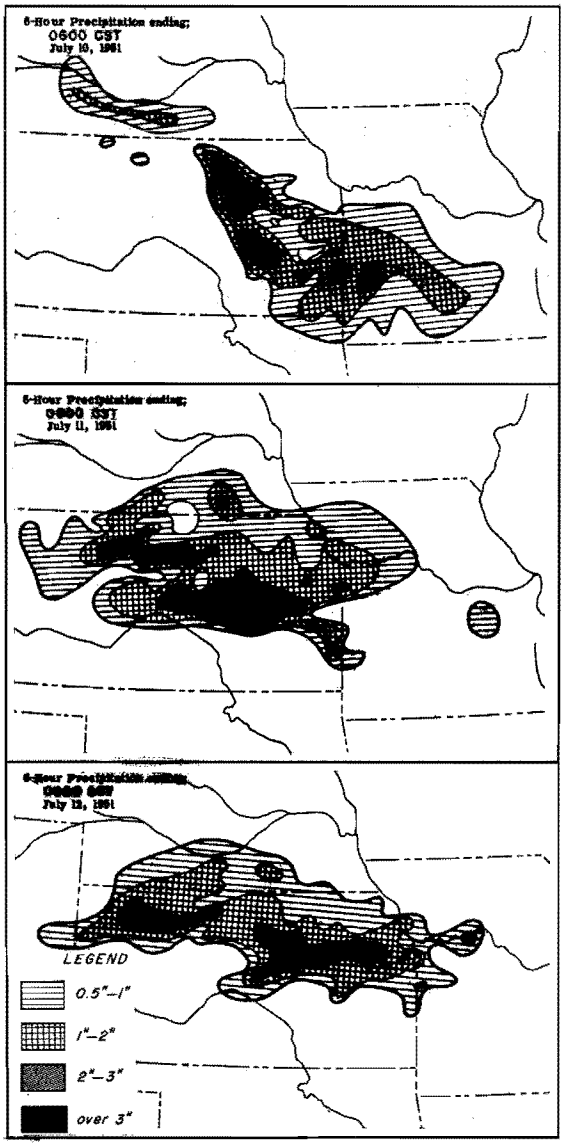

Figure 172. Incremental Isohyetal Patterns

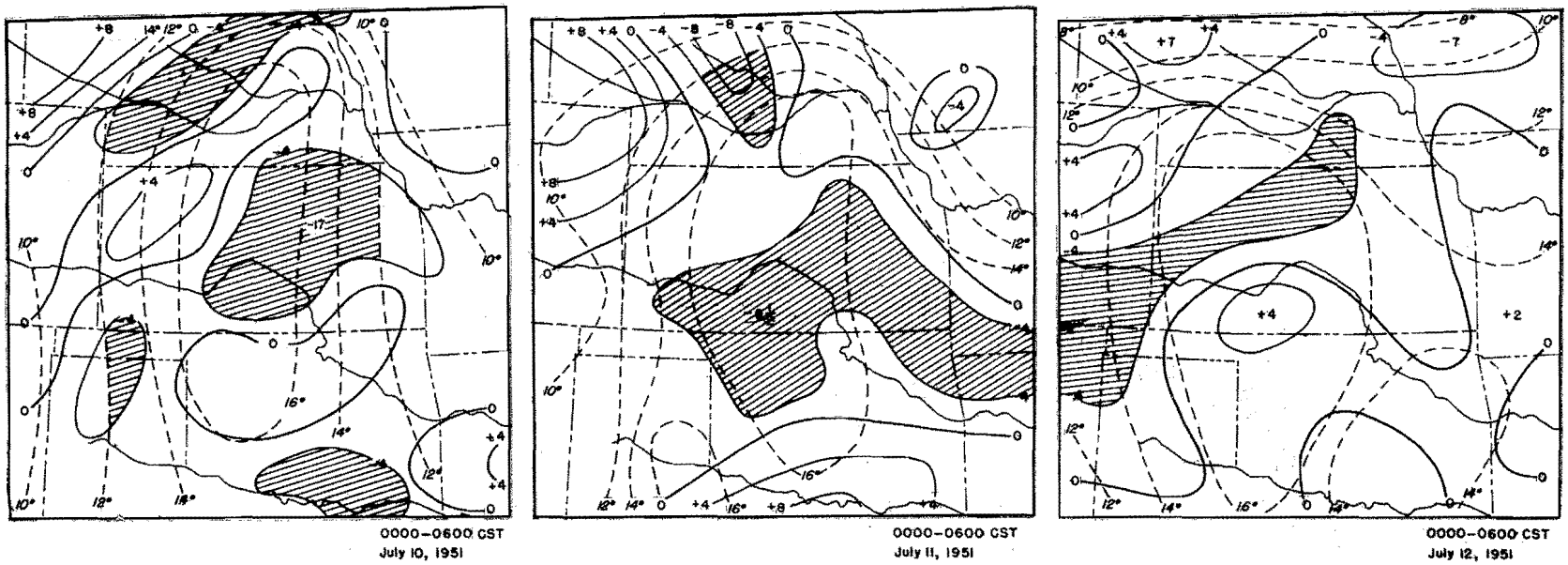

Figure 173. Differential Advection at 700 mbs and Dewpoint Envelope at 850 mbs

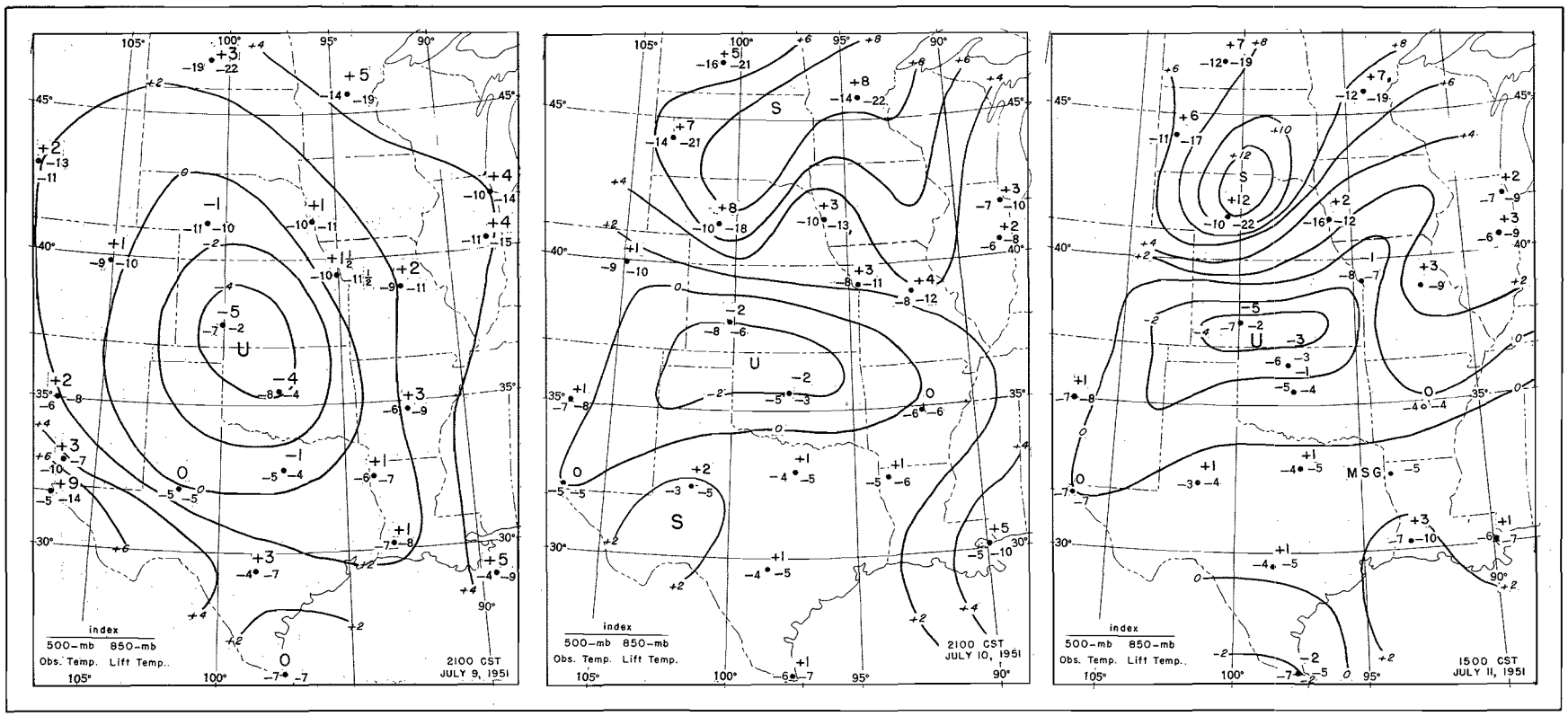

FIGURE 174. CONDITIONAL INSTABILITY, 850-500 MBS (Showalter Index)

☆ U. S. GOVERNMENT PRINTING OFFICE: 1956 O - 398807